Smart Sustainable Mobility

Analytics and Algorithms for Next-Generation Mobility Systems

Karsten Schroer

2022

Smart Sustainable Mobility

Analytics and Algorithms for Next-Generation Mobility Systems

Inauguraldissertation
zur
Erlangung des Doktorgrades
der
Wirtschafts- und Sozialwissenschaftlichen Fakultät
der
Universität zu Köln

2022

vorgelegt
von

Karsten Schroer, B.Eng., M.Phil.

aus

Troisdorf

Promotionsausschuss (Doctoral Committee)

Referent (Referee):	Prof. Dr. Wolfgang Ketter
Koreferent (Co-Referee)	Prof. Dr. Alok Gupta
Vorsitz (Chair):	Prof. Dr. Markus Weinmann
Tag der Promotion (Date of Defense):	June 26, 2023

To my family

Acknowledgments

Without a doubt, pursuing a PhD has been the biggest professional challenge of my life thus far. I joined academia after a few years in industry where I worked as a management consultant advising clients on how to grow revenue, cut costs and increase profits. My decision to pursue a PhD was motivated by the urge to work with and learn about cutting-edge technologies (primarily data analytics and machine learning) and to apply them in sectors where I thought they could make a real-world impact beyond simply driving profits (energy and transportation). Looking back at the past four years, the PhD has certainly delivered on these objectives. Yet, there were obstacles along the way. Overcoming these hurdles and completing my PhD studies successfully has instilled in me a deep confidence that almost any goal can be accomplished if I put my mind to it. As such I consider the PhD as a core milestone in both my professional as well as personal development. It has taught me very valuable life lessons while also affording me the time to acquire highly sought-after technical skills in machine learning, big data-driven causal inference and mathematical programming.

Naturally, none of this would have been possible without the help of a long list of key people including my advisors, colleagues and co-authors many of whom I now count among my friends. I would like to take this opportunity to thank them for the significant parts they played in my PhD undertaking.

First, I would like to thank **Prof. Wolfgang Ketter** who has been an excellent advisor, facilitator and promoter. Thank you very much, Wolf, for believing in my work and for providing the space, support and resources to develop my research. Your steadfast optimism along with a natural tendency to set the bar high continues to inspire me and has pushed me to excel. I also very much appreciate the introduction to key people in your vast network of practitioners and academics. Opportunities like co-authoring World Economic Forum thought pieces or teaching Executive MBA students have been great learning opportunities.

Second, I am very grateful for the support by **Prof. Thomas Y. Lee**. Dear Tom, you have provided invaluable guidance in developing and shaping several of the research projects presented in this Thesis. The in-depth discussions of technical aspects along with your insights on how to best position my work have been immensely valuable. I have always found our exchanges (both via Zoom and in-person in Berkeley) extremely engaging and intellectually stimulating and have benefited tremendously from them.

I would also like to express my gratitude for the continued guidance and support I received from **Prof. Alok Gupta**. Dear Alok, I am immensely grateful for your thoughtful comments and reviews of my work which has undoubtedly pushed it to the next level. Despite your seniority and your many many other obligations you have always found the time to provide feedback, write letters of references or discuss research ideas. The fact that you agreed to serve as co-referee on my PhD committee is another testament to your continued support. Thank you!

I would like to thank **Prof. Dr. Markus Weinmann** who kindly agreed to chair my PhD defense. Dear Markus, it is an absolute honor to have a highly accomplished IS scholar like you chair my PhD committee. I am very grateful for the time and effort you dedicate toward this.

Throughout my PhD **Prof. Dr. Konstantina Valogianni** and **Dr. Micha Kahlen** have been important mentors. As previous PhD students of Wolf's, both have a tremendous amount of experience and expertise that I was able to leverage on multiple occasions. Especially in the early days of my PhD this was a huge help. Dear Micha, thank you for providing important guidance in defining and carrying through my first research project on data-driven management of shared vehicle fleets. Dear Konstantina, thank you for providing deep and thoughtful feedback and contributions during countless iterations and review rounds of our commentary paper.

Importantly, I would like to thank my Uni of Cologne PhD colleagues who have been the most dependable and fun companions during these last four years. **Nastaran** and **Philipp**: I still vividly remember the early days of the Chair when we were suddenly entrusted with developing new course material, managing thesis students and delivering tutorials while simultaneously wrangling with the inner workings of university bureaucracy – all tasks none of us had done before. Yet, like with so many other things, we managed. Over the years you guys have been invaluable sparring partners, sources of feedback and inspiration and just great colleagues to be around. **Muhammed** and **Ramin**: Not only have we co-authored papers together, but we have also become close friends in the process. It has been an absolute pleasure to discuss research, brainstorm solutions to problems we faced, come up with new ideas for papers, or develop exciting startup concepts. Our whiteboarding sessions, first at EWI and later at Pohligstraße, are certainly among my fondest memories of those past four years. **Anna**, **Fred**, **Jannik**, **Lennard**, **Philipp Kai** and **Saber**: You guys have been an excellent addition to the team and our coffee breaks and lunches at "the Indian place" have been a most welcome distraction from PhD life. Let's keep in touch! **Chris**: I really appreciate your help regarding all things admin. No one knows the processes and policies of this university as well as you do and we would all be lost without you. **Dory**: Thank you for your patience in reviewing a number of my papers. I am extremely grateful for the subtle hints on how to improve my writing style.

During my PhD journey I also benefited from several other formative experiences that undoubtedly contributed toward my development as an independent researcher on the one hand and toward a more rounded, open-minded and reflective human being on the other.

First and foremost, I would like to stress the unforgettable and deeply enriching five-months research visit to UC Berkeley, Haas School of Business. I would like to express my deep gratitude to Prof. Thomas Y. Lee for hosting me and making my stay both enjoyable and productive. I would also like to thank **UC Berkeley** and the **German Academic Exchange Service (DAAD)** for providing generous stipends that provided the financial means for my visit. Finally, I would like to thank **Haas School of Business** for including me into the academic community at the School, which has been extremely rewarding and stimulating.

Another formative experience has been the AIS Doctoral Consortium of 2021 in Austin, Texas which I was fortunate to be invited to attend. Learning from some of the leading scholars in the field of Information Systems and engaging with some of the brightest students of the discipline has been both humbling and inspiring. I thank the **Association for Information Systems (AIS)** for sponsoring my stay at the DC and for selecting me as a Consortium Member from the pool of applicants.

I was privileged to attend many academic conferences in some of the most exciting places in the world (Seattle, Austin, Munich, etc.). I thank the **Faculty of Management, Economics and Social Sciences at the University of Cologne** for funding my position and travel.

Let me end on a personal note: I am extremely grateful to those close to me, my mother, **Elke**, and my brother, **Martin**. Both have encouraged me to take the risk and embark on the PhD journey. They have supported me tremendously during my journey by listening, demonstrating excitement for what I was doing and encouraging me during difficult periods. My father, **Peter**, who sadly is not here to witness his son's graduation but without whom I'd never be where I am now. And **Julia**, of course, who has been at my side for the entire journey. Her support cannot be put into words but is most visible in the awesomely designed cover of this Thesis. Thank you all!

Düsseldorf, July 20, 2022
Karsten Schroer

Summary

To this date, mobility ecosystems around the world operate on an uncoordinated, inefficient and unsustainable basis. Yet, many technology-enabled solutions that have the potential to remedy these societal negatives are already at our disposal or just around the corner. Innovations in vehicle technology, IoT devices, mobile connectivity and AI-powered information systems are expected to bring about a mobility system that is connected, autonomous, shared and electric (CASE). In order to fully leverage the sustainability opportunities afforded by CASE, system-level coordination and management approaches are needed.

This Thesis sets out an agenda for Information Systems research to shape the future of CASE mobility through data, analytics and algorithms (Chapter 1). Drawing on causal inference, (spatial) machine learning, mathematical programming and reinforcement learning, three concrete contributions toward this agenda are developed.

Chapter 2 demonstrates the potential of pervasive and inexpensive sensor technology for policy analysis. Connected sensing devices have significantly reduced the cost and complexity of acquiring high-resolution, high-frequency data in the physical world. This affords researchers the opportunity to track temporal and spatial patterns of offline phenomena. Drawing on a case from the bikesharing sector, we demonstrate how geo-tagged IoT data streams can be used for tracing out highly localized causal effects of large-scale mobility policy interventions while offering actionable insights for policy makers and practitioners.

Chapter 3 sets out a solution approach to a novel decision problem faced by operators of shared mobility fleets: allocating vehicle inventory optimally across a network when competition is present. The proposed three-stage model combines real-time data analytics, machine learning and mixed integer non-linear programming into an integrated framework. It provides operational decision support for fleet managers in contested shared mobility markets by generating optimal vehicle re-positioning schedules in real time.

Chapter 4 proposes a method for leveraging data-driven digital twin (DT) frameworks for large multi-stage stochastic design problems. Such problem classes are notoriously difficult to solve with traditional stochastic optimization. Drawing on the case of Electric Vehicle Charging Hubs (EVCHs), we show how high-fidelity, data-driven DT simulation environments fused with reinforcement learning (DT-RL) can achieve (close-to) arbitrary scalability and high modeling flexibility. In benchmark experiments we demonstrate that DT-RL-derived designs result in superior cost and service-level performance under real-world operating conditions.

Table of Contents

Chapter 1

Introduction – Information Systems Research for Smart Sustainable Mobility: A Framework and Call for Action[1]

1.1 Background and Motivation

Transportation is a backbone of modern societies and is changing fast. Rapid innovation in vehicle technology (Ba et al., 2013), connectivity, mobile technology (Hafermalz et al., 2020) and AI-powered information systems (Nishant et al., 2020), among others, heralds what is probably the deepest and most comprehensive transformation the industry has seen since the release of the first production car, Ford's Model T, in 1908 (Sperling, 2018). To this date, however, most mobility ecosystems around the world still operate on an uncoordinated, inefficient and unsustainable basis (Bruun and Givoni, 2015). Most traditional forms of transportation contribute to climate change, produce hazardous pollution (World Health Organization, 2005), cause bodily harm (World Health Organization, 2018) and/or are a major source of inefficiency (Cramton et al., 2018; Cheng et al., 2020). Yet, many technology-enabled solutions that can remedy these societal issues are already at our disposal or are just around the corner.

Researchers agree that tomorrow's mobility system[2] will likely be based on a multi-modal portfolio of connected, autonomous, shared and electric (CASE) mobility resources, i.e., vehicles

[1] Large portions of this Chapter have been published in the following peer-reviewed academic journal: Ketter, W., Schroer, K., & Valogianni, K. (2022). Information Systems Research for Smart Sustainable Mobility: A Framework and Call for Action. Information Systems Research, (September). https://doi.org/10.1287/isre.2022.1167 (rated A+ in the VHB-JOURQUAL 3 ranking).
A preprint of the accepted journal version has been published under the following reference: Ketter, W., Schroer, K., & Valogianni, K., Smart Sustainable Mobility: A Framework and Call for Action. Forthcoming at Information Systems Research, Available at SSRN: https://ssrn.com/abstract=4160719

[2] Throughout this Chapter and Thesis we use the term mobility interchangeably with transportation. Our definition of mobility only refers to physical mobility (as defined in Lyytinen and Yoo (2002)) of goods and people. Broader aspects such as social mobility or labor mobility are outside the scope of this article.

(Burns, 2013; Sperling, 2018). These emerging vehicle technology themes could enable society to achieve a more favourable trade-off between the societal costs and the individual benefits of physical mobility (Bruun and Givoni, 2015). Most scholars argue that, if implemented in an uncoordinated fashion, these CASE vehicle technologies may do more harm than good. Sperling (2018) paints a dystopian "doom and gloom" scenario in which autonomous vehicles lead to increased use of road-based transport versus transit options, worsening congestion and urban sprawl. Technological innovations in mobility, like many other human inventions, seem to be a double-edged sword; a wicked problem with multiple interdependencies and inherent complexities requiring data-driven system-level solution approaches (Ketter et al., 2016a).

Indeed, the wider research community has recognized these challenges. Yet, we find that the IS community, with some exceptions (Greenwood and Wattal, 2017a; Babar and Burtch, 2020; Zhang et al., 2020), has been a relatively silent observer of the intensifying discourse on CASE mobility. We base this conclusion on a comprehensive literature search of leading mobility (Scimago Journal Rank (SJR) Transportation Q1 Basket), management and IS journals (FT 50 list, UT Dallas list, IS Basket of 8) over the past five years, the results of which we have visualized in Figure 1.1. We find that the IS contribution is relatively small in absolute terms. While this may be due to a difference in size of the respective research communities, a trend analysis of research output growth reveals that our community's premier journal basket (IS Scholars' Basket of 8) is the journal category with the lowest relative growth in annual research output over the past five years.

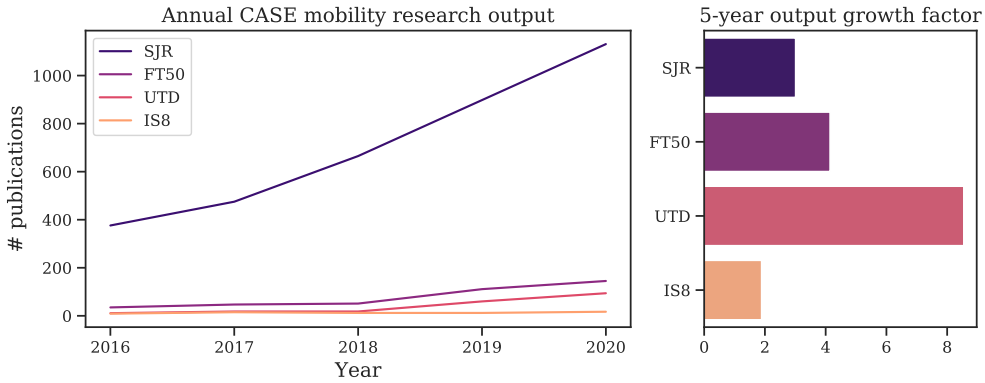

Figure 1.1: Smart mobility research output of domain- and management/IS-focused journal baskets.

Note: SJR = Scimago Journal Rank (Transportation Q1); FT50 = 50 journals used in FT Research Rank; UTD = UT Dallas' Naveen Jindal School of Management 24 leading business journals; IS8 = AIS Senior Scholar's Basket of Eight

We attribute this apparent lack of involvement of our community to the highly interdisciplinary, nascent and complex nature of the field. Yet, it is precisely this complexity coupled with the increasingly digitalized and data-driven nature of the mobility domain that holds great

opportunity for IS and calls for a much stronger involvement of our discipline. With ubiquitous information flows from sensors and mobile devices in spatio-temporal resolution, we have an abundance of information at our disposal which remains to be leveraged. We propose a comprehensive research framework and agenda that will guide IS research endeavours in utilizing this new breadth of information to the benefit of users, mobility providers and the environment. IS researchers are uniquely positioned to address Smart Sustainable Mobility challenges for two reasons. First, IS research can draw on a powerful methodology toolbox comprising advanced technical methods including algorithmic and mechanism design (Bichler et al., 2010), machine learning and econometrics (Abbasi et al., 2015; Adomavicius et al., 2013; Barfar and Padmanabhan, 2017; Dlugosch et al., 2020; Greenwood and Wattal, 2017a). Second, IS researchers combine technical skills with deep expertise in large-scale behavioral and experimental studies and experience in analysing social aspects of various phenomena (Babar and Burtch, 2020; Burtch et al., 2018; Oestreicher-Singer and Zalmanson, 2013; Osterwalder et al., 2005). It is this unique socio-technical lens (Sarker et al., 2019) that differentiates IS researchers from other fields (who might have either technical or social expertise) and enables them to confront large-scale societal challenges head on (Ketter et al., 2016b). For example, IS research already plays a highly active role in driving sustainability in the domains of energy (Dedrick, 2010; Melville, 2010; Watson et al., 2010; Seidel et al., 2013; Ketter et al., 2018) and emissions management (Corbett, 2013), where expertise in social and technical aspects is required.

This Chapter is structured as follows: I start by synthesizing current thinking on the future of mobility and illustrate how four core innovations in vehicle technology (CASE) may result in both intended and unintended consequences for mobility and its adjacent sectors. We then explain why a Smart Sustainable Mobility future is not an inevitable outcome of technological innovation and why achieving it requires careful management and guidance. We proceed by arguing that IS can provide exactly this. We support our argument with a research framework. Building on the developed framework, we formulate and detail seven core research opportunities for IS. We end with a conclusion and call to action for our community.

1.2 Scoping Smart Sustainable Mobility: A Challenge of Societal Scale

For the purpose of this commentary, mobility is defined to comprise physical mobility (i.e., transportation) of goods and people. We consider a mobility system to be smart and sustainable if it can leverage, learn from, and act upon data, information and technology in such a way that a sustainable balance between user preferences, business needs and the environment is struck. Although there are obvious interdependencies between smartness and sustainability, we consider both concepts to be distinct. Smartness refers to the digital nature of a mobility system which enables real-time information exchange, coordination and automation (as afforded by CASE vehicle technology). Sustainability extends beyond important environmental aspects (e.g., Watson et al., 2010; Seidel et al., 2018) to socio-economic sustainability (safety, resource allocation efficiency, user satisfaction, scope for profitable business models, etc.). Sustainability can only be achieved if the coordination and automation opportunities offered by a smart system are leveraged. It then follows that a mobility system can be smart without being sustainable (meaning the system is digital and automated but not geared toward sustainability) but not the other way round (i.e., to be sustainable, the mobility system must necessarily be smart).

There is evidence to suggest that the current mobility system fails to deliver on both smartness and sustainability objectives. As an illustration, consider the following three social negatives of traditional physical mobility consumption. First, conventional combustion-driven mobility is energy intensive and produces greenhouse gas. It thus contributes substantially to the global greenhouse gas emission balance sheet, with an estimated 27-28% of EU[3] and US[4] greenhouse gas emissions attributable to transportation. As such, the sector represents a key lever in the fight against climate change. We will refer to this social negative as SN1 – Climate Impact. Second, road traffic is a major health and safety hazard. Transport-related pollutant emissions that arise from hydrocarbon combustion threaten the health and well-being of urban populations (World Health Organization, 2005). Roughly 1.3m people die in traffic accidents each year across the globe (World Health Organization, 2018) (social negative SN2 – Health & Safety Impact). Third, road transport is space intensive and inefficient. In Los Angeles, America's most congested metropolis, commuters spend 102 hours in peak traffic per year (INRIX Research, 2018). Congestion has become a significant social and economic cost (Cramton et al., 2018), while road and parking infrastructure takes up a significant share of space in urban environments (social negative SN3 – Economic Impact). Below, we provide summary for clarity:

SN1 – Climate Impact: climate impact of mobility related to energy intensity of a vehicle and carbon emissions of the associated fuel (gas or electricity production)

[3] https://www.eea.europa.eu/data-and-maps/indicators/transport-emissions-of-greenhouse-gases/transport-emissions-of-greenhouse-gases-11

[4] https://www.epa.gov/ghgemissions/sources-greenhouse-gas-emissions

SN2 – Health & Safety Impact: health and safety hazards inherent to transportation usage (i.e., health impact of pollutant emissions and road accidents)

SN3 – Economic Impact: economic inefficiencies of transportation (i.e., social impact and economic cost of time lost due to congestion, search for parking spaces, etc. and/or poor access to transportation)

New vehicle technologies, some of which have been developed to address exactly these challenges, promise to improve the sector's sustainability footprint. The transportation community has brought forward diverse visions on the future of mobility technology (e.g, Burns, 2013; Sperling, 2018). Four common themes emerge from this research – mobility is likely to become connected (C), autonomous (A), shared (S) and electric (E). We adopt the acronym CASE to describe these four distinct technological developments (Sperling, 2018)[5]. The concept encapsulates a comprehensive body of research related to economic, strategic, operational and system aspects surrounding electrical vehicles (EVs) (e.g, Papadopoulos et al., 2013; Masoum et al., 2015), autonomous vehicles (AVs) (e.g, Wadud et al., 2016; Maciejewski and Bischoff, 2017), shared vehicles (e.g, Firnkorn and Müller, 2015; Shaheen and Cohen, 2007) or a combination of the three (SAEVs) (e.g, Chen et al., 2016; Dlugosch et al., 2020). We also include a fourth observed attribute – *connected* – which we find important to distinguish particularly given the effect of connected vehicles on the availability of and access to information (Mahmassani, 2016). To varying extents, CASE technology can be applied to all kinds of mobility resources including public transport (electric autonomous buses), micro-mobility (shared e-bikes and e-scooters) and even aviation (e.g., autonomous and electric vertical take-off and landing pods). For clarity, we explicitly define the dimensions of CASE below:

Connected (C): real-time digital signal exchange and communication capabilities of vehicle resources in a ubiquitous computing sense. When connected, the vehicle can interface with other actors and assets in the mobility system as part of a wider internet of things (IoT) allowing for real-time vehicle- and system-level status monitoring and control/coordination (Batty et al., 2012; Qi and Shen, 2018).

Autonomous (A): the ability of any type of vehicle to operate without external assistance, which requires all intelligence to be contained *within* the vehicle. Six levels of automation ranging from no automation (L0), assisted driving (L1), feet-off driving (L2), hands-off driving (L3), eyes-off driving (L4) and full automation (brains-off) (L5) are typically distinguished (SAE, 2018). We consider L5 to be fully autonomous. Autonomy can be enhanced by connectedness (C), i.e., via communication with other smart and connected vehicles (vehicle-to-vehicle) or smart infrastructure (vehicle-to-infrastructure) (Mahmassani, 2016).

[5]Other acronyms like ACES are also sometimes used

Shared (S): the simultaneous and/or sequential use of vehicle assets by a pool of users for transportation purposes. Sharing can take many forms and can range from models similar to renting (e.g., subscription car access like zipcar) to more archetypical sharing models like BlaBlaCar (private ride sharing) (Sundararajan, 2016; Eckhardt et al., 2019).

Electric (E): vehicle propulsion via an electric motor. Two main pure electric vehicle propulsion technologies exist. These are (1) battery electric vehicle (BEV) technology, which draws on a battery pack as the only source of energy supplying one or several on-board electric motors, and (2) fuel cell electric vehicle (FCEV) technology, which uses a fuel cell to convert chemical energy (typically from hydrogen) to electricity, which powers onboard electric motor(s).

CASE mobility technology holds great promise in addressing the three social negatives (SN) of mobility. Importantly, CASE technology, if adopted and utilized in a coordinated effort, represents a core prerequisite and enabler of Smart Sustainable Mobility. Yet, research has also revealed a range of potential adverse effects that may arise from uncoordinated adoption and use of CASE. We synthesize these views in Table 1.1 where we show how each SN might either be alleviated (↓) or aggravated (↑) by new CASE technology. It becomes apparent that the risk of unintended consequences (i.e., a worsening of one or multiple SNs) may be substantial. Thus, CASE technology may afford and result in a smart mobility system, but not necessarily one that is also sustainable (i.e., a system in which unintended consequences are effectively managed and avoided). Delivering on both smartness and sustainability objectives is complex and can only be described as a "wicked problem".

However, CASE vehicle technology also provides the necessary tools to effectively address the wickedness of Smart Sustainable Mobility. For example, ubiquitous data flows from connected vehicles and mobile devices in spatio-temporal resolution provide real-time transparency on the mobility ecosystem. Computational technologies exist that can store and process the resulting data quantities in real time. Connected mobility allows for the broadcasting of instructions, price signals or allocation decisions in real-time. Autonomous technology can ensure flexible and rational execution of such instructions. Finally, shared and electric mobility, if coordinated well, enable an overall more efficient and less resource intensive transport system. In the following section, we describe the integral role that we foresee for IS as a discipline and for its scholars in facilitating the journey toward Smart Sustainable Mobility.

Table 1.1: Possible Societal Implications of CASE Vehicle Technology

Technology	Intended Consequences	Unintended Consequences
Connected (C)	– Lower energy consumption through coordination, optimized routing and flow (Wadud et al., 2016) (↓ SN1) – Reduced congestion through real-time coordination and routing (Batty et al., 2012; Qi and Shen, 2018) (↓ SN3) – Enhanced safety through early warning and crash avoidance systems (Mahmassani, 2016) (↓ SN2)	– Increased demand for road-based transport for convenience and life-style reasons (Mahmassani, 2016) (↑ SN1 & SN3)
Autonomous (A)	– Lower energy consumption as a result of de-emphasized performance, eco-driving, improved traffic flow and routing (Burns, 2013; Wadud et al., 2016) (↓ SN1) – Reduced congestion through real-time coordination and routing (Mahmassani, 2016) (↓ SN3) – Enhanced safety through heavily reduced scope for human error (Mahmassani, 2016; Wadud et al., 2016) (↓ SN2) – Reduced space utilization (e.g., for inner-city parking) (Sperling, 2018) (↓ SN3)	– Increased demand for road-based transport due to improved cost-competitiveness against other options (esp. when shared), therefore, higher energy demand and congestion (Axhausen, 2017) (↑ SN1 & SN3) – Empty rides between pick-up and drop-off resulting in further growth in energy demand and congestion (Wadud et al., 2016) (↑ SN1 & SN3) – Longer commutes being accepted as a result of higher convenience of autonomous transport, therefore, urban sprawl and further traffic and energy demand increase (Sperling, 2018) (↑ SN1 & SN3)
Shared (S)	– Reduced specific energy consumption through higher vehicle utilization (higher trips per vehicle and passengers per trip) (Firnkorn and Müller, 2015) (↓ SN1) – Reduced congestion and space utilization due to fewer vehicles on the road (Firnkorn and Müller, 2015) (↓ SN3)	– Higher demand for road-based transport due to improved cost competitiveness of shared mobility over e.g. transit, therefore more traffic and higher energy intensity (Axhausen, 2017; Sperling, 2018) (↑ SN1 & SN3)
Electric (E)	– Lower energy intensity due to higher efficiency of electric propulsion versus combustion engine technology (Pelletier et al., 2016) (↓ SN1) – Zero emissions possible if fueled entirely with renewable electricity (Pelletier et al., 2016) (↓ SN1)	– Uncoordinated vehicle charging may over-strain the electric grid and/or require substantial infrastructure investment (Valogianni et al., 2019) (↑SN1)

Note: ↓ = alleviates/improves; ↑ = aggravates/worsens; SN1 = Climate Impact; SN2 = Health & Safety Impact; SN3 = Economic Impact

1.3 The IS Perspective on Smart Sustainable Mobility: A Framework

As highlighted by Yoo et al. (2010), the digitization of services, such as mobility, gives rise to a *layered modular architecture* in which an information-based digital layer exists on top of the traditional physical layer. This *layered modular architecture* (Yoo et al., 2010) is the key assumption underlying our mental model of CASE-based future mobility as illustrated in Figure 1.2. Here, the traditional physical layer ("network and device layer" as per Yoo et al.

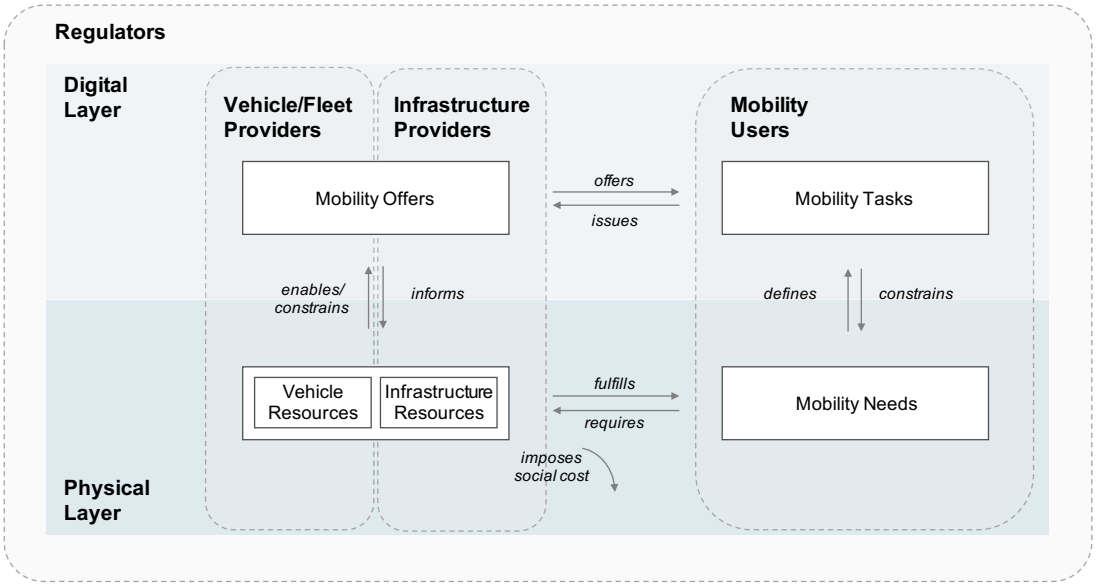

Figure 1.2: Framework for an IS-enabled Smart Sustainable Mobility System.

(2010)) consists of mobility resources (i.e., vehicles), physical infrastructures (roads, parking spots, charging points, the electricity grid, communication networks) and user mobility needs. An information-based instance of this ecosystem resides in the digital layer. The digital layer relies on real-time status information from its underlying physical layer as well as on information exchange with it ("service and content layer" as per Yoo et al. (2010)). The latter is facilitated via ubiquitous sensing and communication technology inherent to connected (C) mobility.

In Figure 1.2, we have also superimposed the stakeholders active in different areas of both physical and digital layers. Mobility Regulators are responsible for establishing a Smart Sustainable Mobility regulatory framework that facilitates and incentivizes system-beneficial and sustainable consumption of mobility, while providing guidance on system architecture, privacy, ethical questions and other aspects of societal relevance. A second stakeholder class is comprised of vehicle/fleet operators or providers (taxi drivers, fleet operators, public transport companies, logistics providers, etc.) who provide Mobility Offers to meet demand originating from a third class of actors, the Mobility Users (private users, online retailers, etc.). In addition, Infrastructure Operators are responsible for supplying and maintaining the right amount of Smart

Sustainable Mobility Infrastructure Resources (e.g., EV charging poles, smart parking lots, road infrastructure, electricity grid capacity, etc.) such that physical Mobility Tasks can be executed to effectively meet Mobility Needs. Finally, Mobility Users express their Mobility Needs in the form of digital-layer Mobility Tasks that can be matched with corresponding Mobility Offers as published digitally by Vehicle Operators.

Figure 1.2 emphasizes the reliance of Smart Sustainable Mobility on a digital and a physical layer. Despite its similarities with digital or cyber-physical systems such as cloud computing and IoT-based production or supply chain systems (e.g., gas pipelines), Smart Sustainable Mobility has distinct characteristics that require unique IS-driven solution approaches. Differences include (1) the considerably higher Sustainable Development Goals (SDG) implications, expanding beyond environmental to health and social/economic (traffic and electricity disruptions, accidents, etc); (2) the much more diverse and combinatorial nature of (physical) resources that is inherent to mobility and leads to (3) a much higher degree of coordination complexity. Digital or cyber-physical systems do not have the same necessity for matching demand and supply in real time. The storage capabilities in such cyber-physical systems (e.g., gas storage) differentiate such systems from Smart Sustainable Mobility systems. In addition, while cyber-physical systems such as gas pipelines, have equally severe mission critical implications (see for example the Colonial Pipeline Cyberattack[6]), Smart Sustainable Mobility failures can result in major interruptions of service level, delays in transportation of goods (including vital items) and health hazards from increased risk of accidents. Finally, (4) the Smart Sustainable Mobility domain is set apart by the larger and more diverse stakeholder landscape in mobility that requires high decision autonomy due to complex preference structures and high dimensionality of the decision spaces. Table 1.2 further details the unique differentiators of Smart Sustainable Mobility and provides examples.

Our layered modular framework accounts for these key differentiators of Smart Sustainable Mobility versus digital and cyber-physical systems. To illustrate this point it may be instructive to consider a concrete example of the user experience in an IS-enabled and digitalized mobility system. Imagine a user who wishes to travel from her current location in the suburbs to a destination in the city center (Mobility Need). Since she does not own a vehicle she issues a Mobility Task; e.g., via an app-based interface provided to her by the mobility platform operator ("service and content layer"). She receives various Mobility Offers with varying characteristics (mode, route, travel time, price, departure time, etc.) that all match her Mobility Task. The app interface indicates that she could save a considerable portion of her trip cost if she opts for an off-peak time slot or a high-occupancy vehicle option. Since she is not in a rush, she opts for a shared bike located just around the corner (i.e., a Vehicle Resource) to cycle to the nearest subway station where she boards a subway train headed toward the city center. Upon her arrival, she selects an e-scooter at the subway exit that has been reserved for her and

[6] https://www.reuters.com/business/colonial-pipeline-ceo-tells-senate-cyber-defenses-were-compromised-ahead-hack-2021-06-08/

Table 1.2: Key differentiators of Smart Sustainable Mobility against other cyber-physical systems

	Cloud Computing	Cyber-physical System	Smart Sustainable Mobility	Core SSM differentiators
Societal Importance				
SDG implications	low	high	high	Besides environmental (CO_2 and pollution) and health (accidents) implications, SSM has also social/economic (access, congestion cost, etc.) implications.
System criticality	mild	severe	severe	Physical implications are severe (physical harm, etc.)
Nature of Resources				
Number of Resource Types	single	single	diverse	Resources are much more diverse, including road space, vehicles, vehicle space, grid capacity, etc.
Divisibility	almost continuous	almost continuous	discrete divisibility	Resources have discrete divisibility (such as journey increments, vehicle space, etc.), as opposed to almost continuous divisibility of cloud jobs or gas and other natural resources.
Combinatorics	individual	individual	combinatorial	Mobility resources are combinatorial with critical paths between different connecting modes/road segments, etc.
Storability	large-scale	large-scale	small-scale	Lack of large-scale storage opportunities (e.g., of mobility demand, electricity) in SSM requires real-time matching of demand/supply
Complexity of Coordination				
Dimensionality	temporal	spatio-tenporal	spatio-tenporal	Decision on when and where to provide mobility service.
Time Horizon	close to real-time	close to real-time	continuous/ real-time	Requirement for online coordination of mobility requests due to lack of storage.
Constraints	few	few	many	Multiple physical resource constraints (e.g., vehicle/road capacity, etc.) and individual preference constraints (time of departure/arrival, mode choice, price, CO2 emissions, etc.), as opposed to mainly capacity constraints.
Stakeholder Interface				
User Preference Structure	relatively homogeneous	relatively homogeneous	highly heterogeneous	Highly diverse mix of use cases (commuting, delivery, leisure trips, etc.) and segments (goods mobility, personal mobility) with heterogeneous preference sets.
Preference Learning	explicit	explicit	largely implicit	High dimensionality of decision space (mode, route, departure, etc.) may require extrapolation and implicit elicitation.
Decision Autonomy	low	medium	high	High automation of real-time choices required due to complexity (e.g., dynamic re-routing, automated pre-booking of connecting modes, etc.).

completes the last leg of her journey ("network and device layer"). On her return journey, she opts for a more convenient and slightly faster travel mode by selecting a pooled electric vehicle, which picks her up from her city location and drops her off at home (having picked up and dropped off other passengers along the way). Her experience is seamless, uninterrupted and highly predictable. She experiences only minimal wait time and no congestion. Note that this is just one illustration of Smart Sustainable Mobility. Our framework generalizes beyond the area of urban road transport and comprises all forms of mobility resources including, for example, air travel or shipping. This is also a direct result of the CASE technology themes transcending into these sub-domains.

Facilitation of such a seamless Smart Sustainable Mobility experience is the purpose of the digital layer. Such facilitation requires the management of a large portfolio of heterogeneous CASE Vehicle Resources (such as shared bikes, demand-responsive transit or ride hailing vehicles to name a few), owned and operated by different platform participants as well as demand for these resources from heterogeneous sectors (e.g., personal mobility or goods mobility). It also requires the management of Infrastructure Resource constraints such as road space, electric grid capacity or available parking spots. The digital layer enables this management, allowing for real-time preference elicitation, predictive analytics, and automated planning and control in time and space. The heterogeneity of actors in our proposed framework is another characteristic of layered modular architectures (Yoo et al., 2010). Indeed, one can already observe in practice the first platforms that exhibit certain aspects of such a *layered modular* ecosystem. Examples include Uber and BlaBlaCar (Sundararajan, 2016), which provide platforms for peer-to-peer ride hailing and ride sharing respectively. Our proposed framework exceeds the somewhat narrow scope of these existing mobility platforms. We define a Smart Sustainable Mobility System as an ecosystem that consolidates and manages many different types of Vehicle Resources, Infrastructure Resources and system participants from diverse sectors, coordinating them against system-level objectives, and drawing on the layered modular architecture attributes (Yoo et al., 2010). In the following section, we further detail the individual components of this IS-enabled Smart Sustainable Mobility System.

1.3.1 Physical Layer

The dimensions of the physical layer are presented in the bottom half of Figure 1.2. We distinguish two types of resources: (1) distributed Vehicle Resources, which can be any vehicle type that affords mobility services to the user population and (2) distributed Infrastructure Resources, which comprises the physical environment in which vehicles operate. These resources are consumed when fulfilling distributed Mobility Needs, such as personal travel, goods mobility or even energy services via the battery storage of an electric vehicle. We use the attribute *distributed* to indicate variability across both a temporal as well as a spatial dimension. Specifically, Vehicle Resources are any connected, autonomous, shared and electrical (CASE) mobility mode

that can provide a mobility or transportation service to users. Our framework allows for the fact that some Vehicle Resources may exhibit only a selection of the four CASE attributes. For instance, micro-mobility options such as shared bikes or e-scooters might not have autonomous capabilities. We do, however, find that some form of *connectedness* and real-time information exchange between physical Vehicle Resources and the digital layer must be guaranteed. Our framework allows for ownership of Vehicle Resources by different stakeholders, including private owners or large-scale professional fleet operators. Infrastructure Resources are any type of infrastructure required to fulfill Mobility Needs via Vehicle Resources. Examples include road segments, parking spots, charging stations or electricity grid capacity. We explicitly also consider the environment as a type of infrastructure resource that is being consumed as part of a mobility service (e.g., by emitting CO_2 emissions). Ownership of Infrastructure Resources may be diverse. For example, non-professional private owners of single charging points or parking spots may coexist with large scale network and infrastructure operators.

1.3.2 Digital Layer

An information-based representation of Vehicle Resources, Infrastructure Resources and Mobility Needs resides in the digital layer of the smart mobility framework. Supply is represented as Mobility Offers that are enabled or constrained by the availability of physical Vehicle Resources (e.g. available units, remaining state of charge, etc.) as well as Infrastructure Resources (e.g. free-flow road capacity, number of charging spots, electricity grid capacity, emission limits, CO_2 targets), both of which must be considered when formulating Mobility Offers. Conversely, Mobility Offers can be used to plan, organize or reallocate Physical Resources. For example, a substantial presence of EV car-sharing providers in a region might require enhancements of the local charging infrastructure (downward arrow in Figure 1.2).

Mobility Tasks are defined by physical Mobility Needs (i.e., preferences). A user may request personal mobility, energy flexibility, logistics or other services in an on-demand fashion. These needs and preferences are encoded in Mobility Tasks in the digital layer. Operators and owners of mobility resources will be able to access these encoded requests and make (tailored) offers. Similarly, Mobility Tasks can incorporate information on the availability of resources and may have to be adapted to a scarcity in supply of these resources. This will necessarily involve some form of demand response on the user side such as (1) time shifting, (2) route shifting, (3) mode shifting or (4) foregoing the intended mobility request (e.g., by substituting with IS-enabled remote options such as online shopping or telework technologies). A matching of both sides is conducted in the digital layer. In addition, Mobility Tasks can affect and shape Mobility Needs. For example, while a user might have an intrinsic preference for a self-driving taxi, such a need and its associated Mobility Task might not (yet) be available (e.g., as a result of technology immaturity). Future technological innovation in Mobility Resources, Offers and Tasks that

include self-driving taxis will allow for such a need to be satisfied; hence, the Mobility Task constrains the Mobility Needs that can be fulfilled.

It is easy to see the requirement for data-driven information systems in this exchange both in terms of preference elicitation and modeling on the supply and demand side as well as in terms of real-time matching of preferences at the interface of offers and tasks. As such, the digital layer serves as a coordination layer that enables matching between various mobility options and mobility demand under the given system capacity constraints such as fleet size, and battery-, road-, and electricity grid-capacity.

1.4 IS Research Opportunities (ROs) Toward Smart Sustainable Mobility

We have argued that Information Systems Research can be an instrumental facilitator of smart sustainable mobility. We now specify this role by formulating seven concrete IS research opportunities (ROs) for the IS community in this domain. These opportunities build on the capabilities of CASE technology and can be mapped onto the dimensions of our framework (see Figure 1.3). Each research opportunity, as well as our proposed framework, is applicable to all four CASE technology themes or combinations thereof, e.g., connected and electric without autonomy features. Naturally, the presence of all four CASE technological themes might increase the complexity of the required solutions.

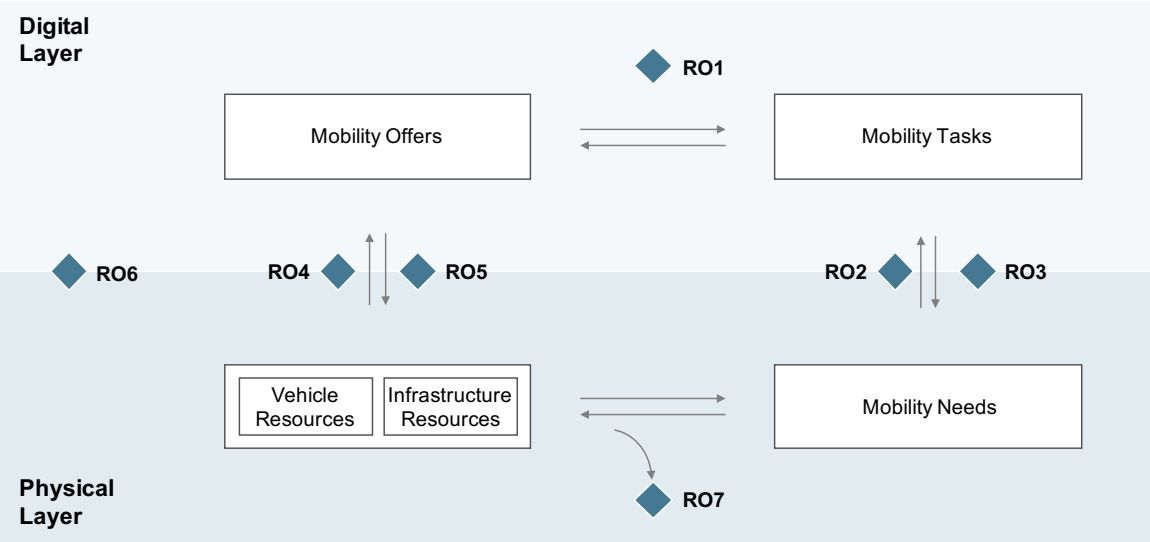

Figure 1.3: IS Research Opportunities (ROs) toward Smart Sustainable Mobility

Note: **RO1**: Designing Real-time Coordination Mechanisms for Smart Sustainable Mobility Environments; **RO2**: Learning and Automating Heterogeneous Smart Sustainable Mobility User Choice Structures; **RO3**: Developing Incentive Designs and Nudging Strategies for Smart Sustainable Mobility Demand Response; **RO4**: Designing & Evaluating AI-Powered Real-Time Decision Support for CASE Mobility Resource Planning and Operations; **RO5**: Developing and Evaluating Digitally-Enabled Smart Sustainable Mobility Business Models; **RO6**: Human-AI collaboration in Smart Sustainable Mobility Systems; **RO7**: Investigating Intended and Unintended Consequences of Smart Sustainable Mobility Interventions

Addressing the ROs will enable IS to directly contribute to making future mobility both smart and sustainable, thus resolving the three social negatives (negative climate, safety and economic impacts) of incumbent transportation systems. For example, RO1 (Designing Real-time Coordination Mechanisms for Smart Sustainable Mobility Environments) could alleviate environmental (SN1) and economic (SN3) negatives, while RO7 can evaluate the impact of new technologies and policies on all three social negatives, and so on.

1.4.1 RO1: Designing Real-time Coordination Mechanisms for Smart Sustainable Mobility Environments

At the heart of the Smart Sustainable Mobility challenge lies a resource allocation problem. Mobility users overutilize capacity-constrained resources such as road space, emission limits or parking contributing to the three social negatives of mobility (Cramton et al., 2018). Therefore, an important element in the digital layer of the smart mobility ecosystem is the efficient matching of resources with demand toward a certain objective. While traditional coordination literature typically optimizes for a narrow definition of social welfare that neglects many externalities, coordination in a Smart Sustainable Mobility system must go beyond individual social welfare objectives and focus on alleviating the social negatives SN1, SN2, leveraging the presence of one or more CASE technology themes.

Real-time matching of Mobility Tasks and Offers that also successfully serves to alleviate these social negatives is complex because of the high-dimensionality of the decision spaces (time horizons, modes of mobility, budget constraints, sustainability constraints, etc.). Additionally, the matching entity (e.g., platform) has to solve combinatorial allocations with dynamically evolving preferences and spaces. Traditional optimization approaches that exhibit the usual NP-hardness characteristics quickly become intractable in these high-dimensional combinatorial spaces. Therefore, heuristic AI-powered algorithms (such as Deep Learning) that derive near-optimal allocation decisions might prove powerful to address such challenges (Karaenke et al., 2019). In contrast to traditional real-time matching problems, system criticality is an additional factor to consider in Smart Sustainable Mobility domains. For example, in a Smart Sustainable Mobility system the social, environmental and financial costs of failures are immense. Because of the special nature of the Smart Sustainable Mobility system (see Table 1.2), the allocation and matching must happen in almost real-time so that customers have uninterrupted service (e.g., matching a request to a mobility or electricity service); therefore, solutions with low computational complexity are required. Challenges related to aligning dimensionality, combinatorics, and computational performance to achieve a practical coordination design can open new paths for future work.

Summarizing, we see tremendous research opportunities around **designing real-time coordination mechanisms for Smart Sustainable Mobility environments** that arise from the above-described challenges. Specific research questions that can guide IS research efforts here include: *What possible coordination approaches capable of fulfilling design guidelines (scalable, real-time, practical, alleviating SNs) exist and how do they compare?*; *Are there trade-offs between design guidelines, and if so how can they be managed?*; *How can the designed approaches be tested ex ante for robustness under close-to-real-world conditions?*; *How does mechanism design impact human/algorithmic behavior?*

The IS field has developed a rich portfolio of contributions in this regard that provide an excellent starting point. Auctions and other smart market-based coordination approaches (Bichler

et al., 2010) have been investigated in depth both from a mathematical and a behavioral point of view in application domains such as server capacity allocation (Bapna et al., 2008a), grid computing (Bhargava and Sundaresan, 2004), combinatorial auctions (Scheffel et al., 2011), and labor markets (Hong et al., 2016), as well as auctions specialized in electric mobility (Kahlen et al., 2018; Valogianni et al., 2019), shared mobility (Lam, 2016) or road pricing (Cramton et al., 2018). However, when designing comprehensive smart market mechanisms for a mobility ecosystem, where vehicles are connected, autonomous, shared and electric, one can appreciate that complexity increases. Each of the framework dimensions represent constraints and influence stakeholder objectives differently, making their management in a smart ecosystem far from trivial. As discussed, due to the complexities of the required coordination in a system with many agents (large-scale, combinatorial), alternatives to traditional analytical solutions may be needed. Testing and benchmarking of different design concepts in large-scale (agent-based) simulations may be fruitful to achieve a consensus on the preferred mechanism design. The Multi-Agent Transport Simulation (MATsim) (Horni et al., 2016) is an example of such a framework - one that could be leveraged for competitive benchmarking of design approaches (Ketter et al., 2016a). In addition, accounting for behavioral characteristics in such mechanisms is of paramount importance for the success of a mechanism. The latter is a unique competency of IS research, which has not only studied the mechanisms themselves but also behavioral attributes that affect behaviors within a mechanism's incentive framework (Cason et al., 2011; Kannan et al., 2019; Lu et al., 2019a,b, 2016b). Note that this established an important link to RO2 (see below), which deals with preference learning and automation in high-dimensional transportation domains. Building on this body of knowledge, IS researchers are uniquely positioned to drive forward, in an iterative fashion, the design of efficient matching instruments and mechanisms. The IS community has expertise both in terms of tools required to address this challenge effectively, and in terms of understanding the complexity posed by interdependencies between physical and digital layers in dynamic environments.

1.4.2 RO2: Learning and Automating Heterogeneous Smart Sustainable Mobility User Choice Structures

Bounded rationality (Simon, 1979), excessive transaction costs (Balduzzi and Lynch, 1999), and cognitive overload (Schwartz, 2016) can result in suboptimal individual decision making and subsequent welfare loss. In high-frequency, high-dimensional Smart Sustainable Mobility environments these issues are particularly relevant. Thus, to achieve the desired real-time coordination as envisioned in RO1, human preferences must be better understood and their decisions supported through IS/IT. Only then can the full potential for alleviating the SNs of mobility be leveraged. Practically speaking, understanding user preferences is key in the translation of physical Mobility Needs to digital Mobility Tasks (upward relationship in Figure 1.3). For example, learning customer preferences about autonomous ride-sharing in the center of a metropolitan

area helps the ride-sharing platform operator allocate the required resources and offer a seamless and uninterrupted service to customers (mitigating SN1, SN2 and possibly SN3). Preference learning is also crucial for identifying the impact of CASE technologies or Mobility Tasks on consumer behavior, i.e. for understanding how Mobility Tasks shape Mobility Needs (downward relationship in Figure 1.3).

Dynamic customer modeling and choice automation can provide these insights and tools. As such, RO2 is targeted at **learning and automating heterogeneous Smart Sustainable Mobility user choice structures** in a high-velocity, high-dimensional Smart Sustainable Mobility system. Specific questions to direct IS research in this area include: *How can multi-dimensional and high-frequency data be used to elicit implicit user preferences in high-dimensional Smart Sustainable Mobility environments?*; *How can consumer choice models be designed to be adaptive to dynamically evolving Smart Sustainable Mobility environments?*; *How should (semi- and/or adjustably-) automated IT artefacts be designed to act upon learned preferences on a user's behalf?*

IS research has longstanding experience in customer modeling and preference elicitation in domains such as B2B auctions (Bapna et al., 2008b; Lu et al., 2016b) online environments (McKinney et al., 2002; Yang et al., 2019), purchasing behavior (Bemmaor and Glady, 2012), online security (Yang and Padmanabhan, 2010), or electricty systems (Peters et al., 2018), among others. Research has looked at causal modeling of current and emerging consumer preference trends and predictive modeling and forecasting of future consumer preferences. Both are necessary for downstream decision support tools that help users navigate the complexities of the above-mentioned domains. Smart Sustainable Mobility environments, however, come with a few notable differences (see also Table 1.2): First, users can exhibit highly heterogeneous and dynamic preference sets depending, for example, on specific travel use cases and other (local) state variables (e.g., local vehicle supply, outside options, weather, etc.). Second, the choice space in mobility is exceedingly large in scale. Users can choose between different departure times, travel modes and routes. Finally, this large set of high-dimensional decisions continues to dynamically evolve as CASE technologies reach maturity and new vehicle types emerge. These novelty characteristics make new preference learning and choice automation approaches necessary.

Therefore, while previous choice modeling research experience may provide a strong basis, significant adaptations to Smart Sustainable Mobility are required. For example, large spatio-temporal datasets that can be used to analyze user patterns in a rapidly changing mobility and energy domain are increasingly abundant and include sensor data, electricity consumption data, mobile GPS traces and geo-tagged transaction data that provide a novel level of granularity of human offline behavioral patterns in the city and its transportation system (Zhang et al., 2020). Explanatory preference modeling powered by these large-scale datasets can uncover drivers of user preferences in unprecedented detail; however, as opposed to previous work, it now requires a combination of data mining and geo-spatial analytics techniques combined with econometric

and statistical analysis. As CASE technology proliferates dynamically, understanding the root cause of evolving consumer needs will be a fruitful avenue for IS research and can provide a basis for formulating utility functions required for choice automation. Second, scalable predictive models (Peters et al., 2018) that can dynamically and cost-effectively (Zheng and Padmanabhan, 2006) forecast mobility needs in the different CASE application fields are needed. For example, segmenting user clusters using unsupervised learning techniques and predicting user behaviour such as willingness to pay (Bapna et al., 2008c) and price elasticity (Cohen et al., 2016) is an important step in leveraging big mobility data. Predicting mobility needs or combined electricity and mobility needs, however, requires consideration of both temporal and geographic dimensions; this aspect generates significantly more complexity compared to other environments, such as e-commerce. For example, Schroer et al. (2022a) and Willing et al. (2017) draw on location analytics techniques to develop statistical mobility demand forecasting models that predict car sharing demand in time and space. Such dynamic spatio-temporal forecasting methods remain highly relevant as contextual contingencies of the mobility ecosystem evolve and play to our IS researchers' strengths in predictive analytics and (spatial) decision support systems (Keenan and Jankowski, 2019).

Accurate customer models are also required when assisting customers in making more efficient decisions by broadening the customer decision spectrum, minimizing information asymmetry barriers and managing bounded rationality issues. In a real-time data-driven world in which a large volume of operational decisions must be made, decision support tools such as recommender agents become necessary enablers of demand response (Adomavicius et al., 2009). IS researchers can capitalize on expertise in choice automation support using advanced machine learning, such as the algorithms implemented in recommender systems (Qiu and Benbasat, 2009; Adomavicius et al., 2013; Collins et al., 2009), marketing applications (Chica and Rand, 2017), smart business networks (Collins et al., 2010), etc.

While not deeply researched in mobility, demand automation is a common notion in the domain of electronic market-based systems such as electricity systems, where it has received some attention from IS research (Watson et al., 2010; Gottwalt et al., 2011; Peters et al., 2013). For example, Valogianni and Ketter (2016) propose a decision support system for consumers combined with a central demand response module that develops effective pricing strategies for different user groups. For applications in Smart Sustainable Mobility, which are subject to a variety of novel challenges and complications (see Table 1.2), new choice automation frameworks must be developed accordingly.

1.4.3 RO3: Developing Incentive Designs and Nudging Strategies for Smart Sustainable Mobility Demand Response

Apart from understanding high-dimensional, heterogeneous customer preferences (RO2) and matching them with available supply in an optimal manner (RO1), there may be a need to

more actively shape consumer demand by encouraging certain desired demand response in the user population. For example, in the event of increased demand for autonomous vehicles in the center of a metropolitan area, prices of alternative modes such as shared bikes could be dynamically discounted thus shifting demand to such outside options while mitigating SN1 and SN3. In general, demand response can take place in terms of (1) time-shifting[7], (2) route-shifting, (3) mode-shifting or (4) curtailing (Vickrey, 1969). Previous research has shown that strategic incentive design (Guda and Subramanian, 2019; Cohen et al., 2016) and non-financial contextual design choices (e.g., Tiefenbeck et al., 2018) can be effective in evoking desired behavioral patterns. The latter approach has commonly become known as nudging and subsumes diverse techniques such as reminders, personalized defaults, rankings, gamification, etc. (Thaler et al., 2013).

We argue that there is a large but under-researched potential for putting such techniques to use in the domain of mobility. Therefore, this research opportunity is directed at **developing effective incentive designs and nudging strategies for Smart Sustainable Mobility demand response**. Research questions that can guide efforts in this area include: *How should effective mobility demand response interventions be designed to steer user behavior in a system-beneficial manner (e.g., via time-,route- or mode-shifting)?*; *Are financial incentive schemes effective in eliciting user demand response in time and space, and if so, what are the boundary conditions?*; *Can traditional nudging techniques influence user behavior toward desired outcomes in high-dimensional spatio-temporal choice spaces like Smart Sustainable Mobility?*; *Which design criteria constitute successful nudging interventions in Smart Sustainable Mobility?*

In terms of examining financial incentive schemes, IS can draw on a wide body of research on revenue maximization and incentive design (Guda and Subramanian, 2019; Cohen et al., 2016). Some early empirical implementations (e.g. Uber surge pricing), although solely profit focused, are also available for empirical investigation. Research on data-driven dynamic tariff designs, by which an agent issues tariffs and observes the market response, are a novel and promising route as well. Near-optimal tariff designs are found by continuously updating tariffs while balancing the cost of exploration with the benefits from exploiting profitable tariffs, for example by using a reinforcement learning approach (Peters et al., 2013). Importantly, empirical investigation and demonstrations of these mechanisms are needed.

We also see research opportunities in non-financial demand response strategies that leverage behavioral nudges. While not yet well-researched in mobility (likely as the result of the above-mentioned challenges), experiences from the energy domain hint at the potential of such approaches. For example, Tiefenbeck et al. (2018) demonstrate that users can be nudged towards more energy conservation simply by removing salience bias through real-time feedback on their consumption behavior, while Costa and Kahn (2013) show that energy conservation nudge-effectiveness is heterogeneous and depends strongly on individual ideology. In a similar

[7] time-shifting can refer to both mobility and electric charging actions

vein, Adena and Huck (2020) explore the potential negative long-term effects of excessive nudging, e.g., by means of too-frequent reminders and asks. Nudging is also a promising research field in mobility and may further augment price-based strategies. Other non-financial incentives comprise the provision of viable alternatives to mobility. Examples include "telework" incentives or "global teams initiatives" that aim to reduce travel. All these require a deep understanding of IT capabilities and human mobility behavior in order to yield the desired outcomes without compromising goals such as productivity or well-being, to name a few.

A particular challenge of research on incentive schemes and nudging in smart mobility systems, as opposed to prior work, is the sheer size of the option space, which is a result of the non-binary nature of mobility choices (see Table 1.2). Users have flexibility both in space (route, mode) and time (departure, arrival). Any incentive or nudging structure should play to both dimensions to achieve the desired outcome of reducing SNs of mobility. For example, to avoid congestion, any pricing schemes should be differentiated both across regions and time periods to accurately reflect supply and demand (Cramton et al., 2018), while on-demand workers in ride hailing networks can also be incentivized via prices to relocate to certain high-demand regions at certain points in time (Guda and Subramanian, 2019; Bimpikis et al., 2019). In addition, highly heterogeneous and dynamic user utilities might make user-specific tailoring of incentives and nudges necessary. For example, travel during rush hour might be avoidable for some users but not for others. Theoretical and empirical research on such spatio-temporal financial and non-financial incentive schemes is highly promising and strongly aligned with IS research methods and tools. Note that (quasi-)experimental research designs must be carefully crafted to isolate the causal effect of certain incentives in these high-dimensional choice spaces. IS research expertise in experimental design and causal inference places our community at the center of addressing the challenges presented here.

1.4.4 RO4: Designing & Evaluating AI-Powered Real-Time Decision Support for CASE Mobility Resource Planning and Operations

As mobility systems become smarter, transportation information flows (supply and demand data, traffic flow data, price data, etc.) are increasingly abundant (see for example open mobility data standards such as the Mobility Data Specification (MDS)[8]). While this creates unprecedented transparency on the status of fleets, traffic flows, etc. it also results in the need to leverage these data streams for better strategic and operational decision making.

In short, as argued previously, digitalization of mobility affords better and real-time coordination and can help remedy the SNs of mobility. Yet, this comes at the cost of higher operational and strategic intricacies for managers of mobility service systems (Abbasi et al., 2016; Beverungen et al., 2019). Therefore, a clear research opportunity for IS research lies in **designing and evaluating AI-powered real-time decision support for CASE mobility**

[8] `https://github.com/openmobilityfoundation/mobility-data-specification`

resource planning and operations. The following exemplary research questions might guide IS research efforts in shaping the agenda here: *Which strategic and operational complexities arise for supply-side actors in Smart Sustainable Mobility environments?*; *How can IS support and automate these decision challenges?*; *What is the value of incorporating ever more abundant (real-time) data-feeds in the strategic and operational decision making process?*

On the strategic level, mobility asset investment decisions are conditioned on expectations of future technology adoption scenarios, changing consumer behavior, and the state of the system (supply, demand, prices) among other factors and are therefore subject to uncertainty. Decisions on how many vehicles to purchase, the level of vehicle autonomy and other capabilities, how many parking spots to create or how many charging points of which capacity to place where within a given region are dependent on expectations of future adoption rates, of the nature and dynamics of consumer behavior (which can often be endogenous to the investment decisions) and on assumptions of how these fleets and infrastructure resources will be managed. Standard optimization approaches quickly become intractable in such volatile, high-dimensional environments, with many interdependencies originating in the sheer size of the optimization problem (see Table 1.2). Large-scale data-driven simulation that uses heuristics to achieve near-optimal results has been shown to be highly successful in these cases (Valogianni et al., 2020). The unprecedented granularity and availability of data afforded by CASE technology enables a new, data-driven and simulation-based approach to vehicle and infrastructure provisioning to which IS can make significant contributions. Such simulation studies, especially agent-based simulation frameworks, also allow for joint evaluation against multiple objectives. This is important as Smart Sustainable Mobility involves trade-offs between firm-level objectives such as sustainability (i.e., the SNs of mobility) and profitability.

At the operational decision level, newly available data streams offer new scope for machine learning and optimization. The vast volumes of data being generated by all entities participating in the CASE-based Smart Sustainable Mobility ecosystem (customers, vehicles, smart infrastructure equipment such as traffic lights, vehicle charging points, etc.) enable advanced spatio-temporal predictions of near-term demand and supply of CASE resources such as vehicles, electricity required to charge the vehicles, price levels of different inputs, etc. IS researchers can address this research opportunity by capitalizing on deep expertise in predictive analytics (Shmueli and Koppius, 2011) in domains such as healthcare (Bardhan et al., 2015; Singh et al., 2018), cybersecurity (Abbasi et al., 2015), presidential elections (Barfar and Padmanabhan, 2017), detecting financial fraud (Abbasi et al., 2012), and forecasting economic regimes (Ketter et al., 2009), among others. Yet, the peculiarities of the Smart Sustainable Mobility sphere (see Table 1.2) lead to a number of specific challenges. Effective decision support systems will usually have a wider scope as they involve multiple uncertainties (e.g., demand and supply in time and space) for which prediction or stochastic algorithms must be devised. Exploring the influence of prediction errors and their interactions (in case of multiple prediction

models) is crucial. Additionally, operational decisions must be made at high frequency and/or with very different time horizons (e.g., weeks-ahead vs. real-time) which can create challenges.

1.4.5 RO5: Developing and Evaluating Digitally-Enabled Smart Sustainable Mobility Business Models

A Smart Sustainable Mobility transition will be successful or, indeed, possible if profitable business models can be conceived that spur private sector adoption and engagement while ensuring societal benefits related to alleviating the SNs of mobility. In this vein, a crucial research opportunity pertains to the creation of such **digitally-enabled Smart Sustainable Mobility business models** that build on the capabilities of CASE technology to create societal value (Osterwalder et al., 2005). Indeed, CASE technology may open up completely new application fields for vehicle resources and mobility, where the social negatives SN1, SN2, SN3 can be alleviated. For example, Vehicle Resources can now be used not only to transport people but also for goods delivery, electricity services and a myriad of further use-cases, many of which are yet to be discovered (in-vehicle commerce and services to name just one example).

Smart Sustainable Mobility business models are enabled through information systems that help manage the complexities associated with the real-time management of these (possibly) multi-purpose vehicle resources (Table 1.2). Specific research questions that may be useful in developing and evaluating different business model options include: *What are viable IS-enabled business models that build on the affordances of CASE mobility technology?*; *How can Smart Sustainable Mobility business models strike an effective balance between efficiency (utilization and profitability), sustainability and customer satisfaction?*; *How resilient and robust are such business models under different Smart Sustainable Mobility scenarios?*

IS research can, in close collaboration with practitioners, contribute to identifying, testing and evaluating these new business model options. Existing business model archetypes may have to be substantially adapted and/or combined to fit the Smart Sustainable Mobility paradigm due to several unique characteristics of this operating environment. First, the previously discussed multi-use characteristics of mobility assets that require ongoing trade-off analyses between the possible markets in which the asset can create value (personal mobility, goods mobility, etc.) may require operating multiple business models in parallel. Yet, if these trade-offs can be managed effectively, new levels of asset utilization, profitability and sustainability may be achieved. For example, a CASE vehicle may transport people during rush hour, perform last-mile parcel delivery in low-demand periods and provide energy services to the grid when connected to a charging station (Kahlen et al., 2018). Second, providing Smart Sustainable Mobility services will require heterogeneous inputs (electricity, parking space, road usage) many of which do and/or increasingly will exhibit high-frequency supply changes in time and space. Managing these inputs such that cost and sustainability targets are achieved is a major operational decision challenge for mobility providers. Finally, business objectives are increasingly multi-dimensional

and extend beyond profitability. This involves continuously trading-off potentially conflicting goals.

Taking an IS Design Science (Hevner and Gregor, 2013), empirical (Oestreicher-Singer and Zalmanson, 2013) or mixed methods approach (Fürstenau et al., 2019), and drawing on the extant literature in the fields of digital platforms and smart service systems (Beverungen et al., 2019), IS can enable the operations of increasingly more complex business models. Methodologically, such work may combine big data analytics, large-scale simulation and/or field tests. In many cases the prototyping of IS decision support tools that are needed for the operation of such data-driven and highly complex business models may be needed (see RO4). Some interesting early work has emerged along these lines. For example, Brandt and Dlugosch (2020) develop a two-stage data-driven framework for ex-ante assessment of operational policies of shared mobility providers. Finally, early examples that build on the capabilities of CASE and combine different business models are emerging. Specifically, Kahlen et al. (2018) present an EV fleet management concept that explicitly considers the trade-off between providing mobility and electricity services in a profit-maximizing manner. While promising, a lot of opportunity for future work exists that further develops existing business models and explores new business model instantiations in a continuously evolving Smart Sustainable Mobility ecosystem.

1.4.6 RO6: Human-AI collaboration in Smart Sustainable Mobility Systems

Smart sustainable mobility systems are operating and evolving with the help of the latest AI methods such as location-based analytics, object recognition using deep learning, dynamic price adjustments, intelligent agents for preference elicitation and decision support, to name a few. Thus, a major question arises: how to facilitate a successful collaboration between human users or decision makers and AI? This question is relevant for all digital-physical intersections, which is why we position RO6 as an overarching RO within our framework (see Figure 1.3)

Trust in AI-based systems in a Smart Sustainable Mobility environment is crucial, as a lack of or partial trust is not expected to enable the ecosystem to reach its full potential and satisfy objectives such alleviating the social negatives SN1, SN2, SN3. At the same time, AI-based systems adoption is challenging, since the domain is nascent, and many of the utilized AI-based applications might be seen as intrusive (e.g., the controversial issue of recording user location by Uber's algorithms[9]) or flawed (e.g., accidents caused by autonomous cars[10]). Literature has shown that when algorithms make mistakes, humans trust them less as opposed to humans who have made similar mistakes (Dietvorst et al., 2015). Especially with regard to autonomy, an active dialogue has been developed in the academic community about minimizing the flaws

[9] https://www.npr.org/sections/thetwo-way/2017/08/29/547113818/uber-ends-its-controversial-post-ride-tracking-of-users-location?t=1586959206306

[10] https://www.theguardian.com/commentisfree/2018/jul/15/crucial-flaw-of-self-driving-cars-always-need-human-involvement

of autonomous vehicles and the responsible entities in case of an accident[11]. In addition, users might be hesitant to adopt AI-based apps that record their preferences in order to offer optimized routing or electric-vehicle charging recommendations. Concerns such as intrusiveness, reliability, bias, or simply resistance to change might arise and require the expertise of IS researchers – who combine social sciences paradigms and technical expertise (Sarker et al., 2019) – to be addressed.

Specifically, Research Opportunity 6, which lies at the intersection of the physical and digital layer of the Smart Sustainable Mobility framework, is concerned with **investigating Human-AI collaboration in Smart Sustainable Mobility systems**. Examples of research questions are: *What design attributes increase human trust toward AI-based applications in Smart Sustainable Mobility systems?; How should privacy-preserving AI-based systems be designed so that they are not perceived as intrusive in Smart Sustainable Mobility platforms?*

IS researchers have already taken some important steps toward exploring human-AI interaction (Berente et al., 2019) and collaboration (Fügener et al., 2021; Breuker et al., 2016; Fügener et al., Forthcoming) in other domains; hence such expertise can be capitalized in Smart Sustainable Mobility environments. IS researchers have also developed expertise in developing AI-based systems (Zhu et al., 2021; Pfeiffer et al., 2020; Wang et al., 2018; Meyer et al., 2014; Sahoo et al., 2012), as well as managing such complex intelligent systems (Ahsen et al., 2019; Du et al., 2014; Chen et al., 2011). However, as opposed to other cyber-physical systems, Smart Sustainable Mobility environments exhibit unique characteristics that require new research contributions (see Table 1.2). Most importantly, the mission criticality of such systems necessitates human-AI collaboration robustness and trust that exceeds levels seen in other domains. Therefore, AI acceptance and human-AI collaboration need to be studied carefully in a Smart Sustainable Mobility context. Tools to achieve the thorough study of human-AI collaboration can be field experiments (similar to the one presented by Cherchi (2017)) or interventions using AI-based artifacts (e.g., Koroleva et al. (2014)).

1.4.7 RO7: Investigating Intended and Unintended Consequences of Smart Sustainable Mobility Interventions

Mobility is a public good and subject to regulation. We realize that the comprehensive transformation of a sector toward smart sustainability, such as is anticipated for the mobility sector, requires a strong foundation in public policy and underlying management approaches. The IS community has made deep contributions in the domains of energy and sustainability (Watson et al., 2010; Melville, 2010; Ketter et al., 2016a; Corbett and Mellouli, 2017), health (Bardhan et al., 2015; Singh et al., 2018) and other areas of high societal relevance. We believe that IS research can be a key facilitator of the Smart Sustainable Mobility transition, not only by developing required decision support tools or coordination mechanisms (as argued in RO 1 through 6), but also by informing policy discussions with hard, causal evidence obtained from rigorous

[11] `https://www.moralmachine.net`

empirical investigation. Therefore, we propose an additional RO that is concerned with **investigating intended and unintended consequences of Smart Sustainable Mobility interventions (as described in Table 1)**. Concrete research questions underlying this opportunity might include: *What are the system- and user-level impacts of new mobility technology, policy or IS artefact introduction?*; *Does a new technology/policy innovation alleviate or aggravate SNs of mobility and under which conditions?*; *What are the temporal and spatial dynamics of macro-level effects?*; and; *What are the implications of these ex-post empirical findings for shaping the ongoing Smart Sustainable Mobility transition with future technologies, policies and managerial approaches?*

Research on the societal impact of technology is deeply rooted in IS (Greenwood and Wattal, 2017a; Burtch et al., 2018; Babar and Burtch, 2020). Furthermore, the IS discipline's prowess in big data analytics for causal inference (Abbasi et al., 2016) – particularly within the economics of IS community – means that our discipline has all the necessary tools at its disposal to engage with this research opportunity. In the evaluation of the social cost of new mobility technologies, IS can contribute extensively by informing policy decisions that are targeted at mitigating unintended consequences of CASE technology (see Table 1.1), while actively promoting the desired effects. For example, Greenwood and Wattal (2017a) investigate the impact of ride hailing platforms on alcohol-related traffic deaths and demonstrate that a significant reduction in drunk driving-related fatalities was achieved. In a similar vein, Babar and Burtch (2020) investigate the heterogeneous effects of ride hailing platforms on public transport. They show that the degree of substitution or complementarity depends on a set of contextual factors and they formulate concrete policy recommendations showing how public transport authorities can benefit from ride hailing platform introduction. Pelechrinis et al. (2016a) find that the introduction of bike sharing platforms replaces some car traffic and thus alleviates traffic and parking pressure. While the above cited studies use highly aggregated data (e.g., monthly or quarterly), increasingly ubiquitous real-time geo-tagged datasets will enable ever more fine-grained empirical investigation. This will allow IS scholars to investigate societal implications of CASE technology (beyond the current IS focus on instantiations of the sharing economy such as ride hailing and ride sharing) in unprecedented detail and to provide considerably more targeted policy and managerial recommendations. There are several challenges endemic to the domain of Smart Sustainable Mobility that make causal analyses difficult. Real-world experimentation is difficult and possibly unethical in Smart Sustainable Mobility environments. Therefore, researchers will rely mostly on observational data sources. With highly granular spatio-temporal mobility data feeds, the detail at which causal inference can be credibly achieved is far superior to what is observed in traditional natural experiment-based causal inference literature. This insight provides opportunity for truly actionable managerial and policy advice beyond the macro-level insights. Yet, when modeling at such granular levels new challenges arise. For example, user utility (and choice) in mobility will heavily depend on local state conditions (e.g., supply of vehicles, weather) and trip

purpose (Table 1.2), which must be taken into account and controlled for. Additionally, effects such as spatial spillovers can make causal analysis challenging when working at low levels of aggregation.

1.5 Enabling IS Smart Sustainable Mobility Research

We now look at where the current state of IS research in Smart Sustainable Mobility research stands with regards to the previously developed Research Opportunities. We have argued that IS has been a relatively silent observer of the recent uptake in Smart Sustainable Mobility research. Here, we explore in more detail why this might be the case, focusing on possible barriers to entry that have thus far prevented wide-spread IS engagement with the field. For this purpose we performed an in-depth review of the IS Basket of 8 papers identified in the initial key-word-based cross-disciplinary survey of the literature (see Figure 1.1).

Several insights are to be highlighted. First and foremost, extant IS research in Smart Sustainable Mobility is limited. Out of the 65 initial papers, only 22 (34%) deal with Smart Sustainable Mobility topics at their core. Second, out of these remaining Smart Sustainable Mobility-related IS papers, most focus on just two out of the seven research objectives (ROs) we propose in this work: RO5 – Developing and Evaluating Digitally-Enabled Smart Sustainable Mobility Business Models and RO7 – Investigating Intended and Unintended Consequences of Smart Sustainable Mobility Interventions. The remainder (eight papers) are distributed more or less equally among the other five ROs. Third, there is a large methodological emphasis on empirical methods (specifically econometrics and interview-based qualitative case studies). Decision support systems for Smart Sustainable Mobility applications are rarely proposed, although we have identified such work as crucial in driving the mobility transition. Finally, the naturally data-intensive empirical research pieces included in our sample are primarily reliant on proprietary data sources with only 6 papers using public or synthetic data.

In sum, the review of current IS research confirms many of previously mentioned suspicions regarding the root causes underlying the IS discipline's relative lack of engagement in the Smart Sustainable Mobility field. These are nascency, complexity, interdisciplinary nature and resource/data intensity.

Nascency implies a lack of domain knowledge in the IS community, creating educational barriers to entry. Indeed, the (limited) extant IS research tends to focus on just two out of the seven ROs we put forward, indicating a lack of awareness of other research opportunities. This commentary is targeted at removing exactly this barrier.

Complexity and interdisciplinary nature suggests a need for methodological prowess in tackling Smart Sustainable Mobility research opportunities. We have argued extensively throughout this article that IS has all the prerequisites to thrive in these environments, as has been demonstrated in other complex domains such as healthcare and cyber-security. Yet, we also observe that extant Smart Sustainable Mobility work is mostly empirical in nature, meaning it is about understanding phenomena rather than providing data-driven and analytics-focused solution frameworks. There clearly is a lack of research on decision support systems that help practitioners navigate complexity in mobility. Again, we attribute this to the nascency and complexity of the field, as well as a possible lack of familiarity with design science and machine-

learning-driven methodologies. In this research commentary, we provide actionable ROs that can guide IS researchers with limited prior domain knowledge to leverage their extensive analytical skillset for meaningful contributions to Smart Sustainable Mobility. In addition, we find that extant Smart Sustainable Mobility research can be resource-intensive – particularly with regard to requiring access to large-scale real-world datasets. Indeed, as we point out above, most of the empirically-focused papers we have reviewed draw from proprietary data sources. In cases where public data is used, the data is not typically geo-tagged and relatively coarse, preventing micro-level analyses envisioned in this commentary. This creates a third adoption barrier for IS researchers. We believe, however, that granular mobility data is increasingly available. Four observations support this argument: (1) First, open standards that facilitate easier mobility data sharing at scale are becoming the norm. Examples of some of the most common standards include: General Bikeshare Feed Specification (GBFS[12]), General Transit Feed Specification (GTFS[13]) or the Mobility Data Specification (MDS[14]). Such standards are already used by many operators (often in combination with open APIs) and their use can even be mandated by local transport authorities as part of open mobility data initiatives (see e.g., LA). (2) Second, empirical evidence also confirms that there already are a number of mobility platform operators that readily share real-time mobility data streams through openly accessible APIs[15]. These sources are available to researchers even today. (3) Third, there are also third-party market research companies[16] that provide real-time data streams including history of most major shared mobility platforms - even those for which open APIs cannot be readily found/queried. While these datasets are not publicly available (yet), they nonetheless provide a viable source of data. (4) Finally, in case real-world data cannot be obtained, large-scale open-source simulation platforms are available that provide realistic synthetic transportation environments and are widely used in the transportation literature (e.g., Horni et al., 2016).

[12] `https://github.com/NABSA/gbfs`

[13] `https://developers.google.com/transit/gtfs/reference/`

[14] `https://github.com/openmobilityfoundation/mobility-data-specification`

[15] As an illustrative example, the following GitHub repository provides a (non-exhaustive) list of (openly accessible) mobility sharing platform APIs including instructions on how to query them `https://github.com/ubahnverleih/WoBike`

[16] e.g., fluctuo (`https://fluctuo.com`) or remix (`https://www.remix.com/solutions/shared-mobility`)

1.6 Navigating this Thesis

Throughout this introductory Chapter, I (and my co-authors) have made the case for IS research to actively shape the future of mobility toward an information-driven Smart Sustainable Mobility ecosystem. I have based this argument on advances in vehicle technology (connected, autonomous, shared and electric (CASE) mobility), which not only provide access to an unprecedented breadth of digital information but also enable real-time analysis and management of the mobility system. I argue that an active management of physical vehicle resources, infrastructure resources and mobility needs is required to promote the positive climate, health & safety and economic effects of CASE mobility, while mitigating unintended consequences of this technology (see Table 1.1). Given the unique characteristics of the envisioned next generation transportation system that clearly set it apart from other cyber-physical systems, a new research agenda is needed to which the IS community can make significant contributions. By laying out a vision for an IS-enabled smart mobility system, I have proposed a framework which can help structure this agenda (see Figures 1.2 and 1.3). I have also proposed seven concrete IS Research Opportunities along this framework for which I discussed promising IS research questions, approaches and methodologies. Despite a previously limited involvement in Smart Sustainable Mobility research, the IS community has all the necessary tools at its disposal to play a pivotal role in the knowledge creation necessary to address the presented research opportunities and pave the way for a successful transition toward a smart and sustainable transportation sector. It is my hope that this work may spur interest to contribute to this exciting agenda and to seize a unique opportunity to positively impact our environment, our economy and our societal welfare at large.

This Doctoral Thesis attempts to contribute to this research journey. In each of the following Chapters, I focus on one or two out of the seven distinct Research Opportunities laid out in this Introductory Chapter. Each Chapter defines and develops an independent research project around important Smart Sustainable Mobility issues associated with the respective Research Opportunity. A mapping of individual Chapters to Research Opportunities is provided in Table 1.3. At a broader level, this Thesis contributes to Smart Sustainable Mobility both in terms of (1) sense-making and (2) decision-making support. Chapter 2 seeks to infer and quantify causal effects of new mobility technologies and policies (i.e., a sense making effort). Chapters 3 and 4 develop mathematical decision algorithms for planning and operating Smart Sustainable Mobility systems against environmental, cost, service level, and other objectives (i.e., a decision support/enablement effort). A brief summary per each remaining Chapter is provided below.

Chapter 2 demonstrates how geo-tagged Internet of Things (IoT) data can be used for tracing out both macro-level and localized causal effects of large-scale policy interventions in the physical world. Drawing on a case from the bikesharing sector, I study the effect that the market entry of electric kick scooters (e-scooter) platforms, a less effortful and

Table 1.3: Chapter Overview and Interface with proposed Framework for an IS-enabled Smart Sustainable Mobility System

Chapter	Title	Research Opportunity (RO)						
		#1	#2	#3	#4	#5	#6	#7
Chapter 1	Information Systems Research for Smart Sustainable Mobility: A Framework and Call for Action	✓	✓	✓	✓	✓	✓	✓
Chapter 2	Identifying Localized Causal Effects from Large-Scale IoT Data Streams: The Case of e-Scooter Introduction and Micromobility							✓
Chapter 3	Data-Driven Competitor-Aware Positioning in On-Demand Vehicle Rental Networks				✓			
Chapter 4	Solving Large-Scale Service System Design Problems with Digital Twins: An Application to Electric Vehicle Charging Hubs		✓		✓			

Note: **RO1**: Designing Real-time Coordination Mechanisms for Smart Sustainable Mobility Environments; **RO2**: Learning and Automating Heterogeneous Smart Sustainable Mobility User Choice Structures; **RO3**: Developing Incentive Designs and Nudging Strategies for Smart Sustainable Mobility Demand Response; **RO4**: Designing & Evaluating AI-Powered Real-Time Decision Support for CASE Mobility Resource Planning and Operations; **RO5**: Developing and Evaluating Digitally-Enabled Smart Sustainable Mobility Business Models; **RO6**: Human-AI collaboration in Smart Sustainable Mobility Systems; **RO7**: Investigating Intended and Unintended Consequences of Smart Sustainable Mobility Interventions

convenience-focused genre of micromobility, has had on the sector. Underlying the analyses is a unique dataset gathered from real-time sensor data streams of shared bicycles. Using state-of-the-art difference-in-differences estimators, I estimate a drop in bicycle trip demand of 22.4% following e-scooter introduction. This breaks down to an annual societal impact of 307M less calories burned by micromobility users, additional emissions of up to 385t of CO^2-equivalent and roughly EUR 1.44M lost revenue across the cities in scope. Policy makers can leverage these results for ex-ante impact assessment of e-scooter entry. I also run a set of localized causal analyses that explore temporal and spatial patterns of substitution, thus fully exploiting the richness of the sensor data. I show that substitution occurs primarily during rush hours in central locations that are in close proximity to transport infrastructure. Substitution is also limited to short point-to-point trips. Platform managers can tailor highly targeted marketing and operational strategies based on

these insights. In sum, by leveraging big urban data for the empirical analysis of transport interventions, this Chapter contributes to Research Opportunity #7.

Chapter 3 studies a novel operational problem that considers vehicle positioning in free-floating on-demand rental networks such as carsharing in the wider context of a competitive market in which users select vehicles based on access. The proposed competitor-aware model combines online machine learning to predict market-level demand and supply with dynamic mixed integer non-linear programming (MINLP) that periodically determine optimal repositioning schedules with the objective of maximizing fleet profit. In extensive simulation experiments based on real-world data from Car2Go and DriveNow the model outperforms conventional models that consider the fleet in isolation by a factor of 2 in terms of profit improvements. The research, thus, addresses Research Opportunity #4 by proposing AI-powered decision support form CASE mobility providers. Specifically, operators of on-demand rental networks can use the developed approach to build a profitable competitive advantage by optimizing access for consumers (i.e., service level) without the need for fleet expansion.

Chapter 4 explores how data-driven Digital Twins (DTs) can be used in multi-stage stochastic design problems. Traditional operations management (OM) decision frameworks such as mathematical optimization rely on analytical solutions and are subject to computational challenges (e.g., NP-hardness). As a result, such frameworks require size reduction and simplification to achieve tractability. DTs, in combination with high-performance search or learning methods, can circumvent these shortcomings. DTs use high-resolution sensor data to achieve realistic and granular digital representations of a system's physical components and processes. The concept is increasingly used for decision problems at an operational level. We propose a general three-stage framework that provides guidance on the use of DTs in earlier stages of a system's life cycle: the design phase. For evaluation purposes we select the application domain of Electric Vehicle (EV) Charging Hubs (EVCHs). We use sensor-derived data including parking, charging, electricity consumption and solar generation data along with microscopic simulations of operational policies to build a realistic representation of the EVCH. Next, using efficient reinforcement learning methods (deep Q-learning), we learn optimal EVCH configurations against a minimum cost objective with service level constraints. In extensive benchmark and sensitivity experiments we demonstrate four core benefits of DT-based service system design versus traditional optimization-based methods: (1) superior planning outcomes due to data-driven approach that captures stochasticity and detail, (2) close-to arbitrary computational scalability, (3) flexibility in system operational scope, and (4) ability to seamlessly carry over the DT into subsequent life cycle phases. Chapter 4 covers aspects of preference learning and AI-powered decision support, thus contributing to Research Opportunities #2 and #4.

1.7 Declaration of Contributions

I (the author) am grateful to a number of co-authors and collaborators who have contributed to varying degrees to the individual research projects (Chapters) presented in this cumulative Doctoral Dissertation (the Thesis). I briefly lay out my own contributions across these research projects and provide details on how my co-authors have contributed to their success.

Chapter 1: The author of this Thesis is the main author of this Chapter and has completed the majority of the work. This includes the conceptualization of the Smart Sustainable Mobility research framework, the development and definition of the Research Objectives and the storylining and write-up of the final manuscript, which is forthcoming at Information Systems Research[17]. Throughout the writing process, the author has benefited significantly from frequent feedback and contributions from two academic advisors: Prof. Konstantina Valogianni and Prof. Wolfgang Ketter. The Chapter in its current form would not have been possible without their contribution, which is gratefully acknowledged.

Chapter 2 The author of this Thesis is the sole author of this Chapter[18]. Prof. Wolfgang Ketter acted as academic advisor and kindly provided feedback and guidance throughout the writing and revision process.

Chapter 3: The author of this Thesis is the main author of this Chapter and has completed the majority of the work. This includes all tasks related to conceptualization, algorithmic modeling, analysis, positioning and write-up of the final paper. He is also the first author of the published journal version of this Chapter[19]. The work has benefited from feedback by Prof. Alok Gupta, Prof. Thomas Y. Lee and Prof. Wolfgang Ketter throughout the writing and revision process. The author would also like to express gratitude for the contribution by Dr. Micha Kahlen who provided the carsharing dataset along with helpful advice during the writing and revision process.

[17] Here you will find a shortened and slightly adapted rendition of this forthcoming journal publication. Apart from several editorial adaptations, an additional Section (1.6) was added to explicitly link the Chapters presented in this cumulative Dissertation and demonstrate their fit with the presented framework of IS Research for Smart Sustainable Mobility.

[18] A precursor study using a similar dataset co-authored with M. Pohl and W. Ketter (Schroer, K., Pohl, M., & Ketter, W. (2020). To Substitute or to Supplement? - Investigating the Heterogeneous Effects of Electric Scooter Platform Introduction on Micromobility. In ICIS 2020 Proceedings. 9) provided inspiration. The author was also the first and main author in this project. The presented Chapter is a completely new paper with a considerably extended experimental sample, fully revamped econometric methodology, novel positioning and new findings and contributions.

[19] This Chapter has been published in its entirety in the following peer-reviewed academic journal:
Schroer, K., Ketter, W., Lee, T. Y., Gupta, A., & Kahlen, M. (2022). Data-Driven Competitor-Aware Positioning in On-Demand Vehicle Rental Networks. Transportation Science, 56(1), 182–200. https://doi.org/10.1287/trsc.2021.1097

Chapter 4: This Chapter was co-authored with Ramin Ahadi. Both co-authors contributed equally in terms of conceptualization, algorithmic/simulation modeling, analysis, positioning and write-up. The work also benefited from frequent feedback kindly provided by Prof. Thomas Y. Lee and Prof. Wolfgang Ketter who both acted as academic advisors on this project.

Chapter 2

Identifying Localized Causal Effects from Large-Scale IoT Data: The Case of e-Scooter Introduction and Micromobility[1]

2.1 Introduction

High-resolution digital trace data such as purchase histories, click stream data, social media connections, online community interactions, and other data types have become widely available. This is particularly true for online settings, where behavioral big data (Shmueli, 2017) has inspired scholars to investigate causal effects of digital interventions both in controlled settings (via experiments) and under quasi-experimental conditions (Abbasi et al., 2016). While large-scale experimentation in the offline world often remains impractical, unethical or prohibitively expensive, measuring human offline behavior at high frequency and granularity is increasingly possible (Zhang et al., 2020). With the emergence of ubiquitous and connected sensing technologies (often referred to as IoT[2] devices), such as smart phones and other connected sensors (e.g., cameras), high-resolution spatio-temporal data streams on human behavior in the offline world are now available to managers and policy makers alike. These data streams offer an opportu-

[1]This Chapter is currently under review at a leading peer-reviewed academic journal.
A precursor study provided inspiration for this work. This precursor study has appeared in the following (non-copyrighted) peer-reviewed academic conferences:
Schroer, K., Pohl, M., & Ketter, W. (2020). To Substitute or to Supplement? – Investigating the Heterogeneous Effects of Electric Scooter Platform Introduction on Micromobility (Full Paper). In ICIS 2020 Proceedings.
Schroer, K. & Ketter, W. (2020). An Empirical Analysis Of The Heterogenous Effects Of Electric Scooter Platform Introduction On Micromobility (Abstract). Informs Annual Meeting 2020
The presented Chapter is a completely new and improved paper with a considerably extended experimental sample, fully revamped econometric methodology, new analyses, novel positioning and new findings and contributions.

[2]Internet of Things

nity for much more fine-grained causal investigations of offline phenomena than is currently the norm. Yet, extant empirical studies of offline interventions in Information Systems, (e.g., Babar and Burtch, 2020; Greenwood and Wattal, 2017b; Burtch et al., 2018), economics (e.g., Cengiz et al., 2019) and other disciplines often leverage highly aggregated datasets (at monthly or even yearly resolution) limiting the level of achievable insight.

In this work, we explore how large-scale geo-tagged sensor-generated data streams can be fully exploited for both aggregate and localized causal analysis of large-scale natural (i.e., non-experimental) interventions in the physical world. To do so, we draw on a recent natural experiment from the transportation domain that has received significant attention in the popular discourse: the swift entry of electric kick scooter (e-scooter) platforms into traditionally bike-based micromobility markets. Micromobility, short-distance and low-speed transportation by means of bikes, electric bikes, e-scooters and similar technologies has been widely hailed as a key component of modern urban transport systems (Shaheen, 2019; Sperling, 2018). Owing in large part to the emergence of digital sharing business models, app-enabled micromobility platforms have become popular. Traditionally, the shared micromobility sector has relied heavily on bicycle sharing schemes. Indeed, bikesharing is often considered a highly successful sharing economy intervention from a social welfare standpoint. It is regarded as a healthy (Xu, 2019; Dill, 2009) and environmentally-friendly (Fishman et al., 2014) transport alternative and is commonly encouraged and subsidized by local municipalities (Pelechrinis et al., 2016b). Starting in late 2018, however, the bike-based micromobility markets experienced a fundamental disruption following the introduction of e-scooter platforms such as Lime and Bird. Originally a US-phenomenon, scooter sharing was introduced in key European cities in mid-2019. E-scooters have sparked extensive policy debate with some observers hailing their positive impacts on traffic, while others cite safety, environmental, public nuisance or health concerns (Shaheen, 2019). With bikes and e-scooters catering to largely similar transportation use cases in terms of speed and range there is a real concern that demand for incumbent bikesharing platforms may have been cannibalized by the introduction of the socially less desirable e-scooter option. To this date, there is a lack of sound empirical analysis to support or refute these claims. Apart from the clear societal implications that arise from this intervention, there are also important managerial and operational aspects to be explored. For example, the question arises of how e-scooter entry affects user rental behavior on the incumbent bike-based platform and how bikesharing operators best respond to the potential competitive threat posed by e-scooters? With Lime, the world's leading e-scooter operator, recently announcing its 100 millionth completed ride[3], e-scooters have become a relevant part of urban transport systems that warrant in-depth empirical investigation.

Our work holds several contributions. First, we contribute to the stream of societal impact of IS (e.g., Greenwood and Wattal, 2017b; Babar and Burtch, 2020; Burtch et al., 2018; Chan and Ghose, 2014) by evaluating and quantifying the (heterogeneous) impact of the introduction

[3] `https://www.li.me/second-street/lime-100-million-rides`

of an IS-enabled platform-based technology in the physical world. Second, we demonstrate the value of fine grained sensor data in achieving a much deeper understanding of the impact of offline interventions beyond aggregate effect estimates. Using high-frequency bicycle position data retrieved from an operator's API[4] over a period of approx. one year we identify both macro-level societal effects (health impacts, climate impact, economic impact), and achieve credible causal estimates of micro-level effects on user behavior shifts, including demand impact by location, time and trip type. Such analyses can reveal crucial effect nuances that hold actionable managerial implications. For example, our analyses pinpoint exactly which trip types are most affected by e-scooter introduction and by how much. This allows managers to tailor highly targeted marketing and operational strategies. Lastly, we offer several important insights that are of relevance to the transportation community. To the best of our knowledge this study is the first and only study of its kind to leverage a multi-city dataset to explore the impact of e-scooter introduction into micromobility systems.

The remainder of this work is structured as follows: We first provide a brief overview of related work. We then proceed with a specification of our difference-in-differences (DiD) identification strategy including a discussion of recent methodological innovations in this sphere. We then present and validate our results. Finally, we offer a brief conclusion and an outlook on future work.

[4] Application Programming Interface

2.2 Related Work

We draw on three core literatures to inform this research: (1) big data-driven policy evaluation, (2) societal impact of information systems (IS), especially digital platforms, and (3) consumer choice in (micro-) mobility. Here, we provide a short overview of these three streams.

2.2.1 IoT Trajectory Data for Policy Evaluation

Newly available IoT data streams, particularly geo-tagged position data that allow inference on movement trajectories have inspired empirical research in recent years. A major focus has been on the use of such large-scale data streams for the prediction of human behavior in time and space. Examples primarily stem from the computer science and transportation communities and include examples such as forecasting spatio-temporal demand of free-floating carsharing (e.g., Schroer et al., 2022b) or predicting the flow of bikes in a bikesharing system (e.g., Chai et al., 2018), among others.

But trajectory data is increasingly used beyond prediction (Athey, 2017b). In their seminal work González et al. (2008) use mobile phone data to trace out patterns in human mobility, showing that it follows much more regular characteristics than predicted by e.g., traditional random walk models. Zhang et al. (2020) use taxi trajectory data to fit analytical models that explain individual preferences and decision making processes of taxi drivers. Similarly, the transportation community has embraced trajectory data for discrete choice modeling in an effort to understand factors that influence mode choice behavior (e.g., Reck et al., 2022). Other authors have studied the value of trajectory data in improving ad targeting by developing and evaluating recommender systems that utilize IoT data in their decision making (e.g., Ghose et al., 2019a,b).

Recently, researchers have increasingly called for the use of IoT data in the causal evaluation of large-scale offline policy interventions (e.g., Athey, 2017b). The core argument being that IoT data streams provide transparency on offline phenomena that were not previously measurable (as opposed to online-only settings where data availability is generally high). For example, Persson et al. (2021) use mobile phone trajectory data to understand the impact of different social distancing policy measures implemented by governments to combat the spread of the COVID-19 pandemic.

In this work we use high-frequency vehicle position data to identify the causal impact of a large-scale natural experiment in the physical world, i.e., the introduction of e-scooters in several major cities. However, as opposed to previous work, we do not only focus on uncovering macro-level societal effects of the intervention (health impacts, climate impact, economic impact). We can also trace out and reliably quantify micro-level effects on the behavioral patterns of users. Such analyses can hold very important implications that extend beyond the policy focus to the operational level.

2.2.2 Societal Impact of IS

We also draw on another key body of literature: research on the societal impact of information systems, a thread deeply rooted in the IS research. It is primarily concerned with the investigation and evaluation of phenomena related to the adoption and impact of new digitally-enabled technologies and platforms. Shared mobility systems are an instantiation of such digital platforms (Tiwana et al., 2010; de Reuver et al., 2018). Previous related studies have explored the societal effects that single- and multi-sided platforms and matching markets have had on a myriad of domains, including the hotel industry (Zervas et al., 2017), housing market (Pelechrinis et al., 2017), durable goods purchases (Gong et al., 2017), sexually transmitted diseases (Chan and Ghose, 2014) and even female homicide rates (Cunningham et al., 2017). A shared view within this emergent discourse is that of a platform either replacing or supplementing incumbent markets, technologies or services (Babar and Burtch, 2020). This, in turn, may result in either positive or negative societal outcomes, depending on situation and domain. We adopt this shared assumption and analyze micromobility platforms through a "substitute vs. complement"-lens. The transportation sector in particular has provided ample scope for empirical studies. For example, Pelechrinis et al. (2017) find that the introduction of bikesharing platforms replaces some car traffic and thus alleviates traffic and parking pressure. Greenwood and Wattal (2017b) show that ride hailing platforms reduce drunk driving fatalities, while Babar and Burtch (2020) investigate the heterogeneous factors that determine whether ride hailing platforms substitute or supplement certain modes of public transport. Burtch et al. (2018) show that Uber entry has a negative impact on entrepreneurial activity, as potential entrepreneurs take up gig employment as Uber drivers instead. Our study ties in with this important body of research on the intended and unintended consequences of IS-enabled platform business models (Tiwana et al., 2010). To the best of our knowledge there is only a small number of empirical studies that deal with the corresponding societal impact of e-scooter introduction. Within this limited academic discourse, a core focus has been on the impact on the environment (Bakker, 2019) and on traffic accident statistics (Badeau et al., 2019). Any societal effects resulting from a replacement of incumbent platforms such as bikesharing have so far been neglected. Indeed, the case of e-scooter platform introduction is unique in the sense that a competing bike-based platform offering objectively similar services is already present. This allows us to investigate how platforms compete with each other and whether new and convenience-focused platform offerings are always desirable.

2.2.3 Consumer Choice in (Micro-)mobility

Previous research has identified a range of important determinants in the choice process that users undergo when selecting between different mobility options. Within the domain of micromobility, a majority of consumer choice research is based on traditional bikesharing systems. Various studies observe a switch from many other incumbent transportation modes to bikesharing following its introduction (Fishman et al., 2014). For example, Campbell and Brakewood

(2017) consider the impact of bikesharing on bus transit and identify a significant decrease in bus ridership. Fishman et al. (2014) and Pelechrinis et al. (2017) uncover a significant reduction in car usage as a result of bikesharing introduction. The research community's understanding of the impact of e-scooter introduction on urban transport systems is considerably less developed and conclusive. Caspi et al. (2020) find that scooters are mostly used in inner city locations and not primarily for commuting, while Bai and Jiao (2020) find usage peaks in the afternoons and on weekends in some cities and stable usage throughout the week in others. A limited number of studies have looked at differences in usage patterns between shared bikes and e-scooters. McKenzie (2019) finds that bikes and e-scooters are not necessarily used in the same way, with bike usage reflecting utilitarian commuting behaviour and scooter use less so. Barnes (2019) on the other hand compare substitution patterns of shared bikes and e-scooters on other modes in San Francisco and find similar patterns for both modes suggesting a likely cannibalization effect of e-scooters on bikes. In support of this, a recent survey among users in Portland concluded that bike usage declined by 5% following e-scooter introduction (Shaheen, 2019). Similarly, Yang et al. (2021) estimate an overall reduction of 10% in demand for shared bike trips following e-scooter introduction in Chicago[5].

Generally, adoption of and choice between (micro-)mobility services depends on a three types of contextual factors (Babar and Burtch, 2020): system-, population- and environment-specific factors. System-specific contextual factors comprise key characteristics related to the scope and quality of a mobility system. Younes et al. (2020) find that free-floating schemes, in which users can commence and complete one-way trips anywhere within a geo-fenced service area, typically enjoy a higher adoption rate compared to station-based sharing schemes. Another key determinant of the quality of service of a mobility system is the notion of coverage and access (Braverman et al., 2019; Benjaafar and Hu, 2020b). In a shared mobility context, access is primarily influenced by the number of vehicles and stations available within a region as well as by how well individual vehicles and stations are distributed geographically (Braverman et al., 2019; Schroer et al., 2022b). Population-specific contextual factors capture important information on the underlying user population in a given market. Indeed, socio-economic characteristics such as population size, income, age or unemployment are often incorporated into empirical demand models in transportation (Greenwood and Wattal, 2017b). Finally, environment-specific contextual factors, have been found to be important for the consumer's choice process. Most commonly, these comprise weather-related factors. Previous research has established that inclement weather such as extreme cold or precipitation can result in rescheduling and cancelling of trips (An et al., 2019). This is especially true for travel modes that are heavily exposed to the elements such as bikes and e-scooters.

[5]Due to the fact that their dataset stems from a single city only (Chicago), the authors had to rely on matching regions inside and outside the e-scooter platform's service area to construct counterfactuals. This raises serious concerns related to selection bias and spatial spillover effects between treated and untreated regions, among others.

As e-scooter platforms continue to expand, further research is needed to deepen our understanding of the technology's impact on urban transportation systems and to clear up inconclusive findings on consumer choice in micromobility (McKenzie, 2019).

2.3 Methodology

2.3.1 Empirical Setting

Our identification strategy exploits the natural experiment of staggered e-scooter introduction into selected (European) markets following the legalization of e-scooters on public roads in mid-2019. While the first e-scooter platforms started to appear in some US cities by mid-2018, scootersharing remained illegal in many Western European markets for another year. Following regulatory approval in mid-2019, e-scooter sharing companies began entering cities throughout Europe. Certain local municipalities, however, upheld a city-wide bans on e-scooters. This constitutes a large-scale natural experiment, in which experimental units (i.e., city-period pairs) have been naturally pre-allocated to a treatment group (e-scooters) and a control group (no e-scooters). This setting is well-suited for the causal estimation of treatment effects via a DiD approach.

As proxy for the traditionally bike-focused micromobility sector, we select Nextbike, Europe's largest operator of bikesharing platforms (Nextbike, 2022). The company is active globally but has a clear focus on Central Europe, in particular Germany, Austria and Switzerland (DACH region), which makes it an ideal candidate for our study. We limit our experimental sample to cities in the DACH region where Nextbike was active over the whole observation period and that have a significantly sized traditional micromobility sector as indicated by a large Nextbike presence. An overview of the resulting experimental sample of 35 cities (18 eventually treated and 17 never treated cities) is presented in Table 2.1.

2.3.2 Data & Sample Construction

To operationalize the DiD specification, we construct a unique dataset combining transaction-level bikesharing data with socio-economic and environmental controls at the city-period or city-period-subgroup level (our units of analyses).

We collect geo-tagged transaction data via Nextbike's public API[6] over close to a full year from January 21, 2019 until January 12, 2020. This provides ample pre- and post-treatment observational panel data and captures daily, weekly and yearly seasonality in transportation demand. We queried the API in 1-minute intervals. Each API query returns the exact coordinates of all currently available vehicles per each city. Individual vehicles are identifiable via a static unique ID. Tracking individual bike IDs appearing and reappearing in our queries allows us to infer the current size of the fleet, individual trips, their start and end positions as well as their duration[7]. In line with Fishman et al. (2014) we only include trips of reasonable length in our analysis, that is, trips which have a duration of at least 2 minutes[8]. We also limit our sample to trips with total duration of below 24 hours, which is the maximum allowable rental time on

[6] `https://api.nextbike.net/maps/nextbike-live.json`
[7] We provide further detail on the imputation of trip level data from position queries in Appendix.
[8] Shorter rentals are usually attributable to technical errors such as lock malfunctions

Table 2.1: Experimental sample of cities $i \in \mathcal{I}$

City	Scooter Entry	City	Scooter Entry
Augsburg (DE)	5-Jul-19	Koeln (DE)	21-Jun-19
Berlin (DE)	15-Jun-19	Leipzig (DE)	-
Bochum (DE)	11-Sep-19	Lippstadt (DE)	-
Bonn (DE)	22-Jun-19	Ludwigshafen (DE)	01-Aug-19
Dortmund (DE)	8-Jul-19	Luzern (CH)	-
Dresden (DE)	25-Jul-19	Mannheim (DE)	1-Aug-19
Duisburg (DE)	-	Marburg (DE)	-
Erfurt (DE)	5-Jul-19	Moenchengladbach (DE)	16-Oct-19
Essen (DE)	22-Aug-19	Muelheim (DE)	-
Frankfurt (DE)	22-Jun-19	Norderstedt	-
Giessen (DE)	-	Offenburg (DE)	-
Hamm (DE)	-	Potsdam (DE)	21-Jun-19
Heidelberg (DE)	3-Aug-19	Ruesselsheim (DE)	-
Innsbruck (AT)	1-Jun-19	St.Poelten (AT)	-
Kaiserslautern (DE)	-	Walldorf (DE)	-
Karlsruhe (DE)	20-Sep-19	Worms (DE)	-
Kassel (DE)	-	Wuerzburg	-
Klagenfurt (AT)	13-Jun-19		

Note: We focus our investigation on Central European (DACH region) cities, where netxbike has a relevant presence (i.e., ≥7,500 bike trips annually) and is present for the entire observation period. We also limit our sample to cities where our data feed is uninterrupted. Scooter Entry describes the exact date of the first scooter platform entry. These data are retrieved from operators' press releases as well as local media reports (see Table 2.19 in Appendix).

Nextbike's platform. Trips that started outside the designated service area or city boundaries are excluded from the analysis. Finally, our data feed experienced full or partial outages for five consecutive days spanning the period March, 15 through March 19, 2019. We exclude the weeks containing these days from our dataset[9].

This leaves us with a raw sample of 7,642,223 individual bikesharing trips across all cities and periods in scope. From this raw data we construct custom datasets by aggregating across city-day or city-day-subgroup, depending on the level of analysis. At the city-day level, the resulting dataset comprises $12,005$ observations. We supplement this dataset with contextual control variables collected from a variety of official channels, primarily country- and city-specific statistical offices (see Table 2.13 for an overview of variables and their data sources).

[9]We exclude the full weeks and not just the individual days to avoid issues stemming from unbalanced week samples in later event studies

Treatment Indicator

The process of e-scooter entry into the European cities contained in our experimental group was rapid and comprehensive. As is commonly observed with platform business models, all entrants followed an aggressive growth strategy by rapidly scaling fleet size in the respective entry city. It follows that scooter sharing companies can be seen as serious and relevant contenders in the micromobility sector from day one after entry. Therefore, we define the date of the first e-scooter platform entry as the start of the intervention. This is consistent with the approach taken by other authors (e.g. Babar and Burtch, 2020; Greenwood and Wattal, 2017b; Burtch et al., 2018) who consider the entry of the first platform operator as the most important and the only relevant treatment identifier. The entry dates per platform and city were retrieved from local media publications and/or the providers' social media feeds.

Dependent Variables

Our main dependent variable (DV) is $Trips_{i,t}$, the absolute trip count of shared bicycle trips in city i and day t. To address normality concerns and ease interpretation of coefficient estimates, we take the natural logarithm of the DV (i.e., $\ln(Trips_{i,t})$). In supplementary localized analyses we also explore the impact of e-scooter introduction by granular bins (or groups) g, thus adding an additional dimension to the model and the DV (i.e., $\ln(Trips_{i,g,t})$).

Figure 2.1 plots $\ln(Trips_{i,t})$ for the control and treatment groups over the full observation period in scope. An early visual inspection of this plot reveals first hints at a parallel pre-treatment trend followed by what looks like a drop in utilization in the treatment group as more and more cities experience scooter introduction (increasing overlap in the confidence intervals).

Subgroups for Localized Analyses

As mentioned, the geo-tagged bicycle sensor data we have available allows us to run in-depth localized analyses on the dynamics of temporal, spatial and other trip characteristics – a level of detail which is not typically attained in causal inference of offline phenomena. There are several advantages to performing these localized analyses. First and foremost, we make full use of the granularity of the data, thus illustrating our argument that large-scale IoT data streams offer potential for causal analysis at an unprecedented detail. Second, we localize the origin of the aggregate effect within the distribution in scope. For example, temporal and spatial patterns of substitution can be readily explored and temporal bins (e.g., $MorningRush$) and spatial areas (e.g., $CityCenter$) that are most (or least) responsible for the observed aggregate effect identified. Finally there are important methodological advantages to decomposing the aggregate treatment effect on the DV by relevant bins (Cengiz et al., 2019). In situations, where only a small number of bins is susceptible to the treatment, aggregate analyses may fail to detect any treatment effects at the full population level. Therefore, we construct different panels that

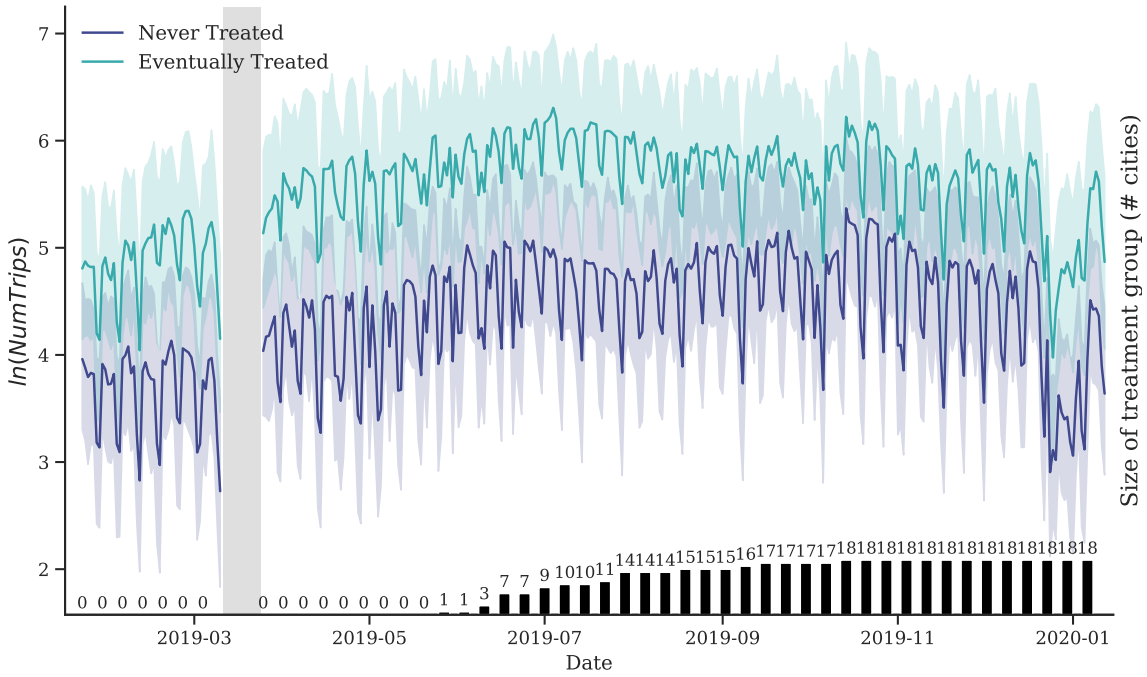

Figure 2.1: Plot of $ln(NumTrips)$ and cumulative number of treated cities over the observation period.

Note: Treatment group is defined as cities that experience scooter platform introduction over the course of the study period. The significant drop in fleet utilization at the end of December coincides with the Christmas holiday. Shaded area (in March) indicates period of missing data that was caused by an API outage. The affected days were subsequently dropped from the dataset.

correspond to key spatio-temporal trip characteristics with the goal in mind to extract the typical trip type that is most/least prone to substitution. We analyze three core trip attributes, which – taken together – provide strong indications for the purpose of a trip: (1) trip timing, (2) spatial characteristics (of trip origin/destination) and (3) trip quality (duration, net distance covered). Per each dimension in scope, we construct a custom set of meaningful bins (or groups). For (1) trip timing, we construct sets of groups (G) that jointly capture weekly and daily seasonality ($G^{\mathcal{T}} = \{WeekdayNight, MorningRush, ..., BarHours, WeekendNight\}$) (Cohen et al., 2016) (see Appendix for details).

Regarding (2) spatial characteristics, we define two additional sets of groups. First, we look at relative distance of trip origins from the city center. For this purpose we compute a $DistanceFromCenter$ metric per each trip in our dataset using the commonly used haversine distance measure. We then normalize these distances at the city level and compute seven quantiles over the normalized range corresponding to seven concentric rings of increasing relative distance to the city center ($G^{\mathcal{D}} = \{CityCenter, ..., Outskirts\}$). The second spatial grouping we conduct is by land use, specifically by most prevalent Points of Interest (POI) class at the trip origin ($G^{POI} = \{ArtsAndCulture, BarsAndRestaurants, ..., Transport\}$) (see Table 2.17 in Appendix). For this purpose, we compute POI densities per each trip location using kernel density estimation (KDE)[10]. We normalize POI densities per class at the city level, then assign each trip to the POI class with highest relative density. Additional details are provided in Appendix.

In terms of (3) trip quality, we construct bins based on trip data from the the pre-treatment period (to avoid endogeneity concerns). We compute 11 bins of relative $TripDuration$, a measure of the duration (in minutes) per each trip, and 11 relative bins of $NetDistancePerHour$, a ratio of the net distance covered to duration, which represents a measure for whether the trip was a round trip or not. Net trip distance is inferred from the origin and destination locations and the shortest path across the (cyclable) road network that connects them[11].

Control Variables

Contextual factors with a simultaneous temporal and regional dimension (as indicated by subscript i,t) are included as dynamic controls $C_{i,t}$ where appropriate as they are not captured by city or day fixed effects (FEs). Specifically, we control for the effect of system-, population- and environment-specific factors.

We capture effects of system-specific contextual factors via two dynamic covariates. A key factor is bike supply as capture by $\ln(NumBikes_{i,t})$ (i.e., the number of active bike in city i on

[10]For each city we first discretize the geographic area using equally spaced hexagonal regions of approx. 200m diameter and count the number of POI instances per each class within each region. We then fit dedicated KDEs per each hexagon center and POI class using a kernel density estimator (KDE) with an Epanechnikov kernel for efficiency. For each trip, the absolute spatial density is retrieved using the fitted KDEs.

[11]We use a road network graph as available in Open Street Maps for shortest path inference

days t), which can be readily expected to influence trip demand (Benjaafar and Hu, 2020b). In addition, the density of the service system as captured by covariate $\ln(NumStations_{i,t})$ (i.e, the number of active bikesharing stations in city i on day t), is likely to co-determine absolute demand. The dynamic population-specific contextual factors we include are $\ln(OvernightStays_{i,t})$ and $\ln(Unemployment_{i,t})$. Anecdotal evidence suggests that tourists may be a highly active adopters of shared mobility, which we control for by including monthly visits. In addition, $Unemployment_{i,t}$ and correspondingly lower income has previously been suggested to drive shared consumption, which is why we control for monthly variations in employment levels. Finally, we control for dynamic environment-specific contextual factors, particularly weather, which we capture by means of the three dummy variables: $RainyPeriod_{i,t}$ (period with precipitation), $HotPeriod_{i,t}$ (period with temperature above 25 °C) and $ColdPeriod_{i,t}$ (period with temperature below 0 °C)).

2.3.3 Difference-in-Differences (DiD) Identification Strategy

The potential outcomes approach postulates that average differences in outcome between a treatment and a control group can be interpreted as the causal effect of the respective treatment, given certain assumptions such as stable unit treatment value (SUTVA) and unconfoundedness are met (Imbens and Rubin, 2015). The most relevant of these assumptions in a group-level observational study like ours, in which treatment is naturally assigned (and unlikely to be fully random[12]), is unconfoundedness. DiD designs manage the threat of confounding by leveraging the longitudinal dimension of the underlying panel data which allows for causal treatment effect estimation via a comparison in trend between treated and untreated units (Athey, 2017a). In our setting, the staggered and regionally selective nature of scooter entry across the sample in scope allows us to use untreated city-period pairs as counterfactuals for treated units under certain assumptions. The target parameter to be estimated by the DiD estimator is the Average Treatment Effect on the Treated (ATT), which is formalized as $ATT = \mathbb{E}[Y_{i,t=post}(1) - Y_{i,t=post}(0)|D_i = 1]$, where $Y_{i,t=post}(1)$ is the outcome of unit i if it is treated in period $post$, $Y_{i,t=post}(0)$ is the outcome had unit i not been treated in period $t = post$ and D_i is a binary indicator of treatment group affiliation. Naturally, $Y_{i,t=post}(0)$ is never actually observed for the treated group. However, given parallel trends of outcomes in treated and untreated units[13] and no anticipation[14], ATT can be identified by taking the difference between the differences in outcomes of treated and untreated units, i.e. $ATT = \mathbb{E}[Y_{i,post}(1) - Y_{i,pre}(1)|D_i = 1] - \mathbb{E}[Y_{i,post}(0) - Y_{pre}(0)|D_i = 0]$. Both expectations in individual outcome differences can be readily observed, thus enabling identification.

[12] Scooter platform operators can be reasonably expected to select/prioritize markets based on factors such as overall market size, income, transport system characteristics or general weather conditions

[13] This can be formalized as $\mathbb{E}[Y_{i,t=post}(0) - Y_{i,t=pre}(0)|D_i = 1] = \mathbb{E}[Y_{i,t=post}(0) - Y_{i,t=pre}(0)|D_i = 0]$, i.e., the trend in outcome in absence of treatment is the same in the eventually treated (D_i=1) and the never treated (D_i=0) cohort

[14] This can be formalized as $Y_{i,t=pre}(0) = Y_{i,t=pre}(1) \ \forall \ i$ with $D_i = 1$

Recent methodological innovations in the difference-in-differences (DiD) literature make recalibration of previously tried and tested identification strategies (i.e., two-way-fixed-effects (TWFE) regression) necessary. We briefly discuss the core implications for our setting, i.e., a setting with staggered, binary and absorbing[15] treatment.

It has been shown that a traditional TWFE estimator is unsuitable in situations where treatment adoption is staggered[16] and treatment effects are heterogeneous across groups and time (e.g., Borusyak et al., 2021; Callaway and Sant'Anna, 2020; de Chaisemartin and D'Haultfœuille, 2020; Goodman-Bacon, 2021). Treatment effect heterogeneity, i.e., differences in treatment effect depending on when and where a treatment is administered, are realistic concerns in most empirical settings. The root cause of TWFE bias in these situations lies in the so-called "forbidden comparison" inherent to TWFE DiD estimators. It has previously been assumed that TWFEs would recover a weighted mean of treatment effects across all treatment periods. Instead, research has shown that a TWFE ATT can be decomposed to weighted averages of all possible 2x2 DiD comparisons of already treated, not-yet-treated and never-treated units (Goodman-Bacon, 2021). The forbidden comparisons are those between two already treated units and can result in negative weights being assigned to some individual ATT estimates (non-convex combination of regression weights). de Chaisemartin and D'Haultfœuille (2020) show that, in extreme cases, TWFE ATT estimates and the true treatment effect may be of opposite signs. Robust alternative estimators have since been developed. These can broadly be categorized into (1) weighted group-time ATT estimators (e.g., Callaway and Sant'Anna, 2020; Sun and Abraham, 2021), (2) stacking individual-level ATTs by normalizing calendar time into relative event time (e.g., Baker et al., 2022; Cengiz et al., 2019) and (3) imputation methods (e.g., Borusyak et al., 2021).

For the purpose of this work, we select the robust stacking estimator described in Baker et al. (2022) (and applied in Cengiz et al. (2019)) as our main DiD estimator, although, for benchmarking purposes, we also present estimation results obtained via weighted group-time estimation (Callaway et al., 2021), imputation DiD strategies (Borusyak et al., 2021) and non-robust traditional TWFE. Stacked DiD estimation avoids the "forbidden comparison" by running individual TWFE models per each treatment event using only the respective treated and all untreated units as comparison group. This results in a then non-staggered design per subsample (i.e., the stack). A key step in the estimation procedure is the preparation of a new, larger dataset that appends all individual stacks with the treatment centered around a common datum. Note that as a result of this process, untreated units will appear multiple times in the combined dataset, a fact which is controlled for by including stack-city specific FEs (Baker et al., 2022). Note also that, much like traditional TWFE, this approach can be applied for both a static 2x2 DiD regression and a dynamic event study specification. Our choice for the stacked DiD estimator is motivated by its close relation to the traditional TWFE DiD model that most readers will be accustomed with and the relative ease with which aggregate ATT estimates can

[15] i.e., units can switch in but not out of treatment

[16] Units enter treated status at different points in time during the observation window T

be computed from the individual stacked estimates. An additional advantage is the ability to readily incorporate control variables in each of the TWFE-based stacks[17]. The core model is a static stacked DiD model of the following form:

$$\ln(NumTrips_{i,t}) = \alpha_{i,s} + \lambda_{t,s} + \delta C_{i,t} + \beta D_{i,t} + \varepsilon_{i,t} \tag{2.1}$$

Treatment is identified by means of binary indicator $D_{i,t}$, which takes a value of 1 if e-scooters are present in city i and time period t, and 0 otherwise. $C_{i,t}$ subsumes several time-varying controls. Note, that for benchmark purposes, we also estimate models without time-varying controls, thus hedging against recently identified possible issues with such control strategies in DiD frameworks (Sant'Anna and Zhao, 2020). $\varepsilon_{i,t}$ is the error term. Note that the city FEs ($\alpha_{i,s}$) and time FEs ($\lambda_{t,s}$) are interacted with each stack s, i.e. they identify which data stack the observation originates from.

We supplement this analysis with an event-study to trace out temporal heterogeneity over time. We limit our investigation to the interval $\mathcal{W}$ = [-12,24] weeks, meaning we investigate 3 months of pre-trends and 6 months of post-trends. For each stack, all data prior or after this period is dropped. This avoids bias from grouping multiple periods into a single relative time bin[18]. The event-time model extends equation 2.1 as follows:

$$\ln(NumTrips_{i,t}) = \alpha_{i,s} + \lambda_{t,s} + \delta C_{i,t} + \sum_{\tau \in \mathcal{W}} \beta_\tau D^\tau_{i,t} + \varepsilon_{i,t} \tag{2.2}$$

Here $D^\tau_{i,t}$ is a binary treatment indicator that is set to one if city i experienced e-scooter introduction τ weeks from day t[19].

For localized effect estimations that trace out the distribution of the treatment's effect across a set of pre-defined temporal or spatial groups $g \in G$, we specify a third group-level model of the following form:

$$\ln(NumTrips_{i,g,t}) = \alpha_{i,g,s} + \lambda_{g,t,s} + \delta C_{i,t} + \sum_{\gamma \in G} \beta_\gamma D^\gamma_{i,g,t} + \varepsilon_{i,g,t} \tag{2.3}$$

Note that this model utilizes an extended dataset which consists of dedicated panel data per group $g \in G$ (hence the added dimension g as identified in the subscript). $\alpha_{i,g,s}$ and $\lambda_{g,t,s}$ are the group-by-city and group-by-period fixed effects (both interacted with the stack s).

[17] Note that it has recently been shown that the inclusion of additional time variant controls only produces credible estimates under several additional assumptions, such as parallel trends in covariates (Sant'Anna and Zhao, 2020). To hedge against this risk, it is recommended that a model without time-varying controls be estimated as a benchmark (Baker et al., 2022). We adopt this recommendation in this work.

[18] Note, that although common practice, such a grouping assumes effect homogeneity in all periods contained in a grouped time bin, which is why we abstain from grouping.

[19] Note that our data comes at daily resolution, yet we measure relative time in weeks, a choice made to achieve a manageable number of pre- and post-treatment periods.

2.4 Results

2.4.1 Main Effects on Bike Demand

We first focus on the main effects of e-scooter introduction on traditional micromobility fleet utilization by reporting the results of static (Eq. 2.1) and event-study (Eq. 2.2) estimates of total population ATTs. The core unit of analysis is the city-day and the DV is $ln(NumTrips_{i,t})$. All reported standard errors (SEs) are clustered by city, the level at which treatment is applied.

Static Model

In Table 2.2 we present the static ATT estimates. Due to the log-transformation of the dependent variables, coefficient estimates of log-transformed covariates can be approximately interpreted as elasticities, while coefficients of untransformed covariates can be interpreted as percentage-changes on the outcome. Since the Baker et al. (2022) estimator readily accommodates additional dynamic controls $C_{i,t}$, we estimate the models in various extended setups with different sets of controls.

Our results indicate that the introduction of e-scooters into a micromobility market results in a statistically highly significant reduction in trip demand on the incumbent bikesharing platform. We estimate, that following e-scooter introduction, demand on incumbent bikesharing platforms decreased by -20% to -22% on average over the post-treatment observation period. We find that these results are robust to the inclusion of dynamic controls $C_{i,t}$ with both absolute coefficient estimates and significance levels remaining largely consistent and in the range of -20% to -22%.

We also find that most of the dynamic controls we include in our model exhibit significant effects on the DV, thus confirming previous insights from the transportation literature that motivated their inclusion. In terms of fleet-specific covariates ($\ln(NumBikes)$ and $\ln(NumStations)$), we find that, on average, more bikes and more stations result in more demand. Specifically, for a 1% increase in the number of bikes or the number of stations, one can expect a 0.8% and 0.7% increase in demand, respectively. This is in line with our expectations (Benjaafar and Hu, 2020b). In terms of dynamic population-specific factors, we find that higher unemployment rates tend to drive demand (elasticity of 1.5). Tourist volumes (as capture by $\ln(OvernightStays)$), seem not to play a major role. Demand is lower on average during cold and inclement weather (-5% and -6%, respectively) and higher on hot days (+6%). Taken together, these estimates confirm that scooter introduction causes undesired substitution shifts within the incumbent user base of bikesharing platforms. Our results support the notion that some users who previously would have opted for a shared bike switch to the self-propelled and less effortful e-scooter option once it becomes available.

Table 2.2: Average treatment effect of *Scooter* on overall bikesharing platform trips ($\ln(NumTrips)$)

DV = $ln(NumTrips)$	(1)	(2)	(3)	(4)	(5)
Scooter	-0.198**	-0.216***	-0.216**	-0.197**	-0.224***
	(0.0936)	(0.0724)	(0.0999)	(0.0933)	(0.0782)
$\ln(NumBikes)$		0.835***			0.840***
		(0.0585)			(0.0568)
$\ln(NumStations)$		0.714***			0.644***
		(0.0637)			(0.0580)
$\ln(OvernightStays)$			0.0706		-0.0281
			(0.0558)		(0.0530)
$\ln(Unemployment)$			1.518***		1.102***
			(0.184)		(0.119)
ColdPeriod				-0.0355***	-0.0522***
				(0.00883)	(0.00943)
HotPeriod				0.0712***	0.0589***
				(0.0185)	(0.0147)
RainyPeriod				-0.0573***	-0.0564***
				(0.00737)	(0.00666)
Model	Baker et al.	Baker et al.	Baker et al.	Baker et al.	Baker et al.
N	93639	93639	93639	93639	93639
adj. R^2	0.887	0.897	0.889	0.887	0.898

Note: *p<0.1; **p<0.05; ***p<0.01. Robust standard errors clustered at city-level reported in parentheses. Estimates based on daily data using specification from Equation 2.1. Higher N for stacked DiD estimator (Baker et al., 2022) results from appending several treatment-centered subsets of the data

Event Study Model

These results are further underpinned by the event-study DiD estimates that trace out temporal variation in treatment effects. Table 2.3 tabulates the coefficient estimates of relative lead/lag variables from 3 months (12 weeks) prior to 6 months (24 weeks) after the intervention for a model without dynamic covariates (Column (1)) and a fully saturated model (Column (2)). A visual representation of coefficient trajectories along with a benchmark against other estimators is provided in Appendix (Figure 2.9). We first highlight that the pre-treatment time dummies oscillate around the zero mark and that none of them are statistically significant. This provides strong support for the parallel trend and no anticipation assumptions underlying our DiD identification strategy (Angrist and Pischker, 2008; Bertrand et al., 2004). Moreover treatment response is swift and sustained. Coefficient estimates turn negative as early as one week after treatment (i.e., relative week 1), depending on the model. Coefficient estimates remain negative over the entire post-treatment period and reach sustained significance levels around week 14 (Model (2)) or 19 (Model (1)).

These results suggest that e-scooter roll-out and adoption is swift and that the aggregate results (as seen in Table 2.6) are not purely attributable to novelty. In fact, the long-term effects of e-scooter introduction may be even higher than estimated in the static models, as the substitution effect seems to grow over time. For example, looking at the period from 3-6months after treatment, an average treatment effect of -0.303 can be observed[20].

[20]This is computed as an average over the twelve individual estimates $\frac{1}{12}\sum_{\tau\in[13,24]}\beta_\tau$

Table 2.3: Event study of effect of *Scooter* on overall bikesharing platform trips ($ln(NumTrips)$)

	(1)		(2)	
Relative Week	Est.	SE	Est.	SE
-12	0.064	0.093	0.083	0.079
-11	0.113	0.085	0.11	0.077
-10	0.116	0.102	0.12	0.087
-9	0.079	0.088	0.071	0.074
-8	0.044	0.100	0.051	0.081
-7	0.027	0.082	0.022	0.062
-6	0.014	0.087	0.002	0.070
-5	-0.018	0.067	-0.038	0.061
-4	-0.015	0.041	-0.043	0.042
-3	0.056	0.048	0.049	0.047
-2	-0.02	0.051	-0.033	0.051
-1	reference		reference	
0	-0.068	0.046	-0.054	0.047
1	-0.165**	0.070	-0.11	0.069
2	-0.123	0.103	-0.103	0.098
3	-0.064	0.120	-0.044	0.098
4	-0.083	0.130	-0.053	0.091
5	-0.15	0.112	-0.13*	0.077
6	-0.133	0.130	-0.1	0.082
7	-0.195	0.140	-0.144	0.093
8	-0.209	0.146	-0.158	0.102
9	-0.172	0.136	-0.172*	0.092
10	-0.131	0.154	-0.133	0.114
11	-0.114	0.151	-0.146	0.115
12	-0.173	0.154	-0.186	0.114
13	-0.254	0.173	-0.245*	0.129
14	-0.273	0.175	-0.28**	0.131
15	-0.228	0.169	-0.24*	0.125
16	-0.212	0.182	-0.226*	0.131
17	-0.278	0.174	-0.291**	0.125
18	-0.27*	0.161	-0.275**	0.121
19	-0.336**	0.159	-0.317***	0.115
20	-0.367**	0.151	-0.369***	0.097
21	-0.428***	0.150	-0.405***	0.109
22	-0.366***	0.141	-0.346***	0.105
23	-0.326**	0.145	-0.351***	0.109
24	-0.298*	0.161	-0.287**	0.115
Day FE	Yes		Yes	
City FE	Yes		Yes	
Controls $C_{i,t}$	No		Yes	
Model	Baker et al.		Baker et al.	
N	93639		93639	
adj R^2	0.887		0.898	

Note: *p<0.1; **p<0.05; ***p<0.01. Robust standard errors clustered at city-level reported in parentheses. Estimates are based on daily data. Higher N for stacked TWFE estimator results from stacking several subsets of the data each of which are centered around the treatment datum

2.4.2 Localized Analyses

We underpin our previous findings with several sets of deep-dive analyses at sub-group level. These analyses distinguish our work from previous empirical studies of offline behavior and demonstrate how granular IoT sensor data can be used beyond identification of aggregate policy effects. Such analyses are useful as they allow managers and policy makers to zoom into the effect dynamics and nuances, thus enabling significantly more targeted measures to extenuate or reinforce an effect, depending on business/policy objectives. We analyze three core trip attributes, which – taken together – provide indications as to the purpose of a trip: (1) trip timing, (2) trip origin and (3) trip quality.

Localized Temporal Effects

Trip timing is highly indicative of trip purpose – in fact it is often used as the sole identifier for inferring user intention (e.g., Cohen et al., 2016). In order to trace out both weekly (i.e., by day of week) and daily (i.e., by hour of day) effect seasonality, we construct custom temporal bins that capture interactions between both weekly and daily effects (see Table 2.16). The results are shown in Figure 2.2. The analysis suggests that the observed aggregate substitution

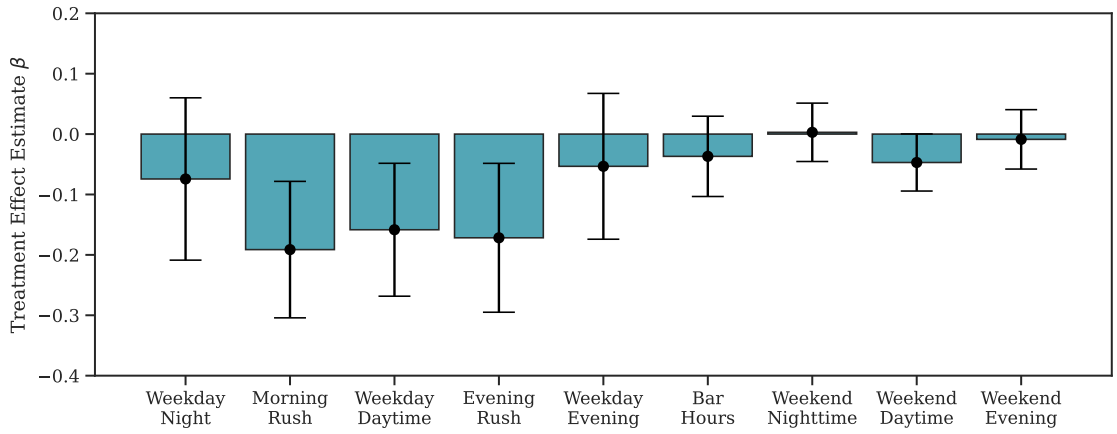

Figure 2.2: Localized Temporal Effects of *Scooter* on ln(*NumTrips*).

Note: DV = ln($NumTrips_{i,g,t}$). Estimates based on Baker et al.'s stacking method and Equation 2.3 (including dynamic controls $C_{i,t}$). Error bars represent the 95% confidence interval based on standard errors clustered at the city level.

effect is a weekday phenomenon only with highest substitution occurring during rush hours (*MorningRush* and *EveningRush*) followed by *WeekdayDaytime*. All three localized effects are significant at the p<0.01 threshold. Other periods are not significantly affected. This suggests that a sizeable portion of users who may have previously opted for a shared bike for commuting purposes (to work, to school or for other purposes) now select e-scooters instead, creating a significant substitution effect away from the incumbent and socially more desirable

bike-based platform. The analysis suggests that observed e-scooter trips outside these time periods are entirely new trips, in the sense that they do not replace bikesharing trips. Instead, they seem to be originate from user segment that have previously been untapped by incumbent bikesharing platforms.

Localized Spatial Effects

In addition, we look at spatial patterns in bike trip substitution. An important aspect to consider is where substitution primarily occurs. A first analysis therefore focuses on whether there is a difference in effect between central versus peripheral locations[21]. The results are shown in Figure 2.3. We find that substitution is limited to central locations only (*InnerRing* and

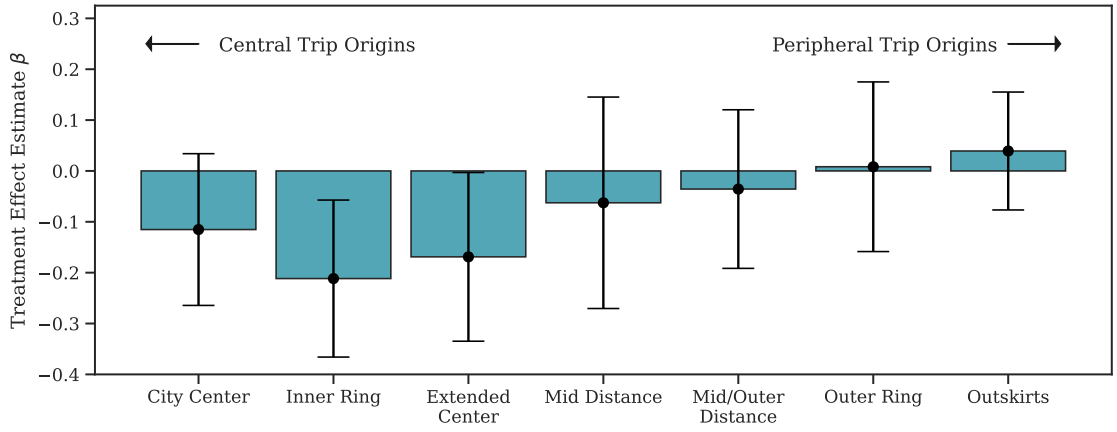

Figure 2.3: Localized Treatment Effects per relative Distance from Center.

Note: DV = $\ln(NumTrips_{i,g,t})$. Estimates based on Baker et al.'s stacking method and Equation 2.3 (including dynamic controls $C_{i,t}$). Error bars represent the 95% confidence interval based on standard errors clustered at the city level.

ExtendedCenter) and becomes insignificant further out from the city center. This reinforces the narrative of commuter-based substitution, which would be expected to occur mostly in central locations (where offices and commercial centers are located). Note also that bike platforms often operate significantly larger service areas compared to e-scooter platforms – especially so in the early phases of platform introduction. Thus, our analysis may also point to the fact that limited competition with e-scooter platforms exists further out from a city's respective center.

We supplement this analysis with a more detailed view on trip location. Specifically, we group trips by most prevalent POI class at the trip origin. The results are shown in Figure 2.4. In line with previous results, we find that trips originating close to transportation-related POIs are most prone to substitution, suggesting that last mile commuter trips are affected most seriously by e-scooter competition.

[21] We consider trip origin locations here.

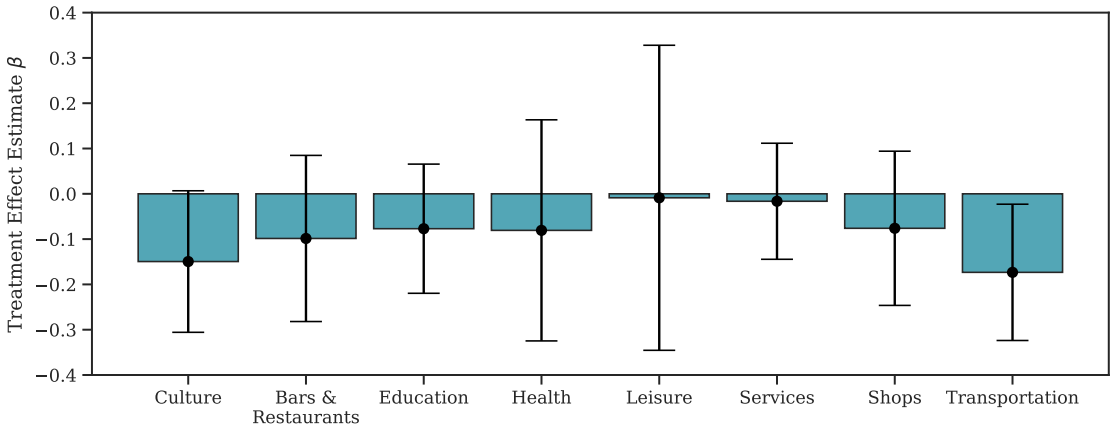

Figure 2.4: Localized Treatment Effects per POI Density Subgroup.

Note: DV = $\ln(NumTrips_{i,g,t})$. Estimates based on Baker et al.'s stacking method and Equation 2.3 (including dynamic controls $C_{i,t}$). Error bars represent the 95% confidence interval based on standard errors clustered at the city level.

Localized Effects on Trip Quality

Apart from analyzing trip timing and origin characteristics, we also explore how core trip quality characteristics may be impacted by e-scooter introduction. We especially look at trip duration and net trip distance covered per hour (an indicator of whether the trip is a roundtrip or a point-to-point trip). Figure 2.5 plots group-specific effect estimates by duration bin. We find that substitution occurs exclusively for very short trips, i.e. those with total durations of 0-15 and 16-30 minutes. Groups of trips with longer durations are not significantly affected. Again, we argue that this underpins previous findings of substitution occuring due to convenience-driven switching to e-scooters for short, largely utilitarian commuting purposes. We see these conclusions supported by the analysis of trip trajectories (see Figure 2.6). Affected trips are primarily point-to-point trips, with round trips being less affected. This is consistent with utilitarian commuter patterns.

In sum, all localized analyses point toward commuter trips being the main source of substitution. This is supported by all localized analyses we run. Specifically, substitution occurs primarily during weekday rush hours and in central locations. Areas with high density of transport infrastructure are disproportionately more affected, again suggesting that convenience-focused former bikesharing users switch to e-scooters for their last-mile commuting needs. The affected trips are mainly short point-to-point trips, again suggesting commuting as the primary source of substitution.

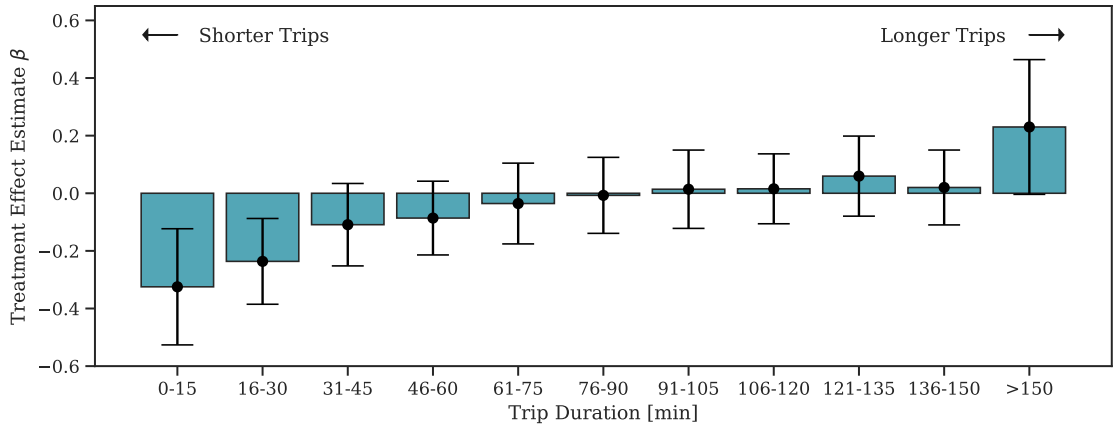

Figure 2.5: Localized Treatment Effects per Trip Duration Subgroup.

Note: DV = $\ln(NumTrips_{i,g,t})$. Estimates based on Baker et al.'s stacking method and Equation 2.3 (including dynamic controls $C_{i,t}$). Error bars represent the 95% confidence interval based on standard errors clustered at the city level.

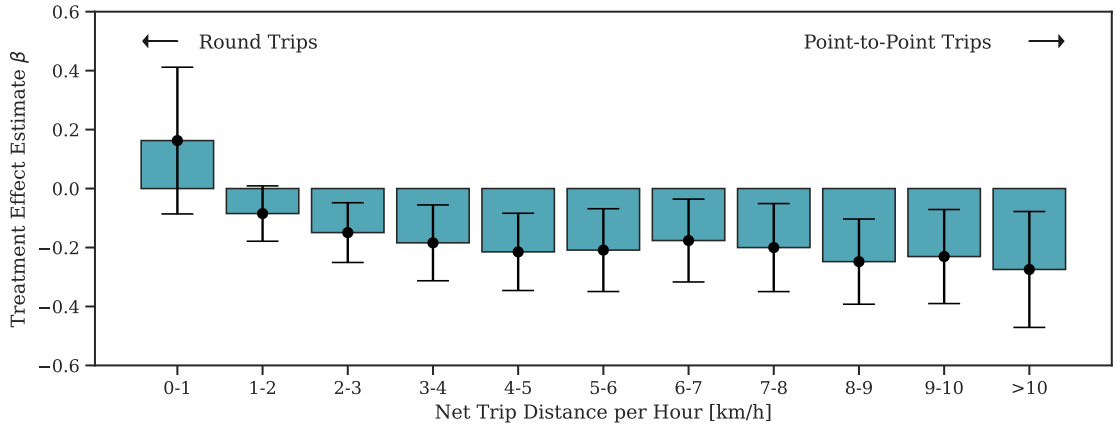

Figure 2.6: Localized Treatment Effects per Net Trip Distance per Hour Subgroup.

Note: DV = $\ln(NumTrips_{i,g,t})$. Estimates based on Baker et al.'s stacking method and Equation 2.3 (including dynamic controls $C_{i,t}$). Error bars represent the 95% confidence interval based on standard errors clustered at the city level.

2.5 Robustness Tests and Validation Analyses

We validate our results by means of a comprehensive set of robustness tests. The specific robustness concerns we address along with their respective validation strategies are summarized in Table 2.4.

2.5.1 Placebo Test for Parallel-Trend and No-Anticipation Assumption

We first validate the parallel trend and no anticipation assumptions, two core prerequisite for the validity of our DiD identification strategy. Note that visual inspection of the dependent variable (see Figure 2.1) and the results from the event study model(s) already lend support to both assumptions being valid. We provide additional evidence here. To do so, we implement two separate falsification tests. First, we run a pseudo-treatment test similar to the one used in Babar and Burtch (2020) by which we artificially move the treatment back 100 days, drop the last 100 days of the dataset and re-estimate Equation 2.1. The results of this analysis are shown in Table 2.5 (Column (1)). We find no evidence for a significant pseudo treatment effect. The second falsification test we run relies exclusively on a non-treated sub-sample (i.e., the period of January 21, 2019 to March 31, 2019 prior to first treatment on June 01, 2019 (see Table 2.1)). We then create placebo treatment vectors by scaling the actual treatment vectors to the (shorter) pre-treatment sub-sample[22]. Again, if the parallel-trend assumption holds, we should expect a non-significant pseudo treatment effect close to zero. Referring to Table 2.5 (Column (2)) this is indeed what we find.

2.5.2 Group-Time Effect Heterogeneity

As mentioned, recent methodological research has revealed certain shortcomings of two-way fixed effects (TWFE) difference-in-differences estimators like the one used throughout this research (de Chaisemartin and D'Haultfœuille, 2020; Callaway and Sant'Anna, 2020). The main concern pertains to the possibility of negative weights when computing the ATT as a weighted sum of group- and period-level ATTs, as is the case with TWFE estimators (de Chaisemartin and D'Haultfœuille, 2020). To test the robustness of our estimations to this concern we estimate group- and period-level average treatment effects following the methodology proposed by Callaway and Sant'Anna (2020).

For reference, we first report results obtained with traditional TWFE estimators (i.e., a log-OLS model and a Poisson quasi-maximum-likelihood (PQML) estimator (Greenwood and Wattal, 2017b)). We then report estimates obtained with the doubly-robust Callaway et al. (2021) weighted group-time estimator, an imputation-based estimator (Borusyak et al., 2021)

[22]For example, if city i was originally treated on day $t \in \mathcal{T}$, where $\mathcal{T}$ is the full set of days, the placebo treatment will set in on day $t^{sub} = \frac{t}{|\mathcal{T}|}|\mathcal{T}^{sub}|$, where $|\mathcal{T}|$ and $|\mathcal{T}^{sub}|$ are the number of days in the full and the pre-treatment sub-sample, respectively

Table 2.4: Overview of robustness concerns, associated validation strategies and results

Robustness concern	Validation strategy	Result	Reference
Core DiD assumptions (pre-treatment parallel trend, not anticipation) do not hold	Event-study model	Non-sig./small pre-treatment eff.	Fig.2.9, Tab.2.18
	Scaled pseudo treatment on Jan-Jun sub-sample	Non-sig./small placebo eff.	Tab.2.5
	Shifted pseudo treatment	Non-sig./small placebo eff.	Tab.2.5
Treatment effect is heterogeneous across time and groups	Review TWFE regressions weights (de Chaisemartin and D'Haultfoeuille, 2021)	All regression weights are non-negative indicating correct effect sign	unreported analyses
	Use of robust DiD estimators	Comparable estimates (size, direction, sig. level) to TWFE	Tab.2.6,2.18
	Specific TWFEs per treatment (Cengiz et al., 2019)	Most treatment coeffs. are significant and negative[a]	Fig.2.10
Serial Correlation in DV leads to underestimation of SEs (Bertrand et al., 2004)	Random assignment test	No sig. effect on DV	Tab.2.7
	Permutation/shuffle test	No sig. effect on DV	Tab.2.7
	Clustering of SEs	Results remain sig.	all results
Incorrect functional form of estimator	Benchmark of variety of DiD estimators of different functional form with and without controls $C_{i,t}$	Results consistent in size, direction and significance	Tab.2.3,2.6,2.18
Effect is driven by novelty of e-scooters and is not sustained over time	Event study model for up to 6 months following treatment	Effect is sustained/grows over time	Fig.2.9, Tab.2.18
Fleet operators strategically adjust network (fleet size, station count) in response to treatment	Regress fleet size and number of stations onto scooter	Eff. is close to 0 and not sig. indicating no network changes after treatment	Tab.2.8
Some cities experience multiple platform entries, others just one	Re-estimate Eq.2.1 on reduced sample excluding cities with multiple entries	Eff. remains sig. and consistent in direction (larger for less entries)	Tab.2.9
Marketing activities of focal bikesharing platform extenuate observed effect	Re-estimate Eq.2.1 on reduced sample excluding affected periods/cities (see Tab.2.20 for details)	Eff. remains sig. and consistent in size	Tab.2.10
Dynamics with competing bikesharing platforms introduce bias	Re-estimate Eq.2.1 on reduced sample only indluding cities, where nextbike is the sole bikesharing operator (see Tab.2.21 for details)	Eff. remains sig. and consistent in size (slightly smaller)	Tab.2.11

Table 2.5: Average pseudo treatment effect on demand for bikesharing ($\ln(NumTrips)$)

DV = $ln(NumTrips)$	(1)	(2)
$PseudoScooterShifted$	-0.0583	
	(0.0738)	
$PseudoScooterScaled$		0.0601
		(0.0526)
Day Fixed Effects	Yes	Yes
City Fixed Effects	Yes	Yes
Dynamic Controls $C_{i,t}$	Yes	Yes
Model	Baker et al.	Baker et al.
N	66,339	31,941
adj. R^2	0.912	0.907

Note: *p<0.1; **p<0.05; ***p<0.01. Robust standard errors (SE) clustered at city-level reported in parentheses. Estimates are based on daily data. Higher N for stacked DiD estimator (Baker et al., 2022) results from appending several treatment-centered subsets of the data

and finally the stacked TWFE regression model based on Baker et al. (2022) (our main estimator). In this benchmark we refrain from including any dynamic controls $C_{i,t}$ to ensure comparability between estimators (some do not allow for the inclusion of controls). The results are reported in Table 2.6. The direction and size of the estimated treatment effect are comparable across all estimators in scope, lending strong support to the robustness of the results. Amongst the robust DiD estimators, there is some minor variability in terms of absolute estimation size ranging from -0.198 to -0.238. Note that the estimate obtained with our fully saturated main model of -0.224 (see Table 2.2) falls within that range. All robust estimates (except for the Callaway et al. (2021) coefficient) are significant, at least at the p=0.05 significance threshold or lower. Event model benchmarks are provided in Table 2.18 and Figure 2.9 and paint a very

Table 2.6: Average treatment effect of *Scooter* on demand for bikesharing (ln($NumTrips$)) as estimated by traditional TWFE models ((1)-(2)) and robust DiD estimators ((3)-(5))

DV = $ln(NumTrips)$	(1)	(2)	(3)	(4)	(5)
Scooter	-0.181	-0.208***	-0.229	-0.238***	-0.198**
	(0.124)	(0.072)	(0.143)	(0.089)	(0.094)
Day Fixed Effects	Yes	Yes	Yes	Yes	Yes
City Fixed Effects	Yes	Yes	Yes	Yes	Yes
Dynamic Controls $C_{i,t}$	No	No	No	No	No
Model	log-OLS	Poisson	Callaway et al.	Borusyak et al.	Baker et al.
N	12,005	12,005	12,005	12,005	93,639
adj. R^2	0.991	-	-	-	0.887

Note: *p<0.1; **p<0.05; ***p<0.01. Robust standard errors clustered at city-level reported in parentheses. Estimates based on daily data. Higher N for stacked DiD estimator (Baker et al., 2022) results from appending several treatment-centered subsets of the data

similar picture.

2.5.3 Random Assignment and Permutation/Shuffle Tests

The second main validity threat for DiD estimators is serial correlation in the DV (Angrist and Pischker, 2008; Bertrand et al., 2004). Note that potential serial correlation should be reflected in the clustered SEs we report throughout this study. Nonetheless we run additional falsification (shuffle) tests, a commonly used strategy to gauge whether model results are robust to serial correlation (e.g., Burtch et al., 2018). We implement two variants. First, we run a pseudo treatment test by which we randomly reassign treatment indicators across the full set of cities as well as the cities that eventually receive treatment (treatment group), respectively. We repeat this procedure for a total of 1000 replications and store the coefficient estimates. The results are shown in Table 2.7 (Columns 1 and 2). As can be seen, the mean placebo effect is approximately equal to zero for both samples with the true effect being in the very

far tail of both distributions of placebo estimates. This lends strong support to the robustness of our results to serial correlation. Second, we randomly reassign (shuffle) the 35 city-specific treatment vectors $Scooter_{i,t}$ across cities (e.g., Berlin receiving treatment vector of Bonn, Bonn receiving treatment vector of Frankfurt, etc.) and re-estimate our basic model. We repeat this process for a total of 1000 replications for both the full sample and the sub-sample of control cities. Our results are reported in Columns 3 and 4 of Table 2.7 and reinforce our previous findings that serial correlation does not pose a problem to our identification strategy. We find that the mean placebo treatment effect is approximately zero. Furthermore, we show that the true treatment effect is in the far tail of the distribution of placebo treatment estimates (see p-value and z-score), which provides strong support for the robustness of our results to serial correlation.

Table 2.7: Permutation/shuffle test swapping entire treatment vectors across cities

	Random Assignment Test		Permutation/Shuffle Test	
μ of Placebo Effect	0.010	0.020	0.014	0.030
σ of Placebo Effect	0.122	0.171	0.110	0.162
Actual Effect Estimate	-0.224	-0.224	-0.224	-0.224
z-Score	-1.922	-1.425	-2.157	-1.561
t-Statistic	60.791	45.048	68.215	49.354
p-Value	<0.001	<0.001	<0.001	<0.001
Replications	1000	1000	1000	1000
Sample	All cities	Never Treated	All cities	Never Treated

Note: Random assignment test involves assigning treatment status fully at random across the sample. Permutation/shuffle test is implemented by shuffling treatment vectors across cities (e.g., Berlin receiving treatment vector of Bonn, Bonn receiving treatment vector of Frankfurt, etc.)

2.5.4 Strategic Adjustment of Networks (Fleet Size and Station Density)

Demand for shared transportation is strongly dependent on service level provided by the incumbent network operator (Benjaafar and Hu, 2020b). In the case of bikesharing, service level can be well approximated by the number of bicycles ($NumBikes_{i,t}$) available in a market as well as the number of docking stations ($NumStations_{i,t}$) installed in the service area. Thus, dynamics in either of the two covariates may raise endogeneity concerns. Therefore, we set out to ensure that the observed reduction in demand for bike trips is not an artefact of the bikesharing operator's decision to strategically adapt fleet size or network structure (i.e., number of stations) in response to new competition from e-scooter platforms. For this purpose, we re-estimate Equation 2.1 for $y_{i,t} = \ln(NumBikes_{i,t})$ and $y_{i,t} = \ln(NumStations_{i,t})$ (without any dynamic controls). Table 2.8 summarizes the results. We find that the effect $Scooter_{i,t}$ on both $\ln(NumBikes_{i,t})$ and $\ln(NumStations_{i,t})$ is close to zero and not statistically significant.

This confirms that bikesharing operators did not change vehicle supply or network density in response to the introduction of e-scooter sharing schemes. Any reduction in bike trips can thus be attributed to the introduction of e-scooters.

Table 2.8: Robustness to network changes ($\ln(NumBikes)$ and $\ln(NumStations)$) in response to treatment ($Scooter$)

	(1) $\ln(NumBikes)$	(2) $\ln(NumStations)$
$Scooter$	0.0151	0.00663
	(0.0456)	(0.0245)
Day Fixed Effects	Yes	Yes
City Fixed Effects	Yes	Yes
Dynamic Controls $C_{i,t}$	No	No
Model	Baker et al.	Baker et al.
N	93,639	93,639
adj. R^2	0.975	0.973

Note: *p<0.1; **p<0.05; ***p<0.01. Robust standard errors (SE) clustered at city-level reported in parentheses. Estimates based on daily data using specification from Equation 2.1. Higher N for stacked TWFE estimator results from stacking several subsets of the data each of which is centered around the treatment datum

2.5.5 Multiple e-Scooter Platform Entries

Some cities experience multiple e-scooter platform entries, others just one or two (see Table 2.19). It may be possible that these dynamics bias our effect estimates. To check for this possibility we drop cities that experience more than one or two significant platform entries over the period of observation from our dataset. We re-estimate Equation 2.1 and report the results in Table 2.9. The ATT remains consistent in direction and significance, indicating that multiple platform entry does not affect our results in a qualitative manner. We attribute the significantly larger coefficient estimates achieved on the sub-samples (Columns (2) and (3) in Table 2.9) to group-specific effect heterogeneity.

2.5.6 Price Promotions and Other Marketing Activities of Incumbent Bikesharing Platform

Price promotions and other marketing activities implemented by the incumbent bikesharing platform during the observational period represent possible confounders that may bias the estimated treatment effects. Reductions in the base price would result in a more attractive competitive positioning of bicycles versus e-scooters, thus extenuating previously observed cannibalization effects. In Table 2.20 we have compiled a list of all marketing activity as advertised on Nextbike's social media channels. In the majority of cases, promotions either affect the full sample, the

Table 2.9: Average treatment effect of *Scooter* on overall bikesharing platform trips ($\ln(NumTrips)$) for different sub-samples with one or two e-scooter entries

	(1)	(2)	(3)
DV = $\ln(NumTrips)$			
Scooter	-0.224***	-0.378***	-0.317***
	(0.0782)	(0.125)	(0.0985)
Day Fixed Effects	Yes	Yes	Yes
City Fixed Effects	Yes	Yes	Yes
Dynamic Controls $C_{i,t}$	Yes	Yes	Yes
Model	Baker et al.	Baker et al.	Baker et al.
Sample	Full	Up to one entry	Up to two entries
N	93,639	43,561	62,083
adj. R^2	0.898	0.896	0.897

Note: *p<0.1; **p<0.05; ***p<0.01. Robust standard errors (SE) clustered at city-level reported in parentheses. Estimates based on daily data using specification from Equation 2.1. Higher N for stacked TWFE estimator results from stacking several subsets of the data each of which is centered around the treatment datum

entire observational period, or both and are therefore controlled for by means of city and period fixed effects. On some occasions, however, only certain cities and periods are affected. We control for these effects by removing single affected days from the sample (for all cities) (see Table 2.20 for an overview of control strategies). We obtain essentially the same coefficient estimates (with only minor deviations in the estimated SE) when re-estimating Equation 2.1 on this reduced sample (see Table 2.10).

Table 2.10: Average treatment effect of *Scooter* on overall bikesharing platform trips (ln(*NumTrips*)) excluding marketing activities

	(1)	(2)
DV = ln(*NumTrips*)		
Scooter	-0.224***	-0.224***
	(0.0782)	(0.0789)
Day Fixed Effects	Yes	Yes
City Fixed Effects	Yes	Yes
Dynamic Controls $C_{i,t}$	Yes	Yes
Model	Baker et al.	Baker et al.
Sample	Full	No marketing activities
N	93,639	90,909
adj. R^2	0.898	0.898

Note: *p<0.1; **p<0.05; ***p<0.01. Robust standard errors (SE) clustered at city-level reported in parentheses. Estimates based on daily data using specification from Equation 2.1. Higher N for stacked TWFE estimator results from stacking several subsets of the data each of which is centered around the treatment datum

2.5.7 Dynamics with Incumbent Bikesharing Platforms

Previous estimation results may be subject to contamination related to competitive dynamics with other incumbent bikesharing systems. To hedge against this risk, we review the number of active incumbent bikesharing competitors (and new entrants) over the observation period (see Table 2.21). We then re-estimate Equation 2.1 on two different subsets of data. First we remove all cities from our experimental sample where Nextbike faces any competition from other bikesharing operators at all, thus removing the possibility of any competitive dynamics present in the sample. We repeat the same analysis for a second sample including only cities where a maximum of one competing bikesharing platform is present. The results are shown in Table 2.11. We find that ATT estimates remain robust in size, direction and significance across the three samples.

Table 2.11: Average treatment effect of *Scooter* on overall bikesharing platform trips ($\ln(NumTrips)$) for different sub-samples of cities with and without competitors

	(1)	(2)	(3)
DV = $\ln(NumTrips)$			
Scooter	-0.224***	-0.162**	-0.204**
	(0.0782)	(0.0723)	(0.0879)
Day Fixed Effects	Yes	Yes	Yes
City Fixed Effects	Yes	Yes	Yes
Dynamic Controls $C_{i,t}$	Yes	Yes	Yes
Model	Baker et al.	Baker et al.	Baker et al.
Sample	Full	No competitors	Up to one competitor
N	93,639	48,020	86,779
adj. R^2	0.898	0.889	0.896

Note: *p<0.1; **p<0.05; ***p<0.01. Robust standard errors (SE) clustered at city-level reported in parentheses. Estimates based on daily data using specification from Equation 2.1. Higher N for stacked TWFE estimator results from stacking several subsets of the data each of which is centered around the treatment datum

2.6 Discussion

Drawing on the much-discussed case of e-scooter introduction into global micromobility markets, we explore how high-fidelity IoT data can be exploited for causal policy and operational insights.

Underlying our analyses is a unique dataset gathered from real-time sensor data streams of shared bicycles. Through regular API queries, we collect a full year (January, 2019 to January, 2020) of granular geo-tagged position data of Nextbike-operated shared bicycles across 35 cities. This data is broadcast continuously via the GPS beacons attached to each shared bike and, when collected and stored at frequent intervals, allows inference on trip origin, destination, departure time, duration and trajectory. 18 of the bikesharing markets in our sample eventually experience e-scooter platform entries, thus creating a natural experiment that we exploit for causal inference. We employ state-of-the-art DiD techniques (Cengiz et al., 2019; Baker et al., 2022) at an aggregate and localized level to explore the impact e-scooters have had on overall demand for shared bike trips and on specific user behavior shifts in the incumbent micromobility user population.

We find that e-scooter introduction has resulted in cannibalization of incumbent bikesharing platforms. In the markets we study we find a statistically significant drop in demand for bike rentals of 22.4%. Our findings suggest that the observed displacement effect stems mostly from convenience-driven substitution of commuter trips. We are able to show that the affected trips are those during morning and evening rush hours, originating in central locations, primarily around transportation infrastructure. We also show that it is mostly short point-to-point trips that are affected by e-scooter competition.

2.6.1 Contributions

Our study offers several contributions. First, we provide new findings related to the societal impact of digital platform business models. We show that e-scooters significantly cannibalize the healthier and environmentally more friendly transport alternative of shared bicycles. This finding adds crucial nuance to the public discussion on the evaluation and regulation of e-scooter platforms, which has largely ignored issues related to undesired mode substitutions and cannibalization. Indeed, our empirical results allow us to quantify the attributable business, health, and environmental impact resulting from bike trip replacement. We estimate that across the 18 treated cities in our sample approximately 1.44M bike trips are replaced annually by e-scooters. Taking into account that mostly shorter trips are affected this breaks down to a replacement of approximately 43.27M active bike minutes annually[23]. We further estimate the resulting business impact for Nextbike to be around EUR 1.44M annually[24]. From a health

[23] Assuming an average trip duration per replaced trip of 15 minutes, i.e., the mid-point of the two most affected duration baskets (0-15min and 16-30min)

[24] Nextbike charges EUR 1 per commenced 30-minute slot in their basic tariff. We therefore account EUR 1 per replaced trip.

perspective, negative impacts are incurred as a result of people moving less (Xu, 2019). We estimate that e-scooter introduction has resulted in the replacement of approximately 307M kcal annually across the treated cities in our sample among Nextbike users alone[25]. Finally, recent studies have shown that e-scooters have a significantly worse full life-cycle carbon footprint performance (126 g CO^2-eq./km) compared to station-based bikesharing (65 g CO^2-eq./km) and free-floating bikesharing (118 g CO^2-eq./km) (Luo et al., 2019). On aggregate, the introduction of e-scooters therefore results in a negative climate impact of 50t-385t CO^2-equivalent purely as a result of replacing bikesharing trips[26]. However, our results also provide cautionary evidence for potential positive societal effects of e-scooters. We show that in many periods e-scooters do not directly cannibalize bikes, and instead cater to users that may previously have been untapped by incumbent micromobility offers. This suggests that e-scooters may be a worthwhile and relevant addition to the transportation mix, especially if it replaces less favorable options, such as cars. These findings also contribute to the literature on transportation mode choice in shared micromobility, a still relatively poorly understood, yet fast growing domain (McKenzie, 2019; Shaheen, 2019).

At a more general level, we show how IoT data can be used to achieve causal inference at a localized level with direct operational and strategic implications for managers. Specifically, we are able to credibly pinpoint and quantify the source of substitution (commuter segment in central locations and in proximity to transport infrastructure), thus enabling targeted strategic and operational response by platform managers. For example, e-scooter platform operators may wish to prioritize the commuter segment in their marketing campaigns given that it is this segment where competition with incumbent bikesharing platforms primarily plays out. Marketing campaigns could explicitly address commuters in the time slots and areas we have identified (e.g., by means of contextual mobile targeting (Ghose et al., 2019a)). Or they may wish to focus on segments where cannibalization has, thus far, not set in. For incumbent bikesharing operators our results provide clear and detailed guidance for possible strategic responses that can help attenuate the business impact of e-scooters. For example, operators may wish to increase coverage and/or try to improve utilization via targeted marketing campaigns in specific time periods and areas that experience higher substitution rates on average. They might also think about incorporating e-bikes into their fleets that offer similar convenience levels as e-scooters and deploying them in the regions and time slots we have identified as most prone to cannibalization.

2.6.2 Future Work

Our study is not without limitations, which provide scope for future research. First, we are limited by the availability of post-treatment data which confines us to the investigation of short-to-medium-term treatment effects. We are confident, however, that our investigation of this

[25] Data suggests that a person of average weight burns roughly 260 kcal for each 30 minutes of moderate cycling whereas standing requires only 47 kcal for the same period (Havard Medical School, 2018).

[26] Assuming moderate cycling speeds of 17.5 km/h

five- to six-month window clearly points toward a prolonged, if not intensifying effect. Also, our observational study is based on European data. Europe has one of the most developed micromobility markets globally, which makes this case particularly relevant. While we expect to see similar effects in other regions, their exact magnitude remains to be verified. Our study is also limited by the fact that we do not have access to user-level data. This limitation is shared with many seminal empirical studies in the area (e.g., Babar and Burtch, 2020; Zervas et al., 2017; Chan and Ghose, 2014). However, contrary to these exemplary studies, the high level of granularity in our data enables us to conduct analyses – especially those related to user behavior shifts – which allow well-grounded assumptions on the underlying user types and travel use cases. Future research exploring the individual user dimension would likely prove useful and could help triangulate the results presented in this study. Finally, our data only allows the analysis of substitution effects of e-scooters on (shared) bicycles. We do not have visibility on cannibalization of other modes. This work also does not attempt to quantify any of the other potential positive (e.g., reduced traffic) or negative (e.g., accident rates, curb crowding, precarious employment) impacts of e-scooter platform introduction. For a full appraisal of the societal benefits and drawbacks of e-scooter platforms, such analyses would be of interest. We leave them for future research.

2.7 Appendix

A. Data Collection

Dependent Variable Data Retrieval and Processing

Table 2.12 shows an excerpt of the raw API data feed for an exemplary bicycle in the city of Berlin. Data feeds like this were collected over the entire observation period across the full experimental sample. Locations per each vehicle (as identified by attribute *bike_ID*) are retrieved and stored every minute by means of a query of Nextbike's application programming interface (API). If the vehicle is rented out, it disappears from the API output. Thus, by tracking individual vehicles disappearing and then reappearing in our records, trip times, trip duration and trip trajectory can be readily inferred. In the example in Table 2.12, bike 22473 was rented out on March 8, 2019 at 18:32 at station 6302589 (Hermannstraße/Briesestraße). The rental was completed approximately ten minutes later (at 18:42) as a free-floating rental (i.e., not returned to a docking station) at location (52.4696115,13.4245992). Note that we do not use station IDs or names for trip trajectory inference. Instead, we utilize observed GPS coordinates (attributes *lat* and *lng*) as broadcast by the bike's GPS sensor. This ensures that trip inference works for both station-based, free-floating and hybrid systems and trips. The API data also allows us to infer the number of vehicles and the number of stations currently in operation. By counting the unique daily values of *bike_ID* and *station_ID* returned by our API queries, we can reliably assess current fleet size and number of stations per each city in our sample.

Table 2.12: Excerpt of raw API output for selected bicycle in the city of Berlin

datetime	city	bike_ID	bike_type	lat	lng	station_ID	station_name
...	...	...	...	...	...	...	...
2019-05-08 18:29:00	Berlin	22473	12	52.476789	13.426652	6302589	Hermannstraße/ Briesestraße
2019-05-08 18:30:00	Berlin	22473	12	52.476789	13.426652	6302589	Hermannstraße/ Briesestraße
2019-05-08 18:31:00	Berlin	22473	12	52.476789	13.426652	6302589	Hermannstraße/ Briesestraße
2019-05-08 18:32:00	Berlin	22473	12	52.476789	13.426652	6302589	Hermannstraße/ Briesestraße
2019-05-08 18:42:00	Berlin	22473	12	52.4696115	13.4245992	-	-
2019-05-08 18:43:00	Berlin	22473	12	52.4696115	13.4245992	-	-
2019-05-08 18:44:00	Berlin	22473	12	52.4696115	13.4245992	-	-
...	...	...	...	...	...	...	...

Note: Column names have been changed from the original API output for easier reading.

Overview and Definition of Variables

In Table 2.13 we provide concise definitions per each variable used in this work and reference their corresponding data sources.

Table 2.13: Summary of Variables and Data Sources

Variable	Description	Source
$ln(NumTrips_{i,(g),t})$	Number of trips originating in group g (optional) of city i during period t (log-transformed)	Nextbike API
$ln(TripDuration_{i,(g),t})$	Mean duration (in minutes) per trip originating in group g (optional) of city i during period t (log-transformed)	Nextbike API
$ln(NetDistance_{i,(g),t})$	Mean net distance (in km) per trip originating in group g (optional) of city i during period t (log-transformed)	Nextbike API,OpenStreeMaps (queried using OSMnx (Boeing, 2017))
$ln(NetSpeed_{i,(g),t})$	Mean net distance per hour (in km/h) per trip originating in group g (optional) of city i during period t (log-transformed)	Nextbike API,OpenStreeMaps (queried using OSMnx (Boeing, 2017))
$Scooter_{i,t}$	Binary indicator of whether an e-scooter platform was present in city i during period t	press search (see Table 2.19)
$ln(NumBikes)_{i,t}$	Count of weekly active vehicles in service area (log-transformed)	Nextbike API
$ln(NumStations)_{i,t}$	Count of weekly dedicated stations in service area	Nextbike API
$ln(Unemployment)_{i,t}$	Unemployment rate in city i and period t (log-transformed, monthly values)	Bundesagentur für Arbeit (2020); AMS (2020); Bundesamt für Statistik (2020)
$ln(OvernightStays)_{i,t}$	Number of overnight stays in city i and period t (log-transformed, monthly data)	state-level statistical offices
$RainyPeriod_{i,t}$	Binary indicator of whether precipitation occurred in city i and period t	The Weather Company (IBM) (2019)
$HotPeriod_{i,t}$	Binary indicator of whether max. temperature in city i and period t exceeded 30°C	The Weather Company (IBM) (2019)
$ColdPeriod_{i,t}$	Binary indicator of whether min. temperature in city i and period t fell below 0°C	The Weather Company (IBM) (2019)

Note: Variables defined for group g in city i and period t

Descriptive Analyses

In Table 2.14, we provide descriptive statistics. In Table 2.15, a correlation matrix is provided. Note that pairwise correlation between covariates (and in particular between the treatment and other covariates) is largely limited, indicating that multicollinearity does not pose a large risk to the robustness of our results. This is, of course, also confirmed by the robustness of ATT estimates to the inclusion of additional dynamic covariates in the model (see Table 2.2).

Table 2.14: Descriptive statistics

	N	**Min**	**Max**	**Mean (μ)**	**St. Dev. (σ)**
$\ln(NumTrips)$	12,005	0.0	8.99	4.97	1.78
$Scooter$	12,005	0.00	1.0	0.26	0.44
$\ln(NumBikes)$	12,005	3.04	7.71	5.26	0.95
$\ln(NumStations)$	12,005	0.69	5.69	3.37	0.96
$\ln(OvernightStays)$	12,005	7.61	15.04	11.07	1.38
$\ln(Unemployment)$	12,005	0.53	2.48	1.76	0.39
$ColdPeriod$	12,005	0.00	1.00	0.12	0.33
$HotPeriod$	12,005	0.00	1.00	0.15	0.36
$RainyPeriod$	12,005	0.00	1.00	0.48	0.50

Note: N reflects size of dataset at daily resolution which is used in most models

Table 2.15: Correlation table of covariates

	(1)	(2)	(3)	(4)	(5)	(6)	(7)	(8)	(9)
(1) $NumTrips$	1.00	0.19	0.63	0.24	0.50	0.12	-0.09	0.08	-0.00
(2) $Scooter$	0.19	1.00	0.32	0.32	0.40	0.13	-0.02	0.00	0.07
(3) $\ln(NumBikes)$	0.63	0.32	1.00	0.78	0.76	0.19	-0.03	0.01	0.00
(4) $\ln(NumStations)$	0.24	0.32	0.78	1.00	0.70	0.14	-0.01	0.01	-0.03
(5) $ln(OvernightStays)$	0.50	0.40	0.76	0.70	1.00	0.01	-0.08	0.05	0.00
(6) $\ln(Unemployment)$	0.12	0.13	0.19	0.14	0.01	1.00	-0.02	-0.02	0.10
(7) $ColdPeriod$	-0.09	-0.02	-0.03	-0.01	-0.08	-0.02	1.00	-0.16	-0.14
(8) $HotPeriod$	0.08	0.00	0.01	0.01	0.05	-0.02	-0.16	1.00	-0.21
(9) $RainyPeriod$	-0.00	0.07	0.00	-0.03	0.00	0.10	-0.14	-0.21	1.00

B. Supplement to Methodology

Temporal Group Identification and Construction

Figure 2.7 visualizes temporal patterns in shared bicycle demand in a quarter-hourly resolution. The analysis reveals clear intra-weekly and intra-daily seasonality. There is a distinction between weekday and weekend patterns with weekdays exhibiting typical commuter patterns (clear rush hours in the morning and afternoon) and weekends usually seeing demand peaks during the daytime.

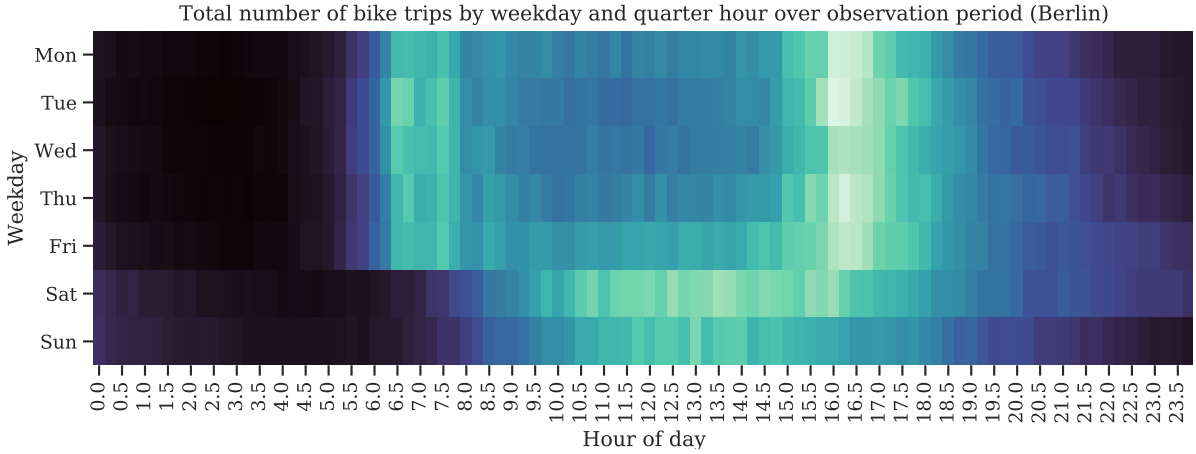

Figure 2.7: Weekly and daily seasonality in bike rental demand.

Shown are number of trip starts per quarter hourly basket and weekday over full observation period. Dark colors indicate low relative trip density, bright colors indicate high relative density of trips. Data is shown for Berlin. Other cities in sample exhibit similar patterns.

We use these insights to define nine distinct temporal sub-groups by adapting commonly used terminology (e.g., Cohen et al., 2016) to the case of bikesharing (see Table 2.16).

Table 2.16: Definition of temporal sub-groups

Time baskets T_t	**Day of Week**	**Time of Day**
Morning rush	Mon - Fri	6:00am - 8:39am
Weekday daytime	Mon - Fri	8:30am - 2:59pm
Evening rush	Mon - Fri	3:00pm - 5:59pm
Weekday evening	Mon - Fri	6:00pm - 9:59pm (except bar hours)
Weekday nighttime	Mon - Fri	10:00pm - 05:59am (except bar hours)
Weekend daytime	Sat & Sun	7:00am - 5:59pm
Weekend evening	Sat & Sun	6:00pm - 10:59pm (except bar hours)
Weekend nighttime	Sat & Sun	11:00pm - 05:59pm (except bar hours)
Bar hours	Fri & Sat	8:00pm - 1:59am (of next day)

Spatial Group Identification and Construction

We report here several details on the construction of the two sets of spatial groups (concentric distance from city center and most prevalent land use as measured by relative POI density). In Figure 2.8 we provide a graphical illustration of both concepts for the example of Berlin. Table 2.17 provides details on the individual POI types contained in the eight POI classes analyzed in this paper.

(a) Distance from center at trip origin **(b)** POI densities at trip origin (ex.: *Transport*)

Figure 2.8: Illustration of spatial trip characteristics (example Berlin)

Table 2.17: Open Street Maps (OSM) POI categories, examplary POIs and categorization adopted in this work

OSM POI Class	Example POI Sub-Class
Arts, Culture & Tourism	arts centre, gallery, museum, place of worship, attraction, fountain, viewpoint, fort, memorial, monument, ruins, tomb, etc.
Bars & Restaurants	bar, beer garden, cafe, fast food, ice cream, pub, restaurant, etc.
Education	school, university, college, kindergarten, library
Health	clinic, dentist, doctors, hospital, nursing home, pharmacy
Leisure & Entertainment	park, garden, playground, stadium, sports center, fitness center, water, beach, peak
Services	atm, bank, beauty, dry cleaning, hairdresser, laundry, tailor, police, post office, town hall, etc.
Shops	clothes, supermarket, bakery, butcher, jewelry, florist, convenience, shoes, etc.
Transport	parking, train station, bus/tram stop, taxi, car sharing, fuel, charging station, etc.

C. Supplement to Empirical Results

Table 2.18 summarizes coefficient estimates obtained by estimating event study models using the the robust DiD estimators most commonly applied in the recent literature (Callaway et al., 2021; Borusyak et al., 2021). To allow for more concise tabulation we report results for 3 months prior (-12 weeks) to 6 months after (+24 weeks) the onset of treatment. A visual representation (with longer pre-treatment period) of the event estimates is provided in Figure 2.9. We see both the parallel trends and the no anticipation assumptions largely confirmed. Estimates turn negative on the week of treatment (week 0) and remain negative from there on.

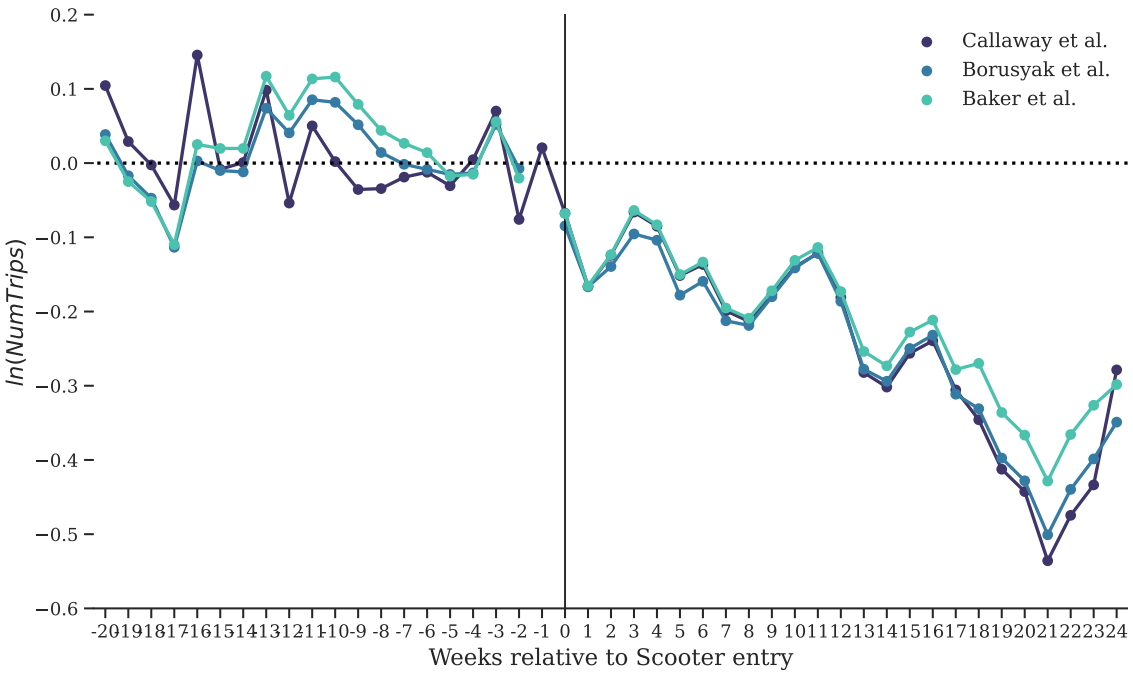

Figure 2.9: Event study coefficient estimates for pre- and post-treatment period.

Note:Reference category is Week -1 (except for Callaway et al. model). Raw regression results shown in Table 2.18

Table 2.18: Event study of *Scooter* on overall bikesharing platform trips ($ln(NumTrips)$)

	(1)		(2)		(3)	
Relative Week	Est.	SE	Est.	SE	Est.	SE
-12	-0.054	0.053	0.041	0.101	0.064	0.093
-11	0.05	0.040	0.085	0.092	0.113	0.085
-10	0.002	0.058	0.082	0.101	0.116	0.102
-9	-0.036	0.056	0.052	0.091	0.079	0.088
-8	-0.034	0.047	0.014	0.095	0.044	0.100
-7	-0.019	0.051	-0.002	0.077	0.027	0.082
-6	-0.012	0.044	-0.008	0.086	0.014	0.087
-5	-0.031	0.045	-0.015	0.060	-0.018	0.067
-4	0.005	0.053	-0.013	0.040	-0.015	0.041
-3	0.07*	0.038	0.052	0.049	0.056	0.048
-2	-0.076	0.049	-0.007	0.051	-0.02	0.052
-1	0.021	0.054	ref	ref	ref	ref
0	-0.068	0.046	-0.085*	0.047	-0.068	0.046
1	-0.166**	0.072	-0.167***	0.060	-0.165**	0.070
2	-0.124	0.107	-0.139**	0.069	-0.123	0.103
3	-0.066	0.125	-0.095	0.078	-0.064	0.120
4	-0.085	0.137	-0.104	0.080	-0.083	0.130
5	-0.152	0.120	-0.178**	0.083	-0.15	0.112
6	-0.137	0.143	-0.159*	0.086	-0.133	0.130
7	-0.199	0.158	-0.213**	0.104	-0.195	0.140
8	-0.213	0.166	-0.219**	0.101	-0.209	0.146
9	-0.177	0.159	-0.18*	0.099	-0.172	0.136
10	-0.14	0.181	-0.141	0.111	-0.131	0.154
11	-0.121	0.176	-0.121	0.108	-0.114	0.151
12	-0.181	0.182	-0.186	0.115	-0.173	0.154
13	-0.282	0.208	-0.278**	0.126	-0.254	0.173
14	-0.302	0.215	-0.294**	0.130	-0.273	0.175
15	-0.256	0.204	-0.25**	0.120	-0.228	0.169
16	-0.239	0.221	-0.232*	0.135	-0.212	0.182
17	-0.306	0.222	-0.311**	0.134	-0.278	0.174
18	-0.346	0.214	-0.331**	0.136	-0.27*	0.161
19	-0.412**	0.208	-0.397***	0.130	-0.336**	0.159
20	-0.443**	0.206	-0.428***	0.136	-0.367**	0.151
21	-0.536**	0.213	-0.501***	0.144	-0.428***	0.150
22	-0.475**	0.191	-0.44***	0.130	-0.366***	0.141
23	-0.434**	0.207	-0.399***	0.142	-0.326**	0.145
24	-0.279	0.216	-0.349**	0.160	-0.298*	0.161
Day FE	Yes		Yes		Yes	
City FE	Yes		Yes		Yes	
Controls $C_{i,t}$	No		No		No	
Model	Callaway et al.		Borusyak et al.		Baker et al.	
N	12,005		12,005		93,639	
adj R^2	-		-		0.898	

Note: *p<0.1; **p<0.05; ***p<0.01. Robust standard errors clustered at city-level reported in parentheses. Estimates based on daily data. Higher N for stacked DiD estimator (Baker et al., 2022) results from appending several treatment-centered subsets of the data

D. Supplement to Robustness Test

Individual-level TWFE Models

In line with Cengiz et al. (2019), we conduct event-by-event analyses by constructing dedicated samples per each treated unit that includes only the treated and all never-treated units (similar to a stack in the stacked DiD estimator). Figure 2.10 shows the resulting individual-level TWFE estimates. While there is considerable heterogeneity in the impact of e-scooter introduction per treated city, the estimations are either highly significant and negative or show no significance. This supports our aggregate estimates.

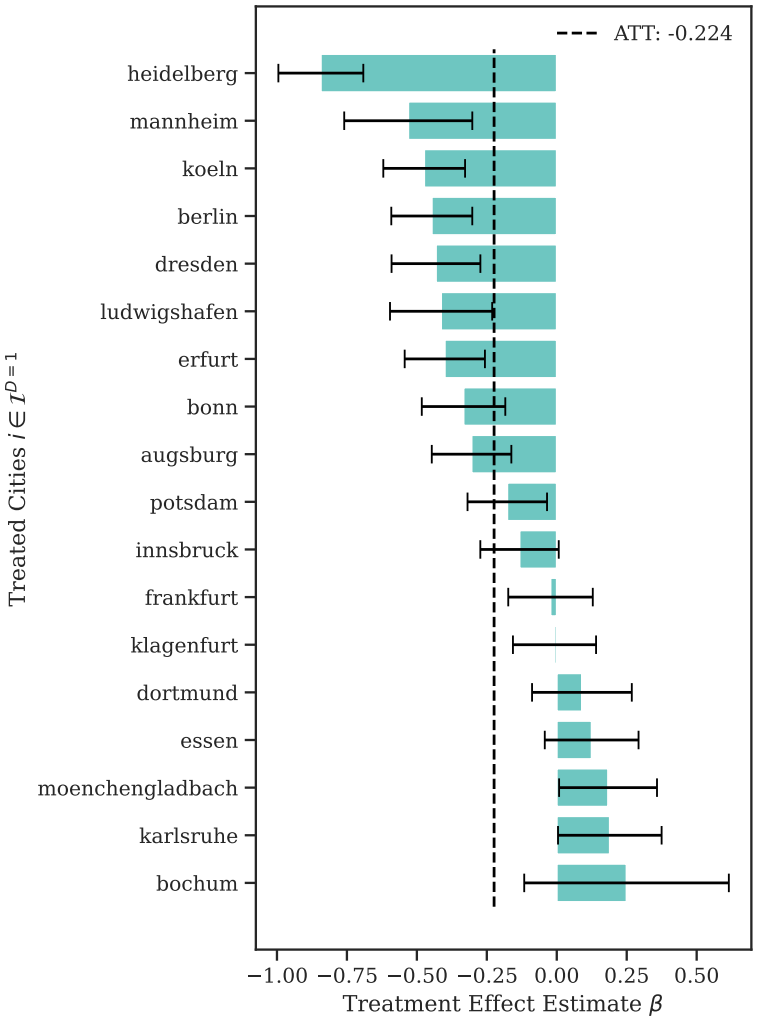

Figure 2.10: Specific TWFE-based coefficient estimates per individual treatment event.

Note: The plot shows individual event-specific point estimates and confidence intervals. Each estimate corresponds to one of the individual the stacks in the Baker et al. (2022) stacked DiD model as described mathematically in Equation 2.1). Standard errors used for the CI computation are clustered at the city-level

Robustness to Multiple e-Scooter Platform Entry

Table 2.19 summarizes the total number of e-scooter platform entries and dates of the first five entries in the cities in scope. To address robustness concerns related to the number of platform entries we perform two robustness checks on limited samples. We first restrict the sample to the subset of cities that experience none or just a single e-scooter platform entry. Second, we construct a less restrictive sample that also includes cities that experience two entries. We re-estimate the static model for both datasets. The results are reported in Table 2.9.

Table 2.19: Electric Scooter Entry Dates (*Scooter*) per City and Data Sources

City	# Entries	1^{st} entry	2^{nd} entry	3^{rd} entry	4^{th} entry	5^{th} entry
Augsburg	1	2019-07-05				
Berlin	5	2019-06-15	2019-06-18	2019-06-21	2019-06-22	2019-08-26
Bochum	3	2019-09-11	2019-08-27	2019-08-30		
Bonn	2	2019-06-22	2019-08-15			
Dortmund	3	2019-07-08	2019-09-05	2019-10-10		
Dresden	1	2019-07-25				
Duisburg	0					
Erfurt	1	2019-07-05				
Essen	3	2019-08-22	2019-10-11	2019-11-18		
Frankfurt	4	2019-06-22	2019-06-27	2019-07-22	2019-08-26	
Giessen	0					
Hamm	0					
Heidelberg	1	2019-08-03				
Innsbruck	3	2019-06-01	2019-07-01	2019-09-02		
Kaiserslautern	1	2020-01-15				
Karlsruhe	1	2019-09-20				
Kassel	0					
Klagenfurt	2	2019-06-13	2019-06-13			
Koeln	4	2019-06-21	2019-06-22	2019-06-22	2019-08-26	
Leipzig	0					
Lippstadt	0					
Ludwigshafen	1	2019-08-01				
Luzern	0					
Mannheim	1	2019-08-01				
Marburg	0					
Moenchengladbach	1	2019-10-16				
Muelheim	0					
Norderstedt	0					
Offenburg	0					
Potsdam	2	2019-06-21	2019-10-01			
Ruesselsheim	0					
St.Poelten	0					
Walldorf	0					
Worms	0					
Wuerzburg	0	2020-10-16				

Note: Presented results were obtained via a press search

Robustness to Nextbike Price Promotions and Marketing Initiatives

In Table 2.20 we have collected marketing and promotional activities of Nextbike over the observation period which were obtained from social media postings. In general, Nextbike's promotional activity is relatively limited. In the majority of cases promotions either affect the full sample, the entire observational period or both, and therefore are controlled for by means of city and period fixed effects. There are, however, some occasions where only certain cities and periods are affected. The control strategies vary from case to case and are elaborated on in column four (control strategy) of Table 2.20. Generally, they involve either removing single affected days from the sample (for all cities) or running a robustness test on a reduced city sample (i.e., excluding the affected city).

Table 2.20: Nextbike marketing activities across the sample and observational period and empirical control strategy

Description	**Regional Scope**	**Temporal Scope**	**Control Strategy**
VRS Collaboration: first 30 min free for VRS-Chipcard owners	Cologne	full period	captured by city FE
Company flatrates for employees	all cities	full period	captured by city FE
Student Special: first 30/60 min free	all university cities	full period	captured by city FE
Customer Survey Bonus: free day pass	all cities	start of period - Jan 11^{th}, 2019	captured by time FE
Strike Special: 2 x 30 min free of charge during strike of public transport workers	Berlin	Feb 15^{th}, 2019	exclude day from sample (for all cities)
Introduction of monthly rate: first 30 min of each rental are free for 10€/month	all cities	May, 7^{th}, 2019 - end of period	captured by time FE
Instagram Promotion: Send a picture of you with a bike and first 50 get monthly pass for free	all cities	Jun 2nd, 2019	captured by time FE
DEK Special: visitors of Deutsche Evangelische Kirchentag get first 120 min of each rent for free	Dortmund	Jun 19^{th} - 23^{rd}, 2019	exclude days from sample (for all cities)
Durstexpress Collaboration: 3 x 30 min for free with every order from Durstexpress	Leipzig	Aug 15^{th}-18^{th}, 2019	exclude days from sample (for all cities)
Crowdfunding Special: support crowdfunding campaign and get 5 x 30 min for free	all cities	Oct 15^{th}, 2019	captured by time FE
Climate Action Promotion: 2 x 30 min free	all cities	Sep 20^{th}, 2019 - Sep, 22^{nd}, 2019	captured by time FE
Fridays 4 Future Special: 2 x 30 min for free	all cities	Nov 29^{th}, 2019	captured by time FE
Customer Survey Bonus: free day pass	all cities	Dec 12^{th}, 2019 - Jan 8^{th}, 2020	captured by time FE

Note: Presented results were obtained via a search of Nextbike's social media channels

Robustness to Dynamics between Incumbent Bikesharing Platforms

Table 2.21 summarizes the competitive environment in the bikesharing market per each city in scope. Nextbike operates in competitive markets in many of the cities in scope. To exclude the risk of confounding from dynamics with incumbent bikesharing operators, we run an additional robustness test on the subsample of cities without competition from other bike-based platforms.

Table 2.21: Overview of active and new entrant bikesharing platforms during the observation period

City	Count	Call-a Bike	Mobike	Donkey Republic	Byke	Jump	LimeBike
Augsburg	0						
Berlin	6	✓	✓	✓	✓	✓	✓
Bochum	0						
Bonn	1	✓					
Dortmund	0						
Dresden	0						
Duisburg	1				(✓)		
Erfurt	0						
Essen	1				(✓)		
Frankfurt	4	✓	✓		(✓)		✓
Gießen	0						
Hamm	0						
Heidelberg	1	✓					
Innsbruck	0						
Kaiserslautern	1	✓					
Karlsruhe	1	✓					
Kassel	0						
Klagenfurt	0						
Köln	2	✓	✓				
Leipzig	0						
Lippstadt	0						
Ludwigshafen	0						
Luzern	0						
Mannheim	1	✓					
Marburg	0						
Mönchengladbach	0						
Mülheim	1				(✓)		
Norderstedt	0						
Offenburg	0						
Potsdam	0						
Rüsselsheim	0						
St. Pölten	0						
Walldorf	0						
Worms	0						
Würzburg	1	✓					

✓= active throughout entire observation period; ✓ = entry during observation period; (✓) = not fully verifiable due to service having been discontinued since; Presented results were obtained via a web search

Chapter 3

Data-Driven Competitor-Aware Positioning in On-Demand Vehicle Rental Networks[1]

3.1 Introduction

A key trend in urban mobility is the consumption of mobility as a service (MaaS) and on-demand (MoD) (Laporte et al., 2018) heralding the age of shared, fleet-based, transportation platforms and rental networks (Benjaafar and Hu, 2020a; Qi and Shen, 2018). On-demand rental networks have emerged for cars (e.g., Car2Go, DriveNow), bikes (e.g., Nextbike) and more recently, scooters (e.g., Lime, Bird). Shared mobility is characterized by the fact that demand is not only influenced by price but also by local supply as defined in terms of availability (e.g., wait time or distance to the nearest vehicle) (Benjaafar and Hu, 2020a). Therefore, regular fleet balancing via physical repositioning actions is required and has been the subject of extensive

[1]This Chapter has been published in its entirety in the following peer-reviewed academic journal:
Schroer, K., Ketter, W., Lee, T. Y., Gupta, A., & Kahlen, M. (2022). Data-Driven Competitor-Aware Positioning in On-Demand Vehicle Rental Networks. Transportation Science, 56(1), 182–200. https://doi.org/10.1287/trsc.2021.1097. (rated A in the VHB-JOURQUAL 3 ranking).
Earlier versions of this Chapter have also appeared in several (non-copyrighted) peer-reviewed academic conferences:
Schroer, K., Ketter, W., Lee, T. Y., Gupta, A., Kahlen, M. (2019). Optimal management of free-floating vehicle sharing systems under competition. In Workshop on Information Systems and Technology (WITS) 2019 (Munich).
Schroer, K., Ketter, W., Lee, T. Y., Gupta, A., Kahlen, M. (2019). An Online Learning and Optimization Approach for Competitor-Aware Management of Shared Mobility Systems. In Proceedings of the SIG GREEN Workshop 2019 (Munich).
Schroer, K., Ketter, W., Lee, T. Y., Gupta, A., Kahlen, M. (2019). Utilizing Real-Time Competitor Information to Boost Profits for One-Way Transportation Companies. In Workshop on Policy, Awareness, Sustainability, and Systems (PASS) 2019 (Cologne)
Schroer, K., Kahlen, M., Ketter, W., Lee, T. Y., Gupta, A. (2019). Fleet Wars: Leveraging Big Urban Data for Competitor- Aware Predictive Analytics in Free-Floating Shared Mobility Systems. In INFORMS Conference on Information Systems and Technology (CIST) 2019 (Seattle)

research (e.g. Lu et al., 2018; He et al., 2019b). A commonly neglected fact in the literature on shared mobility operations is the competitive environment in which shared mobility platforms and rental networks tend to operate in. Participants compete for a finite number of customers who may switch freely between competing networks (multihoming). Given this situation, own vehicle supply should be considered in the wider context of the competitive market in which users select vehicles based on access and availability. It follows that value may be gained from factoring in the competition's supply decisions into a fleet repositioning decision framework. Existing research, however, treats the fleet repositioning problem as a cost-minimizing task aimed at serving an exogenous observed demand. While overall market demand may indeed be exogenous, this is unlikely to be the case for own observed demand. For example, relocating away from a region or reducing the fleet size to serve the same demand can be reasonably expected to result in a relatively worse competitive positioning of the focal fleet to the benefit of competing networks.

In the new digitalized mobility system the necessary data to incorporate competitive dynamics into the operational decision process of a fleet operator has become abundant. We observe a more and more liberal and standardized provision of real-time data across the mobility industry. Open standards such as the General Bikeshare Feed Specification (GBFS) (NABSA, 2021) or the Mobility Data Specification (MDS) (Open Mobility Foundation, 2021) are increasingly adopted by mobility operators who, in many cases, provide open application programming interfaces (APIs) to their digital platforms that allow for automated and real-time data retrieval. Alternatively, real-time data streams of most mobility platforms are now available commercially from third party data analytics providers (e.g., fluctuo). Furthermore, innovations in city-specific regulations increasingly mandate mobility providers to participate in open data initiatives (e.g., Los Angeles). Such developments are only expected to improve real-time mobility data availability in the future.

The question then remains whether there is sufficient value to be gained from this real-time data to warrant investments into the development of a real-time data analytics and decision framework that incorporates competitor supply information into the operational decision making process? In this research we explore this question by focusing on the vehicle positioning problem, a core challenge in the operation of on-demand vehicle rental networks. We explore how fleet operators can leverage real-time competitor information along with other large-scale urban data sources to make optimal competitor-aware vehicle supply decisions to boost overall market share, utilization and profits. What emerges is a novel decision problem which we term the *Competitor-Aware Shared Vehicle Positioning Problem* (CSVP). The key contribution of our work is to compute the value of real-time competitor information in operational decision making of on-demand rental networks by developing a temporally and spatially flexible online learning and optimization framework to solve the CSVP. Specifically, we formulate a novel dynamic mixed-integer non-linear programming (MINLP) model that produces optimal

competitor-aware positioning decisions for a given spatio-temporal resolution. We address the uncertainty associated with the input parameters of this optimization via a high-accuracy learning model and the online nature of our model which incorporates updated contextual information as it becomes available. A core benefit of this approach is that it reduces the complexity of the downstream optimization allowing for close to real-time solution for large problems. Finally, we evaluate our combined model via extensive simulation and counterfactual testing based on a unique combined dataset of Car2Go and DriveNow rental transactions in the city of Berlin.

The remainder of this paper is structured as follows: in the next Section (Section 3.2) we present a short review of related work. We then describe the predictive and prescriptive modeling approaches of our solution approach (Section 3.3). In Section 3.4 we introduce the discrete event simulation (DES), that we use for evaluation, and present results. We end with a discussion (Section 3.5).

3.2 Related Work

3.2.1 Introduction to On-Demand Vehicle Rental Networks

Shared mobility is widely regarded as a core building block of the future mobility system (Savelsbergh and Van Woensel, 2016; Laporte et al., 2018). It entails the consumption of mobility as an on-demand service. Asset ownership is relegated to third parties (Paundra et al., 2017). Benjaafar and Hu (2020a) distinguish three canonical sharing economy applications: (1) peer-to-peer resource sharing (e.g., BlaBlaCar), (2) on-demand service platforms (e.g., Uber, Lyft) and (3) on-demand rental networks (e.g., Car2Go, Lime). This work focuses on on-demand rental networks. On-demand rental networks in mobility have historically been operated as station-based systems in that vehicles are collected and dropped off at a certain number of fixed stations Nair and Miller-Hooks (2011). Recently, free floating vehicle sharing (FFVS) is emerging as an alternative system. In such flexible, one-way systems, customers are free to pick up and drop off a vehicle at any point within a predefined operating area, providing the benefit of direct point-to-point travel. From an operations management perspective, on-demand rental networks exhibit a range of unique characteristics. These are: (1) the inability to book in advance, (2) the spatial distribution of resources and (3) the one-way characteristic of rentals that do not have to be returned to their point of origin (Benjaafar and Hu, 2020a). These characteristics bring with them novel operations management challenges, ranging from strategic issues such as fleet sizing and service area definition to operational challenges such as spatial and temporal fleet positioning (He et al., 2019b). Here we consider FFVS operations when competition is present, with a particular focus on the repositioning challenge.

3.2.2 Predictive Analytics for On-Demand Vehicle Rental Networks

The emergence of big urban data has resulted in new research opportunities in predictive analytics for operations management (Cohen, 2018). Most existing approaches of FFVS positioning rely on known distributions of (1) demand and (2) trip origin-destination pairs across the spatio-temporal network. Machine learning (ML)-based regression techniques allow for a reduction in the uncertainty of future realizations through accurate point estimates. In situations with as many free parameters as the one we study (market level and focal fleet), using point estimates rather than uncertainty sets can significantly enhance performance and scalability while reducing over-conservativeness of some robust optimization approaches (Hao et al., 2019).

In the domain of vehicle sharing, predictive analytics work has focused on demand prediction. For repositioning applications knowledge on vehicle inflows is equally required. Recent work has shown that the same model architectures can be used to predict both supply and demand (e.g., Xu et al., 2018). FFVS predictive analytics research can be differentiated in terms of (1) the type of model used, (2) the spatial discretization, (3) prediction horizon and (4) whether contextual data is used. In terms of (1) models used, we identify traditional statistical time series

approaches using, for example, SARIMA models (Müller and Bogenberger, 2015), traditional machine learning (ML) approaches (Willing et al., 2017; Kahlen et al., 2017) and more recently deep learning frameworks (Xu et al., 2018; Ai et al., 2019; Zhou et al., 2018; Caggiani et al., 2018). ML models and in particular deep learning models have consistently demonstrated superior performance compared to naive and statistical benchmarks. Spatial discretization (2) is relevant for FFVS applications due to the absence of discrete spatial reference points such as rental stations. A common discretization method is the use of ZIP codes (e.g., Lu et al., 2018). However, this technique suffers from various limitations such as arbitrary and non-uniform shapes and sizes of regions. An alternative approach is the use of grids to discretize the service area into regions of uniform size. In most cases static quadratic (e.g., Zhou et al., 2018) or hexagonal (e.g., Schroer et al., 2019) grids are used. Research in the area of discrete spatial simulations suggests the use of hexagonal geodesic discrete global grid system (GDGGS), due to uniform adjacency of hexagons and limited distortion of a geodesic grid. Regarding (3) prediction horizons, myopic single-step predictions are the standard scenario being studied; although Zhou et al. (2018) perform a multi-period prediction using a deep neural network. The use of contextual data varies by type of model. While statistical and certain deep learning models use historic time series data exclusively (Müller and Bogenberger, 2015; Ai et al., 2019), the additional use of contextual data is commonplace. Typical contextual features employed are: temporal metadata (time of day, day of week), meteorological data (e.g., Xu et al., 2018), points of interest (e.g., Willing et al., 2017; Schroer et al., 2019) and events (e.g., Kahlen et al., 2017). Existing predictive approaches are commonly evaluated in static environments with arbitrarily defined period length and region size. Consequently, there is limited clarity regarding their performance in varying temporal and spatial resolutions and different prediction horizons, in which data might become more sparse. As these are important parameters for the performance of the CSVP solution framework, we investigate them in detail in our work.

3.2.3 Prescriptive Analytics and Empty Positioning Problems for On-Demand Vehicle Rental Networks

The problem of vehicle (asset) allocation and positioning is an emerging area of research in operations management (Benjaafar et al., 2017; Benjaafar and Hu, 2020a; He et al., 2019b) and is related to the problem class of empty repositioning, a special case of the assignment problem (Erera et al., 2009). Vehicle allocation and positioning is especially significant in FFVS systems where, due to the unknown target destination of one-way trips, demand and supply imbalances may occur locally (Benjaafar et al., 2017). FFVS are the subject of this work and we therefore focus our review on this thread of literature. The reader is referred to Pal and Zhang (2017) for a comprehensive review of the literature on repositioning in the context of station-based vehicle sharing systems.

The operations management of FFVS has received increasing attention in recent years. Generally, two distinct approaches to facilitate vehicle repositioning in FFVS exist: (1) operator-based repositioning (e.g. Angelopoulos et al., 2018); and (2) user-based repositioning (e.g. Ströhle et al., 2019; Schiffer et al., 2021). Li and Liao (2020) consider self-relocation of autonomous vehicles, which can be understood as a form of operator-based repositioning at lower cost. Either of the two approaches rely on periodic instructions regarding the number of vehicles to be relocated to and from each region in the service network but vary in terms of relocation cost factor and the degree to which positioning actions can be assumed to be deterministic (Laporte et al., 2018). The objective of the underlying positioning framework usually revolves around minimizing a fleet operator's cost of service (He et al., 2019a), or maximizing profitability and/or quality of service (Lu et al., 2018).

Positioning problems are typically modelled using temporal-spatial networks (Erera et al., 2009). Deterministic (Boyaci et al., 2015; Pal and Zhang, 2017; Schiffer et al., 2021; Caggiani et al., 2018), stochastic (Lu et al., 2018) and robust (He et al., 2019b; Hao et al., 2019; Laporte et al., 2018) mathematical programming approaches as well as greedy simulation-based frameworks (Kahlen et al., 2017) have been proposed to solve the positioning challenge for FFVS. Boyaci et al. (2015) propose a deterministic multi-objective model for fleet sizing under repositioning. Caggiani et al. (2018) propose an integrated prediction and optimization model which uses point-estimates of future demand as input into deterministic optimization-based decision support system.Weikl and Bogenberger (2015) propose a two-stage approach with relocations between macroscopic zones and between microscopic zones inside macro zones. Pal and Zhang (2017) develop an optimization model for bike-based FFVS that accounts for the possibility of multi-vehicle repositionings on trucks. Other studies consider the uncertainty inherent in demand and supply prediction and respond with stochastic frameworks for optimization under uncertainty. Lu et al. (2018) develop two-stage stochastic integer programming models for optimizing strategic parking planning and vehicle allocation for station-based and free-floating carshare systems with the objective of maximizing profit and quality of service (i.e., minimizing unserved rentals). A recent example of robust optimization is provided by He et al. (2019a) who produce a myopic and multi-period robust optimization model assuming random realizations of demand based on learned uncertainty sets. They evaluate their model empirically on a temporal-spatial network with up to five regions and three periods. Hao et al. (2019) attempt to address the commonly observed over-conservativeness of robust approaches. The authors include additional contextual covariates in their estimation of uncertainty sets and derive differentiated demand distributions conditional on weather factors.

We identify various gaps in the existing FFVS literature that this study sets out to address. First, previous studies typically assume that demand and origin-destination probabilities follow learnable unconditional spatio-temporal distributions from which random draws materialize at any given instance. Hao et al. (2019) show how this assumption can lead to overly conservative

re-positioning decisions as contextual factors such as weather, points of interest or events are ignored, all of which have impact on demand (Kahlen et al., 2017). We also find that past research assumes that shared vehicle fleets operate in isolation and that their positioning decision will have no impact on user choice. This is a bold assumption, especially for real-time location-based rental networks, where location (or access) can be regarded as a major source of competitive advantage. Indeed, Braverman et al. (2019) postulate that in ride hailing systems, the availability of vehicles directly corresponds to the probability of a ride being served. However, in competitive situations, availability should be viewed in relative terms, i.e., relative to the availability of competitor vehicles (Balac et al., 2019). Spatio-temporal supply decisions can thus be a source of competitive advantage. Finally, existing approaches tend to focus on small networks with correspondingly large regions. In a FFVS network, availability is usually defined in terms of walking distance, making granular networks more beneficial. We develop a scalable solution approach, which can be applied in practice for network sizes of up to 50 regions, greatly exceeding network sizes used in previous research (e.g., He et al., 2019a) and allowing for highly targeted positioning operations.

3.3 Model

We formulate a data-driven, three-stage online learning and optimization model. In Stage ❶, the system retrieves, processes and combines real-time data from a range of different sources, and updates the underlying multivariate dataset. In Stage ❷, this data serves as the basis for machine-learning models that are retrained in each period to estimate key input parameters for the downstream prescriptive model. In Stage ❸, the estimated parameters are used in a dynamic MINLP optimization framework that computes optimal positioning decisions for all periods in the optimization horizon. Positioning actions for the upcoming period are isolated and executed after which Stage ❶ is repeated. In Sections 3.3.1 to 3.3.3 we discuss these three stages in detail. The CSVP relies on the following assumption. First, we assume non-strategic user behaviour, i.e., we assume that users are indifferent between vehicles of all fleets in the market. This assumption is valid, as vehicle types and price levels between competing networks are comparable in most markets. Customers therefore select vehicles based on access and convenience. Both criteria in turn depend on the relative availability of fleet vehicles per competitor in a given region. We, thus, postulate that the probability of capturing a rental within a given region i and period $[t, t+1]$ is directly proportional to the share of vehicles on the ground within that region and period. We test this assumption empirically for the case of Car2Go and DriveNow and find strong support for it (see Appendix B). Second, we assume that competitors are non-strategic, which is currently the case in most markets in which operators do not engage in competitor-aware operations management. From this assumption it follows that early adopters of CSVP positioning can fully exploit the benefits of our solution approach. We also assume that demand is exogenous and observable, i.e., that there is a fixed demand for shared mobility of a certain mode, which can be monitored and predicted (a common assumption in data-driven demand prediction). Finally, we assume that positioning actions are completed within a single planning period and vehicles become available for rental within that same period. We adopt a structured discretization approach in the construction of the underlying spatio-temporal network across which positioning actions are performed. We distinguish between planning times t where new information is retrieved and new assignment schedules are computed and planning periods $[t, t+1]$ for which these assignment schedules are developed. Overall, we define two temporal parameters. First, we define the length of a period Δt (in unit time). Second, we set the length of the optimization horizon by defining the set of optimization periods as $\mathcal{T}^O$. The length of the optimization horizon is then given by $\Delta O = \Delta t|\mathcal{T}^O|$ (in unit time). The spatial framework we adopt is as follows. We construct a hexagonal geodesic discrete global grid system (GDGGS) as defined in Sahr et al. (2004). A GDGGS is more flexible and allows for relatively easy adjustment of spatial resolution due to the hierarchical nature of tile sizes, a property which is helpful if the set of regions $\mathcal{H}$ is to be flexibly defined. We opt for hexagonal tiles, due to their advantage of uniform adjacency.

3.3.1 Stage ❶: Real-time Contextual Data Inputs for Predictive & Prescriptive Analytics

On-demand rental networks operate modern app-based digital interfaces via which users can start, terminate and pay for rentals. A user has access to accurate information at any given point in time about the amount and location of available vehicles in her vicinity. This data is also accessible at a larger and more automated scale via APIs. This allows mobility companies to retrieve and periodically archive real-time geo-tagged competitor supply information from which trip information (start point, end point, duration) can be extrapolated with relative ease (see Appendix A for more details). Our approach also works if individual vehicle trajectories cannot be tracked which is sometimes made difficult by the non-static vehicle ID used for privacy reasons in some data standards such as the General Bikeshare Feed Specification (GBFS) (NABSA, 2021). It is in fact sufficient to track total supply, inflows and outflows per area and time period (irrespective of individual vehicle trajectories) by regularly counting individual vehicles (as identified by their location) per area and tracking changes. Note that this work relies solely on data streams that are generated in the public space, and which are available freely to any user accessing the digital platform interface. We do not use any price data, which may be critical from a competition regulation standpoint.

One challenge with this approach is that it allows the observation of censored demand only, i.e., demand which is limited by the supply of vehicles. We circumvent this challenge in our demand prediction by removing entries where there is either no supply in a region or where supply has been fully exhausted. In addition, we refrain from employing local supply levels as a predictor of demand and subsequent inflows in our predictive model. Our online learning framework relies on the availability of a rich set of independent variables (features) that capture observed and unobserved patterns in mobility behavior. We create spatial and temporal joins between the datasets and obtain rich feature vectors of 238 features for each spatio-temporal instance. These features can be grouped into five sets, which we describe below. A detailed overview is provided in Online Appendix D.

- **Temporal feature vector** $\mathcal{Z} = (z^1, ..., z^z)$: $z = 35$ temporal features, e.g., the hour of the day, the day of the week, and whether the day is a weekend or holiday. They capture temporal patterns in shared mobility usage.
- **Meteorological feature vector** $\mathcal{W} = (w^1, ..., w^w)$: $w = 6$ meteorological features on temperature, precipitation, cloud cover and wind speed are included. Current weather conditions can have a significant impact on mobility choices (Willing et al., 2017).
- **Geographical feature vector** $\mathcal{G} = (g^1, ..., g^g)$: $g = 105$ features related to POIs are retrieved via Google Maps. We include counts and also capture the relative popularity of a location by counting the number of POIs that have a popularity rating and a price rating.

- **Competitor fleet feature vector** $\mathcal{C} = (c^1, ..., c^c)$: We include $c = 46$ lagged outflows (in number of vehicles). We use lags of one, two and three periods prior as well as one to seven days prior to the period in scope, which were selected based on auto-correlation with the target. We also include lagged inflows per region, as these will have an influence on rental starts in the next period (e.g., via round trips). We also include lagged inflows and outflows aggregated across the entire network which determine the total pool of vehicles that become available for rental or are candidates for inflows in the next periods. We apply lags of one, two and three periods. For both inflows and outflows of competitor vehicles we also include the mean and variance over the past seven days as well as weekly differencing variables that capture any trends in inflows and outflows over the past seven weeks. Note that the required position data is easily obtained in real-time by querying a competitor's mobile app interface.
- **Focal fleet feature vector** $\mathcal{F} = (f^1, ..., f^f)$: We use exactly the same features as for the competitor fleet (i.e., $f = c$).

3.3.2 Stage ❷: Online Predictive Model

We use machine learning (ML) models to predict input parameters for the online optimization. We predict total market demand $\hat{D}^M_{i,t}$ in region i during period $[t, t+1]$ as well as total and focal fleet inflows per region and period ($\hat{I}^M_{i,t}$ and $\hat{I}^O_{i,t}$). Since the proposed feature set captures many observed and latent variables, we use the same comprehensive feature vectors to learn models for each of the above target variables. We propose an online learning approach, retrieving and incorporating new information as it becomes available. This allows dynamic trends and evolution of the system such as changes in consumer behavior or changes in competitor relocation schedules to be incorporated by the model as soon as possible. We use a combined data matrix $\mathbf{S}_{[\mathcal{T}^L]}$ of form

$$\mathbf{S}_{[\mathcal{T}^L]} = (\mathbf{z}^1_{[\mathcal{T}^L]}, ..., \mathbf{z}^z_{[\mathcal{T}^L]}, \mathbf{w}^1_{[\mathcal{T}^L]}, ..., \mathbf{w}^w_{[\mathcal{T}^L]}, \mathbf{g}^1_{[\mathcal{T}^L]}, ..., \mathbf{g}^g_{[\mathcal{T}^L]}, \mathbf{c}^1_{[\mathcal{T}^L]}, ..., \mathbf{c}^c_{[\mathcal{T}^L]}, \mathbf{f}^1_{[\mathcal{T}^L]}, ..., \mathbf{f}^f_{[\mathcal{T}^L]})$$

to train our models, where $\mathcal{T}^L$ is the set of training periods and the individual element matrices $\mathbf{e}^n_{[\mathcal{T}^L]} = (e^n_{\mathbf{1}}, ...e^n_{\mathbf{t_L}})$ consist of vectors of form $\mathbf{e}^n_{\mathbf{t}} = (e^n_{i,t})$, i.e., the realizations of independent variable e across all regions $i \in \mathcal{H}$ in period $[t, t+1]$. We normalize the data by subtracting the mean and scaling to unit variance to enhance statistical stability. To increase performance while reducing the risk of overfitting, we employ regularization techniques inherent to the respective algorithm (such as regularization in linear models or dropout for deep neural networks).

We learn new models per period and location based on a fixed-length moving training window of length $|\mathcal{T}^L|$. $|\mathcal{T}^L|$ is problem specific. Similar to the process of hyperparameter tuning, it can be tailored to the individual application case via a heuristic search over a range of possible

lengths. By comparing predictive performance on a validation set, the best lengths can be identified.

We train models in two types of configurations: (1) a single-period prediction and (2) a multi-period prediction. In the single-period prediction we predict market demand $\hat{D}^M_{i,t}$ as well as total and focal fleet inflows $(\hat{I}^M_{i,t}, \hat{I}^O_{i,t})$ as a function of the respective spatio-temporal realization of features as $\phi_{i,t} : \mathcal{S}_{i,t} \rightarrow \hat{y}_{i,t}$, which is obtained by solving an optimization of form $\min_{\phi^y_{i,t}} \sum_{t \in \mathcal{T}^L} \ell(\phi^y_{i,t}(\mathcal{S}_{i,t}), y_{i,t})$, where ℓ is the selected loss function of the machine learning algorithm. Hence, $\hat{\mathbf{y}}_\mathbf{t} = (\hat{y}_{i,t})$ for all $i \in \mathcal{H}$ is computed as follows:

$$\hat{\mathbf{y}}_\mathbf{t} = \boldsymbol{\phi}_\mathbf{t}(\mathcal{S}_\mathbf{t})$$

In the multi-period case, we predict market demand $(\hat{D}^M_{i,t+n})$, total inflows $(\hat{I}^M_{i,t+n})$ and focal fleet inflows $(\hat{I}^O_{i,t+n})$ for region i in any period $[t+n, t+n+1]$. The prediction is repeated for all $(t+n) \in \mathcal{T}^O$, where $\mathcal{T}^O$ is the set of periods in the optimization horizon. We adapt our feature set because our single-period prediction model uses lagged features from the past period that cannot be observed more than one period ahead. One option is to supplement it with predicted values as we move along the prediction horizon. Alternatively, to avoid prediction error propagation, we may iteratively drop lagged features that have become unobservable for the period in scope. We opt for the latter approach and use the reduced feature vector $\mathcal{S}'$ to derive $\hat{y}_{i,t+n}$. Note that $\mathcal{S}'$ will periodically reduce in size the further ahead in time one wishes to predict. Note also that we do not drop any temporal, meteorological or geographical features (i.e., we do not modify $\mathcal{Z}, \mathcal{W}$ and $\mathcal{G}$) as these are either time-independent or we assume that perfect foresight will be available. Thus, for all realizations further than one period ahead we learn models of form $\hat{\mathbf{y}}_{\mathbf{t+n}} = \boldsymbol{\phi'}_{\mathbf{t+n}}$.

Hyperparameter tuning via brute-force grid-searches is performed on a fixed training dataset using time series cross validation. Hyperparameters are parameters of a machine learning model that are not learned during training but chosen by the user directly (e.g., tree depth in a random forest model or the number of nodes per layer in a deep neural network). Since model results can be highly sensitive to these hyperparameters, careful tuning on a training and validation dataset is required. Test metrics of the final tuned model are reported on a completely unseen test dataset. To obtain accurate test metrics, a moving window validation that most accurately reflects the intended real-world application is adopted. We train the model on a fixed amount of periods $|\mathcal{T}^L|$ and evaluate it on the next period. The length of the training window is selected based on predictive performance. We use the mean absolute error (MAE) as main error. The MAE is a measure for the average absolute error in terms of number of vehicles. Mathematically, it is expressed as $MAE = \frac{1}{|\mathcal{H}||\mathcal{T}^E|} \sum_{i \in \mathcal{H}} \sum_{t \in \mathcal{T}^E} |\hat{y}_{i,t} - y_{i,t}|$, where $\mathcal{H}$ is the set of regions in the dataset and $\mathcal{T}^E$ is the set of evaluation periods. One downside of using the MAE is that model performance comparisons between different resolutions and application

fields is not possible because the error is not scaled in accordance with the baseline value. The mean absolute percentage error is a popular relative metric, which is scale-independent. But the MAPE suffers from several problems; the most serious of which (in relationship to this work) is its inability to handle cases in which the true value is zero (Chen et al., 2017). Therefore, the symmetric mean absolute percentage error (SMAPE) is used, which we define here as $\frac{1}{|\mathcal{H}||\mathcal{T}^E|}\sum_{i\in\mathcal{H}}\sum_{t\in\mathcal{T}^E}\frac{|\hat{y}_{i,t}-y_{i,t}|}{|\hat{y}_{i,t}|+|y_{i,t}|}$.

3.3.3 Stage ❸: Online Prescriptive Model

To take advantage of our ability to periodically compute more precise forecasts of parameters based on real-time information, we focus on online optimization approaches. We develop a dynamic model formulated as a mixed integer non-linear program (MINLP). In a vehicle FFVS context, knock-on effects of positionings on future rental performance may be substantial; a dynamic model is able to exploit these to the fleet manager's advantage. Table 4.2 defines the nomenclature adopted in the following formulations. Our optimization objective can be expressed as follows: "For the $|\mathcal{T}^O|$ upcoming periods, position vehicles across the network in a competitor-aware fashion such that fleet contribution margin is maximized over the optimization horizon". We choose the contribution margin as our objective, as we assume fleet size to be exogenously determined. In such a scenario, the fleet operator has an incentive to maximize contribution margin, i.e., to maximize the proportion of sales revenue not consumed by variable costs and thus able to cover the fixed cost base. What results is a special profit-maximizing form of the assignment problem where $i \in \mathcal{H}$ origin regions are matched by the same number of destination regions $j \in \mathcal{H}$, with $\mathcal{H}$ being the set of regions. Let us define the decision variable $x_{ij,t}$ as the number of vehicles that flow from region i to j during period $[t, t+1]$. The decision variables have both revenue and cost implications. The objective function of our general mathematical model can thus be formulated as follows:

$$\underset{x_{ij,t}}{\text{maximize}} \quad \Pi = \sum_{t\in\mathcal{T}^O}\sum_{i\in\mathcal{H}}(D^M_{i,t}\psi^O_{i,t}\hat{\delta}^M_{i,t}(r^{rent}-c^{rent})) - \sum_{t\in\mathcal{T}^O}\sum_{i\in\mathcal{H}}\sum_{j\in\mathcal{H}}(x_{ij,t}c^{reloc}_{ij,t}) \tag{3.1}$$

The first term in Equation 3.1 describes the contribution margin of each captured trip across the network, where the number of captured trips is controlled by the focal fleet's relative availability $\psi^O_{i,t}$:

$$\psi^O_{i,t} = \frac{A^O_{i,t} + I^O_{i,t} + \sum_{j\in\mathcal{H}}(x_{ji,t} - x_{ij,t})}{A^M_{i,t} + I^M_{i,t} + \sum_{j\in\mathcal{H}}(x_{ji,t} - x_{ij,t})} \tag{3.2}$$

This is equivalent to the assumption that the probability of capturing a rental is proportional to a fleet's relative availability within a region (converged to expectation) and lies at the core of the *competitor-awareness* of our model. Repositioning decision are made based on total market demand $D^M_{i,t}$ and supply $A^M_{i,t} + I^M_{i,t}$ per region, thus factoring in where competitor vehicles are positioned and how many additional inflows can be expected over the period in scope. The second

Table 3.1: Optimization model nomenclature

Symbol	Description	Unit
Sets		
$\mathcal{H}$	Set of regions in network with $\mathcal{H} = \{h_0, h_1, ...h_i\}$ and index i,j	set
$\mathcal{T}^O$	Set of planning times/periods in opt. horizon $\mathcal{T}^O = \{t_1, t_2, ...t_{t^O}\}$ with index t	set
Parameters		
$A_{i,t}^{M,base}$	Base market availability without positioning in region i at start of period $[t, t+1]$	vehicles
$A_{i,t}^{O,base}$	Base focal fleet availability without positioning in region i at start of period $[t, t+1]$	vehicles
c_{ij}^{reloc}	Cost of relocating one vehicle from region i to region j	USD
c^{var}	Specific variable cost of vehicle movement (fuel, wear, etc.)	USD/h
d_{ij}	Shortest path between centroids of region i and j across the road network	km
$\hat{D}_{i,t}^{M}$	Total predicted market demand for trips in region i during period $[t, t+1]$	vehicles
$\Delta D_{i,t}^{O}$	Gained trips in region i during period $[t, t+1]$ due to relocations	vehicles
$\hat{\delta}_{i,t}^{M}$	Avg. expected length per rental in region i during period $[t, t+1]$	h
$H_{i,t}^{max}$	Maximum available parking capacity of region i during period $[t, t+1]$	vehicles
$\hat{I}_{i,t}^{M}$	Total predicted inflows of all vehicles in region i during period $[t, t+1]$	vehicles
$\hat{I}_{i,t}^{O}$	Total predicted inflows of focal fleet vehicles in region i during period $[t, t+1]$	vehicles
M_{t}^{max}	Maximum number of relocations during period $[t, t+1]$	relocs
ΔO	Length of optimization horizon	unit time
$\psi_{i,t}^{O,base}$	Relative base vehicle availability of focal fleet in region i during period $[t, t+1]$	ratio
r^{rent}	Specific revenue per rental	USD/h
$s_{i,t}^{O}$	Density share of focal fleet vehicles in region i during period $[t, t+1]$	%
Δt	Length of an individual period $[t, t+1]$	h
ΔW	Length of the planning window	h
$\Delta x_{i,t}$	Net number of relocations to region i during period $[t, t+1]$	vehicles
State variables		
$A_{i,t}^{M}$	Total availability of all fleet vehicles in region i at time t	vehicles
$A_{i,t}^{O}$	Total availability of focal fleet vehicles in region i at time t	vehicles
$D_{i,t}^{M}$	Total market demand in region i during period $[t, t+1]$	vehicles
$I_{i,t}^{M}$	Total market inflows fleet vehicles in region i during period $[t, t+1]$	vehicles
$I_{i,t}^{O}$	Total inflows of focal fleet vehicles in region i during period $[t, t+1]$	vehicles
$\psi_{i,t}^{O}$	Relative vehicle availability of focal fleet in region i during period $[t, t+1]$	ratio
Decision & target variables		
Π	Focal fleet operator's contribution margin over optimization horizon $\mathcal{T}^O$	USD
$x_{ij,t}$	Number of focal fleet vehicles to be relocated from tile i to j in period $[t, t+1]$	relocs

term of the objective function sums the cost of positionings across the network, which depends on $c_{ij,t}^{reloc}$ and the decision variables $x_{ij,t}$. $c_{ij,t}^{reloc}$ denotes the cost of relocating a single vehicle from region i to region j during time-period t. Note, that we are dealing with a concave objective function, which is maximized, as can be readily seen by taking the second derivative (which is negative for all values of $x_{ji,t} - x_{ij,t}$ that lie within the constraints of this problem). Consequently a global optimum exists for the CSVP. The resulting mixed integer non-linear program (MINLP) can be solved with state-of-the-art modeling frameworks (Kröger et al., 2018). Similar to He et al. (2019b) we allow for the fact that the value of an individual rental may vary across time and space, which is captured by the factor $\hat{\delta}_{i,t}^{M}$.

The optimization is subject to a number of constraints. We first ensure that the decision variables only take on positive integer values.

$$x_{ij,t} \geq 0, \quad \forall i,j \in \mathcal{H}, \quad \forall t \in \mathcal{T}^O \tag{3.3}$$

$$x_{ij,t} \in \mathbb{Z}, \quad \forall i,j \in \mathcal{H}, \quad \forall t \in \mathcal{T}^O \tag{3.4}$$

Also, to conserve the number of vehicles, we ensure that the net number of vehicles being relocated from a tile does not exceed the vehicle availability within that tile at the start of a period. This ensures that the relocation schedule can always be executed and that the operator does not have to wait for any natural inflows to arrive in the region i for subsequent repositioning.

$$\sum_{j \in \mathcal{H}} (x_{ij,t} - x_{ji,t}) \leq A^O_{i,t}, \quad \forall i \in \mathcal{H}, \quad \forall t \in \mathcal{T}^O \tag{3.5}$$

Equally, as market demand will be limited by the available vehicles within a region, we implement the following constraints, which guarantee that $D^M_{i,t}$ will be either equal to the lower of predicted demand $\hat{D}^M_{i,t}$ or total available vehicles. Note that as per the definition of $\psi^O_{i,t}$ this also guarantees that own captured demand $D^M_{i,t}\psi^O_{i,t}$ cannot exceed own vehicle availability.

$$D^M_{i,t} \leq \hat{D}^M_{i,t} \quad \forall i \in \mathcal{H} \quad \forall t \in \mathcal{T}^O \tag{3.6}$$

$$D^M_{i,t} \leq A^M_{i,t} + I^M_{i,t} + \sum_{j \in \mathcal{H}} (x_{ji,t} - x_{ij,t}), \quad \forall i \in \mathcal{H}, \quad \forall t \in \mathcal{T}^O \tag{3.7}$$

Consequently, if market demand is not fulfilled, inflows will reduce. We implement this by adjusting state variable $I^M_{i,t}$ by the lost demand in the previous period $\Delta D^M_{t-1} = \sum_{i \in \mathcal{H}} (D^M_{i,t-1} - \hat{D}^M_{i,t-1})$ allocated proportionately across the network. In our simulation we consider the stochasticity in this process by allocating inflows in a probabilistic manner.

$$I^M_{i,t_0} = \hat{I}^M_{i,t_0}, \qquad \forall i \in \mathcal{H} \tag{3.8}$$

$$I^M_{i,t} \leq \hat{I}^M_{i,t} + \Delta D^M_{t-1} * \frac{\hat{I}^M_{i,t}}{\sum_{i \in \mathcal{H}} \hat{I}^M_{i,t}}, \qquad \forall i \in \mathcal{H}, \ \ \forall t \in \{t_1, t_2, ...t_{tO}\} \tag{3.9}$$

We also impose $I^M_{i,t} \geq 0$ as per definition. A further practical constraint is added to the model, reflecting relocation capacity in terms of the maximum number of relocations M^{max}_t:

$$\sum_{i \in \mathcal{H}} \sum_{j \in \mathcal{H}} (x_{ij,t}) \leq M^{max}_t, \quad \forall t \in \mathcal{T}^O \tag{3.10}$$

Finally, we consider the fact that parking capacity $H_{i,t}^{max}$ may be limited in a specific region, for which we add the following constraint:

$$A_{i,t}^{M} + I_{i,t}^{M} + \sum_{j \in \mathcal{H}} (x_{ji,t} - x_{ij,t}) - D_{i,t}^{M} \leq H_{i,t}^{max}, \quad \forall i \in \mathcal{H}, \quad \forall t \in \mathcal{T}^{O} \tag{3.11}$$

We also add constraints to initialize and update the $A_{i,t}^{O}$ and $A_{i,t}^{M}$ state variables in line with the relocation decisions, as well as inflows and outflows.

$$A_{i,t_0}^{O} = A_{i}^{O,base}, \qquad \forall i \in \mathcal{H} \tag{3.12}$$

$$A_{i,t}^{O} = A_{i,t-1}^{O} + I_{i,t-1}^{O} + \sum_{j \in \mathcal{H}} (x_{ji,t-1} - x_{ij,t-1}) - D_{i,t-1}^{M} \psi_{i,t-1}^{O}, \qquad \forall i \in \mathcal{H}, \ \ \forall t \in \{t_1, t_2, ...t_{t^O}\} \tag{3.13}$$

$$A_{i,t_0}^{M} = A_{i}^{M,base}, \qquad \forall i \in \mathcal{H} \tag{3.14}$$

$$A_{i,t}^{M} = A_{i,t-1}^{M} + I_{i,t-1}^{M} + \sum_{j \in \mathcal{H}} (x_{ji,t-1} - x_{ij,t-1}) - D_{i,t-1}^{M}, \qquad \forall i \in \mathcal{H}, \ \ \forall t \in \{t_1, t_2, ...t_{t^O}\} \tag{3.15}$$

As positioning actions typically result in a delta in rentals captured by the focal firm, focal fleet inflows will change by the same amount. Because these effects will not yet be reflected in the forecast of focal fleet inflows ($\hat{I}_{i,t}^{O}$), we use a state variable $I_{i,t}^{O}$ to track additional inflows that result from additional or lost rentals. $I_{i,t}^{O}$ is initialized and updated as follows:

$$I_{i,t_0}^{O} = \hat{I}_{i,t_0}^{O}, \qquad \forall i \in \mathcal{H} \tag{3.16}$$

$$I_{i,t}^{O} \leq \hat{I}_{i,t}^{O} + \Delta D_{t-1}^{O} * \frac{\hat{I}_{i,t}^{M}}{\sum_{i \in \mathcal{H}} \hat{I}_{i,t}^{M}}, \qquad \forall i \in \mathcal{H}, \ \ \forall t \in \{t_1, t_2, ...t_{t^O}\} \tag{3.17}$$

We also impose $I_{i,t}^{O} \leq I_{i,t}^{M}$ as per the definition. ΔD_{t}^{O} is evaluated against an expected total base demand across all regions $\hat{D}_{t}^{O,base}$ that would have materialized if no positionings had taken place. It is defined as:

$$\Delta \hat{D}_{t}^{O} = \sum_{i \in \mathcal{H}} \hat{D}_{i,t}^{M} \psi_{i,t}^{O} - \sum_{i \in \mathcal{H}} \hat{D}_{i,t}^{M} \psi_{i,t}^{O,base} \tag{3.18}$$

Where $\psi_{i,t}^{O,base}$ is computed analogously to $\psi_{i,t}^{O}$ in Equation 3.2 but substituting $A_{i,t}^{O,base}, A_{i,t}^{M,base}$ and $\hat{I}_{i,t}^{O}$, where $A_{i,t}^{O,base}$ and $A_{i,t}^{M,base}$ are initialized and updated analogously to $A_{i,t}^{M}$ and $A_{i,t}^{O}$ in Equations (3.12) through (3.15) but letting $x_{ij,t} = 0$ for all $i, j \in \mathcal{H}$ and $t \in \mathcal{T}^{O}$.

3.4 Experimentation

We employ a simulation experiment to test our model. We simulate positioning actions over a full week. This allows us to capture daily and weekly patterns and to investigate the impact of any cascading effects of positioning actions in later periods. We draw on the case of Car2Go (focal fleet) and DriveNow (competitor fleet), two major free-floating car sharing operators to test our model. Given that fleet size and market shares are comparable for both fleets, the choice of focal fleet is random in our case. We select Berlin, a large competitive car sharing market as geographical focus. While Car2Go and DriveNow have since merged, the case of competitor-awareness in Berlin remains relevant due to the recent entry of WeShare and Miles, two new free-floating car rental networks. In this section we describe the setup of our simulation framework, we introduce the empirical real-time data (Stage ❶), we report results of the learning model (Stage ❷) and discuss the results of the online optimization (Stage ❸).

3.4.1 Discrete Event Simulation Framework

For a realistic evaluation of our model, we construct a discrete event simulation (DES) framework. Exogenous parameters such as market-level demand $D^M_{i,t}$ are retrieved and used as observed in the real world. Factors that are endogenous to the positioning decisions made by our model, i.e., vehicle availability and focal fleet inflows, are updated periodically. We thus capture any future downstream effects that arise from relocation decisions made in a given period. The simplified simulation algorithm is detailed in Appendix C.

We simulate over a randomly selected 1-week window to ensure that weekly and daily seasonality are reflected and that all cascading effects from previous positioning actions are captured. To validate our DES, we run baseline simulations without any positioning actions. These baseline simulations result in minor discrepancies in the number of rentals captured by the focal fleet of just 1.3% versus observed values. Our simulation model thus reflects reality very closely.

3.4.2 Descriptive Statistics on Real-Time Contextual Data (Stage ❶)

We utilize a roughly 5-month window of car sharing demand data covering the period from December 1st, 2016 to April 26th, 2017. The data contains information on availability of vehicles (identifiable via a vehicle ID) and their position at a granularity of five minutes. To construct the hexagonal GDGGS and to create spatio-temporal merges between the datasets, we draw on open source GIS libraries in Python (particularly H3, Geopandas (Jordahl et al., 2020)). We retrieve a network graph representation of Berlin's road network via OpenStreetMap. Distance d_{ij} between regions are determined via shortest path computation across this road network.

We define three spatial sets. First, we define a fine set $\mathcal{H}^f$ with $|\mathcal{H}^f| = 50$ (approx. 1.0km edge length). Using the properties of the underlying GDGGS we aggregate up to a medium-coarse set $\mathcal{H}^m$ with $|\mathcal{H}^m| = 15$ (approx. 3.0km edge length) and a coarse set $\mathcal{H}^c$ with $|\mathcal{H}^c|$

= 4 (approx. 8.5km edge length). For each spatial resolution, we compile two different sets of varying period length with Δt = 1h and Δt = 6h. We choose these to explore trade-offs between temporal resolution and predictive performance. From a practical perspective, different applications may require different resolutions. Table 3.2 shows the information content per spatio-temporal resolution. We report the average number of inflows/outflows per record and their standard deviation (in parentheses). Information on the sparsity of data is crucial in the interpretation of predictive performance.

Table 3.2: Information content (mean and standard deviation (in parentheses) of outflows/inflows per record) per spatio-temporal resolution

	$\mathcal{H}^c$		$\mathcal{H}^m$		$\mathcal{H}^f$	
	1h	6h	1h	6h	1h	6h
Density of $D^M_{i,t}$	152.7 (155.3)	916.2 (878.4)	40.6 (61.3)	243.8 (351.1)	12.1 (14.5)	72.4 (79.9)
Density of $I^M_{i,t}$	152.7 (155.2)	916.2 (872.9)	40.6 (61.7)	243.8 (351.5)	12.1 (14.9)	72.4 (81.4)
Density of $I^O_{i,t}$	70.5 (74.5)	422.9 (422.2)	18.8 (28.1)	112.7 (159.6)	5.6 (6.9)	33.6 (36.6)

We also explore the spatio-temporal patterns in rental demand (inflows exhibit very similar patterns and are not shown here). Figure 3.1 illustrates the considerable similarities in spatial rental patterns clustered along the several sub-centers of Berlin. Figure 3.2 provides an overview

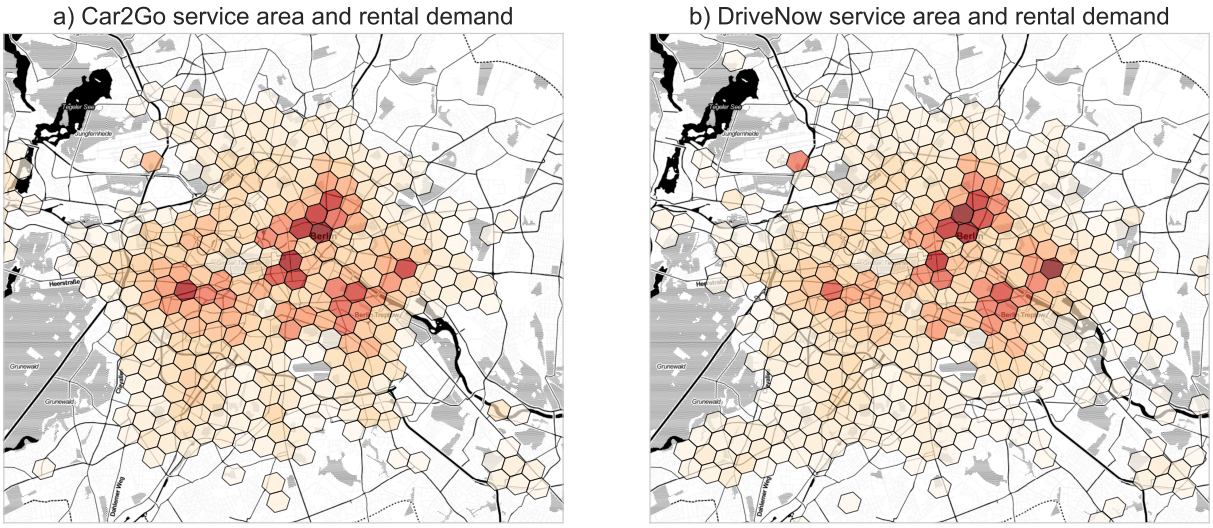

Figure 3.1: Spatial patterns of rental demand in Berlin (Car2Go (left) and DriveNow (right))

of the temporal demand patterns. A weekly trend can be observed in the distributions of daily demand with peaks on Fridays and Saturdays followed by lows on Sundays. Intra-daily seasonality also follows clear patterns with peaks at 5pm and valleys during the night.

3.4.3 Performance of Online Predictive Model (Stage ❷)

We benchmark six different ML models, which we briefly explain in the following.

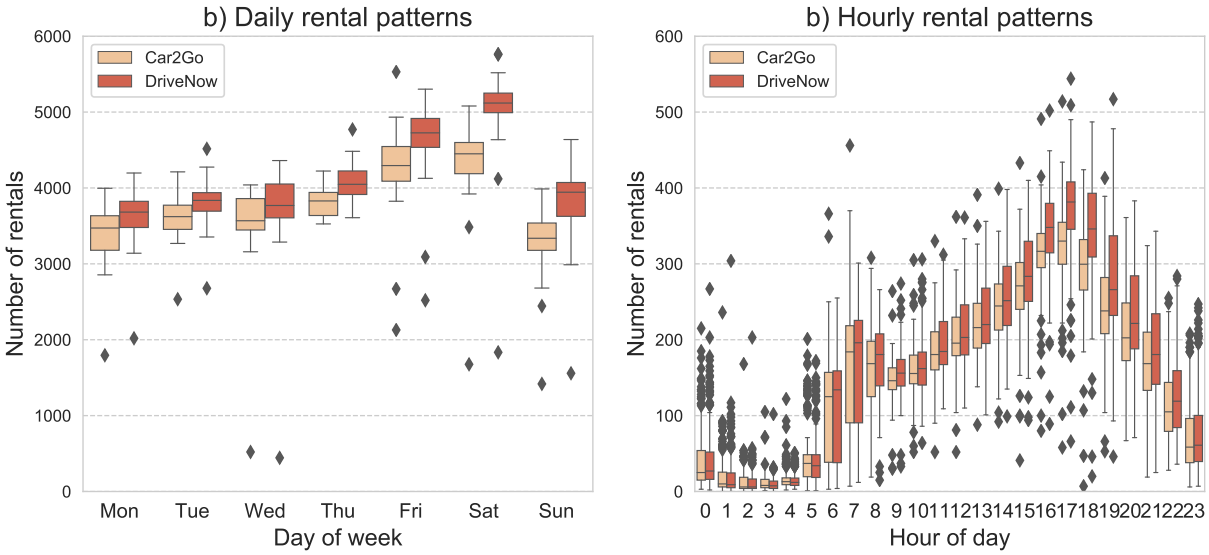

Figure 3.2: Temporal patterns of rental demand in Berlin

- **Linear model (ML-LIN)**: Previous studies have successfully employed linear models for mobility demand prediction in a car sharing context (e.g., Willing et al., 2017). To control model complexity and avoid overfitting, we employ $\ell 1$-regularization. The regularization factor λ is determined via a grid search.
- **Support Vector Machine (ML-SVM)**: Support vector machines have shown to be promising in regression settings. We use a radial-basis-function (RBF) kernel, which is able to capture non-linear relationships. We set ϵ (the margin within which no error is attributed in the training loss function) to 0.4. This will result in no error once rounding has been applied. The regularization C (corresponding to $\ell 2$-regularization) is determined via a grid search.
- **Gradient tree boosting (ML-TREE)**: Gradient-boosted tree-based regression is a non-parametric ML method, using tree-based decision rules to make predictions. Again, inherently non-linear relationships can be represented. Gradient boosting is an ML technique using ensembles of weak models (in our case decision trees) in a step-wise fashion, with each subsequent model minimizing the residuals of the preceding ensemble. We choose MAE as the loss function and determine hyperparameters, including the number of decision trees, the learning rate and the maximum tree depth via a grid search.
- **NN (ML-NN1/2/3)**: We also test three different (deep) neural network (NN) topologies with one, two and three hidden layers respectively. We implement the NNs using Keras (Chollet et al., 2015) and use grid searches to tune the typical hyperparameters in a NN, i.e., batch size, number of epochs, dropout rate (regularization) and the number of neurons per layer. Batch size and epochs define the learning process of the NN. NNs are (re-)trained iteratively on subsets of the training data (batches). One epoch is a full training cycle over

the entire dataset. Regularization (controlled via dropout rate) is a method for controlling overfitting of a ML model. In the case of NNs, this can be achieved by dropping selected nodes to reduce overall model complexity, thus improving predictive performance. We select ADAM (Kingma and Ba, 2015), a common optimization algorithm for deep neural networks as optimizer and use rectifier linear units (ReLU) as activation functions. Each node (neuron) in a NN transmits a signal to the next node only if it is activated by its preceding inputs. The threshold at which this activation happens is determined by the activation function. In NNs, non-linear functions with non-constant derivatives are typically used, of which ReLU is one of the most common and efficient choices. Our loss function is again the MAE, as this is the core metric we want to optimize for (i.e., we want to minimize the absolute number of vehicles the model is off on average).

As additional benchmarks we use the following three models:

- **Persistence (PER) model**: The PER naively predicts that the demand of the next period is equal to the realized demand of the previous period.
- **Historical average (HA) model**: The HA uses a moving average of the three most correlated historical periods to predict the next period. The respective periods are chosen based on auto-correlation with the target over the 80 days training period (see Appendix D).
- **Seasonal Autoregressive Integrated Moving Average (SARIMA) model**: A SARIMA model is used as a third benchmark.

All grid searches are performed using timeseries cross-validation on the 80-day training period (starting from the beginning of the data collection window). The results are documented in Appendix D. To obtain realistic test metrics, we use a moving window validation as described in Section 3.3.2. We keep our training window fixed at 80 days of data (see Appendix D for details on choice of training period). All prediction results are post-processed by rounding to the nearest integer. In Table 3.3 we report MAE and SMAPE per model as evaluated on the full dataset minus the 80 day training window. All ML approaches are superior to both naive prediction methods (PER, HA) as well as statistical time series techniques (SARIMA) across all spatio-temporal resolutions for which we test. This highlights the value of using contextual and competitor data to enhance prediction quality and reduce any uncertainty related to the future realizations of decision parameters. Among the models we test for, deep NN topologies along with the linear model seem to perform best. The advantage of NNs is particularly pronounced where information density is high (coarse spatial and low temporal resolution), a factor which is commonly observed with relatively data-hungry frameworks such as deep learning. The best-in-class models for each resolution are highlighted in Table 3.3. We use these in all further simulations. All best-in-class models can be trained in under 3.0 minutes for their respective spatio-temporal resolution (on a machine with 128 GB RAM and 24 cores) and are therefore suitable for online-learning.

Table 3.3: Benchmark model performance in terms of MAE and SMAPE (in parentheses) for different spatio-temporal resolutions (shown here for $D^M_{i,t}$)

	$\mathcal{H}^c$		$\mathcal{H}^m$		$\mathcal{H}^f$	
	1h	6h	1h	6h	1h	6h
PER	29.0 (17.4%)	553.6 (37.7%)	9.4 (24.7%)	149.1 (35.6%)	4.1 (29.9%)	45.8 (36.9%)
HA	29.3 (18.1%)	394.4 (26.8%)	9.1 (24.5%)	106.3(25.4%)	3.8 (28.1%)	32.6 (26.1%)
SARIMA	18.3 (13.2%)	125.8 (11.4%)	7.0 (21.7%)	38.8 (14.7%)	3.5 (26.3%)	14.9 (15.8%)
ML-LIN	12.7 (10.2%)	54.7 (6.3%)	5.0 (18.1%)	18.7 (9.0%)	2.7 (22.7%)	9.5 (11.1%)
ML-SVM	13.7 (11.1%)	60.4 (6.8%)	5.8 (20.3%)	21.2 (9.7%)	3.1 (24.5%)	10.1 (11.3%)
ML-TREE	13.6 (11.7%)	62.2 (5.7%)	5.3 (18.9%)	19.7 (8.7%)	2.8 (22.9%)	**9.2** (10.4%)
ML-NN1	13.9 (10.8%)	75.1 (6.1%)	5.1 (19.4%)	22.1(9.5%)	**2.7** (22.2%)	10.4 (10.6%)
ML-NN2	12.7 (10.4%)	**49.3** (5.5%)	**5.0** (17.9%)	18.4 (9.0%)	3.0 (24.7%)	9.5 (10.3%)
ML-NN3	**11.6** (10.5%)	49.8 (5.7%)	5.4 (19.9%)	**18.0** (9.0%)	3.0 (23.9%)	9.3 (10.6%)

Note: Best-in-class models highlighted in bold font

In Figure 3.3 we review the impact of resolution on ML performance. We obtain high predictive accuracy achieving a SMAPE of considerably below 10% using the coarsest set of regions $\mathcal{H}^c$ and lowest temporal resolution. This is in line with our expectations, as high aggregation levels tend to smooth out the variance in the data, leading to better predictability. Overall, we achieve nearly identical predictive performance for outflows and inflows, which seems intuitive given their strong time-shifted correlation per location. We also observe performance trade-offs for temporal resolution, with 6h period lengths being considerably more predictable. We find that the performance penalty attributable to temporal resolution is largely constant for the different spatial resolutions (trade-off curve shifted upward in Figure 3.3). Predictive results obtained for $I^O_{i,t}$, while exhibiting similar trade-off characteristics, are typically slightly worse than those obtained for the market-level targets. We explain this with the lower amounts of information content in our data and higher variance compared to the combined market-level data (see Table 3.2). Figure 3.4 shows the relative performance penalty of forecasting further into the future as compared with the MAE of predicting just one period ahead. In general, predicting further ahead into the future comes at a penalty (Ketter et al., 2012). This is to be expected as highly predictive features such as previous realizations become unobservable as we move further into the future. In our case, this penalty can be up to 18% higher MAE versus a single-period forecast for certain spatio-temporal resolutions. We review the impact of these performance penalties on relocation decisions in later simulations.

3.4.4 Performance of Online Optimization Model (Stage ❸)

We implement the online optimization as defined mathematically in Section 3.3.3 in Julia using the Julia Mathematical Programming (JuMP) (Lubin and Dunning, 2015) framework and the Juniper branch and bound MINLP solver (Kröger et al., 2018) with IPOPT (Wächter and Biegler, 2006) as the non-linear programming solver and CPLEX as the mixed-integer program-

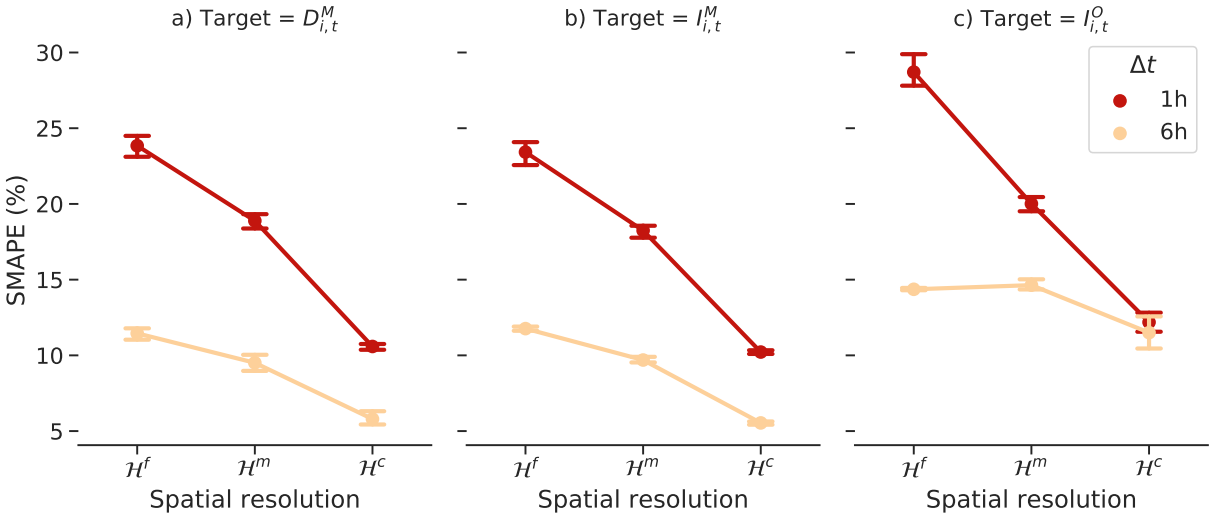

Figure 3.3: SMAPE of best-in-class model for different spatio-temporal resolutions and targets (total demand (a), total inflows (b), focal fleet inflows (c)) (error bars indicate range across prediction horizons)

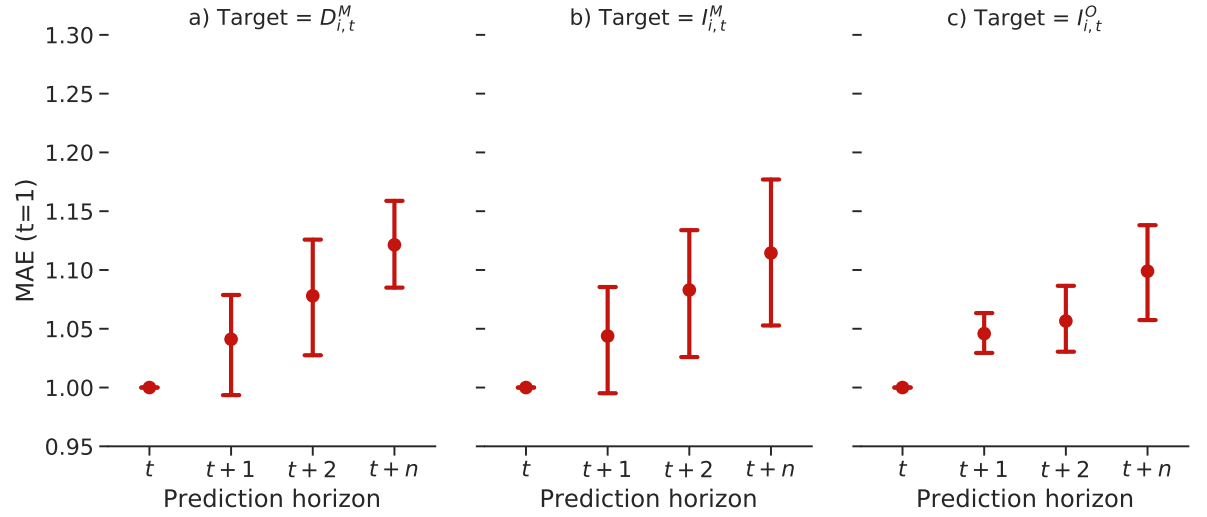

Figure 3.4: Normalized MAE (t=1) of best-in-class model for different prediction horizons and targets (total demand (a), total inflows (b), focal fleet inflows (c)) (error bars indicate range across different spatio-temporal resolutions)

ming solver used in the feasibility pump (Kröger et al., 2018). For practical reasons and given the online nature of our approach we impose a time limit of 900s on the optimization. The optimization runs all solve within that time limit. For a thorough evaluation we vary parameters related to spatial resolution ($\mathcal{H} = [\mathcal{H}^c, \mathcal{H}^m, \mathcal{H}^f]$), temporal resolution ($\Delta t = [1\text{h}, 6\text{h}]$), foresight ($|\mathcal{T}^O| = [1,2]$) and information availability $\mathcal{I}$ (perfect parameter information (PI) and forecast parameters (FI)). This parameterization results in a problem size that is significantly larger than those considered in previous research. He et al. (2019a), for example, test prediction horizons of up to three periods in a network with up to five regions. We argue, however, that in

a micro-mobility setting where location is defined in terms of walking distance, smaller regions are more realistic and accurate.

We parameterize two types of relocation cost c_{ij}^{reloc}: one cost parameter for human operator-based relocation ($c_{ij}^{reloc,hum} = d_{ij}\ (c^{var} + c^{hum})$) and one cost for free relocation (e.g., free rides offered to users or autonomous vehicles) case ($c_{ij}^{reloc,aut} = d_{ij}\ (c^{var} + 0)$). We let the specific variable cost per km c^{var} equal to USD 0.175 per km (includes fuel and degradation cost) and the operator-based relocation cost c^{hum} equal to USD 0.7 per km (i.e., roughly 50% of a NYC taxi fee). We define r^{rent} = USD 0.4 per minute, which corresponds to typical fee levels in car sharing. We let $H_{i,t}^{max}$ equal to the maximum observed market availability plus inflows per region i in the dataset. We do not set a limit for M_t^{max}. For the purpose of the optimization, we let $\hat{\delta}_{i,t}^{M} = \bar{\delta}_{i,t}^{M}$, where $\bar{\delta}_{i,t}^{M}$ is the average rental length across the three most correlated historic periods per region. In the simulation we use the true observed realizations of $\delta_{i,t}^{M}$. For performance evaluation we use three KPIs (all evaluated against the base case of current policies as observed in the data): (1) average number of positioning actions N per period over the simulation horizon, (2) percentage gain in unit revenue ρ over the simulation horizon and (3) percentage gain in unit profit π over the simulation horizon, where profit is defined as the contribution margin Π minus depreciation and fixed costs directly attributable to the vehicle. Tables 3.4 and 3.5 summarize the results. We observe that the finer the spatio-temporal granularity, the higher the theoretical benefits that can be obtained via CSVP positioning. With finer granularity, the potential for identifying local imbalances and opportunities for local availability optimizations rise. As distances between regions become smaller and relocation costs decrease, more positioning actions are initiated to benefit from these opportunities in a profitable manner. This is especially true for high temporal granularity, in which the larger amount of positioning windows over a day drives CSVP performance. Theoretical unit profit gains at the finest granularity ($\Delta t = 1h$, $\mathcal{H}^f$) are up to 7.5% for free positioning and 3.0% for operator-based positioning. Dynamic models are more effective than myopic models in all cases. We also find that prediction quality has a strong impact on performance. While results using predicted values are on par with the perfect information case for the $\mathcal{H}^c$ spatial resolution, the performance penalties at $\mathcal{H}^f$ are considerable - particularly for the dynamic models where prediction errors seem to amplify across the optimization horizon. Another effectiveness driver is positioning costs. While FREE positioning allows for more frequent positioning actions, it is also more susceptible to prediction error compared to OPR positioning, which compensates prediction errors as a result of more conservative positioning strategies due to higher cost.

At $\Delta t = 6h$ the best performing model using forecast parameters is the dynamic model at high spatio-temporal resolution in which a good trade-off is reached and profit gains of 2.8% and 1.5% respectively are achieved. We observe similar patterns for a temporal resolution of $\Delta t = 1$h. While theoretical improvements are higher owing to the larger amount of positioning windows over a day, absolute losses due to prediction errors are also higher. We achieve the

best performance under FREE positioning for predicted values of 3.1% for a dynamic model and $\mathcal{H}^f$. Under OPR positioning, improvements of 1.8% are feasible using a dynamic model and the best performing model at $\Delta t = 6$h is not reached. Given the relatively small improvement for hourly positioning which comes at the cost of considerably more positioning actions and much longer computation times (especially for FREE positioning), we opt for a temporal resolution of $\Delta t = 6h$ in all following simulations. This corresponds to four positioning windows per day with optimization times below 1 minute, which is considered feasible in practice.

Table 3.4: Optimization results for different spatial resolutions ($\mathcal{H}$), different optimization horizon lengths ($|\mathcal{T}^O|$) and different information cases ($\mathcal{I}$) at $\Delta t = 6h$

			Avg. positioning actions (#/period)		Unit revenue gain (%)		Unit profit gain (%)	
$\mathcal{H}$	$\|\mathcal{T}^O\|$	$\mathcal{I}$	FREE	OPR	FREE	OPR	FREE	OPR
$\mathcal{H}^f$	MYO	PI	170.9	56.9	3.4	2.4	3.2	2.1
		FI	130.3	61.8	1.7	1.3	1.4	0.7
	DYN	PI	239.5	62.2	4.5	2.7	4.5	2.5
		FI	252.5	70.5	0.4	1.1	0.2	0.5
$\mathcal{H}^m$	MYO	PI	58.1	4.0	3.0	1.1	3.1	1.2
		FI	61.1	4.0	2.6	1.0	2.6	1.1
	DYN	PI	43.0	5.1	3.4	1.5	3.6	1.6
		FI	46.0	6.0	2.7	1.4	2.8	1.5
$\mathcal{H}^c$	MYO	PI	3.9	0.0	0.7	0.0	0.7	0.0
		FI	2.9	0.0	0.7	0.0	0.7	0.0
	DYN	PI	6.2	0.0	0.9	0.0	1.0	0.0
		FI	4.3	0.0	0.9	0.0	1.0	0.0

Table 3.5: Optimization results for different spatial resolutions ($\mathcal{H}$), different optimization horizon lengths ($|\mathcal{T}^O|$) and different information cases ($\mathcal{I}$) at $\Delta t = 1h$

			Avg. positioning actions (#/period)		Unit revenue gain (%)		Unit profit gain (%)	
$\mathcal{H}$	$\|\mathcal{T}^O\|$	$\mathcal{I}$	FREE	OPR	FREE	OPR	FREE	OPR
$\mathcal{H}^f$	MYO	PI	118.6	22.7	5.5	2.7	4.4	1.4
		FI	101.3	18.6	4.1	1.7	3.1	0.7
	DYN	PI	120.2	23.4	8.2	4.1	7.5	3.0
		FI	111.8	19.7	4.3	2.0	3.1	0.8
$\mathcal{H}^m$	MYO	PI	18.9	0.4	4.8	1.3	4.8	1.4
		FI	15.7	0.5	2.5	1.2	2.3	1.3
	DYN	PI	20.5	0.9	4.9	2.6	4.9	2.8
		FI	18.0	0.9	2.0	1.7	1.6	1.8
$\mathcal{H}^c$	MYO	PI	1.0	0.0	1.4	0.0	1.5	0.0
		FI	0.9	0.0	1.3	0.0	1.4	0.0
	DYN	PI	1.8	0.0	1.2	0.0	1.2	0.0
		FI	1.7	0.0	1.3	0.0	1.3	0.0

3.4.5 Benchmarks and What-if Analyses

We benchmark our results against relevant alternative approaches and test a range of what-if analyses to explore sensitivities. For all instances we choose the previously identified best trade-off model setting under predicted parameters as test case (dynamic, $\mathcal{H} = \mathcal{H}^m$, $\Delta t = 6h$). First, we compare our model against the alternative of purchasing and deploying more vehicles. We increase the focal fleet's vehicle supply by $f_S^O S^M$ proportionately across the network, where f_S^O is the focal fleet vehicle supply growth factor. Our simulations show (see Figure 3.5), that in the absence of smart competitor-aware positioning, the focal fleet would have to increase fleet size by an f_S^O of 7% (FREE positioning) and 4% (OPR positioning) to achieve a comparable increase of 2.7% or 1.5% in absolute revenue respectively. This corresponds to an absolute growth of the fleet of 16.2% and 9.2%. Increasing fleet size, however, has adverse effects on unit economics as shown in Figure 3.5b). Under fleet expansion, unit profit would decline by -13.5% or -7.8 % depending on the positioning case. At the same revenue growth the CSVP model would incur unit profit gain of +2.8% or +1.5%, thus highlighting the value of our approach.

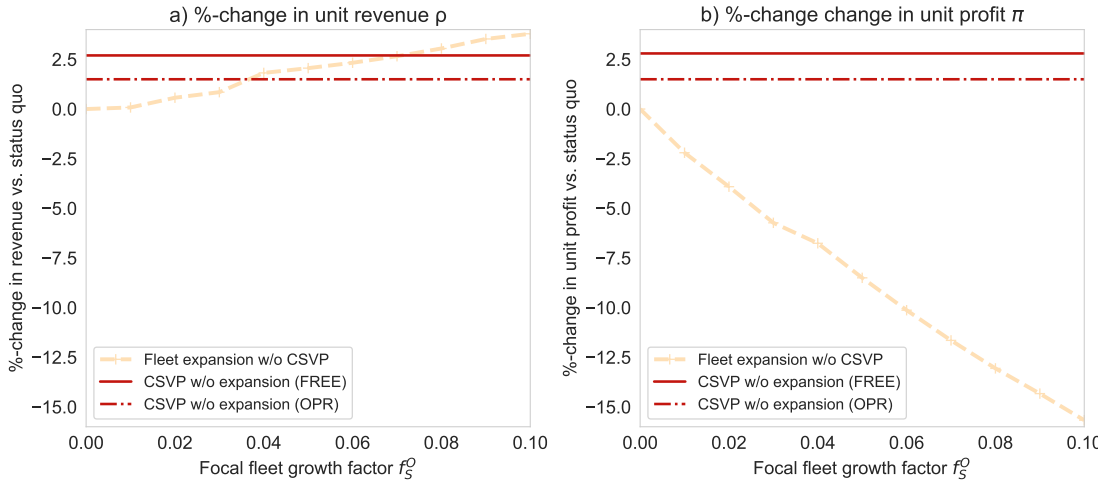

Figure 3.5: Benchmark of fleet expansion vs. CSVP model without fleet expansion (dynamic, forecast parameters, $\mathcal{H} = \mathcal{H}^m$ and $\Delta t = 6h$) in terms of revenue gain (a)) and unit profit gain (b))

Second, we benchmark against a conventional positioning framework, which considers the focal fleet in isolation. We term this an "introvert" model. In the introvert case we let $D_{i,t}^M = D_{i,t}^O$, $I_{i,t}^M = I_{i,t}^O$ and $A_{i,t}^M = A_{i,t}^O$ in Equations 3.1 through 3.18, while the CSVP model formulation remains unchanged. For illustrative purposes and to abstract from the prediction performance, we choose a perfect information case. We also artificially inflate demand by 20% to provide sufficient opportunity for positioning actions in an introvert case. Figure 3.6 shows the results. In an introvert case, positioning benefits stem exclusively from capturing some of the additional demand that otherwise would have been lost or from repositioning to more valuable areas where expected rental length is higher. However, given that competitor vehicles will be present, actual

captured demand will diverge from what is expected a priori. By taking a market-perspective, these relative availabilities are considered in the positioning decisions. It also enables the identification of additional demand pockets which would remain unobserved otherwise. As a result, a fleet operator operating on a CSVP positioning model can achieve more than double (FREE positioning) or just under double (OPR positioning) the unit revenue and profit increases versus a non-competitor-aware model for the scenario we test. Third, we explore our model's performance

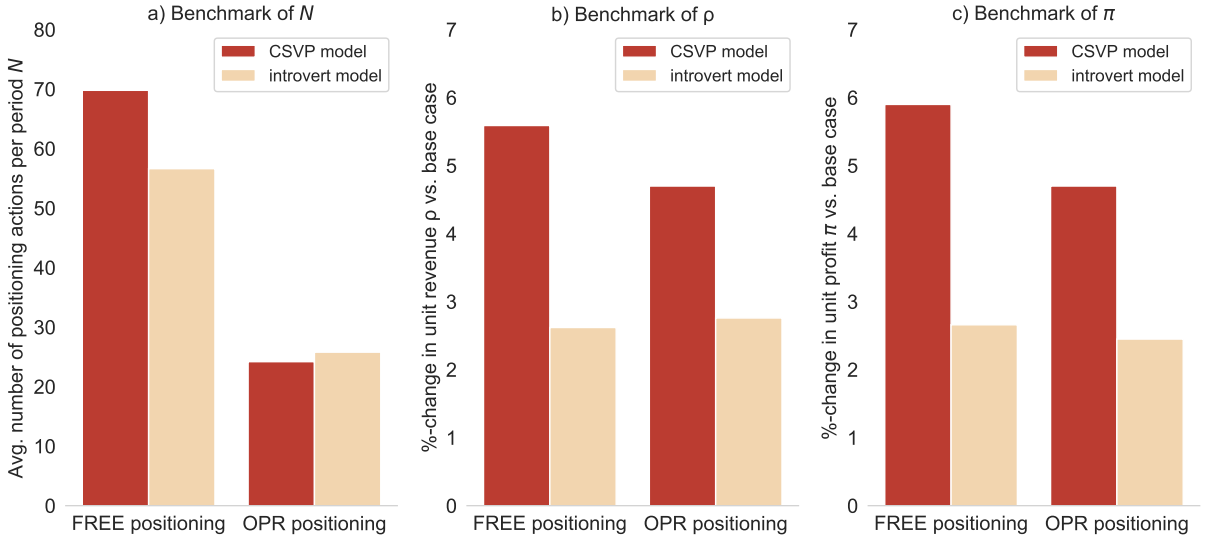

Figure 3.6: Benchmark positioning actions (a), unit revenue (b) and unit profit (c) obtained by non-competitor-aware (introvert) vs. CSVP model (dynamic, perfect information, $\mathcal{H} = \mathcal{H}^m$ and $\Delta t = 6h$) at 20% increase of $\mathbf{D^M}_{[\mathbf{T}]}$ and $\mathbf{D^O}_{[\mathbf{T}]}$

in various realistic scenarios by varying (1) the level of market demand $\mathbf{D^M}_{[\mathbf{T}]}$ and (2) the vehicle supply S^M. We vary demand by increasing $\mathbf{D^M}_{[\mathbf{T}]}$ by factor $(1 + f_D^M)$ proportionally across the network, where f_D^M is the demand growth factor. $\mathbf{I^M}_{[\mathbf{T}]}$ and $\mathbf{I^O}_{[\mathbf{T}]}$ are adjusted depending on how much induced demand is actually served. We increase competitor vehicle supply by adding $f_S^C S^M$ to the initialized availability, where f_S^C is the competitor vehicle supply growth factor. As before, we increase focal fleet vehicle supply by $f_S^O S^M$. Figure 3.7a) provides insights into the effects of growing competitor fleet vehicle supply under different demand growth scenarios. Competing fleet operators may choose to expand their fleets to capture market share (shown for the conservative, high-cost case of operator-based (OPR) positioning). Alternatively, new entrants may raise the supply of competitor vehicles. Market demand may or may not rise in such future scenarios. Comparing the unit profit π against the base case of not engaging in CSVP positioning, we find improvements at all levels of f_S^C and f_D^M we test for. The isolated effect of a demand increase follows a bell-shaped curve (see bottom rows of Figure 3.7) with highest effects versus base case at moderate increases. For large demand increases, the market becomes relatively undersupplied and there is less scope for further improvement. Looking at growth in competitor supply alone (first column), we see stable- to moderately-decreasing effectiveness of

CSVP positioning. This small reduction in effectiveness is noteworthy as a factor $f_S^C = 0.25$ corresponds to a significant loss in relative availability of approx. 10%-points. Our framework remains effective at largely constant rates even as relative availability is considerably reduced. The highest uplifts versus the base case are achieved in scenarios with moderate demand increase and large competitor fleet expansions. The high loss in relative availability, coupled with additional rentals to be captured at a constant own fleet size, provides ample improvement opportunities via CSVP positioning and can result in profit increases versus a base case of 5.0%. The CSVP framework thus provides an effective defensive mechanism against competitor fleet expansion by reducing the impact of the loss in relative availability and by amplifying the decline in unit profitability experienced by the competitor fleet. The CSVP is therefore well suited for accommodating an anticipated growth in market demand even if competitors decide to increase fleet size proportionately. Figure 3.7b) depicts the unit profit gains under operator-based CSVP

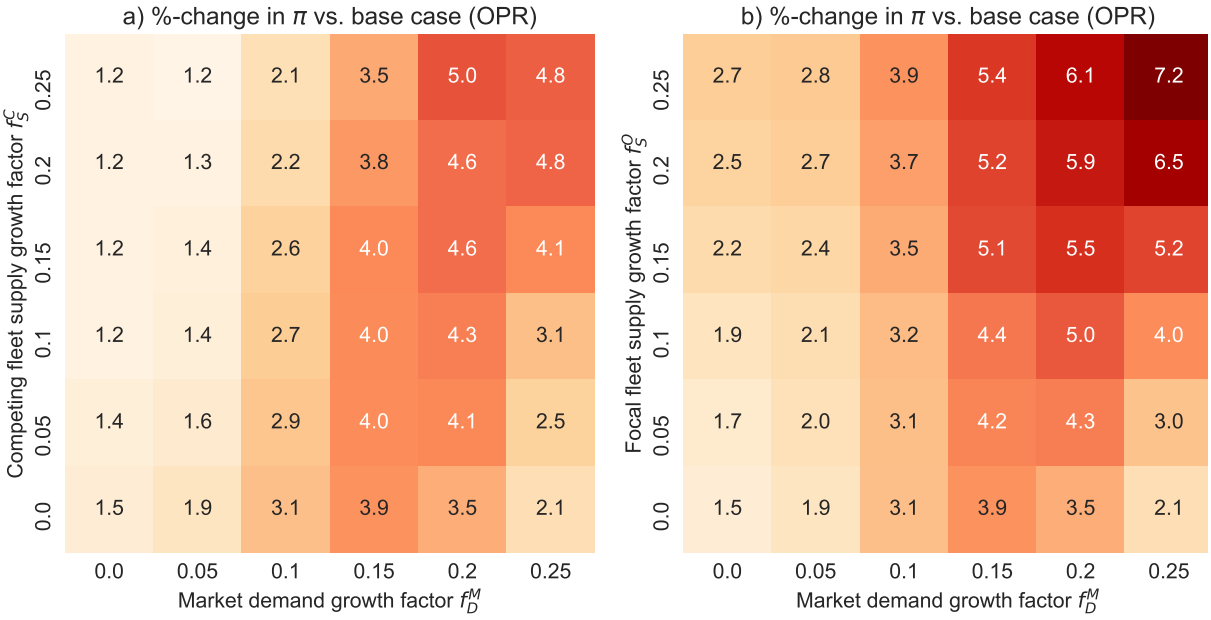

Figure 3.7: Heat map of focal fleets' change in unit profit π under operator-based (OPR) CSVP positioning vs. base case for a) different f_D^M and f_S^C and b) different f_D^M and f_S^O

positioning in the opposite case of focal fleet expansion and different demand growth scenarios. We explore whether the framework can enhance the effectiveness of the focal fleet operator's physical fleet expansions in the market we study by dampening adverse unit economics effects associated with fleet expansion. We find similar effectiveness patterns for changes in f_S^O. However, focal fleet supply effects in isolation (column one in Figure 3.7b)) result in relatively higher effectiveness gains. This can be attributed to the larger vehicle pool the fleet operator can use for CSVP positioning. Effectiveness rises to up to 7.2% unit profit increase in an OPR positioning scenario. Improvements for FREE positioning are even higher and are shown in Appendix E. From these what-if analyses we learn that (1) the level of relative oversupply in the market

plays an important role. As demand growth picks up, CSVP effectiveness rises up to a point when the market becomes undersupplied and the scope for additional gain diminishes. We also find that (2) the relative availability share seems not to have a significant impact on effectiveness. As competitor supply rises, the CSVP remains effective at similar levels. Finally, we find evidence that (3) the vehicle pool size plays a role. As the fleet operator increases her fleet size she not only improves relative availability but also the absolute size of the vehicle pool that can be used for positioning, which drives effectiveness. The CSVP model can thus be expected to perform well in scenarios of growing market demand, growing competitor supply and own fleet expansion. All simulations above assume uninterrupted data flow from competitor APIs. In practice, these may experience occasional outages and malfunctions. In Appendix E we run extensive simulations to test the sensitivity of our results to such outages. We find that our results are highly robust even to reasonably high outage probabilities of 50%. These findings further highlight the real-world readiness of our approach.

3.5 Discussion and Future Work

This research explores how operators of on-demand rental networks can leverage real-time and geo-tagged competitor information in the operations management of their network. Market-level and high-resolution mobility data is widely and publicly available in many geographies. The trend of open-sourcing mobility operator data is continuing (e.g., Mobility Data Specification (MDS) project, or city-level open data initiatives). In an environment evolving towards increased sharing, the question emerges whether operators can profit from incorporating detailed competitor supply and demand information into their operational decision processes. To address this question we focus on the repositioning challenge, a core operational concern in on-demand rental networks. We develop a novel, data-driven, and scalable three-stage framework that enables operators of on-demand rental networks to improve market share and profitability through competitor-aware positioning actions - independent of market structure. We build our model on the assumption that local relative product availability determines the market share that is captured by a fleet in a competitive environment. We test that assumption and develop a machine learning framework to predict market-level demand and supply parameters. Those predictions are input to a multi-period MINLP online optimization framework that periodically determines optimal positioning schedules. Our work offers a new perspective on the shared vehicle positioning problem by incorporating competitor-awareness into the decision process. We demonstrate the effectiveness of our model via benchmarks and counterfactuals tested on real-world data from the case of Car2Go and DriveNow in Berlin. CSVP positioning outperforms the base case observed in our data both in terms of revenue gain and profitability at all spatial and temporal discretizations under consideration. The upper bound is 7.5% unit profit growth. However, given that predictive accuracy diminishes at larger network sizes, the best real-world results are obtained with a dynamic model at medium spatial and low temporal resolution. The optimal unit profit increase ranges from 2.8% to 1.5% depending on positioning cost. We benchmark this setup against the alternative of fleet expansion and against an introverted player that neglects competitor information. Both benchmarks are significantly outperformed. We also find that model effectiveness typically rises under realistic combinations of defensive (competing fleet growth, new entrants), offensive (focal fleet expansion) and demand growth scenarios. We also show that our model readily handles data outages (see Appendix E)

Our work is subject to several limitations, which provide scope for interesting follow-up work. First, our approach relies on the availability of real-time system-level shared mobility data. Throughout this paper we have argued that such data is increasingly and widely accessible. In many cases real-time mobility data streams are provided by the mobility operators themselves via open APIs – either voluntarily or in response to regulatory pressures from governmental authorities. We have also referenced alternative, real-time data sources such as market research companies. Yet, the fact remains that our approach is data hungry. This opens up research opportunities to extend our model to situations where the market environment is only

partially observable in real-time, i.e., where competitor data streams remain untapped. Future work may therefore consider a scenario, where competitor demand and supply information is opaque or unavailable in real-time. Only static, historical data is available. Here, we briefly elaborate on two possible approaches for dealing with such a challenge. A promising methodological extension to handle partial observability, is the use of reinforcement learning (RL), which has received increasing attention in the OR/OM community as a scalable approach in stochastic and sequential environments (Powell, 2011; Gosavi, 2009). One can cast the CSVP as a single-agent, partially observable markov decision process (POMDP). An RL algorithm can then find repositioning policies that maximize a certain reward function (i.e., fleet operator profit) and implicitly incorporate (unobservable) competitor supply and demand information. By learning over many many episodes of historical system states, optimal repositioning policies could likely be found. While such an approach is computationally expensive, once trained, the RL model executes in real-time and would therefore offer real-world utility. The latent modeling technique of Economic Regimes (ER) proposed by Ketter et al. (2009, 2012) also offers a promising avenue. ER models are based on Hierarchical Hidden Markov Models and predict distributions of key market conditions (such as demand and supply volumes) based on limited observable market information (such as a single competitor's supply and demand conditions). Probabilistic modeling is then used to detect and predict changes in economic regimes and derive operational decisions tailored to the specific market/competitive condition.

Second, our model assumes that only the focal fleet conducts competitor-aware positioning actions. This work enables us to quantify the value of real-time market-level data and show that the value is sufficient to warrant investment in the development of a real-time data analytics and decision framework that incorporates competitor supply information. Indeed, as an early adopter, the fleet operator can exploit the full value of the data. Previous research also shows that the overall market efficiency frontier can increase even if only one actor uses the derived competitive strategy (Ketter et al., 2012). The question remains, however, how the situation changes as other competitors with symmetric information may themselves begin to engage in CSVP positioning. One approach to exploring these dynamics is a game-theoretic framework that formalizes interactions between several rational and competitive agents. Due to mathematical tractability, a game-theoretic approach would be limited to evaluating a small number of players and limited set of strategies. A more flexible and scalable alternative is competitive multi-agent simulation (MAS). MAS can find and evaluate different agent strategies and stable combinations thereof (equilibrium) in an evolutionary manner. The MAS approach could also leverage the RL or ER methods mentioned above to derive competitive agent strategies. Several outcomes are conceivable. In a zero sum game, as more and more competitors apply CSVP, the value will increasingly be shared between platforms to the disadvantage of those fleets that either do not use CSVP or those that utilize comparatively worse prediction models. Where competition is not a zero sum game, perhaps because the system is not operating at the efficient

frontier, if all operators use all available information to make more efficient allocations, overall efficiency of the system could increase and a win-win situation might be created. In either situation, while first movers can fully and exclusively benefit from CSVP today, there is also a clear long-term competitive disadvantage from not using competitor-aware vehicle positioning approaches, which highlights the value of the presented approach.

Finally, there is an opportunity to test the CSVP framework on other on-demand rental networks such as bikes or e-scooters. On-demand bike-rental networks typically experience more rental activity and have cheaper positioning cost factors (due to pooling), which could allow for the use of lower network resolutions and more positioning actions, thus increasing effectiveness. On-demand service networks (Uber, Lyft) could also benefit from the proposed framework.

3.6 Appendix

A. Structure of Input Data and Inference of Model Inputs

Table 3.6 contains an excerpt of the raw data (for an exemplary vehicle) that underlies this research. Locations per each vehicle (identifiable via a vehicle ID) are retrieved every five minutes. If the vehicle is rented out it disappears from the API output. Thus, if a vehicle ID is absent from the next API call, it can be assumed that this vehicle was rented over the past five minutes in the region where it last appeared. Conversely, if a vehicle re-appears in the records that particular period and location can be inferred as its rental destination. In sum, this data enables operators to infer (1) the current vehicle availability across the network at the time of data retrieval, (2) the number of rentals starts and ends per each region and time period, and (3) the exact duration and trajectory of a rental (start and end location). Note that this exceeds the data requirements for our model, which only requires availabilities and rental outflows and inflows per period and location. Thus, even if individual vehicle trajectories cannot be tracked, our model works. Note also that APIs that provide

Table 3.6: Excerpt of raw data for selected vehicle

CarID	DateTime	Latitude	Longitude	Fuel	Interior	Exterior
...	...	...	...	...	...	...
B-GO6699	2017-08-01 08:10:00	52.4339	13.5394	71%	good	good
B-GO6699	2017-08-01 08:15:00	52.4339	13.5394	71%	good	good
B-GO6699	2017-08-01 08:20:00	52.4339	13.5394	71%	good	good
B-GO6699	2017-08-01 08:45:00	52.4991	13.4325,	65%	good	good
B-GO6699	2017-08-01 08:50:00	52.4991	13.4325,	65%	good	good
B-GO6699	2017-08-01 08:55:00	52.4991	13.4325,	65%	good	good
B-GO6699	2017-08-01 09:00:00	52.4991	13.4325,	65%	good	good
...	...	...	...	...	...	...

Note: Interior and Exterior refers to the general condition and cleanliness of the vehicle's interior and exterior respectively

data as shown in Table 3.6 are standard in the shared mobility domain. For a non-exhaustive overview of open vehicle sharing APIs see `https://github.com/ubahnverleih/WoBike`. There are also third-party market research companies such as fluctuo (`https://fluctuo.com`) or remix (`https://www.remix.com/solutions/shared-mobility`) who offer real-time data streams of most major shared mobility platforms including those for which open APIs cannot be readily found.

B. Assumptions and Discretization Approach

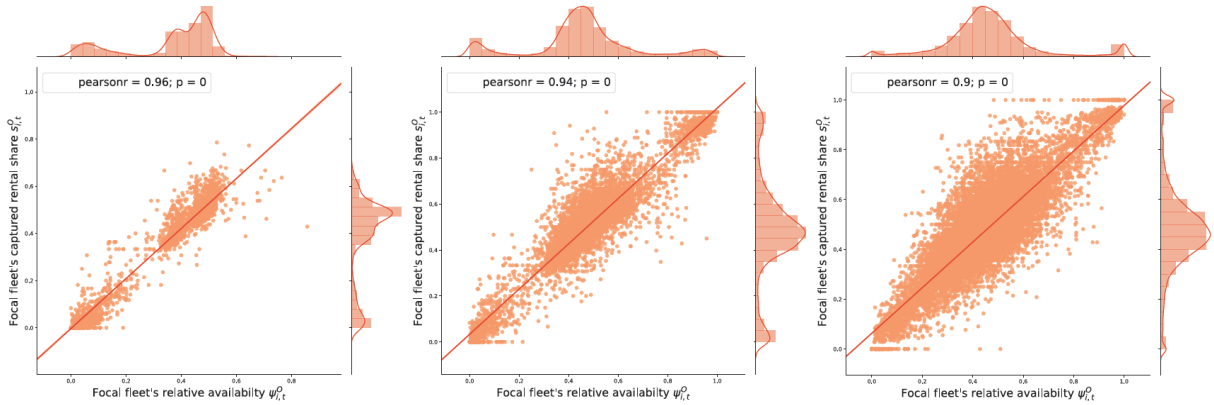

Figure 3.8: Regression of captured demand share $s^O_{i,t}$ against relative availability $\psi^O_{i,t}$ at coarse (left), medium (middle) and fine (right) spatial resolution - There is direct proportionality with $k \approx 1$ at all resolutions.

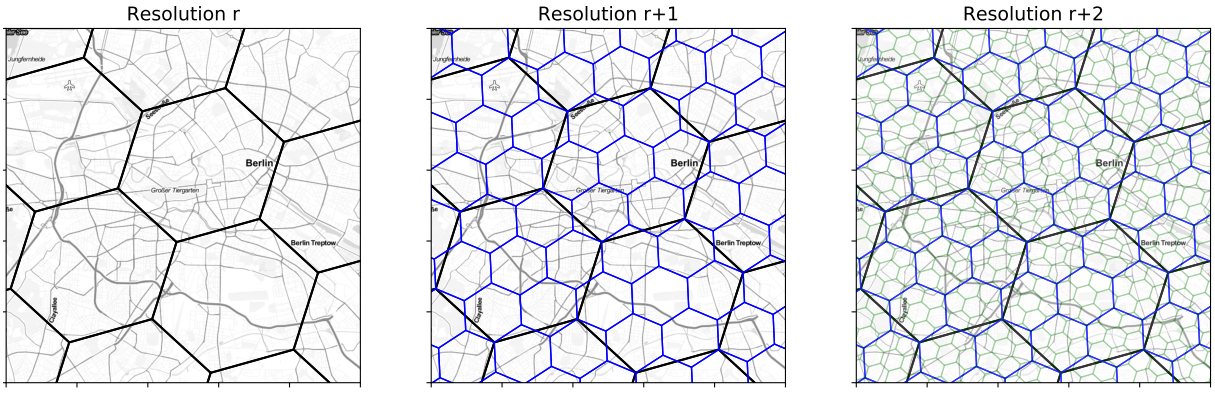

Figure 3.9: Spatial framework - A hexagonal GDGGS (shown for different resolutions at an aperture size of 7)

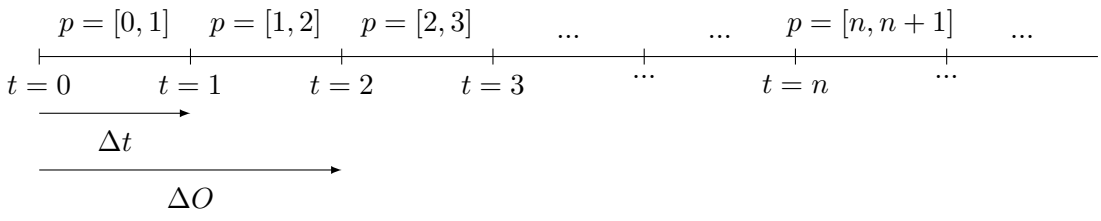

Figure 3.10: Temporal framework - Discrete period length of Δt and user-defined optimization horizon ΔO

C. Discrete Event Simulation

Algorithm 1: CSVPSim()

input : target period: t, set of periods in optimization horizon: $\mathcal{T}^O = \{t, ..., t+n\}$; set of training periods $\mathcal{T}^L = \{1, ..., t-1\}$; set of regions: $\mathcal{H}$, input vector: $\mathcal{S}_\mathbf{t}$; historic realizations of inputs (training data): $\mathcal{S}_{[\mathcal{T}^L]}$; realizations of target parameters: $\mathbf{D^M_t}, \mathbf{I^M_t}, \mathbf{I^O_t}$, historic realizations of targets: $\mathbf{D^M}_{[\mathcal{T}^L]}, \mathbf{I^M}_{[\mathcal{T}^L]}, \mathbf{I^O}_{[\mathcal{T}^L]}$; vehicle supply: $\mathbf{A^M}_t, \mathbf{A^O}_t$; hypertuned ML hypothesis function ϕ and loss function ℓ; CSVP mathematical model Ω (Eq. 1 to 18); rental price: r^{rent}; rental cost: c^{rent}; relocation cost: $\mathbf{c}^{reloc} = (c^{reloc}_{ij})$, actual and hist. avg. rental length: $\boldsymbol{\delta}^M_t$, $\hat{\boldsymbol{\delta}}^M_t$

output: positioning actions: $\mathbf{x}_{[\mathcal{T}^O]} = (x_{ij,t})$ for all $t \in \mathcal{T}^O$ and $i, j \in \mathcal{H}$; revenue: R_t; utilization: U_t; adjusted profit: Π_t, rental gain/loss in target period t: ΔD^O_t, ΔD^M_t

`/* fit` ϕ `for all` P, i, t `and predict future realizations of all` $y_{i,t}$ `*/`

for $P \in [D^M, I^M, I^O]$ **do**
  for $t \in \mathcal{T}^O$, $i \in \mathcal{H}$ **do**
    $\min_{\phi^P_{i,t}} \sum_{t \in \mathcal{T}^L} \ell(\phi^P_{i,t}(\mathcal{S}_{i,t}), P_{i,t})$ `/* learn ML model on` $\mathcal{S}_{[\mathcal{T}^L]}$, $\mathcal{P}_{[\mathcal{T}^L]}$ `*/`
    $\hat{P}_{i,t} = \phi^P_{i,t}(\mathcal{S}_{i,t})$ `/* predict future realizations */`
  end
end

`/* get positioning actions in` $\mathcal{T}^O$ `(`$\mathbf{x}_{[\mathcal{T}^O]}$`); isolate positionings in` t `(`$\mathbf{x_t}$`) */`

$\mathbf{x}_{[\mathcal{T}^O]} = \Omega(t, \hat{\mathbf{D}}^\mathbf{M}_{[\mathcal{T}^O]}, \hat{\mathbf{I}}^\mathbf{M}_{[\mathcal{T}^O]}, \hat{\mathbf{I}}^\mathbf{O}_{[\mathcal{T}^O]}, \mathbf{A}^M_t, \mathbf{A}^O_t, \hat{\boldsymbol{\delta}}^M_t, r^{rent}, c^{rent}, \mathbf{c}^{reloc})$

$\mathbf{x_t} \leftarrow \mathbf{x}_{[\mathcal{T}^O]}[t]$

`/* for target period` t`: execute` $x_{ij,t}$ `and allocate demand and inflows */`

for $i \in \mathcal{H}$ **do**
  Allocate ΔD^M_{t-1} stochastically with $p = \frac{I^M_{i,t}}{\sum_{i \in \mathcal{H}} I^M_{i,t}}$ until exhausted; store as $\mathbf{\Delta I^M_t}$
  Allocate ΔD^O_{t-1} stochastically with $p = \frac{I^O_{i,t}}{\sum_{i \in \mathcal{H}} I^O_{i,t}}$ until exhausted; store as $\mathbf{\Delta I^O_t}$
  Update $A^M_{i,t} \leftarrow A^M_{i,t} + \sum_{j \in \mathcal{H}} x_{ji,t} - x_{ij,t}$ and $A^O_{i,t} \leftarrow A^O_{i,t} + \sum_{j \in \mathcal{H}} x_{ji,t} - x_{ij,t}$
  Update $I^O_{i,t} \leftarrow I^O_{i,t} + round(\Delta D^O_{t-1} \frac{I^M_{i,t}}{\sum_{i \in \mathcal{H}} I^M_{i,t}})$ and $I^M_{i,t} \leftarrow I^M_{i,t} + round(\Delta D^M_{t-1} \frac{I^M_{i,t}}{\sum_{i \in \mathcal{H}} I^M_{i,t}})$
  Compute $D^O_{i,t} = round(\psi^O_{i,t} D^M_{i,t})$ (with $\psi^O_{i,t}$ as per Eq. 2)
end

`/* Compute KPIs and update state variables after demand allocation */`

Compute $R_t = \sum_{i \in \mathcal{H}} (\hat{D}^O_{i,t} \delta^M_{i,t}(r^{rent}))$, $U_t = \frac{\frac{R_t}{r^{rent}}}{V^O \Delta t}$, Π_t (as per Eq. 1), ΔD^O_t, ΔD^M_t

Update $\mathbf{A}^M_{t+1} \leftarrow \mathbf{A}^M_t + \mathbf{I}^M_t - \mathbf{D}^M_t$; $\mathbf{A}^O_{t+1} \leftarrow \mathbf{A}^O_t + \mathbf{I}^O_t - \mathbf{D}^O_t$

D. Prediction Model

Benchmark 1: Historical average model

Figure 3.11 and 3.12 show the autocorrelation plots of $D_{i,t}^{M}$ (similar for the other targets), which were used in the historical average model (HA).

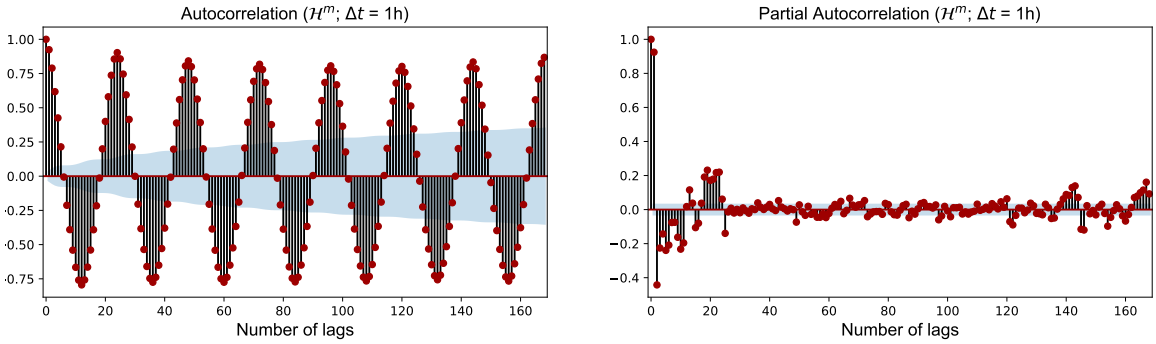

Figure 3.11: 1-week ACF and PACF of $D_{i,t}^{M}$ for a selected region at medium spatial resolution and 1h period length

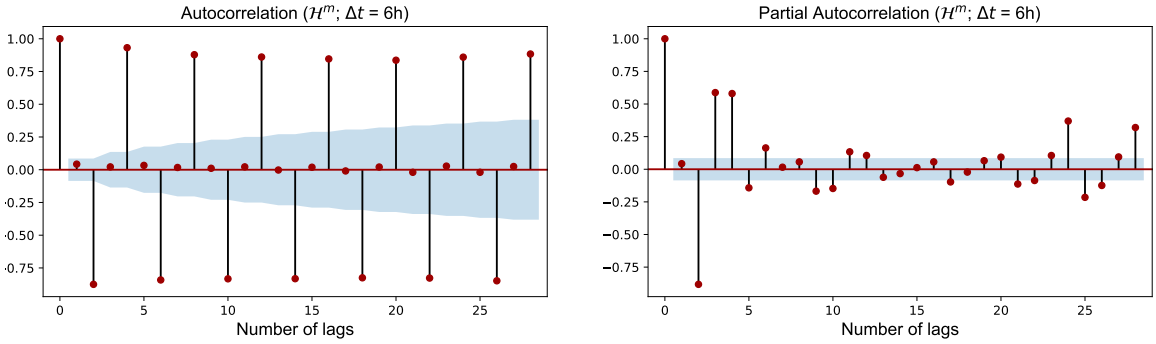

Figure 3.12: 1-week ACF and PACF of $D_{i,t}^{M}$ for a selected region at medium spatial resolution and 6h period length

Benchmark 2: SARIMA model

The SARIMA model uses the following parameters: [(p,d,q)(P,D,Q,m),t]

The first thee hyperparameters are autoregression (p), differencing (d) and moving average (q) like in a normal ARIMA model. We define them as follows:

- Autoregression: p≥1 due to significant autocorrelation at lag 1 in the PACF. We employ a grid search over p = [1,2,3].
- Degree of Differencing: d=0 as there is no visible trend in series
- Moving Average: q≥1 due to significant autocorrelation at lag 1 in the ACF. We employ a grid search over q = [1,2,3].

The remaining hyperparameters are for the seasonal part of the model:

- Autoregression: Autoregression: P≥1 ACF is positive at lag m (24 (1h resolution) or 4 (6h resolution)). We employ a grid search over P = [1,2].
- Differencing: D=1 series has a stable seasonal pattern over time
- Number of Periods: m=24 (1h) or m=4 (6h) due to clear 24- or 4-period seasonality
- Trend t: There is no trend so this parameter is irrelevant

We grid-search models for medium spatial resolution $\mathcal{H}^m$. Results are shown in Table 3.7. For Δt = 1h we choose configuration [(1, 0, 2), (2, 1, 0, 24)], which has strong performance at reasonable training times. For Δt = 6h we choose the best performing configuration [(1, 0, 2), (1, 1, 0, 4)].

Table 3.7: SARIMA grid search results

SARIMA config.	**Δt = 1h (m=24)**		**Δt = 6h (m=4)**	
[(p,d,q)(P,D,Q,m)]	CPU time (s)	MAE (# vehicles)	CPU time (s)	MAE (# vehicles)
[(3, 0, 2), (2, 1, 0, m)]	18855.1	30.8075	36.8	407.6451
[(1, 0, 3), (2, 1, 0, m)]	3074.3	31.1154	24.3	356.0574
[(1, 0, 2), (2, 1, 0, m)]	**2413.3**	**31.1213**	18.6	346.3204
[(2, 0, 2), (2, 1, 0, m)]	4219.9	31.1937	24.7	356.2888
[(2, 0, 3), (2, 1, 0, m)]	7904.6	31.2449	22.9	405.3981
[(3, 0, 3), (2, 1, 0, m)]	7893.6	31.3673	50.2	404.7475
[(3, 0, 1), (2, 1, 0, m)]	3616.3	31.3844	24.3	413.7035
[(2, 0, 2), (1, 1, 0, m)]	1235.0	31.4795	15.9	329.4374
[(1, 0, 3), (1, 1, 0, m)]	859.2	31.4825	14.8	313.8593
[(1, 0, 2), (1, 1, 0, m)]	842.0	31.5256	**12.0**	**311.2128**
[(2, 0, 1), (2, 1, 0, m)]	4114.3	31.5429	7.4	364.2654
[(3, 0, 3), (1, 1, 0, m)]	2173.0	31.619	33.7	380.0744
[(3, 0, 1), (1, 1, 0, m)]	1051.4	31.7426	15.5	404.7965
[(1, 0, 1), (2, 1, 0, m)]	1877.1	31.7549	6.7	377.9798
[(2, 0, 3), (1, 1, 0, m)]	2666.3	31.764	18.0	333.969
[(3, 0, 2), (1, 1, 0, m)]	8185.6	31.8291	17.7	394.75
[(2, 0, 1), (1, 1, 0, m)]	1090.4	31.9805	3.0	334.3803
[(1, 0, 1), (1, 1, 0, m)]	495.6	32.0902	4.0	334.0049

Feature overview

Table 3.8 illustrates the full feature set prior to applying feature reduction.

Table 3.8: Feature overview

No.	Type	Name	Description
0	$\mathcal{Z}$	weekday_yn	Binary indicator if period falls on a weekday
1	$\mathcal{Z}$	weekend_yn	Binary indicator if period falls on a weekend
2	$\mathcal{Z}$	day_0	Binary indicator if period falls on a Mon
3-7	$\mathcal{Z}$	..	...
8	$\mathcal{Z}$	day_6	Binary indicator of whether period falls on a Sun
9	$\mathcal{Z}$	hour_0	Binary indicator if period contains 00.00h window
10-31	$\mathcal{Z}$	...	...
32	$\mathcal{Z}$	hour_23	Binary indicator if period contains 23.00h window
33	$\mathcal{Z}$	bank_holiday	Binary indicator if period falls on a bank holiday
34	$\mathcal{Z}$	school_holiday	Binary indicator if period falls on a school holiday
35	$\mathcal{W}$	temperature_degC	Expected mean temperature during period t in °C
36	$\mathcal{W}$	percipitation_mm	Expected mean precipitation during period t in mm
37	$\mathcal{W}$	wind_mps	Expected mean wind speed in m/s
38	$\mathcal{W}$	humidity_perc	Expected mean relative humidity in %
39	$\mathcal{W}$	clouds_eigth	Expected mean cloud cover in eighth
40	$\mathcal{W}$	percipitation_yn	Binary indicator of whether precipitation is expected
41	$\mathcal{G}$	accounting	Count of POI type 'accounting' in region
42	$\mathcal{G}$	airport	Count of POI type 'airport' in region
43-138	$\mathcal{G}$	...	...
139	$\mathcal{G}$	zoo	Count of POI type 'zoo' in region
140	$\mathcal{G}$	has_rating	Count of POI types with a popularity rating in region
141	$\mathcal{G}$	no_rating	Count of POI types without a popularity rating in region
142	$\mathcal{G}$	has_price	Count of POI types with a price rating in region
143	$\mathcal{G}$	no_price	Count of POI types without a price rating in region
144	$\mathcal{G}$	share_has_rating	Share of POIs with a popularity rating in region
145	$\mathcal{G}$	share_has_price	Share of POIs with a price rating in region
146	$\mathcal{C}$	comp_inflows_p-1	Count of comp. inflows in region 1 period prior
147	$\mathcal{C}$	comp_inflows_p-2	Count of comp. inflows in region 2 periods prior
148	$\mathcal{C}$	comp_inflows_p-3	Count of comp. inflows in region 3 periods prior
149	$\mathcal{C}$	comp_inflows_p-1d	Count of comp. inflows in region 1 day prior
150-154	$\mathcal{C}$	...	...
155	$\mathcal{C}$	comp_inflows_p-7d	Count of comp. inflows in region 7 days prior
156	$\mathcal{C}$	comp_inflows_mean	Mean of inflows in region 1 to 7 days prior
157	$\mathcal{C}$	comp_inflows_var	Var. of inflows in region 1 to 7 days prior
158	$\mathcal{C}$	comp_inflows_std	Std. of inflows in region 1 to 7 days prior
159	$\mathcal{C}$	comp_inflows_diff_6-7d	Diff. in inflows 7 and 6 days prior
160-164	$\mathcal{C}$	...	...
165	$\mathcal{C}$	comp_inflows_diff_0-1d	Diff. in inflows 1 day and 1 period prior
166	$\mathcal{C}$	comp_inflows_all_reg_p-1	Count of comp. inflows (all regions) 1 period prior
167	$\mathcal{C}$	comp_inflows_all_reg_p-2	Count of comp. inflows (all regions) 2 periods prior
168	$\mathcal{C}$	comp_inflows_all_reg_p-3	Count of comp. inflows (all regions) 3 periods prior
169	$\mathcal{C}$	comp_outflows_p-1	Count of comp. outflows in region i 1 period prior
170-190	$\mathcal{C}$	...	analogous to 147-167 for outflows
191	$\mathcal{C}$	comp_outflows_all_reg_p-3	Count of comp. outflows (all regions) 3 periods prior
192-236	$\mathcal{F}_{i,t}$	...	analogous to 147-191 for focal fleet
237	$\mathcal{F}_{i,t}$	own_outflows_all_reg_p-3	Count of focal fleet outflows (all regions) 3 periods prior

An overview of top selected features is shown in Figures 3.13 and 3.14.

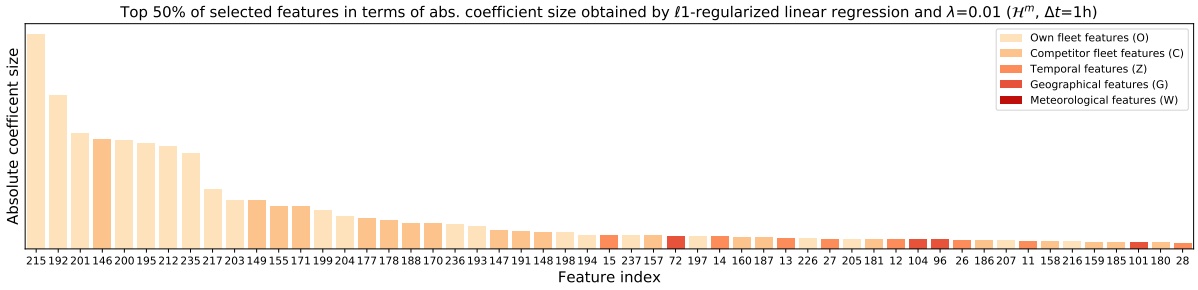

Figure 3.13: Top features for $\mathcal{H}^m$ (Δt=1h)

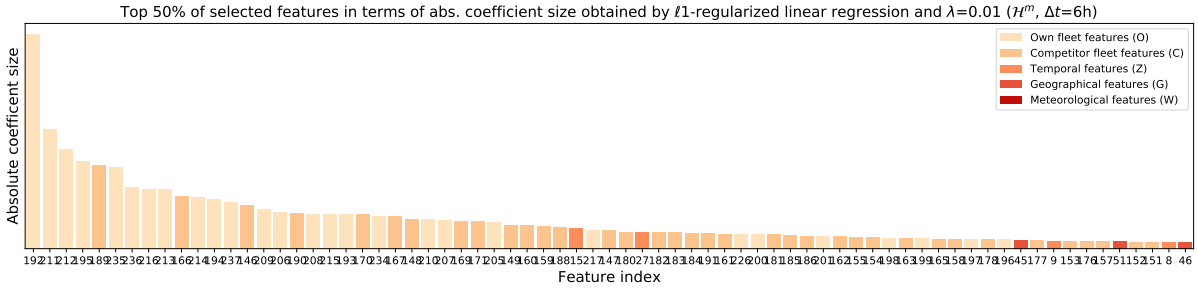

Figure 3.14: Top features for $\mathcal{H}^m$ (Δt=6h)

Selection of training period

We identify the required training length by observing the development of the MAE with increasing training length (see Figure 3.15). MAE plateaus at 80 days of training data, which is the length we adopt.

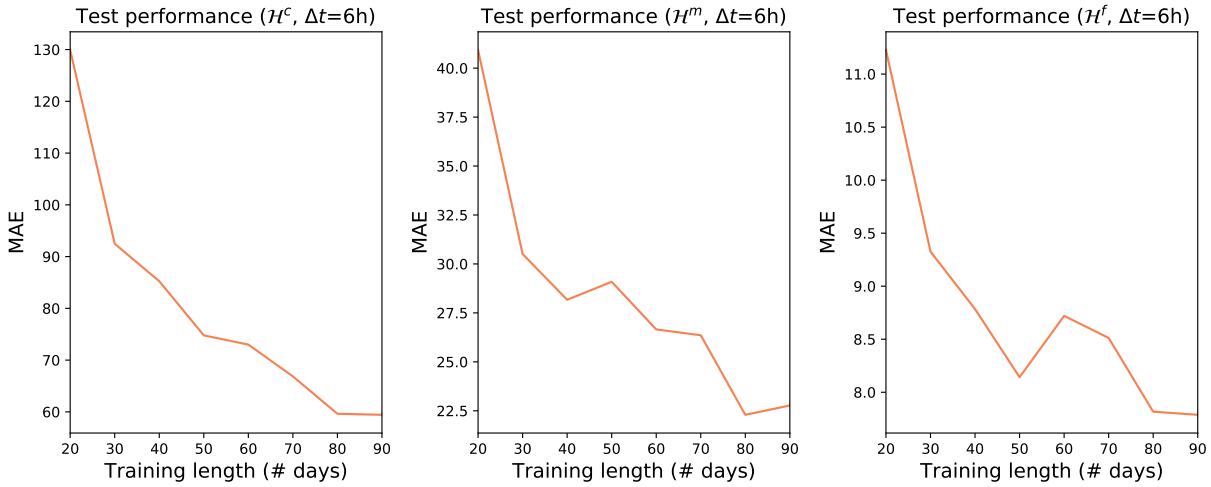

Figure 3.15: Evaluation of MAE with different length in training window (shown here for Δt=6h)

Parameterization of ML models

Table 3.9: Grid-search results of various ML models

			Best performing paramters					
			$\mathcal{H}^c$		$\mathcal{H}^m$		$\mathcal{H}^f$	
Model	**Parameter**	**Search space**	1h	6h	1h	6h	1h	6h
ML-LASSO	regularization	[10^{-3},10^{-2},10^{-1},1,10]	10^{-3}	10^{-3}	10^{-3}	10^{-2}	10^{-1}	1
ML-SVM	cost factor C	[500,10^3,10^4,10^5,10^6]	500	10^5	500	10^4	500	10^4
ML-SVM	epsilon tube ϵ	[0.4]	0.4	0.4	0.001	0.4	0.4	0.4
ML-SVM	kernel	[rbf]	rbf	rbf	rbf	rbf	rbf	rbf
ML-TREE	# of estimators	[250,500,750,1000,1500]	750	750	1000	750	1000	1000
ML-TREE	max. depth	[2,4,6]	2	2	4	2	4	4
ML-TREE	learning rate	[10^{-3},10^{-2},10^{-1}]	10^{-2}	10^{-1}	10^{-1}	10^{-2}	10^{-1}	10^{-1}
ML-TREE	loss	[mae]	mae	mae	mae	mae	mae	mae
NN1	drop rate	[0,10^{-3},10^{-2},10^{-1}]	10^{-3}	10^{-3}	0	10^{-2}	10^{-3}	10^{-3}
NN1	epochs	[100,200]	100	200	100	200	100	200
NN1	batch size	[100,200,300]	300	100	200	100	300	300
NN1	learning rate	[10^{-3}]	10^{-3}	10^{-3}	10^{-3}	10^{-3}	10^{-3}	10^{-3}
NN1	optimizer	[adam]	adam	adam	adam	adam	adam	adam
NN1	activation	[relu]	relu	relu	relu	relu	relu	relu
NN1	loss	[mae]	mae	mae	mae	mae	mae	mae
NN1	hidden layers	[1]	1	1	1	1	1	1
NN1	neurons (f=# features)	[0.75f,1f,1.25f,1.5f]	1.25f	1.5f	1.5f	1f	0.75f	0.75f
NN2	drop rate	[0,10^{-3},10^{-2},10^{-1}]	10^{-3}	10^{-2}	0	0	0	10^{-3}
NN2	epochs	[100,200]	100	200	100	200	100	100
NN2	batch size	[100,200,300]	300	100	300	300	200	300
NN2	learning rate	[10^{-3}]	10^{-3}	10^{-3}	10^{-3}	10^{-3}	10^{-3}	10^{-3}
NN2	optimizer	[adam]	adam	adam	adam	adam	adam	adam
NN2	activation	[relu]	relu	relu	relu	relu	relu	relu
NN2	loss	[mae]	mae	mae	mae	mae	mae	mae
NN2	hidden layers	[2]	2	2	2	2	2	2
NN2	neurons (f=# features)	[0.75f,1f,1.25f,1.5f]	0.75f	1.5f	0.75f	1.5f	1.5f	0.75f
NN3	drop rate	[0,10^{-3},10^{-2},10^{-1}]	10^{-1}	0	0	0	10^{-2}	0
NN3	epochs	[100,200]	100	200	100	100	200	200
NN3	batch size	[100,200,300]	200	200	300	300	300	300
NN3	learning rate	[10^{-3}]	10^{-3}	10^{-3}	10^{-3}	10^{-3}	10^{-3}	10^{-3}
NN3	optimizer	[adam]	adam	adam	adam	adam	adam	adam
NN3	activation	[relu]	relu	relu	relu	relu	relu	relu
NN3	loss	[mae]	mae	mae	mae	mae	mae	mae
NN3	hidden layers	[3]	3	3	3	3	3	3
NN3	neurons (f=# features)	[0.75f,1f,1.25f,1.5f]	1.5f	1.25f	1.5f	1.5f	1.5f	1.5f

E. Optimization Model

CSVP Performance under growth in market demand $D^{M}_{[T]}$ and the vehicle supply S^M

We also plot the heat map of focal fleets' change in unit profit π under free (FREE) CSVP positioning vs. base case for different f_D^M and f_S^C and different f_D^M and f_S^O (see Figure 3.16). The same patterns as for OPR positioning can be observed. Note that at high f_D^M, f_S^C or f_S^O OPR positioning may outperform FREE positioning. We attribute this to the larger susceptibility of FREE positioning to prediction errors, which is amplified by relatively larger negative cascading effects at large demand and supply growth factors. To test this assumption we run the same experiments using perfect information, where FREE positioning outperforms OPR positioning for all cases.

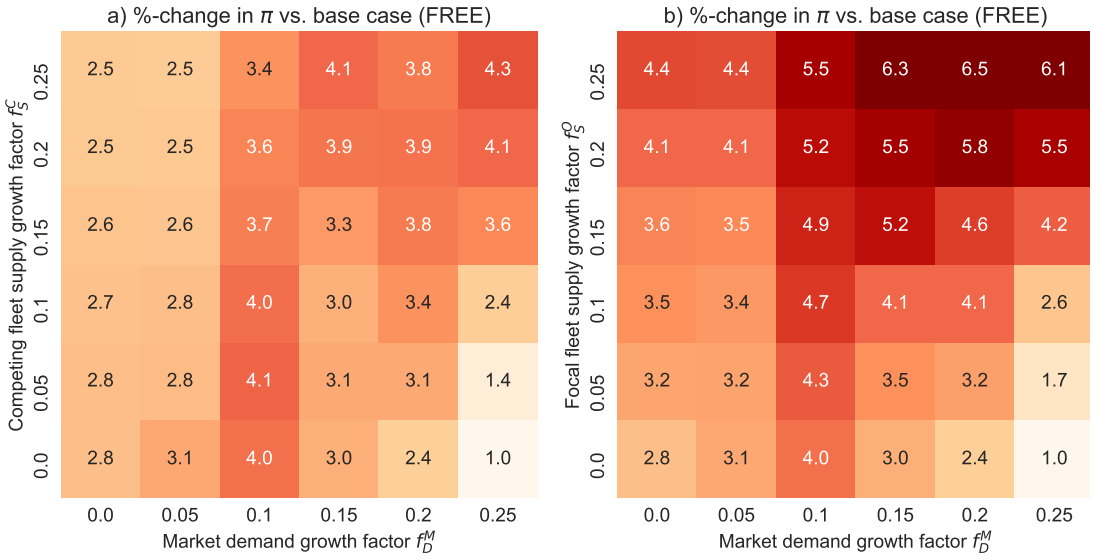

Figure 3.16: Heat map of focal fleets' change in unit profit π under free (FREE) CSVP positioning vs. base case for a) different f_D^M and f_S^C and b) different f_D^M and f_S^O

Sensitivity to API outages leading to missing information

Our model relies on regular and uninterrupted data feeds from third-party APIs. This makes it susceptible to API outages and malfunctions. We review here the impact of such outages and data errors on the robustness of our results. In our simulations we assume the risk of data outages to be limited to the feed of competitor data. This is a reasonable assumption since this data is the only one that an operator engaging in CSVP positioning would need to actively collect via an external API, an arguably error-prone approach which may be subject to technical issues. The focal fleet operator is assumed to have full and error-free visibility regarding the status of his/her own fleet at all times, which is warranted since accessing the focal fleet's data

does not involve external API scraping. API outages can have different repercussions depending on when and how long they persist. In a worst case, an API outage would occur at the beginning of a planning period and persist long enough such that actual demand and inflows cannot be tracked. This would mean that the operator would have no information on the state of the network at the beginning of the period (A_t^M) and would be unable to reliably account for actual realizations of demand and inflows during that period ($D_{i,t}^M$, $I_{i,t}^M$), which are important inputs to the ML model that predicts future realizations of inflows and outflows. To sum up, in a worst case API outage scenario the following issues would be faced: In the current planning period no information on initial market-level fleet vehicle distribution ($A_{i,t}^M$) would be available. In future planning periods missing/unreliable inputs the to prediction model with potential to skew predictions of future inflows and outflows. We account for both effects in our simulations. To simulate API malfunctions we randomly introduce full outages (i.e. missing information) with probability p^0 equal to 10%, 25% and 50%. We focus on the worst case of missing information on both the initial state of the network at the start of the period and missing information on demand and inflows during the period. We initially tested two different response strategies that the focal fleet operator might adopt in cases of API outages. These are: (1) Suspend relocations in affected period, and (2) Extrapolate/predict missing input parameter $A_{i,t}^M$ for the affected period. We find that naive extrapolation of $A_{i,t}^M$ based on past realizations yields worse and sometimes even negative results on average compared to the "suspend relocations" approach. We therefore do not further pursue this approach and instead focus on evaluating the response strategy of suspending relocations in the affected period. We tackle any downstream prediction issue arising from missing inputs for the ML models by dropping missing information on $I_{i,t-1}^M$ and $I_{i,t-1}^O$ (where $t-1$ is the period affected by the API outage). This is analogous to the approach taken for multi-period predictions for which we iteratively drop lagged features that have become unobservable for the period in scope to avoid prediction error propagation.

Per each outage scenario and response strategy we have run 100 simulations. Table 3.10 summarizes mean and standard deviation of the results. We have also visualized them in Figure 3.17.

Table 3.10: Sensitivity of %-change in profitability vs. based case to data outages with varying probability p^0 ($\mathcal{H} = \mathcal{H}^m$, $|\mathcal{T}^O|$ = DYNAMIC, $\mathcal{I}$ = FI, $\Delta t = 6h$)

	Strategy	$p^0 = 0\%$	$p^0 = 10\%$	$p^0 = 25\%$	$p^0 = 50\%$	$p^0 = 75\%$	$p^0 = 100\%$
OPR	Suspend Relocations	1.47 (–)	1.43 (0.072)	1.39 (0.110)	1.22 (0.142)	0.92 (0.319)	0.00 (–)

Note: Results show mean %-change in profitability over 100 simulation runs with standard deviation reported in parentheses

Our results demonstrate that our model is very robust to data outages, even with outage probability of up to p^0=50%. Model performance falls considerably for higher outage rates (p^0=75%), but remains positive. In practice, such high outage probabilities can be consid-

ered extremely rare. The performed API outage scenario simulations can therefore lead strong support to the robustness and real-world applicability of the proposed approach.

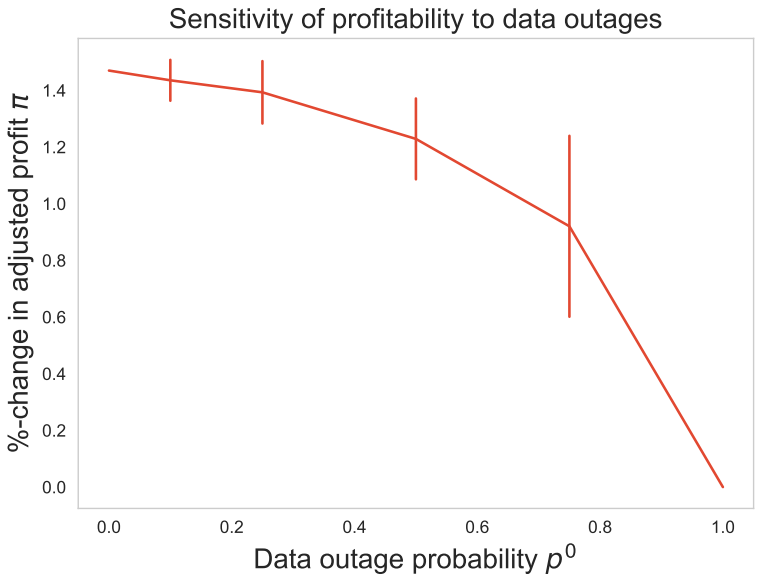

Figure 3.17: Mean and std. of %-change in adjusted profitability π over 100 simulation runs for the following model setting: $\mathcal{H} = \mathcal{H}^m$, $|\mathcal{T}^O|$ = DYNAMIC, $\mathcal{I}$ = FI, $\Delta t = 6h$

Sensitivity to time-variable relocation worker supply

Our simulation considers relocation capacity via a fixed cost parameters. As explained, we parameterize two types of relocation cost c_{ij}^{reloc}: one cost parameter for human operator-based relocation ($c_{ij}^{reloc,hum} = d_{ij}\ (c^{var} + c^{hum})$) and one cost for free relocation (e.g., free rides offered to users or autonomous vehicles) case ($c_{ij}^{reloc,aut} = d_{ij}\ (c^{var} + 0)$), where d_{ij} is the distance from region i to j. In our base simulation we have set c^{var} equal to USD 0.175 per km (includes fuel and degradation cost) and the operator-based relocation cost c^{hum} equal to USD 0.7 per km.

In practice, relocation capacity (e.g., the number of available workers) may, however, vary across time. Specifically, it is conceivable that relocation capacity during the night may be limited. This is true in both an operator-based and a user-based scenario. User-based repositioning capacity can be reasonably assumed to be significantly more abundant in periods of high travel demand during the day and vice versa. The same holds true for operator-based positioning. To account for this fact we have incorporated the notion of variable relocation capacity in the relocation cost parameter. Specifically, we have implemented a time-variable relocation cost surge factor f_t^{Surge} which is applied to the base relocation cost c_{ij}^{reloc}, thus yielding a time-variable relocation cost for operator-based repositioning of $c_{ij,t}^{reloc,hum} = d_{ij}\ (c^{var} + c^{hum} f_t^{Surge})$. Since repositioning cost in a FREE scenario would not be affected by f_t^{Surge} ($c_{ij,t}^{reloc,auto} = d_{ij}\ (c^{var} + 0 f_t^{Surge})$), we parameterize a third case (HYBRID) with base relocation cost of $c^{hybrid} = \frac{c^{hum}}{2}$ =USD 0.35 per km resulting in $c_{ij,t}^{reloc,hybrid} = d_{ij}\ (c^{var} + c^{hybrid} f_t^{Surge})$. In determining the functional form of

f_t^{Surge}, we rely on the average temporal distribution of market demand $\mathbf{D^M_t}$. We re-scale and reverse this distribution to the interval of $[f_t^{Min}, f_t^{Max}]$ letting f_t^{Surge} in the period of highest demand equal to f_t^{Min} and in the period of lowest demand equal to f_t^{Max}. Thus repositioning becomes more expensive in periods of low demand and is cheaper in periods of high demand. Figure 3.18 shows the temporal distribution of f_t^{Surge}. We re-run our simulation for the selected

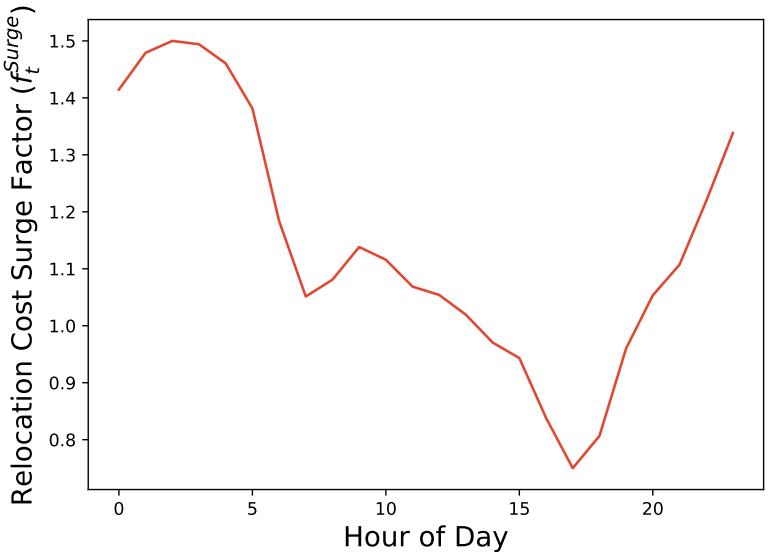

Figure 3.18: Temporal distribution of relocation cost surge factor f_t^{Surge} over the interval $[f_t^{Min} = .075, f_t^{Max} = 1.5]$

best-performing model under predicted parameters as test case (dynamic, $\mathcal{H} = \mathcal{H}^m$, $\Delta t = 6h$). The results are shown in Table 3.11. By increasing the relocation cost in certain time periods the model conducts fewer relocations on average. Profitability is negatively impacted. However, our model still achieves a sizeable profit improvement over the base case.

Table 3.11: Sensitivity to time-variable relocation costs to account for varying supply of labour ($\mathcal{H} = \mathcal{H}^m$, $|\mathcal{T}^O|$ = DYNAMIC and different information cases ($\mathcal{I}$) at $\Delta t = 6h$)

	$\mathcal{I}$	Static relocation cost ($f_t^{Min} = f_t^{Max} = 1$)		Time-variable relocation cost ($f_t^{Min} = 0.75, f_t^{Max} = 1.5$)		Time-variable relocation cost ($f_t^{Min} = 1, f_t^{Max} = 1.75$)	
		Avg. $\sum_{i,j} x_{ij,t}$	%-change in π	Avg. $\sum_{i,j} x_{ij,t}$	%-change in π	Avg. $\sum_{i,j} x_{ij,t}$	%-change in π
OPR	PI	5.1	1.6	3.7	1.3	3.0	1.2
	FI	6.0	1.5	4.2	1.2	3.8	1.1
HYB	PI	12.8	2.6	10.2	2.4	7.8	2.1
	FI	10.8	2.2	10.6	2.1	9.6	1.9

Note: Avg. $\sum_{i,j} x_{ij,t}$ = Avg. number of repositionings per period; %-change in π = % increase in adjusted profit over baseline (no repositioning)

F. Data and Code Supplement

A repository containing a simplified and stream-lined version of the code base along with selected real-world datasets is available via the following link: `https://github.com/KaSchr/CSVP_Code_Supplement`

The provided data and code samples focus on the optimization and simulation aspect of the paper and are intended to facilitate replication and benchmark analyses of the presented research. In particular, the repository contains (1) sample real-world carsharing data, (2) Julia code of the optimization model, (3) Julia code of the simulation framework (4) a basic data processing and evaluation routine to assist the analysis of simulation runs. For ease of use, all code has been compiled into a single jupyter notebook (.ipynb) with extensive annotations and descriptions. Further instructions and requirements are outlined in the online repository.

Chapter 4

Solving Large-Scale Service System Design Problems with Digital Twins: An Application to Electric Vehicle Charging Hubs[1]

4.1 Introduction

In an age of pervasive sensor technology that connect wirelessly in what is often referred to as the internet of things (IoT), fine grained operational and preference data has become abundant. Operations Management (OM) researchers are increasingly interested in incorporating such data into OM frameworks (Qi and Shen, 2018; Cohen, 2018; Choi et al., 2022). A concept that has received increasing attention is the Digital Twin (DT), a close-to exact digital representation of a physical product or operational system that is configured based on primary sensor data, realistic asset models and real-world operational procedures/policies (Choi et al., 2022; Grieves and Vickers, 2017). Digital Twins have traditionally been used for operational questions in the use phase of already-existing operational assets (van der Valk et al., 2020; Grieves and Vickers, 2017). However, several commentators have stressed that DTs could be of use even earlier in an asset's lifecycle – particularly in the design phase (e.g., Boschert and Rosen, 2016). Operations managers traditionally approach strategic planning of service networks via methods such as, mathematical programming (e.g., He et al., 2017, for on-demand vehicle sharing service region

[1]This Chapter is currently under review at a leading peer-reviewed academic journal. Parts of this Chapter have appeared in the following (non-copyrighted) peer-reviewed academic conferences and workshops:
Schroer, K., Ahadi, R., Lee, T. Y., & Ketter, W. (2021). Preference-aware Planning and Operations of Electric Vehicle Charging Clusters : A Data-Driven Prescriptive Framework. In Proceedings of the SIG GREEN Workshop (pp. 1–10). https://aisel.aisnet.org/sprouts_proceedings_siggreen_2021/1
Schroer, K., Ahadi, R., Lee, Y.T., & Ketter, W. (2021). Preference-Aware Planning and Operations of Electric Vehicle Charging Clusters: A Prescriptive Framework. In Workshop on Information Systems and Technology (WITS) 2021 (Austin, TX).

design) or queuing models (e.g., Wang and Odoni, 2016, for last-mile delivery networks). Computational tractability in these frameworks is achieved at the expense of detail and scope of the planning problem (e.g., short planning horizons, coarse temporal discretization, deterministic parameter assumptions, etc.). DTs have the potential to circumvent the need for simplification and problem size reduction, among other theoretical benefits. These benefits include (1) more realistic, data-driven modeling of stochasticity and operational detail, (2) computational scalability, (3) flexible model setup that allows for easy evaluation of many different operational policies and (4) ability to seamlessly carry over the DT into subsequent system life cycle phases (Boschert and Rosen, 2016). Therefore, we set out to answer the following core research question: *How can Digital Twins be leveraged for ex-ante decision support and investment de-risking during the design and configuration phase of service systems?*.

To demonstrate the efficacy of our solution approach, we apply it in the domain of Electric Vehicle (EV) Charging Hubs (EVCHs). Policy makers have traditionally assumed that users would primarily charge their EVs overnight and at home. Indeed, home charging is currently the preeminent charging use case in most markets. As more and more non-homeowners adopt EVs and as commercial fleets are electrified, charging opportunities at the workplace, at popular destinations such as supermarkets, and at fleet depots will be needed (Jun and Meintz, 2018; Lee et al., 2019; Hoover et al., 2021). EVCHs constitute a novel (thus under-researched) operational system class with cross-system interfaces (e.g., with attached buildings or the electricity grid) and a large number of both strategic and operational decision variables (size and configuration of charging stations, on-site storage, charging decisions, etc.) that result in a highly complex planning challenge (Ferguson et al., 2018). Such problem classes (i.e., multi-stage, stochastic) are notoriously challenging for optimization-based methods (Powell, 2014; Hannah, 2015) and therefore provide an ideal test bed.

Our work offers a number of contributions. Methodologically, we propose a framework for the effective use of DTs for ex-ante de-risking and decision support in the design phase of service systems. Our three-phase framework generalizes to any service system and (in combination with high-performance search or learning algorithms) is scalable to almost arbitrarily large system instances. In extensive, real-world-inspired simulation experiments, we show that our framework outperforms extant optimization-based approaches under realistic operating conditions due to a better ability to generalize beyond the training data (i.e., the data based on which the configuration was derived). As such, it provides a novel, high-performing, and actionable method for operations managers to effectively exploit the benefits of big data and high-fidelity DTs from the beginning of a system's life cycle. We also offer numerous domain-specific insights that result from the application of our DT-based framework to the case of EVCH system configuration.

The remainder of this work is structured as follows. In Section 4.2, we review the literature relevant to this work. We then derive a general model for DT-based service system planning and configuration (Section 4.3) and apply it to the case of EVCH planning (Section 4.4). We then

run extensive benchmark simulations (Section 4.5) followed by comprehensive scenario analyses (Section 4.6) to demonstrate performance and flexibility benefits of our DT-based method. We end with a discussion of implications and contributions to theory and practice (Section 4.7).

4.2 Background

Our work draws from two main bodies of literature, which we briefly review here. First, we discuss extant work on DTs and their use for OM decision support. Second, we review traditional OM system design approaches using the example of EVCHs.

4.2.1 Digital Twins (DTs) and their Use in Operations Management

DTs have been hailed as a disruptive trend in OM of the IoT and Industry 4.0 era (Choi et al., 2022). At its most basic level, a DT is a fully digital representation of a specific physical asset or system. DTs can be used as a decision support tool along the entire life cycle of that asset: from design, operations, and maintenance to disposal (Schleich et al., 2017). Various authors, commentators, and software vendors have brought forward diverging notions of the characteristics that make up a DT (van der Valk et al., 2020). For the purpose of this research, we highlight several characteristics that we consider key and which distinguish DTs from, e.g., traditional simulation frameworks (Boschert and Rosen, 2016). The reader is referred to Jones et al. (2020) or Cimino et al. (2019) for comprehensive reviews.

First and foremost, DTs represent a close to real-world representation of the physical system at a granular level using high-fidelity interconnected physical models of system components (Glaessgen and Stargel, 2012). Note that this does not necessarily require identical accuracy but can also mean partial accuracy if this is sufficient for the DT to fulfill its intended use (van der Valk et al., 2020). Second, a DT is data-driven, meaning that it primarily relies on real-world operational data input acquired directly from sensors of the device and the intended application environment (van der Valk et al., 2020). It is often not the case that raw data on all required parameters is available. In such cases, synthetic data from statistical models or simulation frameworks can be used to supplement the data requirements (Sierla et al., 2018). Third, there is eventual synchronization of the DT and the physical asset. This can be achieved via one-directional (physical world to DT) or bi-directional data flows (Tao et al., 2018). DTs have been successfully applied in the use phase of operational systems (Jones et al., 2020). Examples include asset status and health monitoring (Glaessgen and Stargel, 2012), asset optimization, maintenance planning (Cimino et al., 2019), and staff training (Choi et al., 2022).

As argued previously, a core feature of DTs is their reliance on real-world sensor data for asset and process representation in the virtual world. That does not, however, disqualify DTs from the use in design/configuration applications of assets and operational systems that are yet to be built. Indeed, high-granularity data on many aspects of the intended application environment as well as on typical machine/process behavior is likely to already be available. This means that pre-use-phase DTs can be fed with live as well as realistic historic data (Boschert and Rosen, 2016). Indeed, authors have argued that DTs can and should play a core role much earlier in a system's life cycle – particularly the configuration/design phase. Here DTs can act as a test

bed for different design configurations, a concept which Grieves and Vickers (2017) refer to as a "Digital Twin Prototype". Boschert and Rosen (2016), in their influential work, frame DTs as the "next wave" (p.61) in simulation-based system design with a direct linkage to operational data. However, despite these calls, the time of creation of a DT occurs most commonly *after* the production/installation of the physical system (van der Valk et al., 2020).

Our work addresses this gap by developing a novel DT-based solution approach for operational system design. We show that DTs, in combination with scalable search or learning algorithms, can circumvent many of the model simplifications and problem reduction measures unavoidable in traditional mathematical programming, thus providing more realistic asset configurations that can perform better than optimization-derived solutions under real-world conditions. Synchronization of the DT with the physical asset via machine-to-machine communication and data exchange is easily possible following the installation of the derived configuration in the physical world.

4.2.2 Electric Vehicle (EV) Charging Hub Design and Operations

Our work draws heavily on the case of EVCH configuration. EVCHs constitute an example of a complex system of high societal relevance for which DT-based approaches can provide valuable decision support. In this Section, we provide a short overview of the state-of-the-art in EV Charging Hub design and operations.

EVCHs exhibit several unique features that distinguish them from other charging use cases, such as distributed on-street charging, highway charging, and private home charging. First, EVCHs typically represent large locally concentrated loads that may require significant local electricity grid extension making load shaping necessary (Lee et al., 2019). Second, integration with behind-the-meter loads (buildings) and generation units (PV, storage) may be desirable (Nunes et al., 2016) to reduce induced peak loads, drive sustainability and reduce costs (Ferguson et al., 2018). Third, EVCHs typically experience different user behavior compared to other charging use cases such as home charging and this user behavior can vary substantially depending on the use case of the attached facility (workplace, mall, etc.). Fourth, siting of individual charging stations is of no concern in an EVCH context as all chargers will be located in the same space with users being largely indifferent between them. Finally, EVCHs allow for end-to-end control of the full vehicle-level parking and charging journey through what is sometimes referred to as smart EV-capable parking lots (Babic et al., 2022). This enables the assignment of vehicles to chargers and central control over the charging process. It, thus, offers new scope for optimization, e.g., by leveraging parallel or sequential use of charging equipment in an optimal manner (Ferguson et al., 2018). Given that modern parking facilities are typically equipped with connected sensors, high availability of operational data can be assumed. As such, EVCHs represent a timely and challenging environment to develop, implement and test novel data-driven OM methods.

We briefly review state-of-the-art OM approaches in the realms of (1) operating and (2) configuring EVCHs. In terms of EVCH operations, we acknowledge the extensive work on electric vehicle charge scheduling and smart charging (see e.g., Mukherjee and Gupta (2015) for a recent review) that most operations-focused EVCH research is based on. A notable differentiator from the traditional smart charging literature is the inclusion of building/cluster-level constraints and optimization opportunities. Early examples include Huang and Zhou (2015) who develop a mixed-integer optimization framework for workplace charging strategies taking into account different eligibility levels and Wu et al. (2017) who propose a two-stage energy management framework for office buildings with workplace EV charging. Nunes et al. (2016) investigate how charging processes can best be coordinated to use parking lots for EV solar-charging. Ferguson et al. (2018) propose an integrated load management approach to optimize EV charging processes for minimum cost taking into account the building base load and PV generation. A similar site-level load management approach was implemented in practice by Jun and Meintz (2018). Finally, Lee et al. (2019) explore several optimization-driven approaches to operational issues in charging hubs.

Designing EVCH systems has received somewhat less attention. This is likely a result of the complexity of the ensuing design challenge. EVCH configuration is a multi-stage stochastic decision problem that requires large decisions (e.g., the number of charging docks to be installed at each stage in the planning horizon) and small decisions (e.g., charging individual vehicles) to be taken simultaneously. Such problems are notoriously difficult and cannot be solved efficiently with standard stochastic programming or even approximate dynamic programming (Powell, 2014; Hannah, 2015). Some research resolves the ensuing complexity by using simulation-based approaches. For example, in Kazemi et al. (2016) the authors use a genetic search algorithm on top of a simplified simulation model to derive the optimal size of an EV parking lot. Babic et al. (2022) also use a greedy search over a simulation of a parking lot to derive optimal infrastructure decisions. Li et al. (2020) propose a deterministic mathematical programming framework for joint optimization of size and operations of a small-scale, 100-vehicle EV-capable parking lot. Neither of these simulation- or optimization-based studies use high-granularity demand and/or operational data. In addition, extant EVCH design work exhibits low scope and significant simplifications. For example, the studies cited here focus on a single planning stage only, which reduces the problem to a single-stage planning challenge. In addition, the EVCH system scope tends to be considerably simplified (e.g., no consideration of attached building loads, single-use charging docks only, etc.). Using DTs, combined with high-performance search/learning, these simplifications can be avoided.

4.3 A Framework for DT-Based Design of Complex Service Systems

The proposed DT-based service system configuration framework is presented in Figure 4.1. Our three-step approach leverages the unique advantages of DTs (inclusion of stochasticity, high modeling detail, flexibility and scalability) and provides a framework for applying them to service system design problems.

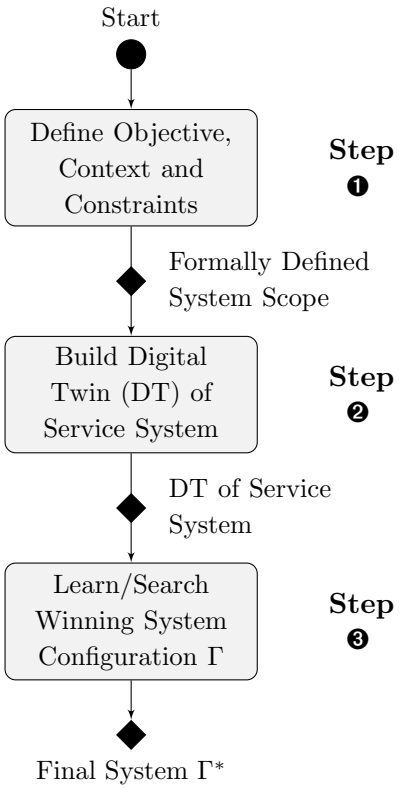

Figure 4.1: Model for the Use of Digital Twins in the Design Phase of Complex Service Systems

4.3.1 Step ❶: Define Objective, Context and Constraints

Step ❶ (see Figure 4.2) comprises the scoping and objective definition of the planning challenge at hand. Operations managers are often interested in achieving some sort of desired system performance at the lowest possible cost (i.e., cost minimization with service level constraint), or, alternatively, maximum profits. More complicated multi-objective settings are also conceivable that might, for example, target a balance between economic and environmental objectives (e.g., Sharifi et al., 2020). The system configuration Γ is optimized against these goals. Thus, defining the corresponding objective function, decision variables (e.g., choice of assets setup), parameters (e.g., costs) and planning horizon (e.g., single year vs. multi-year investment horizon) is a core first step in the service system design process. In addition, local constraints (e.g., space

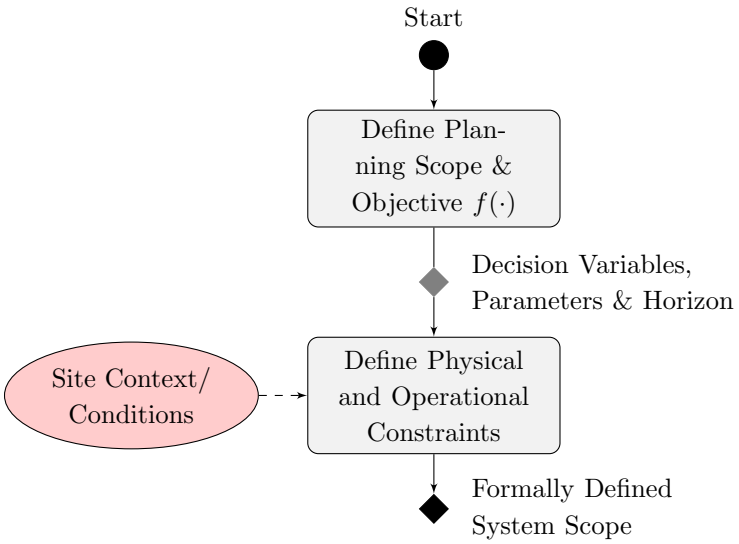

Figure 4.2: Detailed View Step ❶: Define Objective, Context and Constraints

constraints, operational constraints, etc.) are to be identified and incorporated into the problem formulation. At the end of Step ❶ the planning challenge is scoped and formalized to a degree that all information is available for a traditional optimization model to be implemented. Thus, traditional OM methods would typically stop here.

4.3.2 Step ❷: Build and Parameterize Digital Twin of Service System

In Step ❷, a digital representation (i.e., the DT) of the service system components is developed. Three core components make up an operational system (Γ): (1) physical assets (Π), (2) operational policies (Ω) that define how the physical assets are operated, and (3) preference/demand characteristics (Ψ), i.e., the external requests and usage patterns that the service system needs to fulfill. The DT will have to accurately capture all three dimensions while adhering to the system scope and constraints defined in Step ❶.

Figure 4.3 provides details on the process of setting up the DT framework. The DT is populated with realistic asset models Π that simulate physical processes in close-to real-world detail. This avoids oversimplification commonly seen in optimization stemming from attempts to achieve smaller problem sizes. For example, battery degradation is typically heavily simplified to achieve tractability in the optimization of energy systems (Kazhamiaka et al., 2019). The creation of digital asset models per each relevant physical system component should rely on secondary real-world sensor data (e.g., to obtain real-world charging and discharging efficiencies for the case of batteries) along with technical specification sheets, where data from comparable assets is not available.

In addition, realistic operational policy options Ω are implemented that model how the physical assets will be used and managed (if there is active operational management) in practice.

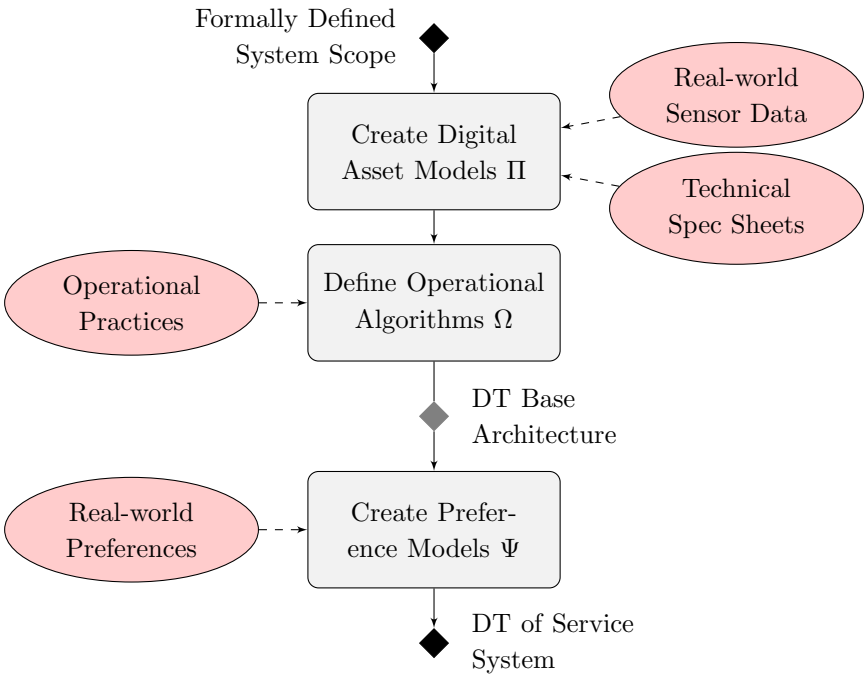

Figure 4.3: Detailed View Step ❷: Build and Parameterize Digital Twin of Service System

Optimization models generally assume optimal operations at low temporal detail. In practice, relatively naive rules-based approaches often replace optimal policies. For example, many of the extant smart charging solutions available on the market charge vehicles on a first-come-first-served basis. Such imperfect operational processes are difficult to model in mathematical programming models and may lead to unrealistic sizing decisions. In a DT environment, multiple realistic operational policy choices can be implemented and evaluated under real-world conditions with ease.

The DT is then supplemented with real-world data from pre-existing sensors to model demand and preference patterns along with other contextual data. Examples include, current electricity demand, user behavioral patters, weather data, or other relevant contextual information. Wherever real-world data is not available, synthetic data may be generated, or data from similar use cases may be transferred to the DT. Note that while traditional mathematical programming frameworks may also draw on real-world data, they will typically require significant simplification/aggregation to achieve tractability.

4.3.3 Step ❸: Learn/Search Winning Service System Configuration

In Step ❸, a search or learning algorithm is initialized, adapted to the problem at hand, and then used to derive a winning system configuration (Γ^*) by iteratively updating and evaluating the candidate solution against the objective defined in Step ❶. This is achieved by following a system configuration policy π to incrementally update and evaluate candidate system configurations Γ'

until a convergence criteria is met. A detailed process description is provided in Figure 4.4. The DT plays an integral part in this process as it provides the environment for evaluating any intermediate system configurations obtained during the search/learning process against the objective function in a close-to real-world stochastic setting.

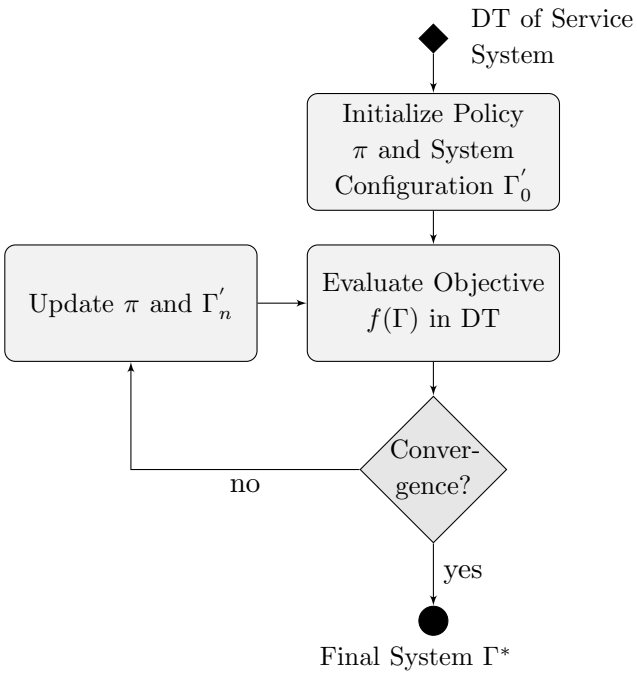

Figure 4.4: Detailed View Step ❸: Learn/Search Winning Service System Configuration

Note that both search (e.g., brute force search, meta-heuristic algorithms) and learning techniques (e.g., reinforcement learning) represent valid solution approaches. Both techniques are general purpose and highly scalable with computing power (Sutton, 2019). They can, thus, be flexibly applied to any real-sized planning environment. Note also that while search first maps the entire solution space and then explores it, learning updates incrementally and refines the solution through interaction with and learning from the environment. Learning, therefore, circumvents the computationally expensive process of full solution space mapping and instead uses iterative updating of the configuration policy π to parameterize the next candidate solution that is to be evaluated in the DT environment. This clearly distinguishes learning from meta-heuristic search solutions that operate on a constant policy for defining the next candidate solution. Both approaches have been explored for this work, although only learning (reinforcement learning using deep Q-learning algorithms) is reported for the case of EVCHs due to its superior computational performance and an ideal fit to the multi-stage nature of the design challenge that results in a sequential decision problem (Hannah, 2015).

4.4 Application to EV Charging Hubs (EVCHs)

We now apply our framework to the case of EVCHs. A table summarizing the nomenclature used throughout this article is provided in the Appendix. EVCHs represent an ideal application domain both from a practical perspective and a methodological viewpoint. In terms of practical relevance, EVCHs are poised to become a key component in the future sustainable mobility nexus (Hoover et al., 2021). Any domain-specific insights generated in this study can therefore be expected to offer relevant practical contributions. Methodologically, EVCH planning represents a large complex multi-stage stochastic decision problem, which is not readily solvable with extant stochastic programming methods (Powell, 2014). Consequently, an opportunity arises for scalable DT-based approaches to step in.

4.4.1 Step ❶: Defining EVCH Planning Objective, Context and Constraints

We define an EVCH as an EV charging-capable parking lot, depot, or garage that will typically be attached to an existing building with a given baseload. Both the building and the EVCH receive power from the same grid connection point, which is constrained to the capacity of the on-site substation. The integrated facility may have additional on-site behind-the-meter generation (photo-voltaic (PV)) and storage (Lithium-Ion battery). A simplified representation of the EVCH system boundary and its components is depicted in Figure 4.5.

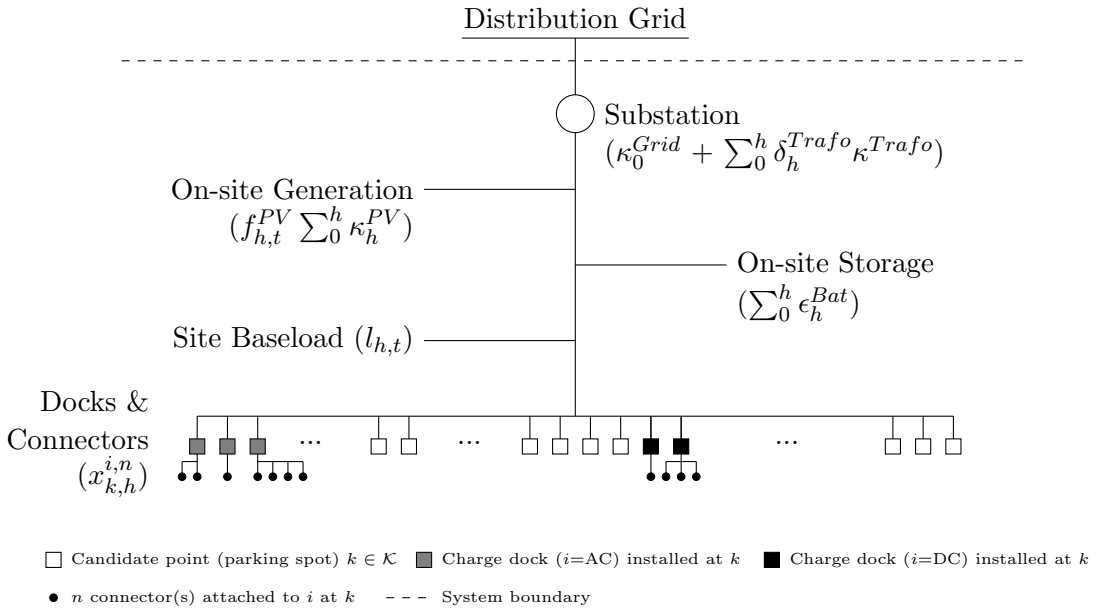

Figure 4.5: EVCH Service System Layout and Asset Components in Planning Stage h

We formulate the EVCH configuration challenge as a feasibility problem that aims to satisfy all or a specified amount of total charging demand in the most resource-efficient manner while considering any exogenous rate, space, and total capacity constraints. The problem then be-

comes a cost minimization planning with the objective to jointly minimize investment costs (C^{Φ}) and operations cost (C^{Ω}) over all stages $h \in \mathcal{H}$ contained in the planning horizon while ensuring a pre-defined service level η^h (typically 100% in the following simulations and benchmarks). Formally, the objective function $f(\Gamma)$ (where Γ is the system configuration) can be expressed as follows:

$$Min_{\Gamma}[C^{\Phi}(x_{k,h}^{i,n}, \delta_h^{Trafo}, \kappa_h^{PV}, \epsilon_h^{Bat}) + C^{\Omega}(\omega_{k,j,h}, \psi_{k,j,h,t}, \beta_{h,t}^{Charge}, \beta_{h,t}^{Discharge}, e_{h,t}^{G})] \tag{4.1}$$

The EVCH infrastructure decision space determining C^{Φ} extends over a large set of decision variables, which we briefly lay out here. First, decisions on the charging infrastructure configuration and scale-up over the investment horizon $\mathcal{H}$ are required. We allow full flexibility regarding the type of EV charging docks (22kW AC or 50kW DC docks) and the number of connectors per dock (ranging from single-connector setups to up to four connectors per dock). Crucially, for charging docks with multiple connectors, we allow for simultaneous charging of EVs, meaning the rated power per dock can be shared dynamically and flexibly by all connected vehicles. This is different from the more prevalent single-server docks, which either possess just a single connector or multiple connectors that may only be operated sequentially. A multi-server setup has the advantage of higher utilization (vehicles that have completed their charging cycle do not block charging docks) (Ferguson et al., 2018). We capture EV charging infrastructure decisions via a set of binary indicator variables of form $x_{k,h}^{i,n}$, indicating whether a dock of type $i \in \{22kW, 50kW\}$ with number of connectors $n \in \{1, 2, 4\}$ is to be installed at candidate point $k \in K$ during planning stage $h \in \mathcal{H}$. The total number of docks and connectors is naturally bounded by the size of the facility (i.e., number of parking spaces) L. Second, the initial size and expansion pathway of possible on-site generation (PV) and/or storage assets (Li-Ion battery) must be defined. We assume that PV generation κ_s^{PV} can be scaled close-to continuously across all stages h in the planning horizon and that it is limited only by local facility space constraints R (e.g., roof space). In terms of on-site storage, we consider Li-Ion battery technology whose energy capacity κ_s^{Bat} (in kWh) can be scaled continuously over $\mathcal{H}$. Finally, a decision is required on whether, by how much and by when the existing substation capacity should be extended to accommodate the desired level of charging service. Note that substations can be purchased in standard sizes (κ^{Trafo}) only. Consequently, the grid connection can only be scaled step-wise in multiples δ_h^{Trafo} of κ^{Trafo}, where δ_h^{Trafo} is an integer value denoting the number of transformer modules to be added to the facility's substation in state h[2]. Given the physical size of substations and the fact that local grid conditions may not allow for an unconstrained scale-up of the existing grid connection, we impose a maximum G on the final size of the substation. In sum, total investment cost over the planning horizon is determined as follows:

[2]We consider any interaction effects with the upstream electrical distribution grid to be out of scope for this problem. Specifically, we assume that the distribution grid is unconstrained and able to accommodate any additional load from the EVCH, provided sufficient substation capacity (i.e., transformers) is installed for voltage regulation.

$C^{\Phi} = \sum_{h\in\mathcal{H}}(c_h^{Trafo}\delta_h^{Trafo}+\sum_{k\in\mathcal{K}}\sum_{i\in\mathcal{I}}\sum_{n\in\mathcal{N}} c_h^{i,n}x_{k,h}^{i,n}+c_h^{PV}\kappa_h^{PV}+c_h^{Bat}\epsilon_h^{Bat})(1+(|\mathcal{H}|-h)\rho^{Maint}))$. Note that this includes the maintenance costs incurred over the planning horizon, which is captured by the factor $(|\mathcal{H}| - h)\rho^{Maint})$. The parameters c_h^{Trafo}, $c_h^{i,n}$, c_h^{PV} and c_h^{Bat} are stage-dependent cost parameters that take into account expected technology cost trajectories over the planning horizon.

Underlying these higher-level infrastructure choices are smaller operational decisions, which determine the operational cost C^{Ω}. Naturally, the operational scope is constrained by the installed infrastructure highlighting the two-way interdependencies between both sets of decisions. Operations decisions focus on the assignment of a vehicle j to a connector k upon arrival (captured by $\omega_{k,j,h}$) and the periodical charging decisions over the duration of stay ($\psi_{k,j,h,t}$). Finally, the on-site battery state is controlled via $\beta_{h,t}^{Charge}$ and $\beta_{h,t}^{Discharge}$, two booleans that control the rate of charge/discharge. We consider PV generation and building baseload to be exogenous parameters that cannot be actively controlled by the EVCH operator. Given the different sources of power (battery, PV, grid), the operator also needs to decide on the power mix per each period t. This involves setting the desired energy drawn from the grid per period in each state $e_{h,t}^{Grid}$. Note that $e_{h,t}^{Grid}$ is typically accounted for based on a two-part tariff including a time-of-use-dependent energy charge $T_{h,t}^{e}$ and a monthly demand charge T_h^p that is a function of the maximum induced power p_h^* in that month. Operational costs are formally defined as follows: $C^{\Omega} = \sum_{h\in\mathcal{H}}(\sum_{t\in\mathcal{T}} T_{h,t}^{e}e_{h,t}^{Grid} + T_h^p p_h^*)$.

4.4.2 Step ❷: Creating Digital Twin of EVCH Service System

The DT environment operates on a discrete-time basis. To reduce any issues/inconsistencies related to discretization, we use very small periods of just one minute. In what follows, we lay out asset models, operational strategies, and preference data sources that constitute the DT.

Creating Digital EVCH Asset Models Π

Figure 4.5 provides an overview of the physical EVCH asset classes that are to be represented digitally in the DT environment. In line with the general approach laid out in Figure 4.3, we draw on asset spec sheets along with real-world machine data to represent the physical EVCH components and the context they operate in as accurately as possible.

Local Substation We model the local substation as an integrated system consisting of transformers, circuit breakers, and other peripheral equipment that connect the site to the higher voltage levels of the distribution grid. The substation capacity is determined by the sum of rated transformer capacities. Although typically very low, we account for transformation losses using an efficiency factor of 1-η^{Trafo}=2%.

On-site Electricity Generation Assets (PV Panels) The only type of electricity generator we consider are photovoltaic (PV) modules – in many senses, a natural supplement to EV charging hubs due to their production patterns, that is highly correlated with occupancy profiles (and thus charging demand) of most parking lots. Naturally, PV power output is dependent on local weather conditions (particularly solar irradiation), which we model via the use of real-world load factors. PV generation is non-dispatchable, i.e., it cannot be actively controlled. PV power is therefore either consumed on-site (by EVs, battery storage, building, etc.) or fed back into the grid. Note that PV installations require DC-AC conversion via inverters. The efficiency losses of AC-DC conversion are accounted for and are typically in the region of 1-η^{Inv}=4%. We use real-world PV load factors ($f^{PV}_{h,t}$) to model PV production from the regions corresponding to the intended EVCH facility locations. Load factors are a measure of real PV panel power output as a ratio of installed capacity (κ^{PV}_{h}) and depend on local solar irradiation conditions[3]. PV production at time t (excluding DC-AC conversion losses) is then given by $f^{PV}_{h,t}\kappa^{PV}_{h}$.

Electricity Storage Assets We model electricity storage as a lithium-ion battery with instantaneous ramp time. To avoid excessive battery degradation, we allow the state of charge to vary over the interval of $[5\%, 95\%]$, thus avoiding deep discharging and over-charging that are particularly strenuous for battery hardware. Setting upper and lower energy content boundaries is a common approach in storage management (Ghiassi-Farrokhfal et al., 2016). We also assume symmetric charge and discharge efficiency of $\eta^{charge} = \eta^{discharge} = 95\%$. Battery operations are simulated using what is sometimes referred to as a C/C/C model[4]. In addition, we implement typical battery constraints related to the maximum charge and discharge rate κ^{Bat} (symmetric). κ^{Bat} is dependent on the size of the battery and is set such that the battery can be charged/discharged to/from full charge within one hour.

Peripheral Building We use real-world building consumption data to model site baseload ($l_{s,t}$) that are served by the same grid connection, thus influencing total available grid capacity at any given period t (see Figure 4.5). Contrary to EV loads, we assume $l_{s,t}$ to be exogenous, i.e., it cannot be dynamically managed or even curtailed. Given the absence of smart energy management hardware in most existing building stock, this is a reasonable assumption. Note that granular consumption data is widely available for commercial buildings above a certain consumption threshold since these consumer classes are typically exposed to time-of-use tariffs as well as demand charges for induced peak load. Our 1-year dataset records peak building loads and consumption at a 15-minute resolution.

[3]This data is available via local transmission system operators (TSOs) and generally comes in 15-minute intervals.

[4]C/C/C models assume constant battery charge/discharge efficiencies, constant energy content upper and lower bounds, and constant voltage (Kazhamiaka et al., 2019)

EV Charging Docks and Connectors We model two different types of charging docks that mainly differ in terms of maximum charging rates κ. Specifically, we allow for AC fast chargers with maximum charging capacity $\kappa^{i=AC}$=22kW and DC super-fast chargers with maximum charging capacity $\kappa^{i=DC}$=50kW. For each charger type $i \in [AC, DC]$ we allow for different connector configurations with $n \in [1, 2, 4]$ connectors per dock. We assume that κ can be shared dynamically and flexibly between all connectors per dock. This means that connected EVs can be served both sequentially and simultaneously via the same dock. Losses related to AC-DC conversion are modeled using an efficiency factor of 1-η^{Inv}=4%[5].

Defining EVCH Operational Algorithms Ω

We also implement a range of realistic operational policies that simulate real-world operations in the DT environment. These policies are inspired by standard operational practices currently used in EV charging operations as well as recent algorithms proposed in the EV charging literature (e.g., Lee et al., 2019; Ferguson et al., 2018). Given that we allow for multi-connector charging docks with simultaneous charging capability, the initial assignment of vehicles to charging stations becomes important due to heterogeneous energy demand and flexibility characteristics. Clearly, since EVs cannot be readily relocated while parked, the initial assignment to a connector influences future available charging capacities for the EV in scope as well as for current and future arrivals that are to be served by the same charge dock.

Vehicle Routing Algorithms Vehicles $j \in \mathcal{J}$ are routed/assigned to a connector k upon entry into the EVCH (captured by $\omega_{k,j,h}$). We implement two heuristic routing algorithms of varying levels of sophistication and varying information requirements.

- **Lowest-utilization-first (LUF)**: This strategy operates on a sorting basis. At each new arrival, the algorithm sorts all available docks based on free capacity. New arrivals are routed to docks with low utilization first. In the case of a tie, the algorithm selects randomly between the charging docks it is indifferent between. An advantage of the lowest-utilization-first approach over other sorting methods (such as lowest-occupancy-first) is that it considers the different charging capacities of AC vs. DC docks in the assignment process.
- **Lowest-laxity-to-highest-capacity matching (LLHC)**: This strategy not only considers the state of individual charging docks but also that of the vehicle that is to be assigned. Specifically, it sorts arriving vehicles into baskets of low, medium, and high laxity (using bins obtained from historical data). Low-laxity vehicles are then matched with charging docks that have a high free capacity and vice versa, thus implicitly provisioning for future arrivals.

[5]For AC charging, the AC-DC inverter is integrated with the vehicle charger unit, whereas for DC charging the inverter sits inside the charging dock

Vehicle Charging Algorithms Vehicle-level charging schedules are re-computed in an online manner every five minutes allowing for updating of pre-computed schedules as new information becomes available. We implement a selection of sorting-based algorithms and optimization-based approaches to periodically determine the charge rate per connector k, vehicle j and time t $\psi_{k,j,h,t}$:

- **First-come-first-served (FCFS)**: Charging requests are served on a first-come-first-served basis at full charging dock capacity until the available power capacity (on-site generation, storage, and grid) is exhausted. This algorithm is largely consistent with standard off-the-shelve load management tools available in the market today.
- **Least-laxity-first (LLF)**: Equivalent to the first-come-first-served algorithm but using a least-laxity-first priority rule meaning that least flexible vehicles are charged first. The algorithm therefore explicitly considers the current state of a vehicle in the charging decision.
- **Optimal**: Optimal operations uses mathematical optimization to periodically (re-)compute cost-optimal charging schedules that satisfy charging demand for the planning period δt in scope. We implement a standard cost-optimal charging framework (e.g., Ferguson et al., 2018). In our simulations, we plan $\delta t = 12$ periods ahead. We also implement a smoothing constraint by limiting the maximum charging ramp rate and considering the parallel use of docks. Since future arrivals and their preference vectors are unknown at the time of planning, we use a carefully tuned safety margin to be able to accommodate these in future periods. Further details are provided in Appendix A.

Electricity Storage Operational Algorithms The third and final system component requiring active operational management is the on-site energy storage system. We implement a heuristic approach that has been demonstrated to perform well under real-world conditions (Gust et al., 2021). We update battery-specific decision variables $\beta_{s,t}^{Charge}$ and $\beta_{s,t}^{Discharge}$ every five minutes[6]:

- **Temporal arbitrage (TA)**: The algorithm exploits the structure of the underlying time-of-use electricity tariff. During off-peak hours, the battery is charged at a constant rate until the upper bound of the allowable energy content is reached. During on-peak periods, the battery is discharged at a constant rate to reduce the amount of electricity purchased at the higher on-peak price.

Creating EVCH Preference Models Ψ

We populate the DT base architecture consisting of the above-described asset models and operational policies with an EVCH-specific high-resolution model of parking and charging prefer-

[6]Note that battery decisions are made after the previously described charging decisions are made and that the available battery capacity at the start of each planning period is available for EV charging.

ences. The charging behavior of EV users is mostly activity-based and depends on identified socio-demographics (gender and age), vehicle characteristics, commute behavior, and workplace charging availability (Lee et al., 2019). Thus, any charging infrastructure should be aligned with these existing preferences such that minimal behavioral adjustment on the user side is needed.

EVCH user preferences (of an individual j) are described by the three-dimensional vector $v_j = (A_j, \delta_j, e_j^d)$ where A_j is the time of arrival, δ_j the duration of stay and e_j^d the requested energy. δ_j and e_j^d define what is referred to as laxity ($lax_j = \delta_j - \frac{e_j^d}{\kappa^i}$) (Nakahira et al., 2017; Lee et al., 2019). $lax_j = 0$ means that a vehicle j needs to charge at the maximum available rate κ^i for the entirety of its stay, while higher laxity values indicate more room for active charging management. Time of entry A_j determines the earliest planning period by which a certain charging event needs to be initiated. We start by building a model of current archetypical parking patterns. We do this in order to understand what typical parker types exist and how the user base composition can vary across facilities. A taxonomy of parker types can also be useful for building synthetic user population datasets based on assumed parker type shares wherever real-world data is not available. We leverage a unique transaction-level parking dataset that was provided by a major European real-estate investor and includes transactions from seven large-scale parking garages (capacities range from 275 to 2200 parking spots)[7]. We use a full year of data to capture daily, weekly and yearly seasonality. 2019 is chosen as the reference year to filter out pandemic-related effects. In total, our data comprises 3.84M parking events. We cluster parking events j based on A_j and δ_j, the two core parameters of interest at this modeling stage. All details related to data pre-processing, selection of clustering algorithms, and robustness tests are provided in Appendix B. In Table 4.1 we summarize our results. The largest proportion of parking events in our dataset is made up of three short-term parker types (*Morning Short*, *Afternoon Short* and *Evening Short*). These users enter a parking lot in the morning, afternoon, or evening respectively and typically stay for periods of 1-2 hours. We also observe a *Business* cluster, which comprises parking events that commence in the early morning (7:26am on average) and last for an average of 8 hours. Two additional segments comprise longer-term parking events. These are *Overnight* parkers, which enter the parking lot in the late afternoon and stay until the next morning (typically 15.8 hours on average), and *Long-term* parkers that stay for periods longer than 24h on average.

We then look at the distribution of parker types across the different facilities in our dataset. Three archetypical facilities can be identified: The first facility type is a typical workplace facility that caters mostly to Business parkers. The second facility type is a destination facility. Apart from a small proportion of Business users, such facilities mostly host Short-term parkers. Finally, we also observe facilities with less conclusive usage patterns experiencing strong demand

[7]Each row in this dataset represents a single parking event j with corresponding arrival and departure preference information. For privacy reasons, individual users cannot be identified

from all segments. We term these mixed-use facility[8]. Typical occupancy profiles for each of the three facility types are shown in Figure 4.6.

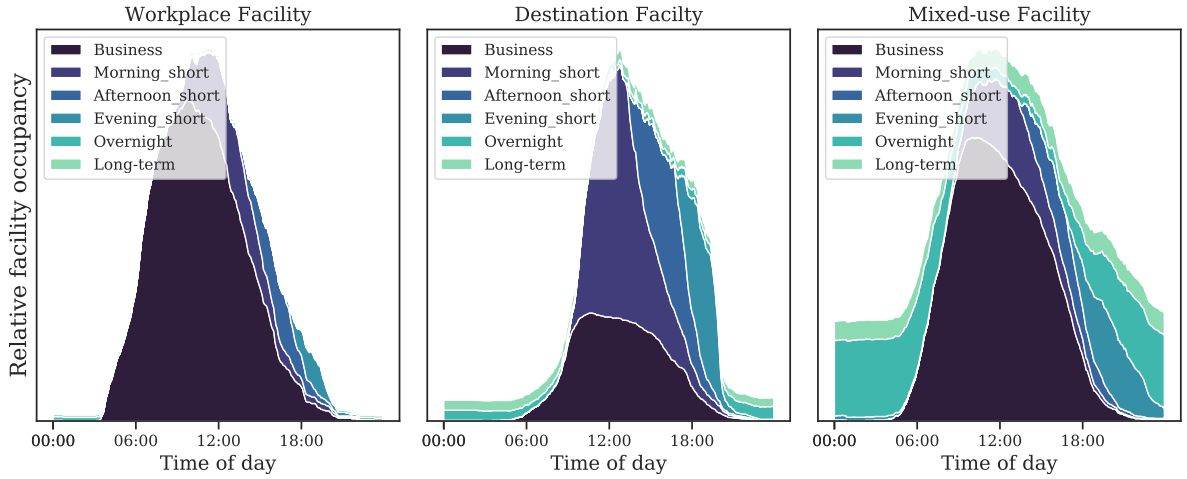

Figure 4.6: Occupancy profiles per parker type (three archetypical parking facilities)

Finally, we focus on the third required preference input variable: the requested energy per vehicle e_j^d. We employ a recently published real-world dataset by Lee et al. (2019) containing >25,000 charging transactions for the year 2019. Per each charging transaction the full preference vector $v_j = (A_j, \delta_j, e_j^d)$ is available. We blend the charging data (which only contains served sessions that are constrained by the available infrastructure) with our parking dataset (which contains all parking requests per facility) using techniques from collaborative filtering. We train a prediction model on the labeled Lee et al. (2019) dataset and use the resulting model to predict charging demand in the parking dataset. We obtain an exponentially distributed charging demand across the entire population of EVs with an average demand of 26.46 kWh (σ = 17.20 kWh) per parking session[9]. The distributional shape of charging demand is consistent with the one seen in other empirical EV charging settings (e.g., Ferguson et al., 2018). Crucially, however, Table 4.1 highlights important implications for charge management resulting from the different compositions of parker types in a facility. As can be seen, the average laxity varies significantly across parker types. Thus, parking facilities with high a proportion of high-laxity parkers (e.g., Business, Long-term) benefit from considerably higher flexibility characteristics with higher scope for optimization through intelligent charge management and parallel charging at lower rates.

[8]The example shown in Figure 4.6 (right panel) is a large-scale inner-city parking facility that caters to workers, visitors and residents.

[9]We also apply some limited post-processing by limiting e_j^d to a realistic maximum bounded by the typical size of batteries (100 kWh) and feasible energy transfer over the duration of stay assuming 50kW maximum charge rate.

[10]assuming 22kW max. charge rate

Table 4.1: Preference characteristics per parker type

		Cluster Size		Characteristics (avg & std. in parentheses)		
k	Name	N	share	A_j	δ_j	lax_j[10]
1	*Business*	671,384	17.47%	7:26am (1.43h)	7.92h (2.73h)	6.29h (2.84h)
2	*Morning Short*	1,279,646	33.30%	11:10am (1.33h)	2.12h (1.90h)	1.31h (1.75h)
3	*Afternoon Short*	985,710	25.65%	3:03pm (1.00h)	1.73h (1.35h)	1.08h (1.30h)
4	*Evening Short*	744,753	19.38%	6:17pm (1.84h)	1.47h (1.30h)	1.11h (1.35h)
5	*Overnight*	129,273	3.36%	5:22 pm (4.01h)	15.84h (4.02h)	12.65h (4.40h)
6	*Long-term*	32,241	0.84%	2:28pm (4.94h)	37.04h (6.70h)	35.80h (6.98h)

Combining Asset Models, Operational Algorithms and Preferences into an EVCH Digital Twin

Combining asset models, operational algorithms, and charging demand preferences yields a high-resolution DT of the envisioned EVCH system. Figure 4.7 and 4.8 highlight the internal mechanics of the DT environment[11]. Figure 4.7 represents the demand side and visualizes load curves for the various load sinks in the EVCH (EV charging, building baseload, battery storage charging) over the simulation horizon. Building load curves follow a recurring daily pattern ramping up during the day and down again during the night. Loads are slightly lower on the weekend (especially on Sunday). Note also the battery storage load which reflects the temporal arbitrage strategy.

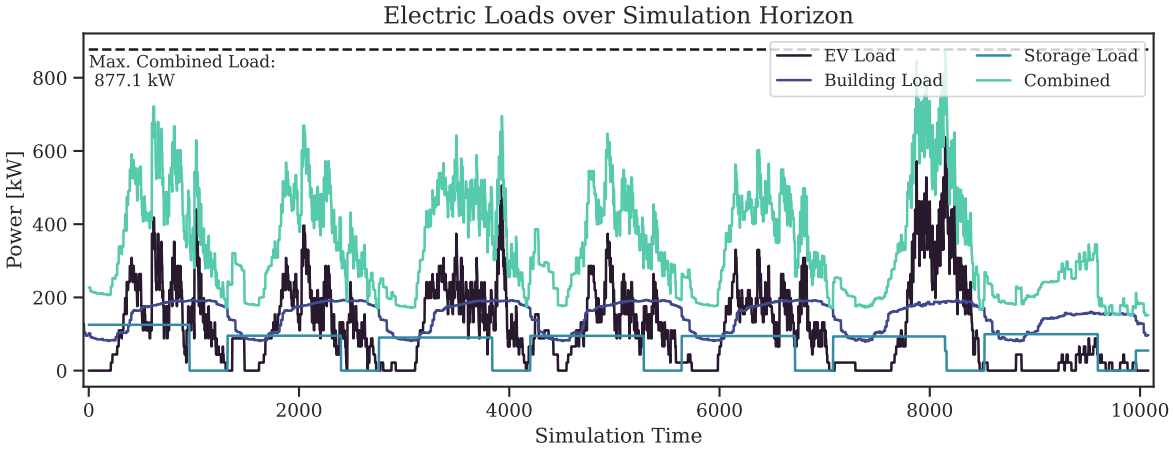

Figure 4.7: Power supply by load sink over one-week simulation horizon (Monday through Sunday, Mixed-use facility)

The power requested by the above-described load sinks is supplied by the grid, the on-site generation unit (PV), or the on-site electricity storage. The behavior of the supply side is shown in Figure 4.8. Note how the exact supply mix heavily depends on the time of day (e.g., no PV

[11] Shown here for a random week in a mixed-use facility using Lowest-laxity-to-highest-capacity routing, optimal charging and temporal arbitrage storage operations

generation after sunset, battery disc) and even weather conditions (note the considerably higher PV output in the middle of the week).

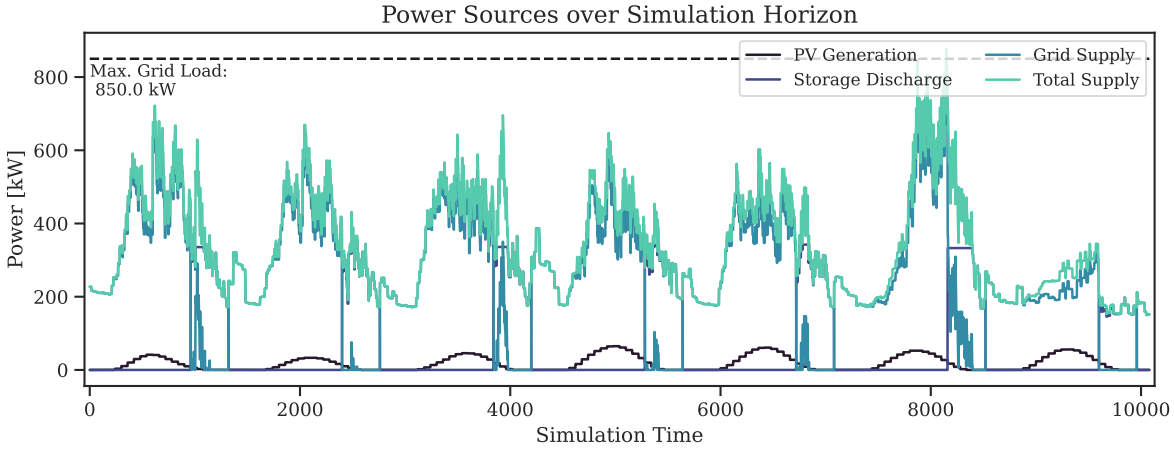

Figure 4.8: Power supply by load source over one-week simulation horizon (Monday through Sunday, Mixed-use facility)

4.4.3 Step ❸: Learning Winning EVCH System Design

Having defined the design objective and the DT environment allows us to use high-performing iterative methods to obtain a (near-optimal[12]) solution to the system design challenge at hand.

A core complication here is the discrete nature of most decision variables (e.g., number of connectors, number of transformers, etc.). This significantly limits the choice of applicable search or learning techniques. Suitable search approaches for discrete solution spaces like ours are meta-heuristic frameworks like, for example, genetic algorithms (GA). GAs have successfully been applied to similar (but mostly lower-dimensional) operations management problems (e.g., Fu, 2002). These random search approaches can perform relatively well provided the search environment is not complex (e.g., a queuing network) and the possible number of decision variables is manageable. In addition, if the environment is highly stochastic, more and more iterations are needed to ensure an accurate objective function estimation. This can quickly lead to intractable solution spaces.

An alternative to meta-heuristic search is learning (Fu, 2015). For the case at hand and given that planning decisions are made over multiple planning stages h in planning horizon $\mathcal{H}$, the problem can be framed as a stochastic sequential decision-making problem. This problem class can be cast as a Markov Decision Process (MDP). An episodic task emerges, which starts at the beginning of the planning horizon ($h = 0$) and runs through the last investment stage $h = |\mathcal{H}|$, with the epochs being the individual decision stages (e.g., beginning of each year). The state $s = (h, s^{chargers}, s^{grid}, s^{PV}, s^{storage})$ is defined as a vector of the time (i.e., the planning

[12]Note that global optimality cannot be guaranteed for most learning or search methods.

stage h) and the already installed equipment which is determined by previous decisions (e.g., the cumulative number of installed chargers, etc.). Actions are described by the vector $a = (a^{chargers}, a^{grid}, a^{PV}, a^{storage})$ and comprise planning decisions, such as the number of fast/slow docks with a specified number of plugs, the number of transformers, the PV capacity and storage to be installed. In line with the planning objective defined in Step ❶, we define the reward for moving from state s_h to s_{h+1} as $r = r(s, a) = C^{\Phi} + C^{\Omega} + C^{\Psi}$, where C^{Ψ} represents the penalty related to unserved charging demand in the corresponding planning stage[13]. Despite a deterministic state transfer function, exact reward functions are stochastic and unknown. In other words, given a decision, the next state is known, while the expected reward is unknown unless the state is evaluated in the EVCH DT environment. Therefore, we employ model-free reinforcement learning to find an optimal EVCH configuration policy π^*. Specifically, we use Q-learning to estimate the action-state value functions $Q(s, a)$. $Q(s, a)$ is updated according to the below Bellman equation, where α is the learning rate with $0 < \alpha \leq 1$ and γ is a discount factor applied to future state-action values.

$$Q(s_h, a_h) \leftarrow Q(s_h, a_h) + \alpha[r(s_h, a_h, s_{h+1}) + \gamma max_{a_{h+1}} Q(s_{h+1}, a_{h+1}) - Q(s_h, a_h)] \tag{4.2}$$

Due to the large state and action space of the EVCH environment and to improve generalizability of our learning agent, we employ deep Q-networks (DQNs) to approximate $Q(s, a)$. We refer the readers to Mnih et al. (2015) for more details. DQN uses a neural network with weights θ as a proxy for action-state values. To train the network, we store transitions (state, action, reward, duration) in an experience replay memory and then update the weights using a random batch of transitions by minimizing the below (squared) loss function:

$$\mathcal{L}(\theta) = \mathbb{E}_{s_h, a_h, s_{h+1}}[(r(s_h, a_h, s_{h+1}) + \gamma max_{a_{h+1}} Q_{\bar{\theta}}(s_{h+1}, a_{h+1}) - Q_{\theta}(s_h, a_h))^2] \tag{4.3}$$

where $Q_{\bar{\theta}}$ is the action-value estimation using a separate network (target network) that is updated less frequent than the main network.

[13] C^{Ψ} can be understood as a constraint that ensures full service level target

4.5 Performance Evaluation and Benchmark

We run several benchmark experiments to demonstrate performance advantages of our DT-based service system design approach versus traditional optimization methods. The benchmark optimization model we use is inspired by the recent EVCH literature (e.g., Li et al., 2020) and is detailed in 4.8. Note that we chose a deterministic mixed-integer programming (MILP) model over stochastic or robust specifications as benchmark. This choice is primarily motivated by concerns related to scalability. As previously discussed, the EVCH configuration problem requires the modeling of both the strategic level (large decisions related to asset investments) and operational level (small decision related to e.g., vehicle routing and charging). This multi-stage nature of the problem makes it susceptible to the curse of dimensionality: the model size grows exponentially with the investment stages $\mathcal{H}$, the decision periods per planning stage $\mathcal{T}$, and the size of the decision space at each planning stage h and time period t, as well as the number of possible outcomes per each stochastic parameter. This poses computational difficulties and significantly limits the degree to which stochasticity in the many input parameters can be considered. Indeed, methods for stochastic multi-stage problems like stochastic programming or approximate dynamic programming (ADP) are limited to short time horizons and coarse time scales (Powell, 2014; Fu, 2015) and are generally considered out of scope for large problems like ours (Powell, 2014).These scalability concerns are further evidenced by the computational performance of the benchmark deterministic MILP. Even with integer relaxation, the model is only tractable for a single day per planning stage at hourly-resolution (approximately 1M decision variables). This means, that any stochastic model would require significant simplification in its formulation (e.g., reducing operational detail to reduce the decision space, increasing period length to reduce the number of periods t or limiting the planning horizon, etc.) simply to achieve tractability. We consider such simplifications to be undesirable and argue that deterministic MILP formulations are the only practical benchmark short of the full-scale DT-RL model we propose that is available to researchers today. We consider the fact that all extant EVCH planning models that we are aware of either use deterministic MILP formulations (e.g., Li et al., 2020), or simplified simulation-optimization based on brute-force search methods (e.g., Ferguson et al., 2018) as further evidence in support of this argument.

4.5.1 Parameterization and Experimental Setup

For benchmarking purposes, we choose a real-world mixed-use facility with attached parking space for which we have access to both building baseload data and transaction-level parking and charging demand. Owing to the size of the problem space, we modify the original dataset by scaling down both parking and building capacities such that tractability of the benchmark mathematical model can be achieved. Specifically, we limit the size of the parking facility to 200 spaces and, correspondingly, scale down peak and minimum baseload. To retain occupancy

seasonality and population characteristics of the full-sized facility we implement a proportional sampling approach to iteratively build the population according to daily parker type proportions until the target occupancy for a respective day is reached. Investment decisions are computed over an investment horizon of 20 years, allowing for an initial investment decision at time 0 and recourse decisions every two years (total of ten states $h \in \mathcal{H}$). Costs and other parameters (such as EV adoption assumptions) and their trajectory over the investment horizon are detailed in Appendix D. What is important to note here is the following: EV adoption rises for 5% in stage 0 to 65% in the final stage; both PV and storage exhibit downward cost curves that reflect technological progress and increasing economies of scale; and grid expansion has an upward cost trajectory that is reflective of an uptake in demand for grid capacity as electrification of mobility, households and other sectors progresses.

4.5.2 CAPEX Decision Comparison

In Figure 4.9 we compare the system configuration plan obtained using DT-based reinforcement learning (DT-RL) and traditional optimization (OPT).

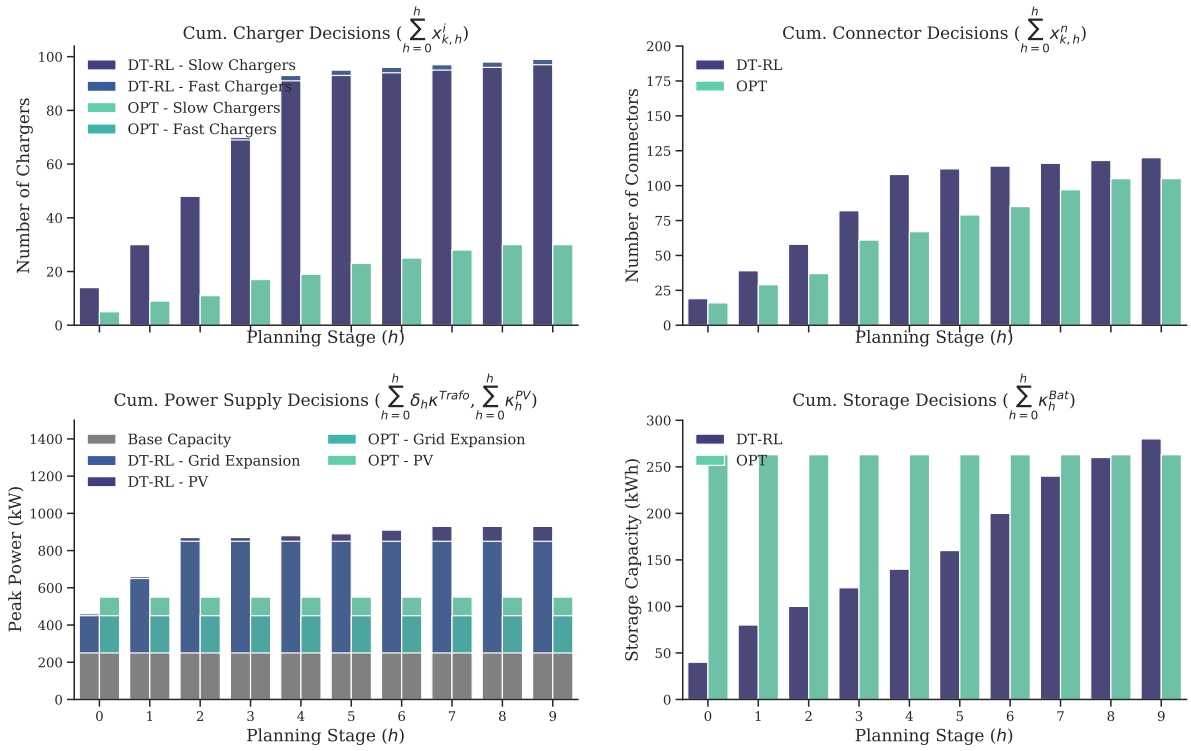

Figure 4.9: Benchmark of Infrastructure Decisions obtained using DT-based Reinforcement Learning (RL) vs. traditional optimization (OPT)

Both EVCH configurations vary significantly in terms of size and composition. The OPT-derived layout requires considerably less charging infrastructure. This is primarily due to its

high reliance on multi-connector docks (3.4 connectors per dock on average vs. 1.2 connectors per dock in the DT-RL case) and is likely an artifact of better optimization opportunities linked to perfect foresight. What's more, the OPT algorithm almost fully avoids the use of the much more expensive fast chargers, while DT-RL relies on some fast charger docks in later system stages to achieve service level objectives but also largely avoids their use for cost reasons. Interestingly, both algorithms draw on multi-connector docks, highlighting the efficiency benefits of this asset class. In terms of power supply and storage decisions, the OPT-derived layouts primarily draw on storage in combination with PV while only investing in limited grid expansion. Under perfect foresight, storage can be optimally used to shave supplemental grid capacity and benefit from energy cost arbitrage opportunities. In a more stochastic setting and under real-world heuristic operational conditions, such theoretically optimal operations perform poorly. The DT-RL algorithm considers these imperfections. As a result, the DT-RL-derived layout draws primarily on predictable grid-supplied energy only gradually expanding PV and storage capacity over time (when these asset classes become comparatively cheaper).

4.5.3 Out-of-sample Operational Performance Benchmark

To benchmark real-world performance of the infrastructure layouts, we run detailed evaluation experiments. Specifically, we test the derived layouts on 12 weeks of out-of-sample operational sensor data (parking transactions, PV generation, building demand, etc.), thus simulating the life-cycle phase of the target EVCH service system (Boschert and Rosen, 2016). The 12-week sample is equally distributed over the entire year and captures daily, weekly and yearly seasonality.

We evaluate two core performance dimensions: service level and cost performance. Figure 4.10 illustrates the results. First, we look at service level (left panel in Figure 4.10). Note that both methods (OPT and DT-RL) optimize for 100% service level fulfillment. We find that the DT-RL-based charging network generalizes better to real world conditions achieving superior service level performance. The DT-RL infrastructure setup achieves a service level of above 99% at each stage of planning horizon, while the service level achieved by the OPT-derived layout eventually drops to below 80% in State 9. Interestingly, the discrepancy in service level grows over time and with the penetration of EVs in the population[14]. Due to the early investments into grid expansion and PV in the OPT model to benefit from lower costs early on in the planning horizon, excess capacity is provisioned which enables high service levels even under real-world conditions. As EV penetration progresses, this excess capacity margin is quickly used up and, given that no major additional investments in grid capacity are made under the OPT investment plan, the target service level cannot be maintained under real-world conditions. This is reflected in the cost performance of both configurations over the investment horizon (see right panel of

[14] As per the parameterization of our experiments, the EV penetration grows from 5% in stage 0 to 65% in stage 9

Figure 4.10). Specific system costs (comprising investment (C^{Φ}), operations (C^{Ω}) and service level penalty (C^{Ψ}) costs) are largely similar in the early stages of the planning horizon, but diverge around stage five in favor of the DT-RL-derived configuration. This is a result of the major opportunity costs incurred by not being able to serve all demand using the OPT-derived system. Taken together, the DT-RL approach outperforms OPT by 36% in terms of cumulative objective over the full optimization horizon. Looking at the final state only, the specific total cost of the DT-RL-derived configuration is 65% lower than that of the OPT-derived system.

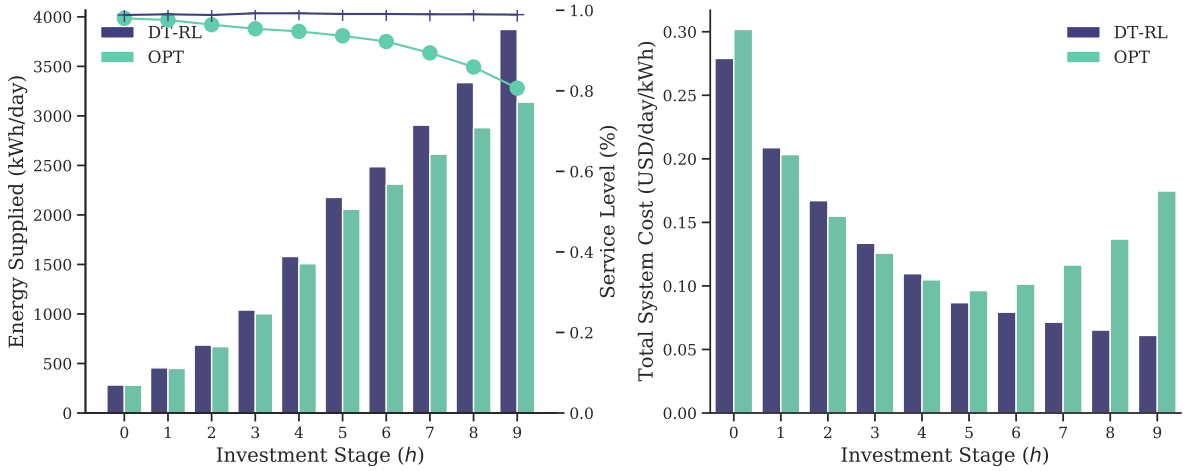

Figure 4.10: Benchmark of service quality and cost of DT-RL-derived and OPT-derived configurations evaluated under real-world conditions on 12 weeks of operational data.

4.5.4 Solution Speed and Scalability Benchmark

While solution speed is usually of limited concern for strategic decisions like investment planning, scalability can play a role. For example, our dataset includes parking facilities with up to 2200 parking spots. It is well established that MILP formulations are NP-hard. This is problematic for large problem instances which can quickly become intractable with standard commercial solvers. Indeed, we find that the solution speed of our benchmark optimization model exhibits an exponential relationship with EVCH size and scope. As a result, the model is only tractable for facility sizes of up to 200 parking spots (given a reasonable cutoff time of 12 hours[15]). Perhaps more importantly, tractability is only achieved at the expense of model granularity, meaning a relatively coarse discretization of time is required along with simplifications of the underlying operational processes to reduce the number of decision variables[16]. Additionally, we can only optimize over a single candidate day; not multiple days or weeks as in the DT-RL case. Finally, the above mentioned performance is only achieved in deterministic settings. As discussed, the use of stochastic or robust approaches would further impact scalability rendering the resulting

[15] Using a machine with 256GB of RAM and an AMD Ryzen Threadripper 3970X 32-Core processor (4.5 GHz)
[16] The model assumes optimal operations throughout and operates at a temporal resolution of 1h per period.

optimization models impractical for real-world use cases. Taken together, scalability constraints of standard optimization models make simplifications necessary (idealized operational processes, deterministic setting, large temporal granularity, small data samples, etc.), which in turn are the core reason behind the comparatively poor performance of derived system design decisions under (near) real-world stochastic conditions (see Figure 4.10). The DT-RL approach is able to achieve almost arbitrary scalability without the need for simplification or removal of uncertainty in input parameters. To be more precise, using Q-learning approaches, we do not only solve for large-scale facilities, but also deal with the stochastic charging demands by incorporating significantly larger and more granular demand datasets. Even with much longer operating periods (e.g., 12 weeks for each time state at one-minute resolution), the learning agent is able to find a high-performing configuration for the benchmark 200-spot facility within just six hours.

4.6 DT-Assisted Scenario Analyses

Another advantage of DT-based approaches to service system optimization is the method's highly flexible nature. This allows for extensive sensitivity testing under real-world conditions, which we perform in this Section. Aspects of particular interest here are: user preference scenarios and operational policy choices. For illustrative purposes, we focus on the final planning state (h=9) (i.e., we neglect the scale-up pathway until that state is reached).

4.6.1 Impact of Variations in User Preferences

In Figure 4.11 we compare DT-RL-derived infrastructure investment decisions for three archetypical EVCH facilities (Destination, Mixed-use, Workplace). The results reveal significant sensitivity of optimal physical layout decisions to user preferences. Recall that Destination facilities are primarily used for short-term parking (large proportion of *Morning Short*, *Afternoon Short* and *Evening Short* parkers), Mixed-use facilities exhibit a heterogeneous user pool, while Workplace facilities are primarily used by commuters with long stays (see Table 4.1 and Figure 4.6). Consequently, average laxity characteristics vary considerably across facility types. We see these differences reflected in the derived EVCH configurations across the three facilities. Specifically, for the facility with the lowest average laxity (Destination facility), the DT-RL algorithm decides to provision primarily single-connector AC docks along with a small number of single-connector fast chargers. A single-connector setup ensures that the full charging power is available at all times but comes at the risk of vehicles blocking an entire dock even after completing a charging cycle. The latter issue seems to be less problematic in a destination parking setting, where users do not stay long on average. At the other end, the infrastructure setup for a Workplace facility tends to favor multi-connector docks, particularly AC double-connector docks, thus taking advantage of the higher laxity of the underlying user population that affords longer charging cycles at lower rates. The third facility type (Mixed-use) falls somewhat in the middle between the previous two extremes. This is consistent with its laxity profile that lies between that of the Destination and Workplace facilities. It is noteworthy that DC charging plays a minor role in any scenario. EVCH charging use cases can mostly be satisfied at lower charging rates.

In terms of power supply infrastructure, the Destination facility requires an additional 200kW transformer to achieve the target service level and satisfy low-laxity charging requests at higher charging rates. Some PV and battery storage is installed in all scenarios.

4.6.2 Impact of Operational Policy Choices

Next, we leverage the flexibility characteristics of the DT approach by investigating the impact of different operational policies on the sizing decisions and the system's cost performance. As mentioned, such analyses would mean major model reformulation for optimization frameworks but are easily implemented in a DT-based model. In Figure 4.12, we explore the impact of

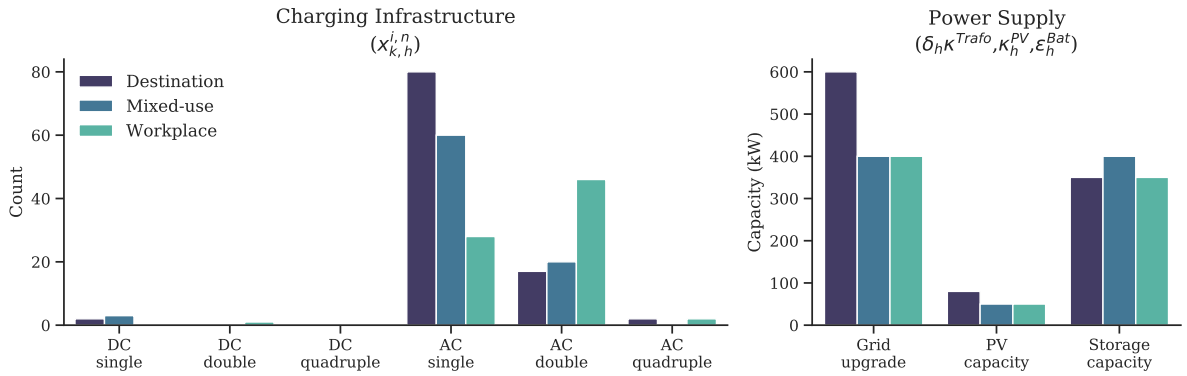

Figure 4.11: DT-RL-derived system configuration decisions for three archetypical EVCH facilities

routing decisions for a Mixed-use facility, assuming FCFS charging operations. We find that the

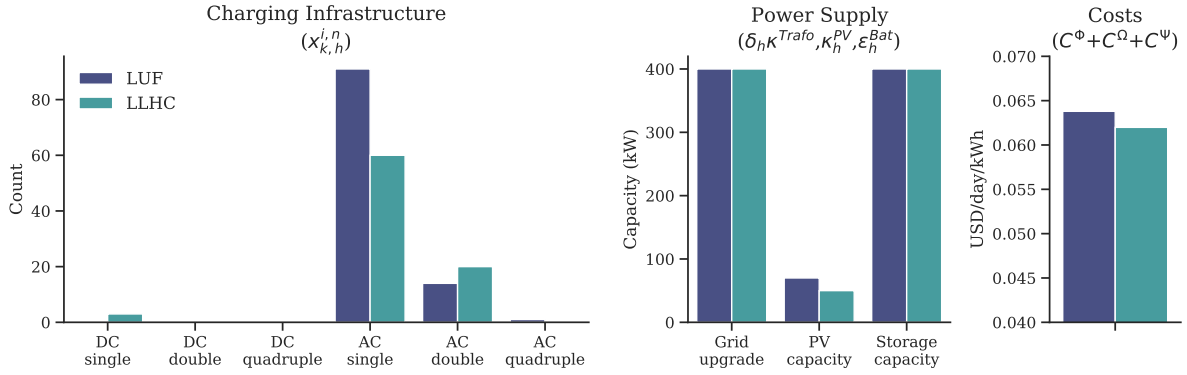

Figure 4.12: DT-RL-derived system configuration and performance against objective for different routing policies and a mixed-use facility

planning outcome is sensitive to the choice of routing strategy, as is the cost performance of the derived system. The more sophisticated routing strategy (LLHC) relies on more multi-connector docks and requires less alternative power sources (PV and storage) in an optimal setup compared to the same facility operated with LUF routing. Total system cost savings amount to 8.4%.

We perform a similar sensitivity analysis for the choice of charging strategy. Figure 4.13 displays DT-RL-derived infrastructure decisions and system cost performance for the same Mixed-use facility, assuming LLHC routing. We observe a largely similar picture here. Planning decisions are sensitive to the choice of charging strategies (e.g., more multi-dock chargers, more PV, and more battery with optimal strategy), as is cost performance (i.e., the best performance of the system with optimal charging with savings of 1.7 to 3.2% against the alternative strategies).

In sum, we show that the physical EVCH configuration (Π) is highly sensitive to Ω, the operational policies that the EVCH operates on. In general, the more sophisticated the operational policies, the lower the total infrastructure requirements and the better the overall cost

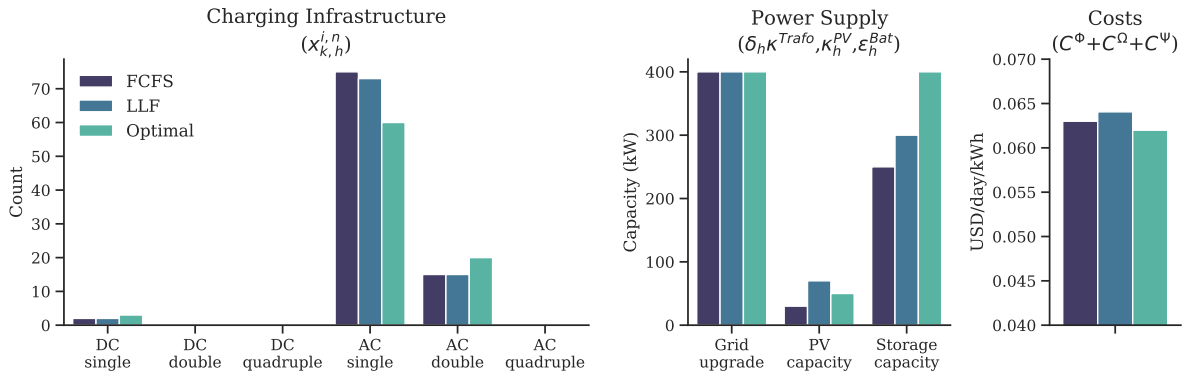

Figure 4.13: DT-RL-derived system configuration and performance against objective for different charging policies and a mixed-use facility

performance of the system. Thus, in order to obtain optimal planning decisions, operations managers need alignment on how they intend to operate the service system. Different operational strategies require different infrastructure layouts to achieve optimal performance and result in different total system costs.

4.7 Discussion

With the advent of large-scale sensor-generated operational data, data-driven OM methods for service system design have come into focus (Choi et al., 2022). DTs, intricate digital representations of the target system and its operational environment, can play an important role here. Indeed, multiple commentators have argued for the increasing use of DTs in the design phase of operational systems (Boschert and Rosen, 2016; Grieves and Vickers, 2017; Jones et al., 2020; Choi et al., 2022). DTs are different from traditional simulation optimization in several ways: First (1), a DT is based on real-world sensor data (historical or real-time) whenever available, coupled with high-resolution virtual asset models. It, thus, represents a detailed technical description of the asset that far exceeds the scope of standard simulation. Second (2), a DT consolidates and integrates into a single model most information on the operational systems that are available and required at any given stage of the life-cycle. Finally (3), a DT seamlessly covers the system's entire life-cycle, not just the design phase. This means that once the physical system has been built, the DT model is simply carried over into the next life-cycle phase (e.g., operations) by feeding it with updated sensor data and updating/re-calibrating the virtual asset models based on this data, thus bridging the gap between design and operations (Grieves and Vickers, 2017). Traditional simulation models do not have these capabilities.

In this work, we have proposed a three-step framework that can guide researchers and OM professionals in using DTs, in combination with state-of-the-art learning methods, for large-scale multi-stage system design problems. We have demonstrated the efficacy of the proposed approach in an application to EV Charging Hub design and benchmarked it extensively against traditional mathematical optimization techniques. As part of our concluding remarks, we now discuss the methodological and managerial contributions of this work.

4.7.1 Methodological Contributions

Our DT-based method holds several important benefits over traditional optimization-driven OM methods. We have shown and quantified these benefits for the case of EVCH planning in this work and summarize them here.

First, the need for simplifying assumptions to achieve mathematical and computational tractability of the configuration task is greatly reduced in DT-based approaches. This can result in better performance of the target system under real-world conditions. Due to their data-driven nature, DT-based approaches can easily accommodate stochasticity and full operational detail. While traditional stochastic or robust optimization approaches can be specified to account for uncertainty in future realizations of parameters, this comes at a significant performance penalty. Incorporating stochasticity in traditional frameworks, therefore, typically involves problem size reduction by, e.g., limiting foresight or selecting coarser planning period durations, again impacting generalizability to real-world conditions. In addition, the full detail of the available

operational data remains untapped. Our experiments show that optimization-derived system configurations can be too optimistic. They do not provide sufficiently for stochasticity in demand and operational imperfections that the DT readily captures. As a result, service level targets are missed by up to 20%, and total systems costs are significantly higher.

Second, DTs are flexible, i.e., they significantly ease the exploration of a broader and less constrained solution space, specifically in terms of operational policies. For example, we have shown how infrastructure requirements change/reduce as asset operations become more sophisticated and make better/more efficient use of the asset base (see Section 4.6). The analysis of this two-way relationship is afforded by the highly flexible DT setup. They are extremely difficult to replicate in more rigid linear programming frameworks. As an example, it is non-trivial to incorporate commonly used naive operational policies such as a first-come-first-served prioritization rule in an optimization model. Likewise, switching between different operational policies requires (potentially extensive) model reformulation.

Third, DT-based planning frameworks, when combined with efficient search or learning methods, can scale to almost arbitrary size. Optimization methods suffer from NP-hardness that limits scalability. This is especially true if stochastic or robust approaches are used, which require further size reduction and simplification. Indeed, in our experiments, using deep reinforcement learning in a DT-based system environment is scalable to any real-world system size, while optimization methods only scale to EVCH facility sizes of approx. 200 parking spots and require significantly coarser discretization to achieve tractability.

In sum, DT-based planning removes many of the drawbacks related to simplification, inflexibility, and scalability of traditional optimization-based planning frameworks. Note that DT-based planning, compared to traditional approaches, comes at the cost of higher data requirements and an increased implementation burden[17]. While we argue that the superior real-world performance of the DT-configured system in itself warrants these costs, there is an additional argument to start DT implementation early: as opposed to traditional OM planning models, a DT-based model is not single-use. Indeed, the DT can be readily bridged-over into the use phase of the service system by simply replacing historical sensor data streams with real-time data flows (Boschert and Rosen, 2016). In the system use phase, the DT then affords real-time system monitoring and optimization (Choi et al., 2022). We aim to exploit this multi-use characteristic in future work by leveraging the developed DT simulation in the development of novel high-performing learning algorithms for real-world EVCH operations.

4.7.2 Managerial Implications

Our framework offers a practical and highly reproducible method for OM practitioners to incorporate data-driven, high-fidelity simulation (i.e., DTs) combined with state-of-the-art reinforcement learning methods (or alternatively traditional meta-heuristic search approaches) in

[17] For example, it involves the creation of an intricate data-driven simulation environment.

the design phase of operational systems. The method generalizes to any envisioned system for which sensor datasets are available that can be reasonably expected to be good proxies for current and future operational conditions and user behavior. With the emergence of inexpensive sensor technology, ubiquitous computing and mobile connectivity, this is already the case for many applications and can be expected to only gain in relevance/volume in the future.

In addition, we offer a range of novel domain-specific insights related to EVCH design that hold important implications for OM managers planning to invest in high-density EV charging infrastructure, such as retrofitting parking garages with charging docks or upgrading fleet depots with charging infrastructure. For instance, we develop a novel data-driven taxonomy of parker types along with an estimation of their future charging demand. We then show how optimal EVCH system configurations vary with the compositions of the user population or with the choice of operational policies. Finally, we demonstrate the value of parallel-server charging docks, particularly when paired with EV routing strategies, among other sensitivity tests. These insights may prove valuable to investors seeking to develop and scale EVCHs as a new and highly relevant charging use case (Hoover et al., 2021).

Note that despite the highly detailed nature of the DT, it is still an abstraction of reality that is subject to several limitations and simplifications. For example, we consider routing and charging decisions separately instead of jointly. We also do not allow for vehicle-to-grid operations and consider loads of the attached building loads to be exogenous, among other simplifications. Such limitations represent exciting avenues for follow-up work, and we leave them for future research.

4.8 Appendix

Table 4.2: Nomenclature

Symbol	Description	Unit
Sets		
$\mathcal{H}$	Set of planning stages in planning horizon with index h	set
$\mathcal{I}$	Set of charging dock types with index i ($\mathcal{I} = \{AC, DC\}$)	set
$\mathcal{J}_h$	Set of unique EVs entering the EVCH during the planning period h with index j	set
$\mathcal{K}$	Set of charging dock candidate points (i.e., parking spots) with index k	set
$\mathcal{N}$	Set of charging dock connector options $\mathcal{N} = \{1, 2, 4\}$ with index n	set
$\mathcal{T}$	Set of time periods per each stage in planning horizon with index t	set
Ξ	Set of decision variables	set
Γ	Full configuration of EVCH system	set
Parameters		
$A_{j,s}$	Arrival time of vehicle j in stage h	period
β^{max}, β^{min}	Maximum charge and maximum discharge rate of energy storage	kW
$c_h^{i,n}$	Cost per EV charging dock of type i with n connectors in stage h	USD
c_h^{Trafo}	Cost per kW of grid connection (i.e., transformer) in stage h	USD/kW
c_h^{PV}	Cost per kWp of PV in stage h	USD/kW
c_h^{Bat}	Cost per kWh of energy storage (battery) in stage h	USD/kWh
δ_j	Duration of stay of vehicle j	hours
Δ_t	Duration of a single planning period t	hours
$D_{j,h}$	Departure time of vehicle j in stage h	period
e_j^d	Total energy requested by vehicle j over duration of stay	kWh
$\eta^{(dis)charge}$	Charge/discharge efficiency of energy storage	ratio
η^{Inv}	AC-DC inversion efficiency	ratio
η_h^{Serv}	Target service level expressed as ratio of fulfilled vs. actual demand	ratio
$f_{h,t}^{PV}$	Avg. PV load factor in period t of stage h	ratio
κ^i	Maximum power per charging dock of type i	kW
κ_0^{Grid}	Existing facility substation capacity	kW
κ^{Trafo}	Standard size of transformer that can be installed	kW
lax_j	Laxity of vehicle j	hours
$l_{h,t}$	Base load of attached facility during period t in stage h	kW
l_h^*	Maximum expected base load of attached facility in stage h	kW
M	big-M cotraint (for linearization)	kW
ρ^{Maint}	Cost ratio for maintenance (as share in total capital stock)	ratio
R	Maximum installable PV capacity (space constraint)	kWp
SoC^{max}	Maximum energy storage level	%
SoC^{min}	Minimum energy storage level	%
L	Space limitation in number of parking spots	count
T_h^p	Cost of induced peak per accounting period (i.e., demand charge) in stage h	USD/kW
$T_{h,t}^e$	Cost of energy in period t of stage h as per TOU tariff	USD/kWh
$U_{j,h,t}$	Indicator of whether vehicle j is present during period t in stage h	boolean
Variables		
$\beta_{h,t}^{Charge}$	Charge rate of EVCH battery storage	kW
$\beta_{h,t}^{Discharge}$	Discharge rate of EVCH battery storage	kW
$\beta_{h,t}^{Direction}$	Indicator of whether the battery is charging (=1) or discharging (=0)	boolean
δ_h^{Trafo}	Number of installed transformers in stage h	integer
C_h^{Φ}	Total normalized investment cost for the EVCH per planning horizon	USD
C^{Ω}	Total cost of operating the EVCH over the planning horizon	USD
C^{Ψ}	Penalty for not serving charging demand	USD
$e_{j,h,t}^S$	Net energy supplied to vehicle j during period t of stage h	kWh
$e_{h,t}^{Grid}$	Net energy supplied from grid during period t of stage h	kWh
ϵ_h^{Bat}	Installed energy storage capacity in stage h	kWh
κ_h^{PV}	Installed PV capacity in stage h	kW
p_h^*	Induced max peak attributable to EVCH operations during stage h	kW
$\psi_{k,j,h,t}$	Charge rate of vehicle j connected to charging dock k during period t of stage h	kW
$SoC_{h,t}$	State variable that tracks state of charge of energy storage	kWh
$w_{k,j,h}$	Indicator for whether a vehicle j is connected to charging dock k in stage h	boolean
$x_{k,h}^{i,n}$	Indicator whether dock (type i, n connectors) is installed at k in stage h	boolean

A. Operational Modeling and Algorithms

Optimal Charging Approach

Our charging model reconsiders the charging rate for connected vehicles at the beginning of each planning interval, thus following an online optimization paradigm.

The objective is to minimize the energy costs while meeting the charging demand of all connected vehicles (up to a predefined service level) over the look ahead planning window $\mathcal{T}^{\Omega}$. As we consider an uncertain case where the perfect information of upcoming vehicles is not available to the decision model, we make this conservative assumptions to ensure that the service level is fulfilled.

First, the planning horizon must be chosen carefully due to its significant effect on model performance. In our simulations, we limit it to 6 hours, which, given a planning interval Δ^{Ω} of 15 minutes, breaks down to 24 decision steps (i.e., charging rates are re-computed every 15 minutes of simulation time). We term the set of decision steps $\mathcal{T}^{\Omega}$

Second, we consider a flexibility margin μ_t to accommodate future, yet unknown demand. Although this model outputs a vector of charging rates for each vehicle, we only use the first charging rate and reconsider decisions in the next charging time step based on the updated systems state including the new arrived vehicles.

$$Min_{\Xi} \sum_{t \in \mathcal{T}^{\Omega}} T_t^e e_t^{Grid} + T^p p^* \tag{4.4}$$

The grid energy consumption e_t^{Grid} accounts for the charging of vehicles (variables) as well as the storage (dis)charging, PV generation and building loads (storage rate is given as parameter before charging management). Constraint EC (3) guarantees that the grid energy consumption does not exceed the grid capacity minus the safety threshold we consider for the following time steps. Accordingly, we compute the induced peak, which is the exceeding grid consumption than the highest post energy peak l^* (Equation EC (4)).

$$e_t^{Grid} = \sum_{j \in \mathcal{J}} \sum_{k \in \mathcal{K}} \Delta_t (\psi_{k,j,t} + \beta_t^{Charge} - \beta_t^{Discharge} - f_t^{PV} \sum_{\tau=0} \kappa_{\tau}^{PV} + l_t) \qquad \forall t \in \mathcal{T}^{\Omega} \tag{4.5}$$

$$\frac{e_t^{Grid}}{\Delta_t} \leq p_t^{Grid} - \mu_t \qquad \forall t \in \mathcal{T}^{\Omega} \tag{4.6}$$

$$p^* \geq \frac{e_t^{Grid}}{\Delta_t} - l^* \qquad \forall t \in \mathcal{T}^{\Omega} \tag{4.7}$$

We also ensure that all vehicles receive at least η percentage of their charging demands. Constraint EC (6) ensures that vehicle can only charge when they are physically present in the EVCH. Finally, Constraint EC (7) restricts the parallel charging of vehicles that are connected to charging dock k to its charging capacity.

$$\sum_{k\in\mathcal{K}}\sum_{t\in\mathcal{T}^{\Omega}}\psi_{k,j,t}\geq\eta e_j^D \qquad \forall j\in\mathcal{J} \tag{4.8}$$

$$0\leq\psi_{k,j,t}\leq U_{j,t}M \qquad \forall k\in\mathcal{K}, j\in\mathcal{J}, t\in\mathcal{T}^{\Omega} \tag{4.9}$$

$$\sum_{j\in\mathcal{J}_k}\psi_{k,j,t}\leq\kappa^k \qquad \forall k\in\mathcal{K}, t\in\mathcal{T}^{\Omega} \tag{4.10}$$

B. Preference Modeling

In this Section we provide details on the clustering routine and robustness test emploied to identify archetypical parking preference types.

We cluster parking events j based on A_j and δ_j, the two core parameters of interest at this modeling stage. To account for the circular nature of arrival time A_j, which is not captured accurately by any distance-based clustering algorithm (for example, entries at 23:59h and 0:00h would be considered furthest apart despite their obvious proximity), we create two circular features $A_j^{sin} = \sin(2\pi(A_j/24))$ and $A_j^{cos} = \cos(2\pi(A_j/24))$. This yields the following vector of clustering variables $v_j^{clust} = (A_j^{sin}, A_j^{cos}, \delta_j)$, which we normalize.

Given the size of our dataset (3.84M observations) we limit our algorithm search to clustering algorithms that are sufficiently scalable. We run initial tests with three clustering algorithms: k-means++, a centroid-based algorithm, Gaussian Mixture Models (GMM) and BIRCH, a scalable density-based clustering algorithm. Overall, we find k-means++ to perform best in terms of runtime and stability. While GMM yields relatively similar results, BIRCH performs very poorly, yielding unstable and non-cohesive clusters suggesting that relative density may not be a good identifier of clusters for the given dataset. We thus focus on fine tuning k-means++. A major challenge in the application of k-means++ is to select the number of centroids (clusters) k that are to be initialized and optimized for. To identify good candidate choices for k, We initially test integer values over an interval of reasonable values $[0, 20]$ and compute Calinski-Harabasz scores per each clustering outcome (Calinski and Harabasz, 1974). These analyses suggest $k = 5$ or $k = 6$ to be good choices. To validate and further narrow down our choice for k, we perform silhouette analyses for both candidate choices (Rousseeuw, 1987). We obtain the highest average silhouette coefficient $\bar{\mathcal{H}}$ for $k = 6$ ($\bar{\mathcal{H}} = 0.420$). Finally, taking $k = 6$ as the best performing choice across the above described internal validity measures, we conduct extensive cross-validation to assess cluster outcome robustness. We iteratively perform 2-1 splits of the data and re-run k-means++ on the larger dataset, then use the fitted algorithm to predict the labels of the smaller (test) dataset. We find our clustering results to be stable with observations in the test set having the same label 99.14% ($\sigma = 0.51$ %, 100 replications) of the time. We run an additional set of robustness analyses, this time focusing on the amount of preference data that is required to identify parker types reliably. This analysis draws on Griffin and Hauser (1993) who looked at the question of how many customer interviews were required for reliable insights. Clearly, there is a benefit to prospective EVCH planners if the need for data was smaller than the full one year period we have considered thus far. We run tests for 2 weeks, 4 weeks and 12 weeks of data per each facility and check the robustness of the clustering results as compared to the clusters obtained on the full one-year facility dataset. Again we adopt the cross-validation approach as outlined in Lu et al. (2016a). We find that high quality clustering results can be obtained with just three weeks of data (95.28%, $\sigma = 3.49$ %) accuracy vs. full one-year facility dataset). Beyond this threshold the value of additional data appears to diminish. At six weeks of data, for

example, we obtain very similar accuracy (95.85% ($\sigma = 1.95$ %)), albeit slightly lower variance. In addition to internal validity and robustness of our clustering results we look at interpretability (or external validity). For this purpose, we presented our final clustering results (for $k = 6$) to a range of practitioners and discussed their implications. The clusters were deemed consistent with the domain experts' experience. In sum, we obtain six parker types that are supported both by internal criteria and real-world observation and can be readily identified with just three weeks of data. Figure 4.14 shows the distributions of the two clustering variables per each final cluster.

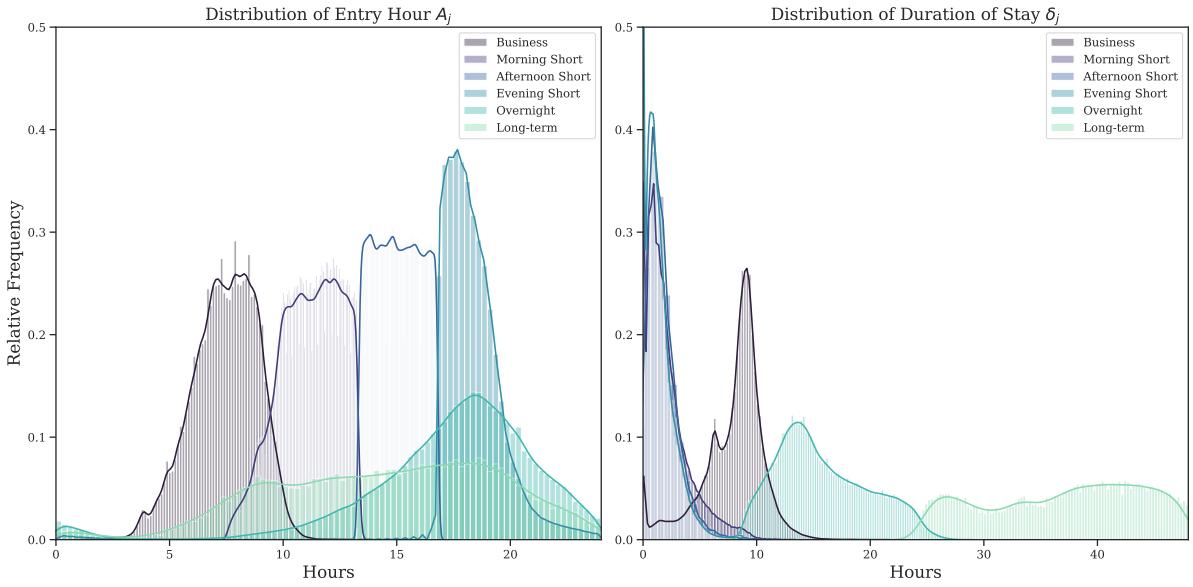

Figure 4.14: Distribution of clustering variables per each cluster

C. Benchmark Optimization Model (OPT)

We formulate the decision challenge as a feasibility problem which aims to satisfy all or a specified amount of total charging demand most resource efficiently while considering rate, space, and total capacity constraints. In doing so we expand on and adapt extant EVCH planning models (e.g., Li et al., 2020).

In line with the planning objective formalized in Section 4.4, we frame the problem as a cost minimization planning with the goal to jointly minimize the investment cost (C^{Φ}) and the operations cost (C^{Ω}) of the EVCH while ensuring a certain service level η_h^{Serv}. Formally, the objective can be expressed as follows:

$$Min_{\Xi}[(C^{\Phi}(x_{k,h}^{i,n}, \delta_h^{Trafo}, \kappa_h^{PV}, \epsilon_h^{Bat}) + C^{\Omega}(\omega_{k,j,h}, \psi_{k,j,h,t}, \beta_{h,t}^{Charge}, \beta_{h,t}^{Discharge})] \tag{4.11}$$

Both cost items are defined as follows. The investment cost (C^{Φ}) is the sum of the grid expansion cost (if any), the cost of EVSEs plus any installed PV and battery capacity over the full investment horizon $\mathcal{H}$. The operations cost (C^{Ω}) is defined as the total sum of electricity costs over the investment horizon, where costs are only incurred on the electricity retrieved from the grid with $e_{h,t}^{Grid}$. Formally:

$$C^{\Phi} = \sum_{h \in \mathcal{H}} [(c_h^T \delta_h^{Trafo} + \sum_{k \in \mathcal{K}} c_h^{i,n} x_{k,j,h}^i + c_h^{PV} p_h^{PV} + c_h^{Bat} \epsilon_h^{Bat})(1 + (|\mathcal{H}| - h)\rho^{Maint})] \tag{4.12}$$

$$C^{\Omega} = \sum_{h \in \mathcal{H}} \sum_{t \in \mathcal{T}} T_{h,t}^e e_{h,t}^{Grid} + T_h^p p_h^* \tag{4.13}$$

Note that $e_{h,t}^{Grid}$ is accounted for on the basis of a two-part tariff charging for both the use of electricity from the grid (excl. PV generation and possible battery discharge $\beta_{h,t}^{Discharge}$) and demand charges arising from the induced peak load attributable to EVCH operations. Demand charges T_h^p are designed to incentivize efficient utilization of the grid (Gust et al., 2021) and are typically based on the monthly peak load induced by the facility. We therefore define p^* as the excess of the expected base facility peak load l^* (excl. EVCH operations) for state h (EC (12)).

$$e_{h,t}^{Grid} = \sum_{j \in \mathcal{J}_h} \sum_{k \in \mathcal{K}} \Delta_t (\psi_{k,j,h,t} + \beta_{h,t}^{Charge} - \beta_{h,t}^{Discharge} - f_{h,t}^{PV} \sum_{\tau=0}^{h} \kappa_{\tau}^{PV} + l_{h,t}) \tag{4.14}$$

$$p_h^* \geq \frac{e_{h,t}^{Grid}}{\Delta_t} - l_h^* \qquad \forall h \in \mathcal{H}, t \in \mathcal{T} \tag{4.15}$$

The optimization is subject to additional operational and physical constraints.

$$\sum_{k\in\mathcal{K}}\sum_{t\in\mathcal{T}}\psi_{k,j,h,t} \geq \eta_h^{Serv} e_j^D \qquad \forall h\in\mathcal{H}, j\in\mathcal{J}_h \tag{4.16}$$

$$x_{k,h}^{i,n}, \omega_{k,j,h} \in \{0,1\} \qquad \forall k\in\mathcal{K}, h\in\mathcal{H}, j\in\mathcal{J}_h, i\in\mathcal{I}, i\in\mathcal{N} \tag{4.17}$$

$$\sum_{k\in\mathcal{K}}\sum_{i\in\mathcal{I}}\sum_{n\in\mathcal{N}}\sum_{h\in\mathcal{H}} x_{k,h}^{i,n} n \leq L \tag{4.18}$$

$$\sum_{h\in\mathcal{H}}\sum_{i\in\mathcal{I}}\sum_{n\in\mathcal{N}} x_{k,h}^{i,n} \leq 1 \qquad \forall k\in\mathcal{K} \tag{4.19}$$

$$\sum_{j\in\mathcal{J}_h} \omega_{k,j,h} U_{j,h,t} \leq \sum_{\tau=0}^{h}\sum_{i\in\mathcal{I}} x_{k,\tau}^{i,n} n \qquad \forall k\in\mathcal{K}, h\in\mathcal{H}, t\in\mathcal{T} \tag{4.20}$$

$$\sum_{k\in\mathcal{K}} \omega_{k,j,h} \leq 1 \qquad \forall h\in\mathcal{H}, j\in\mathcal{J}_h \tag{4.21}$$

$$0 \leq \psi_{k,j,h,t} \leq \omega_{k,j,h} U_{j,h,t} M \qquad \forall k\in\mathcal{K}, h\in\mathcal{H}, j\in\mathcal{J}_h, t\in\mathcal{T} \tag{4.22}$$

$$\sum_{j\in\mathcal{J}_h} \psi_{k,j,h,t} \leq \sum_{\tau=0}^{h}\sum_{i\in\mathcal{I}}\sum_{n\in\mathcal{N}} x_{k,\tau}^{i,n}\kappa^i \qquad \forall k\in\mathcal{K}, h\in\mathcal{H}, t\in\mathcal{T} \tag{4.23}$$

$$\sum_{h\in\mathcal{H}} \kappa_h^{PV} \leq R \tag{4.24}$$

$$SoC_{h,t} = SoC_{h,t-1} + (\beta_{h,t-1}^{Charge} - \beta_{h,t-1}^{Discharge})\Delta_t \qquad \forall h\in\mathcal{H}, t\in\{1,2,...,\mathcal{T}\} \tag{4.25}$$

$$SoC_{h,0} = \sum_{\tau=0}^{h} SoC^{min}\epsilon_\tau^{Bat} \qquad \forall h\in\mathcal{H} \tag{4.26}$$

$$\beta_{h,t}^{Charge} \leq \beta_{h,t}^{Direction}\beta^{max} \qquad \forall h\in\mathcal{H}, t\in\mathcal{T} \tag{4.27}$$

$$\beta_{h,t}^{Discharge} \leq (1-\beta_{h,t}^{Direction})\beta^{max} \qquad \forall h\in\mathcal{H}, t\in\mathcal{T} \tag{4.28}$$

$$\beta_{h,t}^{Charge}\Delta_t \leq \sum_{\tau=0}^{h} SoC^{max}\epsilon_\tau^{Bat} - SoC_{h,t-1} \qquad \forall h\in\mathcal{H}, t\in\{1,2,..\mathcal{T}\} \tag{4.29}$$

$$\beta_{h,t}^{Discharge}\Delta_t \leq SoC_{h,t-1} \qquad \forall h\in\mathcal{H}, t\in\{1,2,..\mathcal{T}\} \tag{4.30}$$

$$e_{h,t}^{Grid} \leq \Delta_t(\kappa_0^{Grid} + \sum_{\tau=0}^{h}\delta_\tau^{Trafo}\kappa^{Trafo}) \qquad \forall h\in\mathcal{H}, t\in\mathcal{T} \tag{4.31}$$

First and foremost, service level is guaranteed in EC (13). Note that the summation is bounded by set $\mathcal{T}_j$, meaning that we consider the total supplied energy at the time of departure. This important constraint ensures that adequate infrastructure is provisioned despite the cost minimization objective.

EV charging infrastructure decisions and operations are controlled by means of decision variables $x_{k,h}^{i,n}$, $\omega_{k,j,h}$ (both binary indicators, see EC (14)) and $\psi_{k,j,h,t}$. First, the number of charging docks and associated connectors is restricted by the space constraints S of the facility (EC (15)). Similarly, EC (16) ensures that candidate points can only be equipped with chargers

once and that this decision cannot be changed over the planning period, i.e., they cannot be removed once installed.

In terms of routing and charging operations, the model assigns vehicles to chargers upon arrival (one-off decision) and periodically adjust the charging power over the duration of their visit. Constraint EC (17) allocates vehicle j to spot k during stage h only if k is equipped with a charging dock and only if j is present in the EVCH (captured via $U_{j,h,t}$). EC (18) ensures that each vehicle connects to at most one charging dock. Constraint EC (19) guarantees that vehicle j receives non-negative energy (bounded by the maximum power of the specific dock in EC (20)) from charging dock k only if it is connected to k.

Battery and on-site generation constraints are set as follows. We assume PV generation to be non-controllable meaning no constraints are necessary to model their operations (in-feed is an exogenous parameter). We simply limit the maximum installable PV capacity $\sum_{h\in\mathcal{H}} \kappa^{PV}$ to the available on-site space (such as rooftop space) R (see EC (21)). EC (22) through (27) implement various battery-related constraints. Constraint (22) incrementally updates the battery state of charge $SoC_{h,t}$. Constraint (23) ensures that the battery SoC remains within a certain interval. Note that we neglect efficiency losses and assume battery depreciation to be independent of operations(Sharifi et al., 2020). We realize that these are simplifications, yet these are necessary to retain tractability of our model. We assume symmetric charge/discharge rate limits which are enforces through constraint EC (24) and (25), where $\beta^{max} \geq 0$. These constraints also ensure that the batter cannot be charged and discharged at the same time.

Our model ensures that the EVCH's base load as well as EV and battery charging loads cannot exceed the total grid capacity (existing and extension) plus current PV generation, which is enforced by EC (28). Note that if the battery was discharging (negative β_t^{Bat}) this would increase the available capacity.

D. Experimental Setup

Table 4.3 summarizes the core parameters used in the benchmark experiments over the investment horizon (10 states $s \in S$).

Table 4.3: Parameterization of benchmark experiments

Parameter[18]	**Unit**	s_0	s_1	s_2	s_3	s_4	s_5	s_6	s_7	s_8	s_9	**Source**
Battery cost (c_s^{Bat})	USD/ kWh	575	507	441	391	352	321	295	273	255	239	Lazard, Bloomberg NEF
AC charger cost[19] ($c_{s,AC}^{EVSE}$)	USD/ unit	4500	4322	4151	3986	3828	3677	3531	3391	3257	3128	industry quotes
DC charger cost[20] ($c_{s,DC}^{EVSE}$)	USD/ unit	50000	49000	47060	45196	43406	41687	40037	38451	36928	35466	California Energy Commission
Connector cost AC	USD/ unit	250	250	250	250	250	250	250	250	250	250	assumption
Connector cost DC	USD/ unit	2500	2500	2500	2500	2500	2500	2500	2500	2500	2500	assumption
EV share[21] (σ_s^{EV})	%	5	8	12	18	27	37	42	49	56	65	Bloomberg NEF
Grid cost[22] (c_s^{Grid})	USD/ kW	250	276	304	335	369	407	449	495	546	602	industry quotes
PV cost (c_s^{PV})	USD/ kWp	2125	2041	1960	1882	1808	1736	1668	1601	1538	1477	Lazard, IEA
Max. PV capacity[23] (R)	kWp	100	100	100	100	100	100	100	100	100	100	-
Number of parking spots (S)	units	200	200	200	200	200	200	200	200	200	200	-

In addition we impose several physical constraints inherent to the various components of the EVCH system. These are summarized in Table 4.4.

Energy costs are based on real-world electricity tariffs from the same region in which the charging data was gathered (i.e., California). Table 4.5 gives an overview of the tariff structure that we use throughout all experiments.

[18] All cost parameters include cost of installation and peripheral equipment (e.g., inverters for battery, PV and DC chargers)

[19] 22kW, single connector

[20] 50kW, single connector

[21] Assuming sales share equals penetration for given facility

[22] Cost of transformer, cabling and contribution to upstream grid upgrades; assuming 5% yearly cost increase

[23] Assuming 500m^2 roof space and PV energy density of 0.2kWp/m^2

Table 4.4: Physical Constraints

	Symbol	**Value**	**Unit**
Maximum EV charging rate	ψ^{EV}	22	kW
EV charging efficiency	η^{EV}	95	%
Energy storage charging/discharging efficiency	η^{Bat}	95	%
Minimum storage SoC	SoC^{Min}	5	%
Maximum storage SoC	SoC^{Max}	95	%
Maximum storage charging rate	β^{Max}	0.5	MW

Table 4.5: Time-of-use tariff and demand charge for large-scale EV charging customers (> 500 kW)

	Summer (Jun - Sep)	**Winter** (all other months)
Super Off-Peak (8am-4pm)	0.08 USD/kWh	0.06 USD/kWh
On-Peak (4pm to 9pm)	0.23 USD/kWh	0.23 USD/kWh
Off-Peak (9pm-8am)	0.08 USD/kWh	0.08 USD/kWh
Demand Charge (monthly)	15.48 USD/kW	

References

A. Abbasi, C. Albrecht, A. Vance, and J. Hansen. Metafraud: a meta-learning framework for detecting financial fraud. *MIS Quarterly*, pages 1293–1327, 2012.

A. Abbasi, F. Zahedi, D. Zeng, Y. Chen, H. Chen, and J. F. Nunamaker Jr. Enhancing predictive analytics for anti-phishing by exploiting website genre information. *Journal of Management Information Systems*, 31(4):109–157, 2015.

A. Abbasi, S. Sarker, and R. H. Chiang. Big data research in information systems: Toward an inclusive research agenda. *Journal of the Association for Information Systems*, 17(2):1–32, 2016. doi: 10.17705/1jais.00423.

M. Adena and S. Huck. Online fundraising, self-image, and the long-term impact of ask avoidance. *Management Science*, 66(2):722–743, 2020. doi: 10.1287/mnsc.2018.3232.

G. Adomavicius, A. Gupta, and D. Zhdanov. Designing intelligent software agents for auctions with limited information feedback. *Information Systems Research*, 20(4):507–526, 2009. doi: 10.1287/isre.1080.0172.

G. Adomavicius, J. C. Bockstedt, S. P. Curley, and J. Zhang. Do recommender systems manipulate consumer preferences? a study of anchoring effects. *Information Systems Research*, 24 (4):956–975, 2013.

M. E. Ahsen, M. U. S. Ayvaci, and S. Raghunathan. When algorithmic predictions use human-generated data: A bias-aware classification algorithm for breast cancer diagnosis. *Information Systems Research*, 30(1):97–116, 2019.

Y. Ai, Z. Li, M. Gan, Y. Zhang, D. Yu, W. Chen, and Y. Ju. A deep learning approach on short-term spatiotemporal distribution forecasting of dockless bike-sharing system. *Neural Computing and Applications*, 31(5):1665–1677, 2019. doi: 10.1007/s00521-018-3470-9.

AMS. Regional Unemployment Statistics NUTS-3, 2020.

R. An, D. Pojani, R. Zahnow, and J. Corcoran. Weather and cycling in New York: The case of Citibike. *Journal of Transport Geography*, 77:97–112, 2019. doi: 10.1016/j.jtrangeo.2019.04.016.

A. Angelopoulos, D. Gavalas, C. Konstantopoulos, D. Kypriadis, and G. Pantziou. Incentivized vehicle relocation in vehicle sharing systems. *Transportation Research Part C: Emerging Technologies*, 97(November 2017):175–193, 2018. doi: 10.1016/j.trc.2018.10.016.

J. D. Angrist and J.-S. Pischker. *Mostly Harmless Econometrics : An Empiricist ' s Companion Mostly Harmless Econometrics : An Empiricist ' s Companion.* Princeton University Press, 2008.

S. Athey. The Impact of Machine Learning on Economics. *NBER AI Workshop 2017*, (Ml): 1–27, 2017a. doi: 10.1257/jep.31.2.87.

S. Athey. Beyond prediction: Using big data for policy problems. *Science*, 355(6324):483–485, feb 2017b. doi: 10.1126/science.aal4321.

K. W. Axhausen. Towards an AV future: Key issues. In *Future Urban Mobility Symposium 2017*, Singapore, 2017. doi: https://doi.org/10.3929/ethz-b-000169534.

S. Ba, L. L. Lisic, Q. Liu, and J. Stallaert. Stock market reaction to green vehicle innovation. *Production and Operations Management*, 22(4):976–990, 2013.

Y. Babar and G. Burtch. Examining the Heterogeneous Impact of Ride-Hailing Services on Public Transit Use. *Information Systems Research*, 31(3):820–834, sep 2020. doi: 10.1287/isre.2019.0917.

J. Babic, A. Carvalho, W. Ketter, and V. Podobnik. A data-driven approach to managing electric vehicle charging infrastructure in parking lots. *Transportation Research Part D: Transport and Environment*, 105:103198, apr 2022. doi: 10.1016/j.trd.2022.103198.

A. Badeau, C. Carman, M. Newman, J. Steenblik, M. Carlson, and T. Madsen. Emergency department visits for electric scooter-related injuries after introduction of an urban rental program. *American Journal of Emergency Medicine*, 37(8):1531–1533, 2019. doi: 10.1016/j.ajem.2019.05.003.

S. Bai and J. Jiao. Dockless E-scooter usage patterns and urban built Environments: A comparison study of Austin, TX, and Minneapolis, MN. *Travel Behaviour and Society*, 20(April): 264–272, 2020. doi: 10.1016/j.tbs.2020.04.005.

A. C. Baker, D. F. Larcker, and C. C. Wang. How much should we trust staggered difference-in-differences estimates? *Journal of Financial Economics*, 144(2):370–395, 2022. doi: 10.1016/j.jfineco.2022.01.004.

S. Bakker. Electric Two-Wheelers, Sustainable Mobility and the City. In *Sustainable Cities - Authenticity, Ambition and Dream*. IntechOpen, feb 2019. doi: 10.5772/intechopen.81460.

M. Balac, H. Becker, F. Ciari, and K. W. Axhausen. Modeling competing free-floating carsharing operators – A case study for Zurich, Switzerland. *Transportation Research Part C: Emerging Technologies*, 98(May 2018):101–117, 2019. doi: 10.1016/j.trc.2018.11.011.

P. Balduzzi and A. W. Lynch. Transaction costs and predictability: Some utility cost calculations. *Journal of Financial Economics*, 52(1):47–78, Apr. 1999. ISSN 0304-405X. doi: 10.1016/S0304-405X(99)00004-5.

R. Bapna, P. Goes, and A. Gupta. Auctioning vertically integrated online services: Computational approaches for real-time allocation. *Journal of Management Information Systems*, 25 (3):65–98, 2008a.

R. Bapna, W. Jank, and G. Shmueli. Price formation and its dynamics in online auctions. *Decision Support Systems*, 44(3):641–656, 2008b. doi: 10.1016/j.dss.2007.09.004.

R. Bapna, W. Jank, and G. Shmueli. Consumer surplus in online auctions. *Information Systems Research*, 19(4):400–416, 2008c.

I. Bardhan, J.-h. Oh, Z. Zheng, and K. Kirksey. Predictive analytics for readmission of patients with congestive heart failure. *Information Systems Research*, 26(1):19–39, 2015.

A. Barfar and B. Padmanabhan. Predicting presidential election outcomes from what people watch. *Big Data*, 5(1):32–41, 2017.

F. Barnes. A Scoot, Skip, and a JUMP away: Learning from shared micromobility systems in San Francisco. Technical report, Institute of Transportation Studies, UCLA, 2019.

M. Batty, K. W. Axhausen, F. Giannotti, A. Pozdnoukhov, A. Bazzani, M. Wachowicz, G. Ouzounis, and Y. Portugali. Smart cities of the future. *European Physical Journal: Special Topics*, 214(1):481–518, 2012. doi: 10.1140/epjst/e2012-01703-3.

A. C. Bemmaor and N. Glady. Modeling purchasing behavior with sudden "death": A flexible customer lifetime model. *Management Science*, 58(5):1012–1021, 2012.

S. Benjaafar and M. Hu. Operations Management in the Age of the Sharing Economy: What Is Old and What Is New? *Manufacturing & Service Operations Management*, 22(1):93–101, jan 2020a. doi: 10.1287/msom.2019.0803.

S. Benjaafar and M. Hu. Operations Management in the Age of the Sharing Economy: What Is Old and What Is New? *Manufacturing & Service Operations Management*, 22(1):93–101, 1 2020b. doi: 10.1287/msom.2019.0803.

S. Benjaafar, X. Li, and X. Li. Inventory Repositioning in On-Demand Product Rental Networks. *SSRN Electronic Journal*, 2017. doi: 10.2139/ssrn.2942921.

N. Berente, B. Gu, J. Recker, and R. Santhanam. Managing AI. *Call for Papers, MIS Quarterly*, 2019.

M. Bertrand, E. Duflo, and S. Mullainathan. How Much Should We Trust Differences-In-Differences Estimates? *The Quarterly Journal of Economics*, 119(1):249–275, feb 2004. doi: 10.1162/003355304772839588.

D. Beverungen, C. F. Breidbach, J. Poeppelbuss, and V. K. Tuunainen. Smart service systems: An interdisciplinary perspective. *Information Systems Journal*, 29(6):1201–1206, 2019. doi: 10.1111/isj.12275.

H. K. Bhargava and S. Sundaresan. Computing as utility: Managing availability, commitment, and pricing through contingent bid auctions. *Journal of Management Information Systems*, 21(2):201–227, 2004.

M. Bichler, A. Gupta, and W. Ketter. Designing smart markets. *Information Systems Research*, 21(4):688–699, 2010. doi: 10.1287/isre.1100.0316.

K. Bimpikis, O. Candogan, and D. Saban. Spatial pricing in ride-sharing networks. *Operations Research*, 67(3):744–769, 2019. doi: 10.1287/opre.2018.1800.

G. Boeing. OSMnx: New methods for acquiring, constructing, analyzing, and visualizing complex street networks. *Computers, Environment and Urban Systems*, 65:126–139, sep 2017. doi: 10.1016/j.compenvurbsys.2017.05.004.

K. Borusyak, X. Jaravel, and J. Spiess. Revisiting Event Study Designs: Robust and Efficient Estimation. pages 1–54, aug 2021.

S. Boschert and R. Rosen. Digital Twin—The Simulation Aspect. In *Mechatronic Futures*, pages 59–74. Springer International Publishing, Cham, 2016. doi: 10.1007/978-3-319-32156-1_5.

B. Boyaci, K. G. Zografos, and N. Geroliminis. An optimization framework for the development of efficient one-way car-sharing systems. *European Journal of Operational Research*, 240(3): 718–733, 2015. doi: 10.1016/j.ejor.2014.07.020.

T. Brandt and O. Dlugosch. Exploratory data science for discovery and ex-ante assessment of operational policies: Insights from vehicle sharing. *Journal of Operations Management*, (May 2019):1–22, 2020. doi: 10.1002/joom.1125.

A. Braverman, J. G. Dai, X. Liu, and L. Ying. Empty-car routing in ridesharing systems. *Operations Research*, 67(5):1437–1452, 2019. doi: 10.1287/opre.2018.1822.

D. Breuker, M. Matzner, P. Delfmann, and J. Becker. Comprehensible predictive models for business processes. *MIS Q.*, 40(4):1009–1034, 2016.

E. Bruun and M. Givoni. Sustainable mobility: Six research routes to steer transport policy. *Nature*, 523(7558):29–31, 2015. doi: 10.1038/523029a.

Bundesagentur für Arbeit. Regional Statitics, 2020.

Bundesamt für Statistik. Arbeitslosenstatistik, 2020.

L. D. Burns. Sustainable mobility: A vision of our transport future. *Nature*, 497(7448):181–182, 2013. doi: 10.1038/497181a.

G. Burtch, S. Carnahan, and B. N. Greenwood. Can You Gig It? An Empirical Examination of the Gig Economy and Entrepreneurial Activity. *Management Science*, 64(12):5497–5520, dec 2018. doi: 10.1287/mnsc.2017.2916.

L. Caggiani, R. Camporeale, M. Ottomanelli, and W. Y. Szeto. A modeling framework for the dynamic management of free-floating bike-sharing systems. *Transportation Research Part C: Emerging Technologies*, 87(January):159–182, 2018. doi: 10.1016/j.trc.2018.01.001.

T. Calinski and J. Harabasz. Communications in Statistics A dendrite method for cluster analysis. *Communications in Statistics*, 3(1):1–27, 1974.

B. Callaway and P. H. Sant'Anna. Difference-in-Differences with multiple time periods. *Journal of Econometrics*, (xxxx):1–31, 2020. doi: 10.1016/j.jeconom.2020.12.001.

B. Callaway, A. Goodman-Bacon, and P. H. C. Sant'Anna. Difference-in-Differences with a Continuous Treatment. 2021.

K. Campbell and C. Brakewood. Sharing riders: How bikesharing impacts bus ridership in New York City. *Transportation Research Part A: Policy and Practice*, 100:264–282, 2017. doi: 10.1016/j.tra.2017.04.017.

T. N. Cason, K. N. Kannan, and R. Siebert. An experimental study of information revelation policies in sequential auctions. *Management Science*, 57(4):667–688, 2011.

O. Caspi, M. J. Smart, and R. B. Noland. Spatial associations of dockless shared e-scooter usage. *Transportation Research Part D: Transport and Environment*, 86:102396, 2020. doi: 10.1016/j.trd.2020.102396.

D. Cengiz, A. Dube, A. Lindner, and B. Zipperer. The Effect of Minimum Wages on Low-Wage Jobs. *The Quarterly Journal of Economics*, 134(3):1405–1454, aug 2019. doi: 10.1093/qje/qjz014.

D. Chai, L. Wang, and Q. Yang. Bike flow prediction with multi-graph convolutional networks. *GIS: Proceedings of the ACM International Symposium on Advances in Geographic Information Systems*, pages 397–400, 2018. doi: 10.1145/3274895.3274896.

J. Chan and A. Ghose. Internet's Dirty Secret: Assessing the Impact of Online Intermediaries on HIV Transmission. *MIS Quarterly*, 38(4):955–976, apr 2014. doi: 10.25300/MISQ/2014/38.4.01.

C. Chen, J. Twycross, and J. M. Garibaldi. A new accuracy measure based on bounded relative error for time series forecasting. *PLoS ONE*, 12(3):1–23, 2017. doi: 10.1371/journal.pone.0174202.

T. D. Chen, K. M. Kockelman, and J. P. Hanna. Operations of a shared, autonomous, electric vehicle fleet: Implications of vehicle & charging infrastructure decisions. *Transportation Research Part A: Policy and Practice*, 94:243–254, 2016. doi: 10.1016/j.tra.2016.08.020.

Y.-D. Chen, S. A. Brown, P. J.-H. Hu, C.-C. King, and H. Chen. Managing emerging infectious diseases with information systems: reconceptualizing outbreak management through the lens of loose coupling. *Information Systems Research*, 22(3):447–468, 2011.

Z. Cheng, M. S. Pang, and P. A. Pavlou. Mitigating traffic congestion: The role of intelligent transportation systems. *Information Systems Research*, 31(3):653–674, 2020. doi: 10.1287/ISRE.2019.0894.

E. Cherchi. A stated choice experiment to measure the effect of informational and normative conformity in the preference for electric vehicles. *Transportation Research Part A: Policy and Practice*, 100:88–104, 2017.

M. Chica and W. Rand. Building agent-based decision support systems for word-of-mouth programs: a freemium application. *Journal of Marketing Research*, 54(5):752–767, 2017.

T. M. Choi, S. Kumar, X. Yue, and H. L. Chan. Disruptive Technologies and Operations Management in the Industry 4.0 Era and Beyond. *Production and Operations Management*, 31(1):9–31, 2022. doi: 10.1111/poms.13622.

F. Chollet et al. Keras, 2015.

C. Cimino, E. Negri, and L. Fumagalli. Review of digital twin applications in manufacturing. *Computers in Industry*, 113:103130, 2019. doi: 10.1016/j.compind.2019.103130.

M. C. Cohen. Big Data and Service Operations. *Production and Operations Management*, 27(9):1709–1723, 2018. doi: 10.1111/poms.12832.

P. Cohen, R. Hahn, J. Hall, S. Levitt, and R. Metcalfe. Using Big Data to Estimate Consumer Surplus: The Case of Uber. Technical report, National Bureau of Economic Research, Cambridge, MA, sep 2016.

J. Collins, W. Ketter, and M. Gini. Flexible decision control in an autonomous trading agent. *Electronic Commerce Research and Applications*, 8(2):91 – 105, 2009. ISSN 1567-4223. doi: https://doi.org/10.1016/j.elerap.2008.09.004. Special Section: Supply Chain Trading Agent Research.

J. Collins, W. Ketter, and M. Gini. Flexible decision support in dynamic inter-organisational networks. *European Journal of Information Systems*, 19(4):436–448, 2010. doi: 10.1057/ejis.2010.24.

J. Corbett. Designing and using carbon management systems to promote ecologically responsible behaviors. *Journal of the Association for Information Systems*, 14(7):339–378, 2013.

J. Corbett and S. Mellouli. Winning the SDG battle in cities: how an integrated information ecosystem can contribute to the achievement of the 2030 sustainable development goals. *Information Systems Journal*, 27(4):427–461, 2017. doi: 10.1111/isj.12138.

D. L. Costa and M. E. Kahn. Energy conservation "nudges" and environmentalist ideology: Evidence from a randomized residential electricity field experiment. *Journal of the European Economic Association*, 11(3):680–702, 2013. doi: 10.1111/jeea.12011.

P. Cramton, R. Geddes, and A. Ockenfels. Set road charges in real time to ease traffic. *Nature*, 560(2 August 2018):23–25, 2018.

S. Cunningham, G. DeAngelo, and J. Tripp. Craiglist's Effect on Violence Against Women. 2017.

C. de Chaisemartin and X. D'Haultfœuille. Two-Way Fixed Effects Estimators with Heterogeneous Treatment Effects. *American Economic Review*, 110(9):2964–2996, 2020. doi: 10.1257/aer.20181169.

C. de Chaisemartin and X. D'Haultfoeuille. Two-Way Fixed Effects and Differences-in-Differences with Heterogeneous Treatment Effects: A Survey. *SSRN Electronic Journal*, pages 1–21, 2021. doi: 10.2139/ssrn.3980758.

M. de Reuver, C. Sørensen, and R. Basole. The digital platform: a research agenda. *Journal of Information Technology*, 33:124–135, 2018. doi: 10.1057/s41265-016-0033-3.

J. Dedrick. Green IS: Concepts and issues for information systems research. *Communications of the Association for Information Systems*, 27(1):173–184, 2010. doi: 10.17705/1CAIS.02711.

B. J. Dietvorst, J. P. Simmons, and C. Massey. Algorithm aversion: People erroneously avoid algorithms after seeing them err. *Journal of Experimental Psychology: General*, 144(1):114, 2015.

J. Dill. Bicycling for transportation and health: The role of infrastructure. *Journal of Public Health Policy*, 30:95–110, 2009. doi: 10.1057/jphp.2008.56.

O. Dlugosch, T. Brandt, and D. Neumann. Combining analytics and simulation methods to assess the impact of shared, autonomous electric vehicles on sustainable urban mobility. *Information & Management*, page 103285, 2020.

A. Y. Du, S. Das, R. D. Gopal, and R. Ramesh. Optimal management of digital content on tiered infrastructure platforms. *Information Systems Research*, 25(4):730–746, 2014.

G. M. Eckhardt, M. B. Houston, B. Jiang, C. Lamberton, A. Rindfleisch, and G. Zervas. Marketing in the Sharing Economy. *Journal of Marketing*, 83(5):5–27, 2019. doi: 10.1177/0022242919861929.

A. L. Erera, J. C. Morales, and M. Savelsbergh. Robust Optimization for Empty Repositioning Problems. *Operations Research*, 57(2):468–483, 2009. doi: 10.1287/opre.1080.0650.

B. Ferguson, V. Nagaraj, E. C. Kara, and M. Alizadeh. Optimal Planning of Workplace Electric Vehicle Charging Infrastructure with Smart Charging Opportunities. *IEEE Conference on Intelligent Transportation Systems, Proceedings, ITSC*, 2018-Novem:1149–1154, 2018. doi: 10.1109/ITSC.2018.8569299.

J. Firnkorn and M. Müller. Free-floating electric carsharing-fleets in smart cities: The dawning of a post-private car era in urban environments? *Environmental Science and Policy*, 45:30–40, 2015. doi: 10.1016/j.envsci.2014.09.005.

E. Fishman, S. Washington, and N. Haworth. Bike share's impact on car use: Evidence from the United States, Great Britain, and Australia. *Transportation Research Part D: Transport and Environment*, 31:13–20, 2014. doi: https://doi.org/10.1016/j.trd.2014.05.013.

M. C. Fu. Optimization for simulation: Theory vs. practice. *INFORMS Journal on Computing*, 14(3):192–215, 2002.

M. C. Fu, editor. *Handbook of Simulation Optimization*, volume 216 of *International Series in Operations Research & Management Science*. Springer New York, New York, NY, 2015. ISBN 978-1-4939-1383-1. doi: 10.1007/978-1-4939-1384-8.

A. Fügener, J. Grahl, A. Gupta, and W. Ketter. Will humans-in-the-loop become borgs? merits and pitfalls of working with ai. *Management Information Systems Quarterly (MISQ)-Vol*, 45, 2021.

A. Fügener, J. Grahl, W. Ketter, and A. Gupta. Cognitive challenges in human-ai collaboration: Investigating the path towards productive delegation. *Information Systems Research*, Forthcoming.

D. Fürstenau, A. Baiyere, and N. Kliewer. A dynamic model of embeddedness in digital infrastructures. *Information Systems Research*, 30(4):1319–1342, 2019.

Y. Ghiassi-Farrokhfal, C. Rosenberg, S. Keshav, and M. B. Adjaho. Joint Optimal Design and Operation of Hybrid Energy Storage Systems. *IEEE Journal on Selected Areas in Communications*, 34(3):639–650, 2016. doi: 10.1109/JSAC.2016.2525599.

A. Ghose, H. E. Kwon, D. Lee, and W. Oh. Seizing the commuting moment: Contextual targeting based on mobile transportation apps. *Information Systems Research*, 30(1):154–174, 2019a. doi: 10.1287/isre.2018.0792.

A. Ghose, B. Li, and S. Liu. Mobile targeting using customer trajectory patterns. *Management Science*, 65(11):5027–5049, 2019b. doi: 10.1287/mnsc.2018.3188.

E. Glaessgen and D. Stargel. The Digital Twin Paradigm for Future NASA and U.S. Air Force Vehicles. In *53rd AIAA/ASME/ASCE/AHS/ASC Structures, Structural Dynamics and Materials Conference
20th AIAA/ASME/AHS Adaptive Structures Conference
14th AIAA*, number April, Reston, Virigina, apr 2012. American Institute of Aeronautics and Astronautics. doi: 10.2514/6.2012-1818.

J. Gong, B. N. Greenwood, and Y. Song. Uber Might Buy Me a Mercedes Benz: An Empirical Investigation of the Sharing Economy and Durable Goods Purchase. *Ssrn*, 2017. doi: 10.2139/ssrn.2971072.

M. C. González, C. A. Hidalgo, and A. L. Barabási. Understanding individual human mobility patterns. *Nature*, 453(7196):779–782, 2008. doi: 10.1038/nature06958.

A. Goodman-Bacon. Difference-in-differences with variation in treatment timing. *Journal of Econometrics*, 225(2):254–277, 2021. doi: 10.1016/j.jeconom.2021.03.014.

A. Gosavi. Reinforcement learning: A tutorial survey and recent advances. *INFORMS Journal on Computing*, 21(2):178–192, 2009. doi: 10.1287/ijoc.1080.0305.

S. Gottwalt, W. Ketter, C. Block, J. Collins, and C. Weinhardt. Demand side management-A simulation of household behavior under variable prices. *Energy Policy*, 39(12):8163–8174, 2011. doi: 10.1016/j.enpol.2011.10.016.

B. N. Greenwood and S. Wattal. Show Me the Way to go Home: An Empirical Investigation of Ride-Sharing and Alcohool Related Motor Vehicle Fatalities. *MIS Quarterly*, 41(1):163–187, 2017a.

B. N. Greenwood and S. Wattal. Show me the way to go home: An empirical investigation of ride-sharing and alcohol related motor vehicle fatalities. *MIS Quarterly*, 41:163–187, 2017b. doi: 10.25300/MISQ/2017/41.1.08.

M. Grieves and J. Vickers. *Digital Twin: Mitigating Unpredictable, Undesirable Emergent Behavior in Complex Systems*, pages 85–113. Springer International Publishing, 2017. ISBN 978-3-319-38756-7. doi: 10.1007/978-3-319-38756-7_4.

A. Griffin and J. R. Hauser. The Voice of the Customer. *Marketing Science*, 12(1):1–27, feb 1993. doi: 10.1287/mksc.12.1.1.

H. Guda and U. Subramanian. Your Uber Is Arriving: Managing On-Demand Workers Through Surge Pricing, Forecast Communication, and Worker Incentives. *Management Science, Articles in Advance*, (March):1–20, feb 2019. doi: 10.1287/mnsc.2018.3050.

G. Gust, T. Brandt, S. Mashayekh, M. Heleno, N. DeForest, M. Stadler, and D. Neumann. Strategies for microgrid operation under real-world conditions. *European Journal of Operational Research*, 292(1):339–352, 2021. doi: 10.1016/j.ejor.2020.10.041.

E. Hafermalz, R. B. Johnston, D. S. Hovorka, and K. Riemer. Beyond 'mobility': A new understanding of moving with technology. *Information Systems Journal*, 2020.

L. A. Hannah. Stochastic Optimization. In *International Encyclopedia of the Social & Behavioral Sciences*, volume 23, pages 473–481. Elsevier, second edi edition, 2015. ISBN 9780080970875. doi: 10.1016/B978-0-08-097086-8.42010-6.

Z. Hao, L. He, Z. Hu, and J. Jiang. Robust Vehicle Pre-Allocation with Uncertain Covariates. *Production and Operations Management*, 0(0):1–18, 2019. doi: 10.1111/poms.13143.

Havard Medical School. Calories burned in 30 minutes for people of three different weights, 2018.

L. He, H. Y. Mak, Y. Rong, and Z. J. M. Shen. Service region design for urban electric vehicle sharing systems. *Manufacturing and Service Operations Management*, 19(2):309–327, 2017. doi: 10.1287/msom.2016.0611.

L. He, Z. Hu, and M. Zhang. Robust Repositioning for Vehicle Sharing. *Manufacturing & Service Operations Management*, (May):msom.2018.0734, apr 2019a. doi: 10.1287/msom.2018.0734.

L. He, H.-y. Mak, and Y. Rong. Operations Management of Vehicle Sharing Systems. In M. Hu, editor, *Sharing Economy*, chapter 19, pages 461–484. Springer Nature, Berlin, 2019b. doi: 10.1007/978-3-030-01863-4_19.

A. R. Hevner and S. Gregor. Positioning and Presenting Design Science Research for Maximum Impact. *MIS Quarterly*, 37(2):337–355, 2013. doi: 10.2753/MIS0742-1222240302.

Y. Hong, C. Wang, and P. A. Pavlou. Comparing open and sealed bid auctions: Evidence from online labor markets. *Information Systems Research*, 27(1):49–69, 2016.

Z. Hoover, E. Polymeneas, and S. Sahdev. How to integrate electric-vehicle charging into existing building and grid infrastructure. Technical report, McKinsey & Company, 2021.

A. Horni, K. Nagel, and K. W. Axhausen. *The Multi-Agent Transport Simulation MATSim.* Ubiquity Press, London, aug 2016. doi: 10.5334/baw.

Y. Huang and Y. Zhou. An optimization framework for workplace charging strategies. *Transportation Research Part C: Emerging Technologies*, 52:144–155, 2015. doi: 10.1016/j.trc.2015.01.022.

G. W. Imbens and D. B. Rubin. *Causal Inference for Statistics, Social, and Biomedical Sciences: An Introduction.* Cambridge University Press, New York, USA, 2015.

INRIX Research. Inrix Global Traffic Scorecard. Technical report, 2018.

D. Jones, C. Snider, A. Nassehi, J. Yon, and B. Hicks. Characterising the Digital Twin: A systematic literature review. *CIRP Journal of Manufacturing Science and Technology*, 29: 36–52, 2020. doi: 10.1016/j.cirpj.2020.02.002.

K. Jordahl, J. V. den Bossche, M. Fleischmann, J. Wasserman, J. McBride, J. Gerard, J. Tratner, M. Perry, A. G. Badaracco, C. Farmer, G. A. Hjelle, A. D. Snow, M. Cochran, S. Gillies, L. Culbertson, M. Bartos, N. Eubank, maxalbert, A. Bilogur, S. Rey, C. Ren, D. Arribas-Bel, L. Wasser, L. J. Wolf, M. Journois, J. Wilson, A. Greenhall, C. Holdgraf, Filipe, and F. Leblanc. geopandas/geopandas: v0.8.1, July 2020.

M. Jun and A. Meintz. Workplace Charge Management with Aggregated Building Loads. *2018 IEEE Transportation and Electrification Conference and Expo, ITEC 2018*, pages 519–524, 2018. doi: 10.1109/ITEC.2018.8450227.

M. Kahlen, T. Y. Lee, W. Ketter, and A. Gupta. Optimal Prepositioning and Fleet Sizing to Maximize Profits for One-Way Transportation Companies. In *Thirty Eighth International Conference on Information Systems, South Korea 2017*, pages 0–17, 2017.

M. T. Kahlen, W. Ketter, and J. van Dalen. Electric Vehicle Virtual Power Plant Dilemma: Grid Balancing Versus Customer Mobility. *Production and Operations Management*, 27(11): 2054–2070, nov 2018. doi: 10.1111/poms.12876.

K. N. Kannan, V. Pamuru, and Y. Rosokha. Using machine learning for modeling human behavior and analyzing friction in generalized second price auctions. *Available at SSRN 3315772*, 2019.

P. Karaenke, M. Bichler, and S. Minner. Coordination is hard: Electronic auction mechanisms for increased efficiency in transportation logistics. *Management Science*, 65(12):5884–5900, 2019.

M. A. Kazemi, M. Sedighizadeh, M. J. Mirzaei, and O. Homaee. Optimal siting and sizing of distribution system operator owned EV parking lots. *Applied Energy*, 179:1176–1184, 2016. doi: 10.1016/j.apenergy.2016.06.125.

F. Kazhamiaka, C. Rosenberg, and S. Keshav. Tractable lithium-ion storage models for optimizing energy systems. *Energy Informatics*, 2(1), 2019. doi: 10.1186/s42162-019-0070-6.

P. B. Keenan and P. Jankowski. Spatial Decision Support Systems: Three decades on. *Decision Support Systems*, 116(October 2018):64–76, 2019. doi: 10.1016/j.dss.2018.10.010.

W. Ketter, J. Collins, M. Gini, A. Gupta, and P. Schrater. Detecting and forecasting economic regimes in multi-agent automated exchanges. *Decision Support Systems*, 47(4):307–318, 2009. doi: 10.1016/j.dss.2009.05.012.

W. Ketter, J. Collins, M. Gini, A. Gupta, and P. Schrater. Real-Time tactical and strategic sales management for intelligent agents guided by economic regimes. *Information Systems Research*, 23(4):1263–1283, 2012. doi: 10.1287/isre.1110.0415.

W. Ketter, M. Peters, J. Collins, and A. Gupta. Competitive Benchmarking: An IS Research Approach to Address Wicked Problems with Big Data and Analytics. *MIS Quarterly*, 40(4): 1–53, 2016a.

W. Ketter, M. Peters, J. Collins, and A. Gupta. A Multiagent Competitive Gaming Platform to Address Societal Challenges. *MIS Quarterly*, 40(2):447–460, 2016b.

W. Ketter, J. Collins, M. Saar-Tsechansky, and O. Marom. Information Systems for a Smart Electricity Grid. *ACM Transactions on Management Information Systems*, 9(3):1–22, 2018. doi: 10.1145/3230712.

D. P. Kingma and J. Ba. Adam: A Method for Stochastic Optimization. In *ICLR*, pages 1–15, 2015. doi: http://doi.acm.org.ezproxy.lib.ucf.edu/10.1145/1830483.1830503.

K. Koroleva, M. Kahlen, W. Ketter, L. Rook, and F. Lanz. Tamagocar: Using a simulation app to explore price elasticity of demand for electricity of electric vehicle users. *Proceedings of the 35th International Conference on Information Systems (ICIS)*, 2014.

O. Kröger, C. Coffrin, H. Hijazi, and H. Nagarajan. Juniper: An Open-Source Nonlinear Branch-and-Bound Solver in Julia. In *CPAIOR 2018: Integration of Constraint Programming, Artificial Intelligence, and Operations Research*, volume 2, pages 377–386. 2018. doi: 10.1007/978-3-319-93031-2_27.

A. Y. Lam. Combinatorial Auction-Based Pricing for Multi-Tenant Autonomous Vehicle Public Transportation System. *IEEE Transactions on Intelligent Transportation Systems*, 17(3): 859–869, 2016. doi: 10.1109/TITS.2015.2490800.

G. Laporte, F. Meunier, and R. Wolfler Calvo. Shared mobility systems: an updated survey. *Annals of Operations Research*, 271(1):105–126, 2018. doi: 10.1007/s10479-018-3076-8.

Z. J. Lee, T. Li, and S. H. Low. ACN-Data: Analysis and applications of an open EV charging dataset. *e-Energy 2019 - Proceedings of the 10th ACM International Conference on Future Energy Systems*, pages 139–149, 2019. doi: 10.1145/3307772.3328313.

Q. Li and F. Liao. Incorporating vehicle self-relocations and traveler activity chains in a bi-level model of optimal deployment of shared autonomous vehicles. *Transportation Research Part B: Methodological*, 140:151–175, 2020. doi: 10.1016/j.trb.2020.08.001.

S. Li, F. Xie, Y. Huang, Z. Lin, and C. Liu. Optimizing workplace charging facility deployment and smart charging strategies. *Transportation Research Part D: Transport and Environment*, 87:1–12, 2020. doi: 10.1016/j.trd.2020.102481.

M. Lu, Z. Chen, and S. Shen. Optimizing the Profitability and Quality of Service in Carshare Systems Under Demand Uncertainty. *Manufacturing & Service Operations Management*, 20 (2):162–180, may 2018. doi: 10.1287/msom.2017.0644.

Y. Lu, A. Gupta, W. Ketter, and E. V. Heck. Exploring Bidder Heterogeneity in Multichannel Sequential B2B Auctions. *MIS Quarterly*, 40(3):645–662, 2016a. doi: 10.25300/MISQ/2016/40.3.06.

Y. Lu, A. Gupta, W. Ketter, and E. v. Heck. Exploring bidder heterogeneity in multichannel sequential b2b auctions. *MIS Quarterly*, 40(3):645–662, 2016b.

Y. Lu, A. Gupta, W. Ketter, and E. van Heck. Dynamic Decision Making in Sequential Business-to-Business Auctions: A Structural Econometric Approach. *Management Science*, (June), 2019a. doi: 10.1287/mnsc.2018.3118.

Y. Lu, A. Gupta, W. Ketter, and E. Van Heck. Information transparency in business-to-business auction markets: The role of winner identity disclosure. *Management Science*, 65(9):4261–4279, 2019b.

M. Lubin and I. Dunning. Computing in operations research using julia. *INFORMS Journal on Computing*, 27(2):238–248, 2015. doi: 10.1287/ijoc.2014.0623.

H. Luo, Z. Kou, F. Zhao, and H. Cai. Comparative life cycle assessment of station-based and dock-less bike sharing systems. *Resources, Conservation and Recycling*, 146(March):180–189, 2019. doi: 10.1016/j.resconrec.2019.03.003.

K. Lyytinen and Y. Yoo. Research commentary: The next wave of nomadic computing. *Information Systems Research*, 13(4):377–388, 2002. doi: 10.1287/isre.13.4.377.75.

M. Maciejewski and J. Bischoff. Congestion effects of autonomous taxi fleets. *Transport*, pages 1–10, 2017. doi: 10.3846/16484142.2017.1347827.

H. S. Mahmassani. 50th Anniversary Invited Article—Autonomous Vehicles and Connected Vehicle Systems: Flow and Operations Considerations. *Transportation Science*, 50(4):1140–1162, 2016. doi: 10.1287/trsc.2016.0712.

A. S. Masoum, S. Deilami, A. Abu-Siada, and M. A. Masoum. Fuzzy Approach for Online Coordination of Plug-In Electric Vehicle Charging in Smart Grid. *IEEE Transactions on Sustainable Energy*, 6(3):1112–1121, 2015. doi: 10.1109/TSTE.2014.2327640.

G. McKenzie. Spatiotemporal comparative analysis of scooter-share and bike-share usage patterns in Washington, D.C. *Journal of Transport Geography*, 78:19–28, 2019. doi: https://doi.org/10.1016/j.jtrangeo.2019.05.007.

V. McKinney, K. Yoon, and F. Zahedi. The measurement of web-customer satisfaction: An expectation and disconfirmation approach. *Information Systems Research*, 13(3):296–315, 2002.

N. Melville. Information Systems Innovation for Environmental Sustainability. *MIS Quarterly*, 34(1):1–21, jun 2010.

G. Meyer, G. Adomavicius, P. E. Johnson, M. Elidrisi, W. A. Rush, J. M. Sperl-Hillen, and P. J. O'Connor. A machine learning approach to improving dynamic decision making. *Information Systems Research*, 25(2):239–263, 2014.

V. Mnih, K. Kavukcuoglu, D. Silver, A. A. Rusu, J. Veness, M. G. Bellemare, A. Graves, M. Riedmiller, A. K. Fidjeland, G. Ostrovski, et al. Human-level control through deep reinforcement learning. *nature*, 518(7540):529–533, 2015.

J. C. Mukherjee and A. Gupta. A Review of Charge Scheduling of Electric Vehicles in Smart Grid. *IEEE Systems Journal*, 9(4):1541–1553, 2015. doi: 10.1109/JSYST.2014.2356559.

J. Müller and K. Bogenberger. Time series analysis of booking data of a free-floating carsharing system in Berlin. *Transportation Research Procedia*, 10(July):345–354, 2015. doi: 10.1016/j.trpro.2015.09.084.

NABSA. General Bikeshare Feed Specification (GBFS), 2021.

R. Nair and E. Miller-Hooks. Fleet Management for Vehicle Sharing Operations. *Transportation Science*, 45(4):524–540, 2011. doi: 10.1287/trsc.1100.0347.

Y. Nakahira, N. Chen, L. Chen, and S. Low. Smoothed least-laxity-first algorithm for EV charging. In *e-Energy 2017 - Proceedings of the 8th International Conference on Future Energy Systems*, pages 242–251, 2017. doi: 10.1145/3077839.3077864.

Nextbike. Nextbike - company. https://www.nextbike.net/en/, 2022. Accessed: 2022-06-24.

R. Nishant, M. Kennedy, and J. Corbett. Artificial intelligence for sustainability: Challenges, opportunities, and a research agenda. *International Journal of Information Management*, 53: 102104, 2020.

P. Nunes, R. Figueiredo, and M. C. Brito. The use of parking lots to solar-charge electric vehicles. *Renewable and Sustainable Energy Reviews*, 66:679–693, 2016. doi: 10.1016/j.rser.2016.08.015.

G. Oestreicher-Singer and L. Zalmanson. Content or community? a digital business strategy for content providers in the social age. *MIS Quarterly*, pages 591–616, 2013.

Open Mobility Foundation. Mobility Data Specification (MDS), 2021.

A. Osterwalder, Y. Pigneur, and C. Tucci. Clarifying business models: origins, present, and future of the concept. *Communications of the Association for Information Systems*, 15(May): 1–43, 2005. doi: 10.1.1.83.7452.

A. Pal and Y. Zhang. Free-floating bike sharing: Solving real-life large-scale static rebalancing problems. *Transportation Research Part C: Emerging Technologies*, 80:92–116, 2017. doi: 10.1016/j.trc.2017.03.016.

P. Papadopoulos, N. Jenkins, L. M. Cipcigan, I. Grau, and E. Zabala. Coordination of the charging of electric vehicles using a multi-agent system. *IEEE Transactions on Smart Grid*, 4(4):1802–1809, 2013. doi: 10.1109/TSG.2013.2274391.

J. Paundra, L. Rook, J. van Dalen, and W. Ketter. Preferences for car sharing services: Effects of instrumental attributes and psychological ownership. *Journal of Environmental Psychology*, 53:121–130, 2017. doi: 10.1016/j.jenvp.2017.07.003.

K. Pelechrinis, B. Li, and S. Qian. Bike Sharing and Car Trips in the City: The Case of Healthy Ride Pittsburgh. 2016a.

K. Pelechrinis, B. Li, and S. Qian. Bike sharing and car trips in the city: The case of Healthy Ride Pittsburgh. Technical report, University of Pittsburgh, 2016b.

K. Pelechrinis, C. Zacharias, M. Kokkodis, and T. Lappas. Economic impact and policy implications from urban shared transportation: The case of Pittsburgh's shared bike system. *PLoS ONE*, 12(8):1–21, 2017. doi: 10.1371/journal.pone.0184092.

S. Pelletier, O. Jabali, and G. Laporte. 50th Anniversary Invited Article—Goods Distribution with Electric Vehicles: Review and Research Perspectives. *Transportation Science*, 50(1): 3–22, 2016. doi: 10.1287/trsc.2015.0646.

J. Persson, J. F. Parie, and S. Feuerriegel. Monitoring the COVID-19 epidemic with nationwide telecommunication data. *Proceedings of the National Academy of Sciences of the United States of America*, 118(26), 2021. doi: 10.1073/pnas.2100664118.

M. Peters, W. Ketter, M. Saar-Tsechansky, and J. Collins. A reinforcement learning approach to autonomous decision-making in smart electricity markets. *Mach Learn*, 92:5–39, 2013. doi: 10.1007/s10994-013-5340-0.

M. Peters, M. Saar-Tsechansky, W. Ketter, S. A. Williamson, P. Groot, and T. Heskes. A scalable preference model for autonomous decision-making. *Machine Learning*, 107(6):1039–1068, 2018. doi: 10.1007/s10994-018-5705-5.

J. Pfeiffer, T. Pfeiffer, M. Meißner, and E. Weiß. Eye-tracking-based classification of information search behavior using machine learning: evidence from experiments in physical shops and virtual reality shopping environments. *Information Systems Research*, 31(3):675–691, 2020.

W. B. Powell. *Approximate Dynamic Programming*. Wiley Series in Probability and Statistics. John Wiley & Sons, Inc., Hoboken, NJ, USA, aug 2011. doi: 10.1002/9781118029176.

W. B. Powell. Energy and uncertainty: Models and algorithms for complex energy systems. *AI Magazine*, 35(3):8–21, 2014. ISSN 07384602. doi: 10.1609/aimag.v35i3.2540.

W. Qi and Z.-J. M. Shen. A Smart-City Scope of Operations Management. *Production and Operations Management*, 0(0):1–14, 2018. doi: 10.1111/poms.12928.

L. Qiu and I. Benbasat. Evaluating anthropomorphic product recommendation agents: A social relationship perspective to designing information systems. *Journal of Management Information Systems*, 25(4):145–182, 2009.

D. J. Reck, H. Martin, and K. W. Axhausen. Mode choice, substitution patterns and environmental impacts of shared and personal micro-mobility. *Transportation Research Part D: Transport and Environment*, 102(December 2021):103134, 2022. doi: 10.1016/j.trd.2021.103134.

P. J. Rousseeuw. Silhouettes: A graphical aid to the interpretation and validation of cluster analysis. *Journal of Computational and Applied Mathematics*, 20(C):53–65, 1987. doi: 10.1016/0377-0427(87)90125-7.

SAE. J3016_201806: Taxonomy and Definitions for Terms Related to Driving Automation Systems for On-Road Motor Vehicles, 2018.

N. Sahoo, P. V. Singh, and T. Mukhopadhyay. A hidden markov model for collaborative filtering. *MIS quarterly*, pages 1329–1356, 2012.

K. Sahr, D. White, and A. J. Kimerling. Geodesic Discrete Global Grid Systems. *Cartography and Geographic Information Science*, 30(2):121–134, 2004. doi: 10.1559/152304003100011090.

P. H. Sant'Anna and J. Zhao. Doubly robust difference-in-differences estimators. *Journal of Econometrics*, 219(1):101–122, 2020. doi: https://doi.org/10.1016/j.jeconom.2020.06.003.

S. Sarker, S. Chatterjee, X. Xiao, and A. Elbanna. The Sociotechnical Axis of Cohesion for the IS Discipline: Its Historical Legacy and its Continued Relevance. *MIS Quarterly*, 43(3): 695–719, jan 2019. doi: 10.25300/MISQ/2019/13747.

M. Savelsbergh and T. Van Woensel. 50th Anniversary Invited Article—City Logistics: Challenges and Opportunities. *Transportation Science*, 50(2):579–590, 2016. doi: 10.1287/trsc.2016.0675.

T. Scheffel, A. Pikovsky, M. Bichler, and K. Guler. An experimental comparison of linear and nonlinear price combinatorial auctions. *Information Systems Research*, 22(2):346–368, 2011.

M. Schiffer, G. Hiermann, F. Rüdel, and G. Walther. A polynomial-time algorithm for user-based relocation in free-floating car sharing systems. *Transportation Research Part B: Methodological*, 143:65–85, 2021. doi: 10.1016/j.trb.2020.11.001.

B. Schleich, N. Anwer, L. Mathieu, and S. Wartzack. Shaping the digital twin for design and production engineering. *CIRP Annals*, 66(1):141–144, 2017. doi: 10.1016/j.cirp.2017.04.040.

K. Schroer, W. Ketter, T. Y. Lee, A. Gupta, and M. Kahlen. An Online Learning and Optimization Approach for Competitor-Aware Management of Shared Mobility Systems. In *Proceedings of the SIG GREEN Workshop*, pages 1–12, 2019.

K. Schroer, W. Ketter, T. Y. Lee, A. Gupta, and M. Kahlen. Data-Driven Competitor-Aware Positioning in On-Demand Vehicle Rental Networks. *Transportation Science*, 56(1):182–200, jan 2022a. doi: 10.1287/trsc.2021.1097.

K. Schroer, W. Ketter, T. Y. Lee, A. Gupta, and M. Kahlen. Data-Driven Competitor-Aware Positioning in On-Demand Vehicle Rental Networks. *Transportation Science*, 56(1):182–200, jan 2022b. doi: 10.1287/trsc.2021.1097.

B. Schwartz. *The Paradox of Choice: Why More Is Less, Revised Edition: Amazon.de: Barry Schwartz: Amazon.De*. Harper Perennial, 2016.

S. Seidel, J. Recker, and J. vom Brocke. Sensemaking and Sustainable Practicing: Functional Affordances of Information Systems in Green Transformations. *MIS Quarterly*, 37(4):1275–1299, 2013. doi: 10.25300/MISQ/2013/37.4.13.

S. Seidel, L. Chandra Kruse, N. Székely, M. Gau, and D. Stieger. Design principles for sensemaking support systems in environmental sustainability transformations. *European Journal of Information Systems*, 27(2):221–247, 2018. doi: 10.1057/s41303-017-0039-0.

S. Shaheen. Shared micromobility policy toolkit: Docked and dockless bike and scooter sharing. Technical report, UC Berkeley, 2019.

S. Shaheen and A. Cohen. Growth in Worldwide Carsharing: An International Comparison. *Transportation Research Record: Journal of the Transportation Research Board*, 1992:81–89, 2007. doi: 10.3141/1992-10.

P. Sharifi, A. Banerjee, and M. J. Feizollahi. Leveraging owners' flexibility in smart charge/discharge scheduling of electric vehicles to support renewable energy integration. *Computers and Industrial Engineering*, 149(July):106762, 2020. doi: 10.1016/j.cie.2020.106762.

G. Shmueli. Research Dilemmas with Behavioral Big Data. *Big Data*, 5(2):98–119, 2017. doi: 10.1089/big.2016.0043.

G. Shmueli and O. R. Koppius. Predictive analytics in information systems research. *MIS Quarterly*, 35(3):553–572, 2011.

S. Sierla, V. Kyrki, P. Aarnio, and V. Vyatkin. Automatic assembly planning based on digital product descriptions. *Computers in Industry*, 97:34–46, 2018. doi: 10.1016/j.compind.2018.01.013.

H. A. Simon. Rational Decision Making in Business Organizations. *THE AMERICAN ECONOMIC REVIEW*, page 22, 1979.

V. K. Singh, U. Shrivastava, L. Bouayad, B. Padmanabhan, A. Ialynytchev, and S. K. Schultz. Machine learning for psychiatric patient triaging: an investigation of cascading classifiers. *Journal of the American Medical Informatics Association*, 25(11):1481–1487, 2018.

D. Sperling. *Three revolutions: steering automated, shared, and electric vehicles to a better future*. Island Press, Washington, D.C., USA, 2018. doi: 10.1080/01441647.2018.1481892.

P. Ströhle, C. M. Flath, and J. Gärttner. Leveraging Customer Flexibility for Car-Sharing Fleet Optimization. *Transportation Science*, 53(1):42–61, feb 2019. doi: 10.1287/trsc.2017.0813.

L. Sun and S. Abraham. Estimating dynamic treatment effects in event studies with heterogeneous treatment effects. *Journal of Econometrics*, 225(2):175–199, 2021. doi: 10.1016/j.jeconom.2020.09.006.

A. Sundararajan. *The Sharing Economy: The End of Employment and the Rise of Crowd-Based Capitalism*. The MIT Press, Cambridge, MA, 2016. doi: 10.1177/0972262917712390.

R. Sutton. The Bitter Lesson, 2019.

F. Tao, J. Cheng, Q. Qi, M. Zhang, H. Zhang, and F. Sui. Digital twin-driven product design, manufacturing and service with big data. *The International Journal of Advanced Manufacturing Technology*, 94(9-12):3563–3576, feb 2018. doi: 10.1007/s00170-017-0233-1.

R. H. Thaler, C. R. Sunstein, and J. P. Balz. Choice Architecture. In E. Sharfir, editor, *The Behavioral Foundations of Public Policy*, chapter 25, pages 428–439. Princeton University Press, Princeton, NJ, USA, 2013. doi: 10.2139/ssrn.1583509.

The Weather Company (IBM). IBM Weather Solutions, 2019.

V. Tiefenbeck, L. Goette, K. Degen, V. Tasic, E. Fleisch, R. Lalive, and T. Staake. Overcoming Salience Bias: How Real-Time Feedback Fosters Resource Conservation. *Management Science*, 64(3):1458–1476, mar 2018. doi: 10.1287/mnsc.2016.2646.

A. Tiwana, B. Konsynski, and A. A. Bush. Platform evolution: Coevolution of platform architecture, governance, and environmental dynamics. *Information Systems Research*, 21(4): 675–687, 2010. doi: 10.1287/isre.1100.0323.

K. Valogianni and W. Ketter. Effective demand response for smart grids: Evidence from a real-world pilot. *Decision Support Systems*, 91:48–66, 2016. doi: 10.1016/j.dss.2016.07.007.

K. Valogianni, A. Gupta, W. Ketter, S. Sen, and E. van Heck. Multiple vickrey auctions for sustainable electric vehicle charging. *Proceedings of the 40th International Conference on Information Systems (ICIS)*, 2019.

K. Valogianni, W. Ketter, J. Collins, and D. Zhdanov. Sustainable Electric Vehicle Charging using Adaptive Pricing. *Production and Operations Management*, 29(6):1550–1572, 2020. doi: 10.1111/poms.13179.

H. van der Valk, H. Haße, F. Möller, M. Arbter, J. L. Henning, and B. Otto. A Taxonomy of Digital Twins. *26th Americas Conference on Information Systems, AMCIS 2020*, pages 1–10, 2020.

W. Vickrey. Congestion Theory and Transport Investment. *The American Economic Review*, 59(2):251–260, 1969.

A. Wächter and L. T. Biegler. On the implementation of an interior-point filter line-search algorithm for large-scale nonlinear programming. *Mathematical Programming*, 106(1):25–57, mar 2006. doi: 10.1007/s10107-004-0559-y.

Z. Wadud, D. MacKenzie, and P. Leiby. Help or hindrance? The travel, energy and carbon impacts of highly automated vehicles. *Transportation Research Part A: Policy and Practice*, 86:1–18, 2016. doi: 10.1016/j.tra.2015.12.001.

H. Wang and A. Odoni. Approximating the Performance of a "Last Mile" Transportation System. *Transportation Science*, 50(2):659–675, 2016. doi: 10.1287/trsc.2014.0553.

Q. Wang, B. Li, and P. V. Singh. Copycats vs. original mobile apps: A machine learning copycat-detection method and empirical analysis. *Information Systems Research*, 29(2):273–291, 2018.

R. T. Watson, M.-C. Boudreau, and A. J. Chen. Information Systems and Environmentally Sustainable Development: Energy Informatics and New Directions for the IS Community. *MIS Quarterly*, 24(4):665–694, 2010. doi: 10.2307/3250951.

S. Weikl and K. Bogenberger. A practice-ready relocation model for free-floating carsharing systems with electric vehicles - Mesoscopic approach and field trial results. *Transportation Research Part C: Emerging Technologies*, 57:206–223, 2015. doi: 10.1016/j.trc.2015.06.024.

C. Willing, K. Klemmer, T. Brandt, and D. Neumann. Moving in time and space – Location intelligence for carsharing decision support. *Decision Support Systems*, 99:75–85, 2017. doi: 10.1016/j.dss.2017.05.005.

World Health Organization. Health effects of transport-related air pollution. Technical report, World Health Organization (WHO), 2005.

World Health Organization. GLOBAL STATUS REPORT ON ROAD SAFETY. Technical Report 4, World Health Organization, 2018.

D. Wu, H. Zeng, C. Lu, and B. Boulet. Two-Stage Energy Management for Office Buildings with Workplace EV Charging and Renewable Energy. *IEEE Transactions on Transportation Electrification*, 3(1):225–237, 2017. doi: 10.1109/TTE.2017.2659626.

C. Xu, J. Ji, and P. Liu. The station-free sharing bike demand forecasting with a deep learning approach and large-scale datasets. *Transportation Research Part C: Emerging Technologies*, 95(July):47–60, 2018. doi: 10.1016/j.trc.2018.07.013.

D. Xu. Burn Calories, Not Fuel! The effects of bikeshare programs on obesity rates. *Transportation Research Part D: Transport and Environment*, 67:89–108, 2019. doi: 10.1016/j.trd.2018.11.002.

H. Yang, J. Huo, Y. Bao, X. Li, L. Yang, and C. R. Cherry. Impact of e-scooter sharing on bike sharing in Chicago. *Transportation Research Part A: Policy and Practice*, 154(September): 23–36, 2021. doi: 10.1016/j.tra.2021.09.012.

M. Yang, Y. Ren, and G. Adomavicius. Understanding user-generated content and customer engagement on facebook business pages. *Information Systems Research*, 30(3):839–855, 2019.

Y. C. Yang and B. Padmanabhan. Toward user patterns for online security: Observation time and online user identification. *Decision Support Systems*, 48(4):548–558, 2010.

Y. Yoo, O. Henfridsson, and K. Lyytinen. Research commentary—the new organizing logic of digital innovation: an agenda for information systems research. *Information systems research*, 21(4):724–735, 2010.

H. Younes, Z. Zou, J. Wu, and G. Baiocchi. Comparing the temporal determinants of dockless scooter-share and station-based bike-share in washington, d.c. *Transportation Research Part A: Policy and Practice*, 134:308 – 320, 2020. doi: https://doi.org/10.1016/j.tra.2020.02.021.

G. Zervas, D. Proserpio, and J. W. Byers. The rise of the sharing economy: Estimating the impact of airbnb on the hotel industry. *Journal of Marketing Research*, 54(5):687–705, 2017. doi: 10.1509/jmr.15.0204.

Y. Zhang, B. Li, and R. Krishnan. Learning individual behavior using sensor data: The case of global positioning system traces and taxi drivers. *Information Systems Research*, 31(4): 1301–1321, 2020. doi: 10.1287/isre.2020.0946.

Z. Zheng and B. Padmanabhan. Selectively acquiring customer information: A new data acquisition problem and an active learning-based solution. *Management Science*, 52(5):697–712, 2006. doi: 10.1287/mnsc.1050.0488.

X. Zhou, Y. Shen, Y. Zhu, and L. Huang. Predicting multi-step citywide passenger demands using attention-based neural networks. *WSDM 2018 - Proceedings of the 11th ACM International Conference on Web Search and Data Mining*, 2018-Febua:736–744, 2018. doi: 10.1145/3159652.3159682.

H. Zhu, S. Samtani, R. A. Brown, and H. Chen. Adeep learning approach for recognizing activity of daily living (adl) for senior care: Exploiting interaction dependency and temporal patterns1. *MIS Quarterly*, 45(2):859–896, 2021.

Eidesstattliche Erklärung nach § 8 Abs. 3 der Promotionsordnung vom 17.02.2015

Hiermit versichere ich an Eides Statt, dass ich die vorgelegte Arbeit selbstständig und ohne die Benutzung anderer als der angegebenen Hilfsmittel angefertigt habe. Die aus anderen Quellen direkt oder indirekt übernommenen Aussagen, Daten und Konzepte sind unter Angabe der Quelle gekennzeichnet.
Weitere Personen, neben den ggf. in der Einleitung der Arbeit aufgeführten Koautorinnen und Koautoren, waren an der inhaltlich-materiellen Erstellung der vorliegenden Arbeit nicht beteiligt. Insbesondere habe ich hierfür nicht die entgeltliche Hilfe von Vermittlungs- bzw. Beratungsdiensten in Anspruch genommen. Niemand hat von mir unmittelbar oder mittelbar geldwerte Leistungen für Arbeiten erhalten, die im Zusammenhang mit dem Inhalt der vorgelegten Dissertation stehen.
Die Arbeit wurde bisher weder im In- noch im Ausland in gleicher oder ähnlicher Form einer anderen Prüfungsbehörde vorgelegt.
Ich versichere, dass ich nach bestem Wissen die reine Wahrheit gesagt und nichts verschwiegen habe.
Ich versichere, dass die eingereichte elektronische Fassung der eingereichten Druckfassung vollständig entspricht.
Die Strafbarkeit einer falschen eidesstattlichen Versicherung ist mir bekannt, namentlich die Strafandrohung gemäß § 156 StGB bis zu drei Jahren Freiheitsstrafe oder Geldstrafe bei vorsätzlicher Begehung der Tat bzw. gemäß § 161 Abs. 1 StGB bis zu einem Jahr Freiheitsstrafe oder Geldstrafe bei fahrlässiger Begehung.

Düsseldorf, den 20. Juli, 2022

Karsten Schroer

About the Author

Karsten Schroer, born in 1992 in Troisdorf, Germany, holds a Master's degree in Industrial Engineering from Cambridge University and a Bachelor's degree in Mechanical Engineering from the University of Birmingham. Prior to embarking on his academic career he gained extensive industry experience at leading management consultancies including Roland Berger and McKinsey & Company.

In April of 2018, Karsten joined the University of Cologne as a PhD Candidate under the supervision of Prof. Dr. Wolfgang Ketter. His research focuses on the application of data and analytics to understand and resolve societal challenges – with a particular focus on issues in sustainable energy and transport. In his work he draws on causal inference, (spatial) machine learning, mathematical programming and reinforcement learning to achieve two general research objectives: (1) to infer and quantify causal effects of new (energy/mobility) technologies and policies on human behavior, society and the environment and (2) to develop mathematical decision algorithms for planning and operating digital energy/mobility systems. Karsten's research has been presented at leading Operations Management (OM) and Information Systems (IS) conferences[24] and is published in highly ranked IS and OM journals[25]. He has also contributed to several policy papers related to his field of expertise, such as co-authoring a World Economic Forum whitepaper on road pricing[26].

Apart from his research activities, Karsten has been involved in developing and teaching Data Science and Machine Learning courses and seminars at Bachelor's and Master's level. He has also been a regular guest lecturer in the Cologne-Rotterdam EMBA elective on Smart Sustainable Mobility.

[24] INFORMS Annual Meeting, International Conference on Information Systems (ICIS), European Conference on Information Systems (ECIS), INFORMS Conference on Information Systems and Technology (CIST), Workshop on Information Technology and Systems (WITS)

[25] e.g., Transportation Science, Information Systems Research

[26] Eckhardt, C.-F., Gray, K., Haon, S., Ketter, W., Shann, L.W., Ma, W. Ang, J.M., **Schroer, K.** (2021). *Sustainable Road Transport and Pricing.* World Economic Forum Whitepaper. Available at: `https://www3.weforum.org/docs/WEF_Sustainable_Road_Transport_and_Pricing_2021.pdf`

Research Portfolio

Publications in Peer-Reviewed Academic Journals

– Ketter, W., **Schroer, K.**, Valogianni, K.[27] (2022). *Information Systems Research for Smart Sustainable Mobility: A Framework and Call for Action.* Information Systems Research for Smart Sustainable Mobility: A Framework and Call for Action. Information Systems Research, (September). https://doi.org/10.1287/isre.2022.1167

– **Schroer, K.**, Ketter, W., Lee, T. Y., Gupta, A., & Kahlen, M. (2022). *Data-Driven Competitor-Aware Positioning in On-Demand Vehicle Rental Networks.* Transportation Science, 56(1), 182–200. https://doi.org/10.1287/trsc.2021.1097

– Herreros, J. M., **Schroer, K.**, Sukjit, E., Tsolakis, A. (2015). *Extending the environmental benefits of ethanol–diesel blends through DGE incorporation.* Applied Energy, 146(x), 335–343. https://doi.org/10.1016/j.apenergy.2015.02.075

Working Papers

– **Schroer, K.**, Ketter, W. (2022). *Identifying localized causal effects from large-scale IoT data streams: The case of e-scooter introduction and micromobility.* (1^{st}-round)

– Kahlen, M., **Schroer, K.**, Ketter, W., Gupta A. (2022). *Smart Markets for Real-Time Allocation of Multi-Product Resources: The Case of Shared Electric Vehicles.* (2^{nd}-round)

– **Schroer, K.**, Ahadi, R., Lee, T. Y., Ketter, W. (2022). *Data-Driven Service System Design using Digital Twins: An Application to Electric Vehicle Charging Hubs.* (1^{st}-round)

– **Schroer, K.**, Demircan, M., Ketter, W. (2022). *Dynamic Pricing to Manage On-demand Vehicle Rental Network Operations: An Empirical Study of ShareNow.* (currently being prepared for submission)

[27] authors in alphabetical order

Publications & Presentations in Peer-Reviewed Academic Conference Proceedings

- Demircan, M., **Schroer, K.**, Fritze, M.P., Ketter, W. (2022). *To Differentiate or not to Differentiate? The Role of Product Characteristics in the Sharing Economy* (Full Paper). In European Conference on Information Systems (ECIS) 2022 (Timisoara). `https://aisel.aisnet.org/ecis2022_rp/164`
- **Schroer, K.**, Ahadi, R., Lee, Y.T., Ketter, W. (2021). *Preference-aware Planning and Operations of Electric Vehicle Charging Clusters: A Data-Driven Prescriptive Framework.* In Proceedings of the SIG GREEN Workshop 2021 (Austin, TX). `https://aisel.aisnet.org/sprouts_proceedings_siggreen_2021/1/`
- **Schroer, K.**, Ahadi, R., Lee, Y.T., Ketter, W. (2021). *Preference-Aware Planning and Operations of Electric Vehicle Charging Clusters: A Prescriptive Framework.* In Workshop on Information Systems and Technology (WITS) 2021 (Austin, TX).
- **Schroer, K.**, Demircan, M., Ketter, W. (2021). *Dynamic Pricing to Manage On-demand Vehicle Rental Network Operations: An Empirical Study of ShareNow.* INFORMS 2021 Annual Meeting (Anaheim, CA).
- Demircan, M., **Schroer, K.**, Fritze, M.P., Ketter, W. (2021). *Examining the Role of Product Differentiation in the Sharing Economy.* In INFORMS Conference on Information Systems and Technology (CIST) 2021 (Newport Beach, CA).
- **Schroer, K.**, Pohl, M., Ketter, W. (2020). *To Substitute or to Supplement? Investigating the Heterogeneous Effects of Electric Scooter Platform Introduction on Micromobility* (Full Paper). In International Conference on Information Systems (ICIS) 2020 (India) `https://aisel.aisnet.org/icis2020/societal_impact/societal_impact/9`.
- **Schroer, K.**, Ketter, W. (2020). *An Empirical Analysis Of The Heterogenous Effects Of Electric Scooter Platform Introduction On Micromobility.* INFORMS 2020 Annual Meeting (Virtual).
- **Schroer, K.**, Ketter, W., Lee, T. Y., Gupta, A., Kahlen, M. (2019). *Optimal management of free-floating vehicle sharing systems under competition.* In Workshop on Information Systems and Technology (WITS) 2019 (Munich).
- **Schroer, K.**, Ketter, W., Lee, T. Y., Gupta, A., Kahlen, M. (2019). *An Online Learning and Optimization Approach for Competitor-Aware Management of Shared Mobility Systems.* In Proceedings of the SIG GREEN Workshop 2019 (Munich) `https://aisel.aisnet.org/sprouts_proceedings_siggreen_2019/2`
- **Schroer, K.**, Ketter, W., Lee, T. Y., Gupta, A., Kahlen, M. (2019). *Utilizing Real-Time Competitor Information to Boost Profits for One-Way Transportation Companies.* In Workshop on Policy, Awareness, Sustainability, and Systems (PASS) 2019 (Cologne)

– **Schroer, K.**, Kahlen, M., Ketter, W., Lee, T. Y., Gupta, A. (2019). *Fleet Wars: Leveraging Big Urban Data for Competitor- Aware Predictive Analytics in Free-Floating Shared Mobility Systems.* In INFORMS Conference on Information Systems and Technology (CIST) 2019 (Seattle).

Non-Academic Publications

– Ketter, W., M., Loan, Eckhardt, C.F., Wolff, C., and **Schroer, K.** (2021). *How road pricing is tackling congestion and pollution in cities like London and Singapore.* World Economic Forum Blogpost. Available at: `https://www.weforum.org/agenda/2021/12/how-road-pricing-is-tackling-congestion-and-pollution-in-cities/`
– Eckhardt, C.-F., Gray, K., Haon, S., Ketter, W., Shann, L.W., Ma, W. Ang, J.M., **Schroer, K.** (2021). *Sustainable Road Transport and Pricing.* World Economic Forum Whitepaper. Available at: `https://www3.weforum.org/docs/WEF_Sustainable_Road_Transport_and_Pricing_2021.pdf`
– Lilienkamp, A., Kienscherf, P., **Schroer, K.**, Gierkink, M. (2020). *Analyse zukünftiger Elektrofahrzeugdaten auf Basis von App-Daten.* Energiewirtschaftliche Tagesfragen, 70(11), 53–55.
– Ketter, W., **Schroer, K.** (2020). *Accessing new revenue pools through virtual power planting of electric vehicle fleets.* Wundermobility Blog. Available at: `https://www.wundermobility.com/blog/`
– Ketter, W., **Schroer, K.** (2020). *Virtuelle Kraftwerke aus Elektrofahrzeugen.* MitUns, 14–15. Available at: `https://verwaltung.uni-koeln.de/mituns/content/e88/e188369/RZmitunsMrz2020_web_DS_ger.pdf`

Teaching Portfolio

Lecturing & Tutoring

As PhD candidate at the University of Cologne I had the opportunity to gain valuable (co-) lecturing and tutoring experience at Bachelor's, Master's and MBA level. I was involved in the creation of a completely new data science and machine learning curriculum targeted at information systems students. This involved the strategic planning of the curriculum, lecture content development and the creation of entirely new programming tutorials. I have taught courses and tutorials across these topics. My tasks included leading weekly programming tutorials (in Python), preparing lecture materials, co-lecturing, and preparing, conducting and assessing examinations. A list of specific lecturing activity is provided below.

Bachelor's

Data Science & Machine Learning (DSML) – Co-Lecturer and Tutor) [WirtInf/BWL Summer 18,19,20,21]

– I held co-teaching and tutoring responsibility for the Bachelor's course on Data Science & Machine Learning. The curriculum, which I co-developed, covers the entire data science and machine learning life cycle from data preparation (feature engineering and reduction techniques), model building including in-depth lectures on supervised learning algorithms for regression (linear, SVM, polynomial, RBFs) and classification (logistic regression, decision trees, Bayesian methods) along with their mathematical definitions/intuition and evaluation (test metrics, evaluation workflows). Unsupervised methods (PCA, hard and soft clustering) and advanced methods including deep neural networks are also discussed and applied.

– Accompanying the lectures I offered weekly programming tutorials (Python data science stack). I also coached groups of students on their team assignments which consists of a real-world data science and prediction problem and is typically based on a large-scale mobility or energy dataset.

Master's

Advanced Topics in Information Systems for Sustainable Society (ATIS3) – Co-Lecturer and Tutor [WirtInf/BWL, Winter 18/19, 19/20]

– I co-developed and taught a new course on IS for sustainability targeted at equipping IS and management students with the necessary domain knowledge (energy markets, technological constraints, etc.) and tools (data analytics, mathematical programming/optimization) needed to effectively develop and deploy IS technology solutions in the energy and smart mobility domains.

Advanced Seminar for Information Systems for Sustainable Society (ASIS3) – Seminar Tutor [WirtInf/BWL, Winter 18/19, 19/20, 20/21, 21/22]

– ASIS3, is held in an interactive seminar format that draws on literature from mechanism design, online markets, decision support systems, and empirical analysis of these artifacts. Students are asked to present and discuss papers from the compiled reading list in class. I co-lead the seminar sessions, assessed student presentations and moderated in-class paper discussions.

MBA

Elective on Operations Management for Future Mobility Systems – Guest Lecturer [Cologne-Rotterdam EMBA 2017-18, 2018-19, 2020-21, 2021-22]

– I was a Guest Lecturer in the annual Cologne-Rotterdam Executive MBA elective on Future of Mobility where I delivered two-hour self-designed interactive lecture sessions on core technology trends and implications/opportunities for data-driven operations management. Drawing from case studies from my own research on e.g., virtual power plants of EVs, real-time management of shared vehicle fleets as well as the latest OM/IS research in the area, I presented concrete examples of how technology can be used to solve some of society's most pressing issues.

– As part of the lecture session I also developed and moderated in-class group case studies that the students prepared, presented and discussed in class.

Thesis Supervision (Total Count: 30)

In addition to teaching, I held main supervision and coaching responsibility for 30 Master's, MBA and Bachelor's theses. These typically aligned with my research interests in data-driven and automated management and empirical analysis of new energy and mobility systems. As part of my supervision responsibilities I helped students develop their research question, provided data sets, held regular feedback/discussion meetings and graded the final thesis. A complete list of supervised theses titles is provided below.

Master's & MBA Theses (Count: 12)

- *A simulation-driven approach to optimize EV charging clusters: A more sustainable parking facility* (2021)
- *Supporting Cities in Decision-making with Shared Mobility Data* (2021)
- *Predicting Rental Length and Endpoints in Free-Floating Vehicle Sharing Systems - An Analysis using Geotagged Rental Data* (2020)
- *Platform competition for the worse? The influence of electric scooters on bike sharing usage* (2019)
- *Last-Mile Delivery with Shared Autonomous Vehicles: A mixed rental-delivery strategy for fleet operators* (2019)
- *An auction-based mechanism for road pricing in autonomous urban transport systems* (2019)
- *Emco entering the e-scooter sharing operations business in Spain* [MBA Thesis] (2019)
- *Reinforcement Learning Portfolio Optimization of Electric Vehicle Virtual Power Plants* (2019)
- *Improving spatio-temporal Demand Predictions for Free Floating Car Sharing Services - A Machine Learning Approach with Novel Features* (2019)
- *Predicting Dockless Bikesharing Demand Across Time and Space using Machine Learning* (2019)
- *Implementation Framework for EVs in the Commercial Sector in Urban Areas* [MBA Thesis] (2018)
- *Predicting Economic Regimes in Electricity Markets* (2018)

Bachelor's Theses (Count: 18)

- *Consumer Models of EV Charging - How, When, Where and How much do People Charge their EVs* (2021)
- *Using Big-Behavioral Data to Estimate Future Charging Demand in Parking Lots* (2021)
- *Mobility in times of COVID-19 - An Empirical Analysis of Policy Compliance* (2021)
- *A spatio-temporal analysis of usage patterns in free-floating shared mobility* (2021)
- *Understanding and predicting shared mobility usage patterns* (2021)
- *Leveraging Parking Preference Data for EV Charging Infrastructure Planning* (2021)

- *Determining the Sustainability Footprint of New Mobility* (2020)
- *Understanding and Quantifying EV Usage Patterns* (2020)
- *Examining the Effect of COVID-19 policy interventions using large-scale mobility data* (2020)
- *Carsharing at the Multi-Residential Building Scale with Renewable Energy - an IT-Enabled Business Model for Building Operators* (2020)
- *Driving Sustainability in Transportation through IS-Enabled Eco Nudging* (2020)
- *Information Systems Research for Connected Autonomous, Shared and Electric Mobility: A Literature Review* (2020)
- *Uncovering the relationship between public transit and shared mobility concepts: An empirical investigation* (2019)
- *Free and yet predictable: Value of big urban data in predicting free-floating car sharing demand* (2019)
- *Smart planning of charging infrastructure for connected, shared and electric vehicles using real-world data* (2019)
- *Possible approaches to avoid traffic congestion in an autonomous mobility future* (2019)
- *Eine demografische Untersuchung der Elektroautobesitzer in Deutschland* (2018)
- *Scenario of a Sustainable Germany: A Technology-Based Approach* (2018)

KARSTEN SCHROER

Version: July, 2022

karsten.schroer@icloud.com ◇ karstenschroer.github.io

EDUCATION

University of Cologne, DE *2022 (exp.)*
Ph.D. in Operations & Information Management
Advisor: Prof. Wolfgang Ketter

University of California at Berkeley, US *2022*
Visiting Ph.D. Scholar in Data Science & Operations Management
Advisor: Prof. Thomas Y. Lee

University of Cambridge, UK *2015*
M.Phil in Industrial Systems, Manufacture & Management
Grade: Distinction (top 5% of cohort)

University of Birmingham, UK *2013*
B.Eng in Mechanical Engineering with Business Management
Grade: First Class (top 5% of cohort)

International German School Brussels, BE *2010*
High School Diploma (Abitur)
Grade: 1.4

EXPERIENCE

University of Cologne Apr '18 – Jun '22
PhD Researcher & Academic Staff *Cologne, DE; Berkeley, US*

- Researched data-driven decision making (econometrics/statistics, machine learning, optimization, simulation, reinforcement learning) with focus on future energy and mobility systems (EV charging, fleet management); 5-months research visit at UC Berkeley
- Published first-authored papers at leading international operations management and information systems conferences and high-impact journals
- Taught *"Data Science and Machine Learning"* (Bachelor), *"Analytics and Applications"* (Master), *"Advanced Seminar on Information Systems"* (Master/Ph.D.) and gave annual guest lecture on *"Smart Sustainable Mobility"* (MBA/EMBA); Supervised theses in data science and operations management at Bachelor's, Master's and MBA level
- Co-led DE- and EU-level grant proposals (total funds acquired: EUR 228k) and initiated two active company research collaborations

Institute of Energy Economics at the University of Cologne (EWI) Oct '19 – Oct '21
Affiliated Researcher/Data Scientist *Cologne, DE*

- Co-led data-driven applied research projects in the area of smart electric vehicle charging and charging infrastructure planning; managed teams of up to three researchers
- Developed proposal materials for project acquisitions and delivered senior management and investor presentations (e.g., results presentations, workshop series on AI and the Smart Grid)
- Contributed to EWI's thought-leadership in the area of electric mobility by co-authoring technical reports

Roland Berger Feb '16 – Mar '18
Management Consultant, Energy & Utilities Practice *Duesseldorf, DE*

- Led own work streams in large international strategy development and restructuring assignments in Europe and the Middle East for clients in the utilities, oil&gas, chemicals and healthcare industries; extensive senior management exposure
- Managed teams of up to three interns and junior consultants; acted as mentor for summer interns and new hires
- Contributed to project acquisitions by crafting proposal documents and participating in pitch presentations with senior management attendance; co-developed new RB offering in the area of AI-powered maintenance and prognostics

McKinsey & Company Mar '14 – May '14
Visiting Associate (Intern) *Berlin, DE*

- Supported an operational excellence and store concept re-launch project for a global fashion retailer

Innogy Consulting (formerly RWE Consulting) Dec '13 – Feb '14
Junior Consultant (Intern) *Essen, DE*

- Supported the development of a scenario-based outlook on the future of the Polish energy ecosystem and identified strategic implications for RWE (now Innogy)

Simon-Kucher & Partners Aug '13 – Nov '13
Associate Consultant (Intern) *Bonn, DE*

- Supported the conceptualization and implementation of a web-based decision support tool for price promotions at a major German supermarket chain

HONOURS & AWARDS

AIS Doctoral Consortium Member 2021, Association for Information Systems (AIS)
One of only 40 PhD students globally to be invited to the prestigious ICIS Doctoral Consortium 2021 in Austin (Texas); competitive peer review-based selection process; fully funded.

DAAD PhD Research Scholarship, German Academic Exchange Service (DAAD)
Full scholarship (fees and maintenance grant) to fund research visit to UC Berkeley

The Frederick Alfred Warren Prize, University of Cambridge
Price received for the highest mark overall in project work and research dissertation

DAAD Postgradual Scholarship, German Academic Exchange Service (DAAD)
Full scholarship (fees and maintenance grant) to pursue postgraduate studies at Cambridge

Ellis, Linning and Sandifer Prize, University of Birmingham
Prize awarded annually to the academically most outstanding student in the final year of the B.Eng. program in Mechanical Engineering.

Gilbert Walker Prize in Mech Eng and Commerce, University of Birmingham
Prize awarded annually to the academically most outstanding student of the double Honours course in Mechanical Engineering and Business Management

First Class Scholarship 2010-2013, University of Birmingham
Scholarship awarded for excellent academic accomplishments. Awarded for three consecutive years.

SKILLS

Programming	Python, R, Julia, STATA, SQL, Git, LaTeX
APIs & Technologies	machine learning (scikit-learn, TensorFlow, Keras), optimization (commercial (CPLEX, Gurobi) and non-commercial (GLPK, Ipopt) solvers, higher-level frameworks (JuMP, Pyomo)), large-scale simulation (SimPy), causal inference/econometrics (R and Python statistics packages), GIS (geopandas, h3, kepler.gl), big data/cloud technologies
Languages	English, German (native), French, Dutch

SOCIETAL SERVICE & PERSONAL INTERESTS

Academic Service	Regular ad hoc reviewing activities for leading Information Systems conferences (ICIS, ECIS, WI) and journals (Journal of Information Technology)
Sports	Rowing at competitive level: currently at RG Benrath Rowing Club; previously at University of Cologne Rowing Club (2018-2020), Wolfson College Cambridge Boat Club (Boat Captain, 2014-15), Cercles des Régates de Bruxelles Rowing Club (2007-10), Siegburger RV Rowing Club (2004-07)
Societies	Berkeley Energy and Resource Collective (BERC), Haas Technology Club, Wolfson College Cambridge Mayball Organizing Committee (2015)